

UC Berkeley

UC Berkeley Electronic Theses and Dissertations

Title

Semiclassical Analysis of Fundamental Amplitudes in Loop Quantum Gravity

Permalink

<https://escholarship.org/uc/item/6c65v5sg>

Author

Hedeman, Austin J.

Publication Date

2014

Peer reviewed|Thesis/dissertation

Semiclassical Analysis of Fundamental Amplitudes in Loop Quantum Gravity

by

Austin J Hedeman

A dissertation submitted in partial satisfaction of the

requirements for the degree of

Doctor of Philosophy

in

Physics

in the

Graduate Division

of the

University of California, Berkeley

Committee in charge:

Professor Robert Littlejohn, Chair

Associate Professor Ori Ganor

Professor William Miller

Fall 2014

Semiclassical Analysis of Fundamental Amplitudes in Loop Quantum Gravity

Copyright 2014
by
Austin J Hedeman

Abstract

Semiclassical Analysis of Fundamental Amplitudes in Loop Quantum Gravity

by

Austin J Hedeman

Doctor of Philosophy in Physics

University of California, Berkeley

Professor Robert Littlejohn, Chair

Spin networks arise in many areas of physics and are a key component in both the canonical formulation (loop quantum gravity) and the path-integral formulation (spin-foam gravity) of quantum gravity. In loop quantum gravity the spin networks are used to construct a countable basis for the physical Hilbert space of gravity. The basis states may be interpreted as gauge-invariant wavefunctionals of the connection. Evaluating the wavefunctional on a specific classical connection involves embedding the spin network into a spacelike hypersurface and finding the holonomy around the network. This is equivalent to evaluating a “ g -inserted” spin network (a spin network with a group action acting on all of the edges of the network). The spin-foam approach to quantum gravity is a path-integral formulation of loop quantum gravity in which the paths are world-histories of embedded spin networks. Depending on the spin-foam model under consideration the vertex amplitude (the contribution a spin-foam vertex makes to the transition amplitude) may be represented by a specific simple closed spin network. The most important examples use the $6j$ -symbol, the $15j$ -symbol, and the Riemannian $10j$ -symbol. The semiclassical treatment of spin networks is the main theme of this dissertation.

To show that classical solutions of general relativity emerge in the appropriate limits of loop quantum gravity or spin-foam gravity requires knowledge of the semiclassical limits of spin networks. This involves interpreting the spin networks as inner products and then treating the inner products semiclassically using the WKB method and the stationary phase approximation. For any given spin network there are many possible inner product models which correspond to how the spin network is “split up” into pieces. For example the $6j$ -symbol has been studied in both a model involving four angular momenta (Aquilanti *et al* [1]) and a model involving twelve angular momenta (Roberts [2]). Each of these models offers advantages and disadvantages when performing semiclassical analyses. Since the amplitude of the stationary phase approximation relies on determinants they are easiest to calculate in phase spaces with the fewest dimensions. The phase, on the other hand, is easiest to compute in cases where all angular momenta are treated on an equal footing, requiring a larger phase space.

Surprisingly, the different inner product models are *not* related by symplectic reduction (the removal of a symmetry from a Hamiltonian system). There *is* a connection between the models, however. On the level of linear algebra the connection is made by considering first not inner products but matrix elements of linear operators. A given matrix element can then be interpreted as an inner product in two different Hilbert spaces. We call the connection between these two inner product models the “remodeling of an inner product.” The semiclassical version of an inner product remodeling is a generalization of the idea that the phase space manifold that supports the semiclassical approximation of a unitary operator may be considered the graph of a symplectomorphism. We use the manifold that supports the semiclassical approximation of the linear map to “transport” features from one space to another. Using this transport procedure we can show that the amplitude and phase calculations in the phase spaces for the two models are identical. The asymptotics of a complicated spin network, and thus the fundamental amplitudes of loop quantum gravity and spin-foam gravity, may be computed by first setting up an inner product remodeling and then picking and choosing which features of the calculation to perform in which space.

In this dissertation we first introduce the remodeling of an inner product and the semiclassical features of the remodeling. We then apply the remodeling to the well-studied cases of the $3j$ -symbol and the $6j$ -symbol. Finally we explore how the remodel procedure applies to more complicated spin networks such as the $15j$ -symbol and the g -inserted spin networks of loop quantum gravity.

To my family and friends.

In loving memory of Jack Hedeman.

Contents

Contents	ii
List of Figures	vi
List of Tables	viii
1 Introduction	1
2 The Remodeling of an Inner Product	8
2.1 Hilbert and Phase Space Models	9
2.1.1 The Remodeling Algebra	9
2.1.2 The Remodeling Geometry	12
2.1.3 Lagrangian Manifolds in the Remodeling Geometry	14
2.1.4 Momentum Maps and Densities	16
2.1.5 Semiclassical Inner Product Models	19
2.2 The Transport of a Manifold	21
2.2.1 The Stationary Phase Approximation for $\psi_\beta(x)$	21
2.2.2 Geometric Construction of $\mathcal{T}_M(\mathcal{L}_b)$	22
2.2.3 The Transport of an Isotropic Manifold is Isotropic	25
2.2.4 The Transport of a Manifold in Cases of Symmetry	26
2.3 The Transport of the Density	28
2.3.1 The WKB Amplitude of ψ_β	28
2.3.2 The WKB Amplitude in Cases of Symmetry	31
2.3.3 The Transported Density on $\mathcal{T}_M(\mathcal{L}_b)$	32
2.3.4 The Transported Density in Cases of Symmetry	34
2.3.5 Equality of the WKB and Transported Densities	35
2.4 The Transport of a Momentum Map	37
2.4.1 The Core Isomorphism of \hat{M}	37
2.4.2 Observables of the β -State	39
2.4.3 Subspaces and Symplectic Reduction	40
2.4.4 The Core Geometry and Symplectomorphism	42
2.4.5 Momentum Maps in the Core Geometry	45

2.4.6	The Density on \mathcal{L}_β Using β	47
2.5	Phases in the Remodeling Geometry	51
2.5.1	Relative Phases	52
2.5.2	Paths in the Remodeling Geometry	53
2.5.3	The Action Integrals	55
2.5.4	Maslov Indices	56
2.5.5	The Signature Index	58
2.5.6	Quantization	59
2.6	Summary	61
3	Models of the $3j$-Symbol	63
3.1	Linear Algebra of the $3j$ -Symbol	64
3.1.1	The Wigner Intertwiner and the $3j$ -Symbol	64
3.1.2	The Remodeling Algebra of the $3j$ -Symbol	65
3.1.3	Schur's Lemma and the $3j$ -Intertwiner	69
3.1.4	The $2j$ -Intertwiner State	74
3.1.5	Observables of $3j$ -Remodeling Algebra	75
3.1.6	The Clebsch-Gordan Coefficients and Map	77
3.2	Remodeling Geometry for the $3j$ -Symbol	79
3.2.1	Phase Spaces	79
3.2.2	Lagrangian Manifolds	80
3.2.3	The Transport of \mathcal{L}_b Through \mathcal{L}_W	86
3.2.4	The Core Geometry	87
3.2.5	The Core Symplectomorphism	89
3.3	Analysis of the Inner Product Models	92
3.3.1	Stationary Phase Sets	92
3.3.2	Amplitude Determinants	95
3.3.3	The Action Integral	98
3.3.4	Maslov and Signature Indices	100
3.4	Summary	102
4	Models of the $6j$-Symbol	104
4.1	Intertwiner States	105
4.1.1	The $2j$ -Intertwiner ("Diangle") States	106
4.1.2	The $3j$ -Intertwiner ("Triangle") States	107
4.1.3	The $4j$ -Intertwiner ("Butterfly") States	108
4.2	Remodeling Algebra of the $6j$ -Symbol	111
4.2.1	Hilbert Spaces for the Remodels of the $6j$ -Symbol	112
4.2.2	The First Remodeling Algebra	114
4.2.3	The Second Remodeling Algebra	117
4.3	Remodeling Geometries of the $6j$ -Symbol	120
4.3.1	Phase Spaces and Lagrangian Manifolds	121

4.3.2	Transporting Manifolds	122
4.3.3	Stationary Phase Sets	124
4.3.4	Reduction of the $4j$ -Model	127
4.4	Action Integrals in the $6j$ -Remodeling Geometry	129
4.4.1	The Action Integral in the $12j$ -Model	130
4.4.2	The Action Integral in the $4j$ -Model	133
4.5	Asymptotics of the $6j$ -Symbol	136
4.5.1	Computing the Amplitude in the $4j$ -Model	137
4.5.2	Computing the Maslov Index in the $4j$ -Model	138
4.5.3	The Asymptotic Expression for the $6j$ -Symbol	140
4.6	Summary	140
5	Other Applications	142
5.1	$3nj$ -Symbols ($n \geq 2$)	142
5.1.1	Inner Product Models of the $3nj$ -Symbol	143
5.1.2	Remodeling Algebras for the $3nj$ -Symbols	148
5.1.3	Remodeling Geometries for the $3nj$ -Symbols	153
5.2	g -Insertions	154
5.2.1	Models of the D -Matrix	156
5.2.2	$L^2SU(2)$ and $T^*SU(2)$	158
5.2.3	g -Inserted Intertwiners	160
5.2.4	g -Inserted Spin Networks	163
5.3	Co-Isotropic Manifolds	168
5.3.1	Quantization of I	170
5.4	Conclusions	172
	Bibliography	173
	A Representations of Angular Momenta	182
A.1	The Schwinger Hilbert Space	182
A.2	The Schwinger Phase Space	183
A.3	Group Actions	185
A.4	Representations in the Schwinger Phase Space	186
	B Symplectic Geometry	188
B.1	Symplectic Manifolds	188
B.2	Momentum Maps	190
B.3	Level Sets, Orbits, and Lagrangian Manifolds	191
B.4	Symplectic Reduction	192
B.5	The Lagrangian Signature	194
	C The Semiclassical Approximation	196

C.1	The WKB Wavefunction	196
C.2	Densities	198
C.3	The Wigner-Weyl Transform	200
C.4	WKB Approximation of Inner Products	201
C.5	Phases in the WKB Inner Product Approximation	203

List of Figures

2.1.1 The remodeling algebra for $\langle a \hat{M} b\rangle$	12
2.1.2 Phase spaces and maps in the remodeling geometry	14
2.2.1 The transport of a manifold	24
2.2.2 Branches of the intersection manifold	25
2.2.3 Tangent maps in the remodeling geometry	25
2.2.4 Projection of the intersection manifold in cases with symmetry	28
2.3.1 The branch index \tilde{k}	30
2.4.1 The core isomorphism	38
2.4.2 The core geometry	44
2.5.1 Paths on \mathcal{L}_β , \mathcal{L}_M , and \mathcal{L}_b	54
2.5.2 Paths on \mathcal{L}_{ab}	55
3.1.1 The remodeling algebra for the $3j$ -symbol	68
3.2.1 Phase spaces and maps in the remodeling geometry for the $3j$ -symbol	80
3.2.2 A point on the $2jm$ -manifold	82
3.2.3 A point on the Wigner manifold	84
3.2.4 A point on the “coupled” manifold	85
3.3.1 The reduced $2j$ -phase space Φ_{2j}^R	101
4.1.1 A point on the diangle manifold	107
4.1.2 A point on the butterfly manifold	111
4.1.3 A point in L_Z defines a tetrahedron	112
4.2.1 The remodeling algebras for the $6j$ -symbol	112
4.3.1 Phase spaces and maps in the remodeling geometries for the $6j$ -symbol	122
4.3.2 A point in the $12j$ -model stationary phase set	126
4.3.3 A point in the $8j$ -model stationary phase set	127
4.4.1 The closed path in the $12j$ -model.	130
5.1.1 Spin network models of the $9j$ -symbol	147
5.1.2 Spin network models for the $15j$ -symbols	148
5.1.3 The remodeling algebras for the $3nj$ -symbols	149
5.1.4 Phase spaces and maps in the remodeling geometries for the $3nj$ -symbols	154

5.2.1 The remodeling algebras for the D -matrix	159
5.2.2 The remodeling algebras for the g -inserted $6j$ -symbol	164
5.2.3 The embedding of a spin network edge	166
5.3.1 The symplectic reduction and remodeling geometry for the inclusion map	169
5.3.2 The symplectic reduction and remodeling geometry for the projection map . . .	171

List of Tables

2.1	States in the remodeling algebra	11
2.2	Lagrangian manifolds in the remodeling geometry	18
2.3	Spaces involved in the transport of \mathcal{L}_b through \mathcal{L}_M	24
3.1	Subspaces and states in the remodeling algebra for the $3j$ -symbol	78
3.2	Phase spaces in the remodeling geometry for the $3j$ -symbol	80
3.3	Lagrangian manifolds in the remodeling geometry for the $3j$ -symbol	85
3.4	Manifolds in the transport of \mathcal{L}_b through the Wigner manifold	87
4.1	Hilbert spaces in the remodeling algebras for the $6j$ -symbol	114
4.2	States in first remodeling algebra for the $6j$ -symbol	117
4.3	States in the second remodeling algebra for the $6j$ -symbol	121
4.4	Inner product models of the $6j$ -symbol	121
4.5	Phase spaces in the remodeling geometries for the $6j$ -symbol	122
4.6	Lagrangian manifolds in the remodeling geometries of the $6j$ -symbol	123
5.1	States in the two remodeling algebras for the $3nj$ -symbols.	152
5.2	Phase spaces for models in the remodeling geometries of the $3nj$ -symbols	154

Acknowledgments

Many people helped me in the development of the work presented in this dissertation and are richly deserving of thanks. First and foremost is my advisor Robert Littlejohn who taught me to appreciate the beauty of semiclassical physics and has been a mentor and guide throughout the back half of my graduate career. I am grateful for the amount of attention and consideration that Professor Littlejohn gave to my project and thoroughly enjoyed all of the stimulating intellectual detours we have taken in the course of completing this dissertation. I also want to thank all the other members of the Littlejohn group, notably Hal Haggard, Eugene Kur, and Ilya Esterlis, who were always eager to discuss this work and whose insights and feedback have helped me work through tricky details.

I would like to thank the entire Physics support staff at UC Berkeley for the amazing job they do. Anne Takizawa and Donna Sakima in particular have provided me with many opportunities and have helped me out of many jams.

To all of my friends at Berkeley I thank you for your companionship and for helping make the completion of this dissertation possible. You are all special to me but I especially want to mention Susan Amrose and Jackson and Theresa DeBuhr. Susan, you have been a dear friend since I started graduate school and your friendship and support has meant the world to me. Theresa, thank you for always being around and providing an excuse to talk about non-physics things. Jackson, thank you for co-founding the “No Strings Attached” alternatives to Quantum Gravity journal club with me! This journal club brought me into Professor Littlejohn’s orbit and finally connected me with an advisor whose interests aligned with mine.

Finally, I give my deepest thanks to my family: my father and mother, who nurtured my interest in all things math and science from the beginning; my sister Juliana and my grandmother, who were always there for me; and my grandfather, who I always perceived as the root of my family’s love of science.

Chapter 1

Introduction

Spin networks were first introduced by Penrose [3] as a way of creating a discrete model of three-dimensional spatial geometry. Spin networks and their role in quantum gravity have been reviewed in Major [4]. They are a diagrammatic way of representing certain group-theoretic concepts such as the coupling of group representations. As defined in Rovelli [5], a (closed) spin network is a graph containing a number of nodes and oriented links (“edges”) between the nodes with labels on each of the nodes and links representing group-theoretic quantities. For a given group the edges are labeled by a group representation. In this work we deal exclusively with $SU(2)$ spin networks so the irreducible representations are labeled by j , a non-negative integer or positive half-integer. The nodes are intertwiners, linear maps between carrier spaces of group representations that commute with the action of the group. If the nodes are trivalent (so only three edges connect to the node) then the intertwiner is uniquely determined up to a normalization and phase. If the nodes are of higher valence (so four or more edges connect to the node) then there is a non-trivial vector space of possible intertwiners the node could represent. Thus a further decoration or “coloring” is required for each node of valence four or higher to indicate the precise intertwiner the node represents. Note that this abstract definition of a spin network is *not* a graph embedded in some space, though embeddings are used to form the basis states of loop quantum gravity.

These spin networks are closely related to the graphical technique used by Levinson [6] and Yutsis *et al* [7] to describe calculations in $SU(2)$ group theory. In their work each closed spin network evaluates to a number. The Yutsis spin networks also contain links that contain free ends. These ends are labeled with azimuthal quantum numbers m and represent angular momenta with definite z -components. This idea was expanded upon in Stedman [8] where the open ends are left unlabeled, in which case the spin network represents a state in the Hilbert space of angular momenta rather than a number.

There is another approach to spin networks, sometimes called the chromatic evaluation, which is more directly connected to Penrose’s original idea [3]. The fundamental object in this approach is a “loop,” which is essentially a spin network with no nodes whose edge carries a $j = 1/2$ representation label. Any closed $SU(2)$ spin network can be decomposed into finite linear combinations of loops. The decomposition uses the fact that the carrier

space for the j -irrep of $SU(2)$ can be expressed as the symmetrized product of $2j$ carrier spaces for the fundamental ($j = 1/2$) representation. A spin network edge labeled with irrep j is therefore interpreted as a symmetrized product of $2j$ strands (segments of a loop) (see, for example, Section 6.3.2 of Rovelli [5]). The intertwiners at the nodes encode how the strands that end at each node are connected. Thus the spin network becomes a linear combination of closed loops. Kauffman and Lins [9] provide a more thorough overview of this approach. It is this conception of spin networks that allows spin networks to be interpreted as functionals of the connection in loop quantum gravity [5].

Spin networks arise in many areas of physics, ranging from atomic, molecular, and nuclear physics to quantum computing and quantum gravity [10, 11]. They are a key component in both the canonical formulation (loop quantum gravity) and the path-integral formulation (spin-foam gravity) of quantum gravity [5]. Spin networks also provide a rich playground for semiclassical analysis since their semiclassical approximations involve integrable systems.

Loop quantum gravity is a canonical, background-independent quantum field theory for quantum gravity. Review articles and texts for loop quantum gravity include Rovelli [5], Ashtekar and Lewandowski [12], and Thiemann [13]. Historically loop quantum gravity grew out of the ADM formalism and the Cartan formulation of the first-order Palatini formalism. In the ADM formalism [14] general relativity is described as a Hamiltonian system with first-class constraints and in the Cartan formulation the Palatini action is expressed in terms of a tetrad and a Lorentz connection, the metric being a function of the tetrad and the curvature being a function of the connection [15, 5]. The formalism of loop quantum gravity is built out of the Ashtekar’s “new variables” [16] which reformulate the ADM formalism as a type of $SU(2)$ Yang-Mills gauge theory, with the fundamental field an $SU(2)$ connection, which is the self-dual part of the complexified Palatini Lorentz connection.

Given a gauge theory in the canonical formalism we may use the connection of the gauge theory to form a representation for the quantization of the theory. In this connection representation physical quantum states are interpreted as gauge-invariant functionals of the connection. Just as the classical configuration space in elementary quantum mechanics specifies a set of basis states whose wavefunctions are delta functions in the configuration variables, the space of connections specifies the connection basis states. However, the wavefunctionals for these basis states are not gauge-invariant and therefore the connection basis states do *not* represent physical states. Moreover, the Hilbert space on which these connection basis states live is non-separable and therefore an uncountably infinite number of connection basis states is required. In the context of quantum gravity this Hilbert space is the space of Ashtekar’s $SU(2)$ connections. Rovelli [5] calls this the “kinematical state space.” The physical Hilbert space is obtained by performing a quotient operation in which the gauge freedoms and constraints of the theory are eliminated. One of the early triumphs of loop quantum gravity was Rovelli and Smolin’s construction of a countable basis for a (separable) physical Hilbert space of gravity [17]. This basis is made up of “s-knot” states and is labeled by a decorated spin network and a knot class. In this work we call this basis the spin network basis.

Since loop quantum gravity is a canonical (Hamiltonian) formulation of gravity we need to perform a 3+1 split of spacetime. Let the spacetime locally be foliated into a family of

spacelike hypersurfaces. Interpreting the geometric properties of a spin network basis state involves first embedding the spin network in a three-dimensional spacelike hypersurface Σ . Let $|S\rangle$ be a spin network basis state, A a connection, and $|A\rangle$ the corresponding connection basis state. Just as a state in ordinary quantum mechanics can be identified with a function of the classical configuration (the wavefunction), a state in gauge theory can be interpreted as a gauge-invariant functional of the classical connection (the wavefunctional) [18]. Thus we may interpret spin network states in loop quantum gravity as wavefunctionals of the Ashtekar $SU(2)$ connection, $\Psi_S[\mathbf{A}] = \langle A|S\rangle$. These are the fundamental amplitudes in loop quantum gravity, taking one from the connection basis to the spin network basis [5]. The semiclassical treatment of these amplitudes is the main theme of this dissertation.

As discussed earlier we may interpret an embedded spin network as a linear combination of embedded loops. In this interpretation each of the individual loops evaluated against the connection is a Wilson loop (this terminology is standard but confusing - it is *not* a loop in the sense that we have defined them but the trace of the closed-path holonomy *around* a loop) and thus the spin network evaluated against a connection may be interpreted in terms of holonomies. The evaluation of spin networks as in Yutsis *et al* [7] is recovered when the spin network is evaluated against a flat connection (so all holonomies are the identity). For a non-flat connection there is an open-path holonomy g along each of the embeddings of an edge. Evaluating the wavefunctional $\Psi_S[\mathbf{A}]$ on a specific classical connection then involves inserting a group action operator $\hat{U}(g)$ on each of the legs of the spin network. We call such operations “ g -insertions”. The fundamental amplitudes of loop quantum gravity are therefore the evaluations of g -inserted spin networks.

Diffeomorphism invariance in gravity is manifested as the invariance of physical quantities on the embedding given a specific knot class (diffeomorphisms cannot map a spin network embedding in one knot class into another which is why the spin network basis must specify both a spin network *and* a knot class). An area operator \hat{A}_S and volume operator \hat{V}_R may be defined for each two-dimensional surface S and three-dimensional region R in Σ . A spin network basis state for a given four-valent spin network where all four-valent nodes are colored by volume eigenvalues is an eigenstate of all area operators [19] and volume operators [20] on Σ . The spin network basis may therefore be considered a “geometry” basis, in contrast to the standard “connection” basis of quantum field theories [5, 13].

The origins of the idea of treating the g -inserted spin networks as the amplitudes of loop quantum gravity trace back a long way. As described in Rovelli [5], it is a modern version of Faraday’s insight that electromagnetic phenomena may be treated in terms of “lines of force.” If we take the Faraday approach seriously then the relevant physical variables are the holonomies of the $U(1)$ electromagnetic gauge potential along paths. To gain physical insight into loop quantum gravity we can compare with the loop representation of electromagnetism, which is described in Ashtekar and Rovelli [21] and Gambini and Pullin [22]. Since electromagnetism is an abelian $U(1)$ gauge theory the $SU(2)$ spin network basis states of loop quantum gravity can be replaced by “loop states,” although now the loop states are *not* invariant under diffeomorphisms and thus the states in the loop representation have to also contain complete information about the embedding (this is one of the very few instances

where the treatment of gravity is simpler than electromagnetism!). A loop state then is a state where the electric field is zero everywhere *except* for the loop, along which it is tangent. The loop state thus represents a singular electric field line. Since this state represents a definite electric field it is a simultaneous eigenstate of the electric field operator $\hat{\mathbf{E}}(x)$ at every point in space. In Maxwell theory the electric field is the conjugate momentum to the connection one-form and thus the loop representation is related to a “momentum representation” while the typical basis built out of the second quantization of the potential is related to a “configuration representation” (up to subtleties that are irrelevant for this discussion). We can also create an electric flux operator associated with each two-dimensional surface S in space. The electric flux “counts” how many electric field lines pierce the surface and thus we can interpret the edges of a loop state as carrying quanta of electric flux. This is exactly analogous to loop quantum gravity where the spin network edges carry quanta of area. This is the statement made in Section 4.1.1 of Rovelli [5], “the area of a surface is the flux of the gravitational electric field across the surface”, where the gravitational electric field is roughly the conjugate momentum to the induced Ashtekar connection on Σ .

Spin networks are also a central object in spin-foam models of quantum gravity. The spin-foam approach is a path-integral formulation of loop quantum gravity. The “paths” in this case are the world-history of the embedded spin network, called a “spin-foam.” Spin network nodes becomes spin-foam edges and spin network edges become spin-foam faces. A given spin-foam graphically shows one possible way for one spin network to evolve into a different spin network. This usually involves creating or destroying spin network nodes. This occurs at the vertices of the spin-foam. For example, three spin-foam edges meeting at a spin-foam vertex and leaving as a single spin-foam edge represents three spin network nodes coalescing to become a single spin network node. As in the Feynman diagram approach to quantum field theory the transition amplitudes of spin-foam models are presented as sums-over-histories. Review articles and texts for the spin-foam approach to gravity include Baez [23], Oriti [24], Perez [25, 26], and Rovelli [5]. Spin networks enter this spin-foam approach in a second way, distinct from their use in the spin network states of loop quantum gravity. The contribution of a specific spin-foam to the transition amplitude is dependent in part on the spin-foam vertices. Depending on the spin-foam model under consideration the vertex amplitude may be represented by a specific simple closed spin network. The “Ponzano-Regge model” presented in Ponzano and Regge [27] is a state-sum model for $3d$ -Euclidean quantum gravity treated as an $SU(2)$ gauge theory. It was the first spin-foam model ever presented and uses the $6j$ -symbol as a fundamental building block. The $6j$ -symbol is a central object in angular momentum theory and represents the unitary matrix elements involved in a change-of-basis between the various recoupling schemes of three angular momenta [28]. The $6j$ -symbol provides the one of the simplest non-trivial examples of a closed-spin network and will be discussed extensively in Chapter 4. Turaev and Viro [29], unaware of the previous work by Ponzano and Regge, defined a similar state sum. They also expanded the formalism and created a state sum using the “ q -deformed” $6j$ -symbol, which is the $6j$ symbol for the Hopf algebra $SL_q(2)$. This state sum represents a spin-foam model for $3d$ -Euclidean quantum gravity with a cosmological constant. Ooguri [30] created a $4d$ -Lorentzian spin-

foam model for BF theory. The vertex amplitude in the Ooguri model is a $15j$ -symbol. The Archer [31, 32], Crane-Yetter [33], and Roberts [34] models are versions of the Ooguri model which use the q -deformed $15j$ -symbol as the vertex amplitude and are spin-foam models for $4d$ -Lorentzian BF theory with cosmological constant. The Barrett-Crane model [35] is a spin-foam model that uses the “Riemannian $10j$ -symbol” as the vertex amplitude. The spin network for the $10j$ -symbol contains ten edges linking five four-valent nodes. The irrep labels on the ten edges are related to the areas ten triangular 2-faces of a four-simplex. Each of the four-valent nodes is colored with an eigenvalue of the volume operator and represents the volume of each of the five tetrahedral 3-faces of the four-simplex. One unfortunate feature of the Barrett-Crane models is “ultra-locality,” the virtual absence of correlations between the amplitudes of neighboring simplices. More recent spin-foam models for $4d$ -gravity proposed by Engle, Pereira, and Rovelli [36] and Freidel and Krasnow [37] are free from this problem. These models also use the $15j$ -symbol as a fundamental building block of transition amplitudes.

One of the outstanding problems in both loop quantum gravity and spin-foam models of quantum gravity is to show that classical solutions of general relativity emerge in the appropriate limits. This requires knowledge of the semiclassical limits of spin networks as the quantum numbers (the irrep values that label the edges) become large. The asymptotics of certain fundamental spin networks has been studied extensively. The semiclassical behavior of the Wigner $3jm$ -symbol (which in the rest of this work we refer to as simply the “ $3j$ -symbol”) and the Wigner $6j$ -symbol (which is related to the Racah W -coefficient by a phase) have been studied in such works as Ponzano and Regge [27], Neville [38], Miller [39], Schulten and Gordon [40, 41], Biedenharn and Louck [42], Roberts [2], Charles [43], and Aquilanti *et al* [44, 1]. The asymptotics of other simple spin networks have been studied by Haggard and Littlejohn [45] (the $9j$ -symbol), Haggard [46] (the $6j$ and $9j$ -symbols), Yu [47] and Bonzom and Fleury [48] (the $3nj$ -symbols with both large and small quantum numbers), and Baez *et al* [49] and Freidel and Louapre [50] (the $10j$ -symbol), among others.

One of the Littlejohn group’s main approaches to studying the asymptotics of spin networks (see, for example, Aquilanti *et al* [44, 1] and Hedeman *et al* [51]) has been to treat the spin networks as inner products and to treat the inner product semiclassically using the WKB method and the stationary phase approximation. For an overview of features of the WKB method relevant for this work see Appendix C and for modern treatments of WKB theory, see Martinez [52] or Mishchenko *et al* [53]. The semiclassical calculation can be broken up into two main components, the phase and the amplitude. We are mainly concerned with the *relative* phases that occur between the terms of the semiclassical expressions rather than the absolute phases (which depend on the phase conventions of the states in the inner products). The relative phase itself may be broken up into two pieces, an “action integral” and a discrete Maslov correction, which are described in Sections C.1 and C.5. The action integral and Maslov indices are dependent on paths in phase space. As shown in Littlejohn [54], the amplitude can be expressed in terms of the determinant of matrix of Poisson brackets on phase space, which we call the “amplitude determinant”. The Maslov correction can also be expressed in terms of determinants of matrices of Poisson brackets, as discussed in

Esterlis *et al* [55].

In preparing to analyze a spin network a specific inner product model must be chosen. For any given spin network there are many possible models, which correspond to how the spin network is “split up” into pieces (each piece representing a vector in a Hilbert space). For example, in Roberts [2] a “ $12j$ -model” of the $6j$ -symbol was used. The states in the $12j$ -model inner product are states in a Hilbert space describing twelve angular momenta (two for each of the six irrep labels of the $6j$ -symbol). In contrast Aquilanti *et al* [1] used a “ $4j$ -model,” in which the states are states in a Hilbert space describing four angular momenta (with four of the six irrep labels of the $6j$ -symbol assigned to these four angular momenta and the remaining two irrep labels used to describe intermediate couplings between the original four angular momenta). Each of these models offers advantages and disadvantages when performing semiclassical analyses. Since the amplitude determinant and the Maslov correction calculations rely on determinants they are easiest to calculate in phase spaces with the fewest dimensions. In the case of the $6j$ -symbol this phase space is the symplectic reduction (a way of eliminating a symmetry from a classical system, as described in Section B.4) of the semiclassical $4j$ -model. The action integral in the phase, on the other hand, is easiest to compute in cases where all angular momenta are treated on an equal footing, such as in the $12j$ -model.

Surprisingly, the different inner product models are *not* related by symplectic reduction. We discovered this in our analysis of the $3j$ -symbol. In Aquilanti *et al* [44] a “ $3j$ -model” was used to study the $3j$ -symbol, which is constructed by considering the coupling of three angular momenta to zero. The semiclassical analysis took place on a 12-dimensional phase space, which may be reduced to a four-dimensional phase space by symplectic reduction. Meanwhile, the $3j$ -symbol is closely related to the Clebsch-Gordan coefficients (up to the action of a “ $2j$ -intertwiner,” as discussed in Chapter 3), which may be considered a “ $2j$ -model” of the $3j$ -symbol. This model is constructed by considering the coupling of two angular momenta to a third, non-zero angular momentum. The semiclassical analysis of the $2j$ -model takes place on an 8-dimensional phase space, which may be reduced to a two-dimensional phase space by symplectic reduction. There is no symplectic reduction that connects the four-dimensional reduced $3j$ -model with the two-dimensional reduced $2j$ -model.

There *is* a connection between the models, however. On the level of linear algebra the connection is made by considering first not inner products but matrix elements of linear operators. A given matrix element can then be interpreted as an inner product in two different Hilbert spaces, a “product” Hilbert space in which the linear operator of the matrix element is a vector, and a “target” Hilbert space which contains the range of the linear operator. We call the connection between these two inner product models the “remodeling of an inner product.” The semiclassical version of an inner product remodeling is a generalization of the idea in Miller [39] that the phase space manifold that supports the semiclassical approximation of a unitary operator may be considered the graph of a symplectomorphism. We use the manifold that supports the semiclassical approximation of the linear map to “transport” features from one space to another. Using this transport procedure we can show that the amplitude and phase calculations in the phase spaces for the two models are identical. The

asymptotics of a complicated spin network, and thus the fundamental amplitudes of loop quantum gravity and spin-foam gravity, may be computed by first setting up an inner product remodeling and then picking and choosing which features of the calculation to perform in which space.

The structure of this dissertation is as follows:

In Chapter 2 we introduce and discuss the remodeling of an inner product. We explore the remodeling of an inner product first through the linear algebra and then through the phase space geometry (and set up what we refer to as the “remodeling algebra” and “remodeling geometry,” respectively). Then we define in the “transport of a manifold,” a geometric construction that is used to relate semiclassical objects in different phase spaces. The remainder of the chapter is then devoted to showing that the various aspects of the semiclassical evaluations of an inner product are identical for the different models of the matrix element.

In Chapter 3 we apply the remodeling of an inner product to the $3j$ -symbol and see explicitly how the constructions of Chapter 2 apply. In particular we show how a remodeling algebra and geometry is constructed. We show how the transport procedure maps the manifolds of the $3j$ -model to the manifolds of the $2j$ -model and explicitly demonstrate the how the remodeling geometry produces the expected densities, amplitudes, and phases in the two models.

In Chapter 4 we apply the remodeling of an inner product to the $6j$ -symbol. In the case of the $6j$ -symbol *two* remodeling algebras are required to connect the “symmetric” $12j$ -model of Roberts [2] to the “small” $4j$ -model of Aquilanti *et al* [1]. With the remodeling algebras and geometries in place we re-derive the asymptotic formula for the $6j$ -symbol, choosing to do different pieces of the calculation in different models in order to simplify the calculation.

In Chapter 5 we consider other applications of the remodeling of an inner product. In particular we show how different models may be constructed for the $3nj$ -symbol and set up the remodeling algebras and geometries connecting these models. Then we consider g -insertions in spin networks and show how the remodeling algebras and geometries are affected. Finally, we analyze how the remodeling geometry may be used to associate a Lagrangian manifold in a certain product phase space to a co-isotropic manifold. This relationship enables us to consider the quantization of co-isotropic manifolds.

The Schwinger model of angular momentum, which is used heavily in all of our spin network applications, is summarized in Appendix A. Appendix B reviews the various aspects of symplectic geometry that are crucial to this work. Finally, relevant features of the WKB method are reviewed in Appendix C.

Chapter 2

The Remodeling of an Inner Product

One way to simplify the semiclassical evaluation of an inner product is through symplectic reduction [56]. We can do that when there is symmetry in the system. However, symplectic reduction is not the only way that a semiclassical calculation can be put on a different phase space. Rather than reducing the phase space we can “remodel” the inner product so that the calculation takes place in a different phase space. Remodeling shuffles computational complexity between various aspects of a calculation whereas a symplectic reduction simplifies things (and can be considered a “step down” on the complexity ladder) by removing the redundancies in the system due to the symmetry.

For example, the inner product defining the $6j$ -symbol can be evaluated using either the “ $4j$ -model” or the “ $12j$ -model” of the $6j$ -symbol as described in Aquilanti *et al* [1]. Under a symplectic reduction the $4j$ -model reduces to a two-dimensional phase space. However, calculations of the action integrals are more complicated due to the asymmetric nature in which the six angular momenta of the $6j$ -symbol are treated. The angular momenta are treated symmetrically by the $12j$ -model, at the cost of living in a 48-dimensional phase space. However the symmetric treatment of the 12 angular momenta allows an easy and straightforward calculation of the semiclassical phase. The $4j$ - and $12j$ - models cannot be connected by symplectic reductions but *can* be by two remodels, as will be shown in Chapter 4.

The goal of this chapter is to define and explore the remodeling procedure. In Section 2.1 the linear algebra and symplectic geometry connecting the various inner product models is described. Then in Section 2.2 the “transport of a manifold,” a geometric construction that is used to relate semiclassical objects in different phase spaces, is defined. The remainder of the chapter is devoted to showing that the various aspects of the semiclassical evaluations of an inner product are identical for the different models of the matrix element. Section 2.3 shows how a density may be geometrically constructed on the transported manifold and then shows that this density is identical to the density that naturally arises from a stationary phase evaluation. Section 2.4 shows how a momentum map description of the transported manifold also reproduces this density. This result is used to show that the different inner product models yield the same amplitudes in the semiclassical evaluation of the inner products.

Finally in Section 2.5 we prove that the relative phases that occur in the stationary phase evaluation are identical.

As will be shown in spin network calculations in future chapters, the phase is often easiest to calculate in phase spaces of a large dimension where all of the angular momenta are treated symmetrically. The amplitude, on the other hand, involves evaluation of a determinant and thus is easier to evaluate in phase spaces of the lower dimensionality. Knowledge that the various pieces of the stationary phase calculation are identical in different models allows for the separate evaluation of these pieces in different models.

2.1 Hilbert and Phase Space Models

In this section we define the remodeling procedure and explore the various quantum and semiclassical structures associated with each of the models. In Section 2.1.1 the “remodeling algebra,” a collection of related Hilbert spaces, states, and inner product models is described. Then in Section 2.1.2 the “remodeling geometry,” a collection of classical phase spaces and maps between them, is constructed. The remodeling geometry contains the phase spaces on which semiclassical evaluations of the various inner product models introduced in Section 2.1.1 is carried out. The wavefunctions and associated semiclassical manifolds for the quantum states and operators are described in Section 2.1.3. Finally, Section 2.1.4 provides a description of the states and manifolds of the remodeling geometry in terms of a group theory structure.

2.1.1 The Remodeling Algebra

Consider two Hilbert spaces \mathcal{H}_1 and \mathcal{H}_2 . In this discussion vectors in \mathcal{H}_1 and \mathcal{H}_2 will be written as kets. The formalism developed in this chapter, however, extends to cases where \mathcal{H}_1 or \mathcal{H}_2 are spaces of bras, linear maps, or tensor products of such spaces. The chapter on the $3j$ -symbol, for example, will deal with the case where \mathcal{H}_1 is a space of kets and \mathcal{H}_2 is a space of bras.

Let $\hat{M} : \mathcal{H}_2 \rightarrow \mathcal{H}_1$ be a linear map. The Hilbert spaces \mathcal{H}_1 and \mathcal{H}_2 will be called the “target” and “source” Hilbert spaces, respectively. Let $|a\rangle \in \mathcal{H}_1$ and $|b\rangle \in \mathcal{H}_2$ be two normalized vectors, called the “ a -state” and the “ b -state,” respectively. In this work, “state” refers to a vector in a Hilbert space following the common physics usage. Given vectors $|a\rangle \in \mathcal{H}_1$ and $|b\rangle \in \mathcal{H}_2$, one can form the matrix element

$$\langle a|\hat{M}|b\rangle, \tag{2.1.1}$$

which can be interpreted as an inner product in different ways. Such interpretations are what we call the various “models” of the matrix element.

We will be dealing exclusively with integrable systems in this work, which implies that the states described in this section can all be described as the simultaneous non-degenerate eigenstates of sets of observables. The set of observables defining a state do not need to

commute globally on the Hilbert space but they do commute when acting on the state [44]. For example, the Wigner state $|j_1 j_2 j_3 \mathbf{0}\rangle$ is a simultaneous eigenvector of the three observables $\hat{\mathbf{J}}$ at eigenvalue $\mathbf{0}$. On the $\mathbf{0}$ eigenspace, the three components of $\hat{\mathbf{J}}$ mutually commute. The observables defining a state will usually be the generators for a unitary representation of some group on the Hilbert space. For example, the operators $\hat{I}_1, \hat{I}_2, \hat{I}_3, \hat{\mathbf{J}}$ that are used to define the Wigner state are the generators of a $U(1)^3 \times SU(2)$ representation on the $3j$ -Hilbert space. In this case we say that the operators form the direct sum of three copies of the $\mathfrak{u}(1)$ Lie algebra and the $\mathfrak{su}(2)$ Lie algebra under the commutator. We will assume that all sets of operators defined below form Lie algebras under the commutator.

Let there be n_1 degrees of freedom in \mathcal{H}_1 so that n_1 independent operators are needed to form a complete set of observables on \mathcal{H}_1 . Let the a -state be the unique state (up to a normalization and phase) such that $\hat{A}_i|a\rangle = \mu_{a,i}|a\rangle$, where $\{\hat{A}_i\}$ are a set of n_1 observables on \mathcal{H}_1 satisfying

$$[\hat{A}_i, \hat{A}_j]|a\rangle = 0. \quad (2.1.2)$$

Assume that the set of operators \hat{A}_i form a Lie algebra under the commutator so that the operator identity $[\hat{A}_i, \hat{A}_j] = f_{ij}^k \hat{A}_k$ holds for some constants f_{ij}^k . Then the set of operators \hat{A}_i may act as the generators of a group G_A on \mathcal{H}_1 , where f_{ij}^k are the structure constants of the Lie algebra \mathfrak{g}_A . The observables are then interpreted as the components of the \mathfrak{g}_A^* -valued operator $\hat{\mathbf{A}} : \mathcal{H}_1 \rightarrow \mathfrak{g}_A^* \times \mathcal{H}_1$ with respect to some basis. With respect to this basis, the eigenvalues $\mu_{a,i}$ are considered the components of a momentum $\mu_a \in \mathfrak{g}_A^*$. For 2.1.2 to be satisfied we need μ_a to be a fixed point of \mathfrak{g}_A^* under the co-adjoint action of G_A on \mathfrak{g}_A^* . Given such a μ_a we may express the eigenstate $|a\rangle$ using the notation

$$|a\rangle = \left| \begin{array}{ccc} \hat{A}_1 & \dots & \hat{A}_{n_1} \\ \mu_{a,1} & & \mu_{a,n_1} \end{array} \right\rangle = \left| \begin{array}{c} \hat{\mathbf{A}} \\ \mu_a \end{array} \right\rangle, \quad (2.1.3)$$

where the top row is a list of operators and the bottom row is a list of quantum numbers and $\mu_a \in \mathfrak{g}_A^*$.

Similarly, \mathcal{H}_2 describe a system with n_2 degrees of freedom and let the b -state be described as the simultaneous eigenstate

$$|b\rangle = \left| \begin{array}{ccc} \hat{B}_1 & \dots & \hat{B}_{n_2} \\ \mu_{b,1} & & \mu_{b,n_2} \end{array} \right\rangle = \left| \begin{array}{c} \hat{\mathbf{B}} \\ \mu_b \end{array} \right\rangle, \quad (2.1.4)$$

where $\{\hat{B}_I\}$ are a set of n_2 observables on \mathcal{H}_2 satisfying $[\hat{B}_I, \hat{B}_J]|b\rangle = 0$. Let \hat{B}_I close under commutation and generate a Lie group G_B .

Define the “ β -state,” as the map \hat{M} acting on the b -state,

$$|\beta\rangle \equiv \hat{M}|b\rangle. \quad (2.1.5)$$

We assume in this work that the β -state can be expressed as the simultaneous eigenstate of a set of n_1 observables $\{\hat{\beta}_i\}$ at eigenvalues $\mu_{\beta,i}$. The relationship between $\hat{\beta}_i$, the map \hat{M} ,

State	Hilbert Space	Observables	Eigenvalues	Group
$ a\rangle$	\mathcal{H}_1	\hat{A}_i	$\mu_{a,i}$	G_A
$ \beta\rangle$	\mathcal{H}_1	$\hat{\beta}_i$	$\mu_{\beta,i}$	G_β
$ b\rangle$	\mathcal{H}_2	\hat{B}_I	$\mu_{b,I}$	G_B
$ a\rangle\langle b $	\mathcal{H}_{12}	$\hat{A}_i^{(12)}, \hat{B}_I^{(12)}$	$\mu_{a,i}, \mu_{b,I}$	$G_A \times G_B$
\hat{M}	\mathcal{H}_{12}	$\hat{O}_{M,\alpha}$	$\mu_{M,\alpha}$	G_M

 Table 2.1: States in the remodeling algebra of $\langle a|\hat{M}|b\rangle$.

and the observables $\hat{\mathbf{B}}$ will be discussed in Section 2.4.2. In terms of $|\beta\rangle$, the matrix element 2.1.1 can be expressed as

$$\langle a|\hat{M}|b\rangle = \langle a|\beta\rangle, \quad (2.1.6)$$

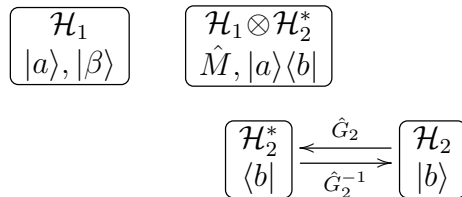
Since $|a\rangle$ and $|\beta\rangle$ are vectors in \mathcal{H}_1 , Eq. 2.1.6 is called the “target space model” of matrix element 2.1.1.

The “dual source Hilbert space” \mathcal{H}_2^* is the space of linear maps $:\mathcal{H}_2 \rightarrow \mathbb{C}$. If \mathcal{H}_2 is a space of kets then \mathcal{H}_2^* is a space of bras and vice versa. There is a natural antiunitary map $\hat{G}_2 : \mathcal{H}_2 \rightarrow \mathcal{H}_2^*$ that acts on vectors in \mathcal{H}_2 via the Hermitian conjugate, $\hat{G}_2(|b\rangle) = (|b\rangle)^\dagger = \langle b|$. There is a natural mapping from operators $\hat{B} : \mathcal{H}_2 \rightarrow \mathcal{H}_2$ on the source Hilbert space to operators \hat{B}^\top on the dual source Hilbert space. As discussed in Section A.1, \hat{B}^\top is the natural action of \hat{B} on dual vectors from the right.

Define the “product Hilbert space” $\mathcal{H}_{12} \equiv \mathcal{H}_1 \otimes \mathcal{H}_2^*$ to be the tensor product of the target Hilbert space with the dual source Hilbert space. The product Hilbert space can be identified with the space of linear maps $:\mathcal{H}_2 \rightarrow \mathcal{H}_1$. By construction \mathcal{H}_{12} describes a system with $(n_1 + n_2)$ degrees of freedom. Thus \hat{M} is interpreted both as a linear map and as a vector in \mathcal{H}_{12} . The map \hat{M} will be called the “map state” or the “ M -state” when considered as a vector in the product Hilbert space. We assume that \hat{M} , considered as a state in \mathcal{H}_{12} , may be described as the simultaneous eigenstate of a set of $(n_1 + n_2)$ observables $\{\hat{O}_{M,\alpha}\}$ on \mathcal{H}_{12} satisfying $[\hat{O}_{M,\alpha}, \hat{O}_{M,\gamma}]\hat{M} = 0$ that generate a Lie group G_M .

Another vector in \mathcal{H}_{12} can be constructed by taking the outer product of the a -state with the dual of the b -state, $|a\rangle \otimes \langle b| \in \mathcal{H}_1 \otimes \mathcal{H}_2^*$. This will be called the “product state” or the “ ab -state.” We will usually omit the tensor product symbol for brevity, writing the product state as simply $|a\rangle\langle b|$. Operators on the target or source Hilbert spaces can be extended to operators on the product Hilbert space. Let $\hat{A}_i^{(12)} : \mathcal{H}_{12} \rightarrow \mathcal{H}_{12}$ and $\hat{B}_I^{(12)} : \mathcal{H}_{12} \rightarrow \mathcal{H}_{12}$ be defined as $\hat{A}_i^{(12)} = \hat{A}_i \otimes \hat{I}d_2^\top$ and $\hat{B}_I^{(12)} = \hat{I}d_1 \otimes \hat{B}_I^\top$, where $\hat{I}d_1$ and $\hat{I}d_2$ are the identity operator on \mathcal{H}_1 and \mathcal{H}_2 . The superscript (12) is used to emphasize that the operators act on \mathcal{H}_{12} and may be dropped if the space the operators are acting on is clear from context. The ab -state may be described as the simultaneous eigenstate of the $(n_1 + n_2)$ observables $\hat{A}_i^{(12)}$ and $\hat{B}_I^{(12)}$ at eigenvalues $(\mu_{a,i}, \mu_{b,I})$. This set of observables generates the group $G_A \times G_B$.

The space of linear maps between Hilbert spaces carries a natural inner product. The inner product of two vectors \hat{O}_a and $\hat{O}_b \in \mathcal{H}_{12}$ is given by $\text{tr}(\hat{O}_a^\dagger \hat{O}_b)$. The matrix element


 Figure 2.1.1: The remodeling algebra for $\langle a|\hat{M}|b\rangle$.

2.1.1 can be expressed as such an inner product,

$$\langle a|\hat{M}|b\rangle = \text{tr}((|a\rangle\langle b|)^\dagger \hat{M}). \quad (2.1.7)$$

The right-hand side of Eq. 2.1.7 is the inner product of vectors $|a\rangle\langle b|$ and \hat{M} in the product Hilbert space $\mathcal{H}_1 \otimes \mathcal{H}_2^*$ and is called the “product space model” of matrix element 2.1.1.

We call the above collection of Hilbert spaces, states, and inner product models of the matrix element 2.1.1 the “remodeling algebra” of the matrix element. A diagram showing the spaces and states in the remodeling algebra is shown in Fig. 2.1.1. A list of the states and the observables that define them is given in Table 2.1.

It is also possible to act \hat{M} to the left in the matrix element 2.1.1 to form a state $\langle \alpha| \in \mathcal{H}_2^*$ and thus make a “source space model” $\langle \alpha|b\rangle$. However, this is equivalent to setting up the remodeling algebra for \hat{M} interpreted as a map $:\mathcal{H}_1^* \rightarrow \mathcal{H}_2^*$ and so does not need to be considered separately.

2.1.2 The Remodeling Geometry

Since the different inner product models Eqs. 2.1.6 and 2.1.7 are carried out in different Hilbert spaces, the semiclassical approximations of the models will occur in different phase spaces. Since the approximations are for the same object 2.1.1, it is expected that the semiclassical evaluations in the different models will be closely related to one another. The set of phase spaces for the different models, the relations between them, semiclassical objects that live in them will be referred to as the “remodeling geometry.”

A Hilbert space \mathcal{H} may be represented semiclassically by a phase space which is specified by a manifold Φ and a symplectic form ω on the manifold, (Φ, ω) . In a slight abuse of notation we will usually use the symbol Φ to refer to the manifold equipped with the symplectic form. If the number of independent operators necessarily to form a complete set in \mathcal{H} is n then the phase space has dimension $2n$.

The target Hilbert space \mathcal{H}_1 is associated with the “target phase space” (Φ_1, ω_1) , where $\dim \Phi_1 = 2n_1$. A point in Φ_1 will be labeled z_1 and local Darboux coordinates on Φ_1 are chosen to be (x_i, p_i) , where lowercase index i runs from 1 to n_1 . In these coordinates, the symplectic form is $\omega_1 = \sum_i dp_i \wedge dx_i$ or $dp \wedge dx$, where a sum over hidden index i is implied. The Darboux coordinate define a local x -representation, for which the symplectic potential is $\theta_1 = \sum_i p_i dx_i$ which we write as $p dx$.

Similarly, the source Hilbert space \mathcal{H}_2 is associated with the “source phase space” (Φ_2, ω_2) , where $\dim \Phi_2 = 2n_2$. A point in Φ_2 will be labeled z_2 and local Darboux coordinates on Φ_2 are chosen to be (y_I, r_I) , where uppercase index I runs from 1 to n_2 . In these coordinates, the symplectic form is $\omega_2 = \sum_I dr_I \wedge dy_I$ or $dr \wedge dy$, where a sum over hidden index I is implied. The Darboux coordinate define a local x -representation, for which the symplectic potential is $\theta_2 = \sum_I r_I dy_I$ which we write as $r dy$.

The phase space for the dual source Hilbert space \mathcal{H}_2^* is the “dual source phase space” $(\bar{\Phi}_2, \bar{\omega}_2) = (\Phi_2, -\omega_2)$, where the bar on the subscript distinguishes the symplectic form on the dual space from the form on the original space. The manifold Φ_2 with the symplectic form ω_2 will be written as Φ_2^* . The dual source phase space is identical as a manifold to the source phase space but has the opposite symplectic form. There is a natural antisymplectic isomorphism between these spaces,

$$G_2 : \Phi_2 \rightarrow \bar{\Phi}_2 : z_2 \mapsto z_2. \quad (2.1.8)$$

This is different from the identity map because the two copies of z_2 belong to spaces with different symplectic structures. The map is antisymplectic since $G_2^* \bar{\omega}_2 = -\omega_2$. The map G_2 is called the “dual map” and G_2 and G_2^{-1} can be used to pull back or push forward structures between a space and its dual. For example, submanifolds keep their symplectic character under the dual map. That is, the push-forward of an isotropic/Lagrangian/co-isotropic submanifold of Φ_2 under G_2 is an isotropic/Lagrangian/co-isotropic submanifold of $\bar{\Phi}_2$. Coordinates (y, r) define a local y -representation on Φ_2 . With respect to this representation the symplectic potential is $\theta_2 = -r dy = -G_2^{-1*} \bar{\theta}_2$.

The product Hilbert space \mathcal{H}_{12} is associated with the “product phase space” (Φ_{12}, ω_{12}) . The manifold Φ_{12} is the Cartesian product of the manifolds Φ_1 and Φ_2 and thus is $2(n_1 + n_2)$ -dimensional. The symplectic form ω_{12} is the sum of the pull-backs of the symplectic forms on the component phase spaces by the natural projection maps π_1 and π_2 associated with the Cartesian product, $\omega_{12} = \pi_1^* \omega_1 + \pi_2^* \omega_2$. In a slight abuse of notation, this will be expressed as $\omega_{12} = \omega_1 - \omega_2$.

A point $z \in \Phi_{12}$ will be described as the pair (z_1, z_2) , where $z_1 = \pi_1(z)$ and $z_2 = \pi_2(z)$. Local coordinates $(x_i, p_i; y_I, r_I)$ on Φ_{12} are the pull-backs of the coordinates on the target and dual source phase spaces. In these coordinates, the symplectic form is

$$\omega_{12} = \sum_{i=1}^{n_1} dp_i \wedge dx_i - \sum_{I=1}^{n_2} dr_I \wedge dy_I. \quad (2.1.9)$$

We will usually use Φ_{12} to refer to the manifold with this symplectic structure and write $\Phi_{12} = \Phi_1 \times \bar{\Phi}_2$, where the phase space $\Phi_1 \times \bar{\Phi}_2$ is the pair $(\Phi_1 \times \Phi_2, \omega_1 - \omega_2)$. Coordinates $(x, p; y, r)$ define a local xy -representation on Φ_{12} , for which the symplectic potential is

$$\theta_{12} = \pi_1^* \theta_1 + \pi_2^* \theta_2 = \sum_{i=1}^{n_1} p_i dx_i - \sum_{I=1}^{n_2} r_I dy_I. \quad (2.1.10)$$

Note that $d\theta_{12} = \omega_{12}$, as required.

The phase spaces and the various maps between them are summarized in Fig. 2.1.2.

$$\begin{array}{ccc}
 \Phi_1 & \xleftarrow{\pi_1} & \Phi_1 \times \Phi_2^* \\
 & & \downarrow \pi_2 \\
 & & \Phi_2^* \xrightleftharpoons[G_2^{-1}]{G_2} \Phi_2
 \end{array}$$

Figure 2.1.2: Phase spaces and maps in the remodeling geometry.

2.1.3 Lagrangian Manifolds in the Remodeling Geometry

In this work, we will assume that the states described in Section 2.1.1 all have wavefunctions that are well-approximated by the WKB form. The WKB wavefunctions will be expressed in the x -, y -, and (x, y) -representation for states in the target, source, and product Hilbert spaces, respectively. As discussed in Section C.1, the phase function in the WKB wavefunction generates a Lagrangian manifold in the relevant phase space associated with the Hilbert space. The amplitudes and phase functions in the following discussion all carry a hidden branch index and the functions are to be interpreted locally. Each of the branches of the WKB wavefunctions carries a Maslov index μ . The Maslov indices for the various wavefunctions and the relationships between them will be discussed in Section 2.5.4. We assume that all states defined in the remodeling algebra are normalized and explicitly include normalization constants N in the WKB wavefunctions below. This will allow us to express the amplitudes in terms of Poisson brackets and the normalization constant in terms of group volumes in Section 2.1.4.

The vector $|a\rangle \in \mathcal{H}_1$ has a WKB wavefunction in the x -representation of Φ_1 given by

$$\psi_a(x) = \langle x|a\rangle = N_a \sum_{k_a} A_a(x) e^{iS_a(x) - i\mu_a\pi/2}, \quad (2.1.11)$$

where k_a is the branch index, $A_a(x)$ is the amplitude, $S_a(x)$ is the phase function, and μ_a is the Maslov index. The amplitude, phase function, and Maslov index all carry a hidden branch index in the above sum. The functions $S_a(x)$ are the generating functions for the Lagrangian manifold $\mathcal{L}_a \subset \Phi_1$. Points on the “ a -manifold” \mathcal{L}_a have coordinates $(x, p_a(x))$, where

$$p_a(x) \equiv \frac{\partial S_a}{\partial x}. \quad (2.1.12)$$

Note that each branch of the WKB wavefunction carries a different phase function and thus generates a different x -representation branch of the Lagrangian manifold.

Similarly, the vector $|\beta\rangle \in \mathcal{H}_1$ has WKB wavefunction

$$\psi_\beta(x) = \langle x|\beta\rangle = N_\beta \sum_{k_\beta} A_\beta(x) e^{iS_\beta(x) - i\mu_\beta\pi/2}. \quad (2.1.13)$$

The function $S_\beta(x)$ generates the Lagrangian manifold $\mathcal{L}_\beta \subset \Phi_1$. Points on the “ β -manifold” \mathcal{L}_β have coordinates $(x, p_\beta(x))$, where

$$p_\beta(x) \equiv \frac{\partial S_\beta}{\partial x}. \quad (2.1.14)$$

The vector $|b\rangle \in \mathcal{H}_2$ has a WKB wavefunction in the y -representation of Φ_2 given by

$$\psi_b(y) = \langle y|b\rangle = N_b \sum_{k_b} A_b(y) e^{iS_b(y) - i\mu_b\pi/2}. \quad (2.1.15)$$

The function $S_b(y)$ is the generating function for the Lagrangian manifold $\mathcal{L}_b \subset \Phi_2$. Points on the “ b -manifold” \mathcal{L}_b have coordinates $(y, r_b(y))$, where

$$r_b(y) \equiv \frac{\partial S_b}{\partial y}. \quad (2.1.16)$$

Similarly, the WKB wavefunction for the dual vector $\langle b| \in \mathcal{H}_2^*$ is given by

$$\psi_{\bar{b}}(y) = \langle b|y\rangle = N_b \sum_{k_b} A_b(y) e^{iS_{\bar{b}}(y) - i\mu_{\bar{b}}\pi/2}. \quad (2.1.17)$$

Since $\psi_{\bar{b}}(y) = \psi_b^*(y)$, the phase function is $S_{\bar{b}}(y) = -S_b(y)$ and $\mu_{\bar{b}} = -\mu_b$. The amplitude for $\psi_{\bar{b}}$ is real and is therefore the same as the amplitude for ψ_b . The Lagrangian manifold $\mathcal{L}_{\bar{b}} \subset \Phi_2^*$ is generated by $S_{\bar{b}}(y)$. Points on the “dual b ” or “ \bar{b} -manifold” $\mathcal{L}_{\bar{b}}$ have coordinates $(y, r_{\bar{b}}(y))$, where

$$r_{\bar{b}}(y) \equiv -\frac{\partial S_{\bar{b}}}{\partial y} = +\frac{\partial S_b}{\partial y} = r_b(y). \quad (2.1.18)$$

The negative sign in the definition of $r_{\bar{b}}(y)$ is due to the fact that the symplectic form is $\omega_2 = -dr \wedge dy$. Note that the manifold $\mathcal{L}_{\bar{b}} \subset \Phi_2^*$ is described by the same momentum functions as $\mathcal{L}_b \subset \Phi_2$. Therefore $\mathcal{L}_{\bar{b}}$ is the image of the manifold \mathcal{L}_b under the dual map Eq. 2.1.8, $\mathcal{L}_{\bar{b}} = G_2(\mathcal{L}_b)$.

The M -state, interpreted as a vector in $\mathcal{H}_1 \otimes \mathcal{H}_2^*$, has a WKB wavefunction in the (x, y) -representation of Φ_{12} given by

$$\psi_M(x, y) = \langle x|\hat{M}|y\rangle = N_M \sum_{k_M} A_M(x, y) e^{iS_M(x, y) - i\mu_M\pi/2}. \quad (2.1.19)$$

The function $S_M(x, y)$ is the generating function for the Lagrangian manifold $\mathcal{L}_M \subset \Phi_1 \times \Phi_2^*$. Points on the “ M ” or “map manifold” \mathcal{L}_M have coordinates $(x, y, p_M(x, y), r_M(x, y))$, where

$$p_M(x, y) \equiv \frac{\partial S_M}{\partial x}; \quad r_M(x, y) \equiv -\frac{\partial S_M}{\partial y}. \quad (2.1.20)$$

The product state $|a\rangle\langle b| \in \mathcal{H}_1 \otimes \mathcal{H}_2^*$ has a WKB wavefunction in the (x, y) -representation of Φ_{12}^* given by

$$\psi_{ab}(x, y) = \langle x | (|a\rangle\langle b|) | y \rangle = N_{ab} \sum_{k_{ab}} A_{ab}(x, y) e^{iS_{ab}(x, y) - i\mu_{ab}\pi/2}. \quad (2.1.21)$$

The function $S_{ab}(x, y)$ is the generating function for the Lagrangian manifold $\mathcal{L}_{ab} \subset \Phi_1 \times \Phi_2^*$. Points on the “ ab –” or “product manifold” \mathcal{L}_{ab} have coordinates $(x, p_{ab}(x, y); y, r_{ab}(x, y))$, where

$$p_{ab}(x, y) \equiv \frac{\partial S_{ab}}{\partial x}; \quad r_{ab}(x, y) \equiv -\frac{\partial S_{ab}}{\partial y}. \quad (2.1.22)$$

Since $\psi_{ab}(x, y) = \psi_a(x)\psi_b^*(y)$, we may express Eq. 2.1.21 as This may also be expressed as

$$\psi_{ab}(x, y) = N_a N_b \sum_{k_a k_b} A_a(x) A_b(y) e^{iS_b(y) - iS_a(x) - i(\mu_b - \mu_a)\pi/2}. \quad (2.1.23)$$

Therefore the phase function $S_{ab}(x, y)$ is the difference $S_a(x) - S_b(y)$ and Eq. 2.1.22 becomes

$$p_{ab}(x, y) = p_a(x); \quad r_{ab}(x, y) = r_b(y). \quad (2.1.24)$$

Points on \mathcal{L}_{ab} can be described by coordinates $(x, p_a(x); y, r_b(y))$ and therefore \mathcal{L}_{ab} may be expressed as the Cartesian product $\mathcal{L}_a \times \mathcal{L}_{\bar{b}}$. In particular,

$$\mathcal{L}_{ab} = \pi_1^{-1}(\mathcal{L}_a) \cap \pi_2^{-1}(\mathcal{L}_{\bar{b}}), \quad \pi_1(\mathcal{L}_{ab}) = \mathcal{L}_a, \quad \pi_2(\mathcal{L}_{ab}) = \mathcal{L}_{\bar{b}}. \quad (2.1.25)$$

2.1.4 Momentum Maps and Densities

As discussed in Littlejohn [54] and Aquilanti *et al* [44, 1], the simultaneous eigenstate condition defining a state translates to a level set condition that defines the Lagrangian manifold that supports the semiclassical approximation for the state. For example, the Lagrangian manifold \mathcal{L}_a is the simultaneous level set for the classical observables A_i associated with \hat{A}_i at the quantized contour values $\mu_{a,i}$. As discussed in Sections A.2 and C.3, the classical observables A_i are the Weyl symbols of operators \hat{A}_i . The \mathcal{L}_a is described using the notation similar to the eigenstate notation introduced in Eq. 2.1.3,

$$\mathcal{L}_a = \begin{pmatrix} A_1 & \cdots & A_{n_1} \\ \mu_{a,1} & \cdots & \mu_{a,n_1} \end{pmatrix}, \quad (2.1.26)$$

where the top row is a list of classical observables and the bottom row is a list of contour values.

The set of classical observables defining a Lagrangian manifold can often be described as the components of a momentum map for some symplectic group action on phase space. All groups in this section are assumed to be connected, semisimple Lie groups to ensure the existence of Ad*-equivariant momentum maps, as discussed in Section B.2. Consider a

group G with a symplectic group action on a $2n$ -dimensional phase space Φ . Let $\mathbf{P} : \Phi \rightarrow \mathfrak{g}^*$ be an Ad^* -equivariant momentum map for the group action and let generalized momentum μ be a fixed point of \mathfrak{g}^* under the co-adjoint action. Following Section B.3, the level set $\mathbf{P}^{-1}(\mu)$ is then a co-isotropic manifold. The group orbits through points on the level set are isotropic manifolds completely contained in $\mathbf{P}^{-1}(\mu)$ and the level set is the union of these group orbits.

Let $\{\xi_i\}$ be a basis of the Lie algebra \mathfrak{g} and let P_i be the components of \mathbf{P} with respect to this basis. Let $X_i \equiv \omega^{-1}(dP_i)$ be the set of Hamiltonian vector fields for the momentum map components. As discussed in Section B.3, if the set of vectors X_i at a point $z \in \Phi$ has rank m then the group orbit through z has dimension m and the level set containing z has co-dimension m . If $\dim G = n$ (half the dimension of Φ) and if the set of vectors $\{X_i\}$ are full rank on the level set $\mathbf{P}^{-1}(\mu)$ then the level set and the group orbit through any point on $\mathbf{P}^{-1}(\mu)$ are n -dimensional and thus Lagrangian. We assume that all Lagrangian manifolds in this section are connected and therefore are covered by a single group orbit. Let $\{\lambda_i\}$ be the set of n one-forms on the Lagrangian manifold that are dual to $\{X_i\}$ on $\mathbf{P}^{-1}(\mu)$, $\lambda_i(X_j) = \delta_{ij}$. Let $\sigma \equiv \bigwedge \lambda_i$ on the Lagrangian manifold $\mathbf{P}^{-1}(\mu)$ be the form on \mathcal{L} as defined in Eq. C.2.2. This is locally the push-forward of the Haar measure on G . The isotropy subgroup $H_{\mathcal{L}} \subset G$ is defined as the elements of G that leave points on \mathcal{L} invariant under the symplectic action. The volume of \mathcal{L} with respect to σ is the volume of the group G with respect to the Haar measure divided by the cardinality of the isotropy subgroup $H_{\mathcal{L}}$, $V_{\mathcal{L}} = V_G / |H_{\mathcal{L}}|$. The normalization of the WKB wavefunction is then $N = 1/\sqrt{V_{\mathcal{L}}}$. Given an x -representation on Φ the density σ defines a set of density functions $\Omega_k(x)$ indexed by the branches of \mathcal{L} in the x -representation. As in Section C.2, the density functions are defined through $\sigma|_z = \Omega_k(x) dx_1 \wedge \cdots \wedge dx_n$, where z is the point on the k -th branch of \mathcal{L} over point x . As shown in Littlejohn [54] the density functions can be expressed using the determinant of an $n \times n$ matrix of Poisson brackets evaluated at z , $\Omega_k(x) = (\det \{x_i, P_j\})^{-1}$ in which case the amplitudes of the WKB wavefunction are expressed as $A_k(x) = \sqrt{\Omega_k(x)}$.

We now apply these general ideas to the states defined in Section 2.1.1 and the Lagrangian manifolds described in Section 2.1.3. We assume that each of the states can be described as simultaneous non-degenerate eigenstates of a set of observables and that the manifolds can be described as the level set of an Ad^* -equivariant momentum map. Note that all of the states and Lagrangian manifolds that occur in spin network applications may be described in such a way.

Let the a -manifold \mathcal{L}_a be the level set $\mathbf{A}^{-1}(\mu_a)$, where G_A is an n_1 -dimensional connected, semi-simple Lie group with Ad^* -equivariant momentum map $\mathbf{A} : \Phi_1 \rightarrow \mathfrak{g}_A^*$ and μ_a is a fixed point of \mathfrak{g}_A^* . Let $\{\xi_i^A\}$ ($i = 1, \dots, n_1$) be a basis of \mathfrak{g}_A . Let X_i^A be the Hamiltonian vector field for momentum map component A_i with respect to this basis. Let λ_i^A be the forms dual to X_i^A on \mathcal{L}_a and let σ_a be the volume form on \mathcal{L}_a , as described above.

Similarly let G_{β} , G_B , and G_M be n_1 -, n_2 -, and $(n_1 + n_2)$ -dimensional groups with momentum maps β , \mathbf{B} , and \mathbf{M} . Let μ_{β} , μ_b , and μ_M be fixed-point generalized momenta so the Lagrangian manifolds can be expressed as momentum map level sets, as listed in Table 2.2.

Lagrangian Manifold	Space	Group	Dimension	Momentum Map	Generalized Momentum
\mathcal{L}_a	Φ_1	G_A	n_1	\mathbf{A}	μ_a
\mathcal{L}_β	Φ_1	G_β	n_1	β	μ_β
\mathcal{L}_b	Φ_2	G_B	n_2	\mathbf{B}	μ_b
$\mathcal{L}_{\bar{b}}$	Φ_2^*	G_B	n_2	$-\mathbf{B}$	$-\mu_b$
\mathcal{L}_M	Φ_{12}	G_M	$n_1 + n_2$	\mathbf{M}	μ_M
\mathcal{L}_{ab}	Φ_{12}	$G_A \times G_B$	$n_1 + n_2$	$(\mathbf{A}, -\mathbf{B})$	$(\mu_a, -\mu_b)$

Table 2.2: Lagrangian manifolds in the remodeling geometry. These manifolds may be expressed as group orbits of a group or as level sets of a momentum map at a particular generalized momentum.

Let $\{\xi_i^\beta\}$, $\{\xi_I^B\}$, and $\{\xi_\alpha^M\}$ be bases of the Lie algebras, where lower case Latin indices run from 1 to n_1 , upper case Latin indices run from 1 to n_2 , and Greek indices run from 1 to $(n_1 + n_2)$. Let σ_β , σ_b , and σ_M be the volume forms on \mathcal{L}_β , \mathcal{L}_b , and \mathcal{L}_M with respect to these ordered choices of basis. The momentum map β is related to maps \mathbf{B} and \mathbf{M} as will be shown in Section 2.4.

The symplectic group action φ^B of G_B on Φ_2 induces a symplectic group action $\varphi^{\bar{B}}$ on the dual space Φ_2^* via conjugation with the dual map,

$$\varphi_g^{\bar{B}} \equiv G_2 \circ \varphi_g^B \circ G_2^{-1}, \quad \forall g \in G_B. \quad (2.1.27)$$

Let $X_I^{\bar{B}}$ be the infinitesimal generators of $\varphi^{\bar{B}}$ corresponding to the basis vectors ξ_I . Since $\omega_2 = -(G_2^{-1})^* \omega_2$, $X_I^{\bar{B}} = -G_{2*} X_I^B$. Therefore the momentum map $\bar{\mathbf{B}} : \Phi_2^* \rightarrow \mathfrak{g}_B^*$ is the negative of the pull-back of \mathbf{B} ,

$$\bar{\mathbf{B}} = -\mathbf{B} \circ G_2^{-1}. \quad (2.1.28)$$

Since G_2^{-1} is the identity map on the points of Φ_2^* , the momentum map $\bar{\mathbf{B}}$ acting on a point of Φ_2^* is the same as $-\mathbf{B}$ acting on the same point of Φ_2 . In a slight abuse of notation we will write $\bar{\mathbf{B}}$ as simply $-\mathbf{B}$. The Lagrangian manifold $\mathcal{L}_{\bar{b}}$ is therefore the level set

$$\mathcal{L}_{\bar{b}} = \left(\begin{array}{c} \bar{\mathbf{B}} \\ -\mu_b \end{array} \right) = \left(\begin{array}{c} -\mathbf{B} \\ -\mu_b \end{array} \right) = \left(\begin{array}{c} \mathbf{B} \\ \mu_b \end{array} \right), \quad (2.1.29)$$

where we use the notation introduced in Eq. 2.1.26 for a level set of momentum maps. The one-forms $\lambda_{\bar{b}}^I \in \Omega^1(\mathcal{L}_{\bar{b}})$ dual to $X_I^{\bar{b}}$ on $\mathcal{L}_{\bar{b}}$ are given by $\lambda_{\bar{b}}^I = -(G_2^{-1})^* \lambda_b^I$ and therefore the density on $\mathcal{L}_{\bar{b}}$ is

$$\sigma_{\bar{b}} = (-1)^{n_2} (G_2^{-1})^* \sigma_b \in \Omega^{n_2}(\mathcal{L}_{\bar{b}}). \quad (2.1.30)$$

Finally, group actions φ^A of G_A on Φ_1 and $\varphi^{\bar{B}}$ of G_B on Φ_2^* induce a $G_A \times G_B$ action φ^{AB} on the product space Φ_{12} ,

$$\varphi_{(g,h)}^{AB} : (z_1, z_2) \mapsto (\varphi_g^A z_1, \varphi_h^{\bar{B}} z_2), \quad \forall g \in G_A, h \in G_B. \quad (2.1.31)$$

The Lie algebra of $G_A \times G_B$ is the direct sum of Lie algebras $\mathfrak{g}_A \oplus \mathfrak{g}_B$ and the dual Lie algebra is the direct sum $\mathfrak{g}_A^* \oplus \mathfrak{g}_B^*$. The momentum map $\mathbf{P}_{AB} : \Phi_{12} \rightarrow \mathfrak{g}_a^* \oplus \mathfrak{g}_b^*$ for this action is given by

$$\mathbf{P}_{AB} : (z_1, z_2) \mapsto (\mathbf{A}(z_1), \bar{\mathbf{B}}(z_2)), \quad (2.1.32)$$

which we write as just $\mathbf{P}_{AB} = (\mathbf{A}, -\mathbf{B})$, as in Table 2.2. The product Lagrangian manifold $\mathcal{L}_{ab} = \mathcal{L}_a \times \mathcal{L}_{\bar{b}}$ is the level set $\mathbf{P}_{AB}^{-1}(\mu_{ab})$, where $\mu_{ab} = (\mu_a, -\mu_b)$. Interpreting \mathbf{A} and \mathbf{B} as functions on Φ_{12} defined via the pullbacks by π_1 and $G_2^{-1} \circ \pi_2$, respectively, \mathcal{L}_{ab} is thus the simultaneous level set of \mathbf{A} at μ_a and \mathbf{B} at μ_b . We also express this as

$$\mathcal{L}_{ab} = \begin{pmatrix} \mathbf{P}_{AB} \\ \mu_{ab} \end{pmatrix} = \begin{pmatrix} \mathbf{A} & -\mathbf{B} \\ \mu_a & -\mu_b \end{pmatrix} = \begin{pmatrix} \mathbf{A} & \mathbf{B} \\ \mu_a & \mu_b \end{pmatrix}, \quad (2.1.33)$$

where the top row is a list of momentum maps or classical observables and the bottom row is the corresponding generalized momenta or contour values.

Let $\{\xi_\alpha^{AB}\}$ be a basis of $\mathfrak{g}_a \oplus \mathfrak{g}_b$, with $\xi_\alpha^{AB} = \xi_i^A$ for $\alpha = i \leq n_1$ and $\xi_\alpha^{AB} = \xi_I^B$ for $\alpha = n_1 + I$. The $(n_1 + n_2)$ components of the momentum map \mathbf{P}_{AB} are then the n_1 components of \mathbf{A} and the n_2 components of \mathbf{B} . With this basis, the volume form on \mathcal{L}_{ab} is given by

$$\sigma_{ab} = (\pi_1^* \sigma_a) \wedge (\pi_2^* \sigma_{\bar{b}}) \in \Omega^{(n_1+n_2)}(\mathcal{L}_{ab}). \quad (2.1.34)$$

2.1.5 Semiclassical Inner Product Models

The target space inner product model Eq. 2.1.6 and the product space inner product model 2.1.7 of matrix element 2.1.1 are evaluated semiclassically in the target phase space and product phase space, respectively. Both are expressed as integrals of the WKB wavefunctions defined in Section 2.1.3.

The target space model is expressed as

$$\langle a | \beta \rangle = N_a N_b \sum_{k_a, k_\beta} \int dx A_a(x) A_\beta(x) e^{iS_b(x) - iS_a(x) - i(\mu_b - \mu_a)\pi/2}, \quad (2.1.35)$$

where the sum is taken over the branches of $\psi_a(x)$ and $\psi_\beta(x)$ and branch indices on the amplitudes and phase functions have been suppressed. Each of the points in the intersection $I^{(1)} \equiv \mathcal{L}_a \cap \mathcal{L}_\beta$ corresponds to a stationary phase point of one of the integrals in Eq. 2.1.35, where the conjugate momentum coordinates p of the intersection determine the branch indices k_a and k_β [44]. We first consider the case when the stationary phase set $I^{(1)}$ is composed of a discrete set of points. Applying Eq. (3) of Aquilanti *et al* [44] to the target space model yields

$$\langle a | \beta \rangle = \frac{(2\pi i)^{n_1/2}}{\sqrt{V_a V_\beta}} \sum_k |\Omega^{(1)}(z_{1,k})|^{1/2} e^{i\varphi_k^1}, \quad (2.1.36)$$

where k indexes points $z_{1,k} \in I^{(1)}$, $\Omega^{(1)}(z_{1,k})$ is the ‘‘amplitude determinant’’ $(\det \{A_i, \beta_j\})^{-1}$ evaluated at $z_{1,k}$ and φ_k^1 is the phase. Let $z_{1,k}$ be on the k_a -th branch of \mathcal{L}_a and the k_β -th

branch of \mathcal{L}_β over representation point x_k . Then the phase is

$$\varphi_k^1 = S_{\beta, k_\beta}(x_k) - S_{a, k_a}(x_k) - (\mu_{b, k_\beta} - \mu_{a, k_a}) \frac{\pi}{2} + \sigma_{z_{1,k}}(\beta, a) \frac{\pi}{4}, \quad (2.1.37)$$

where μ_{b, k_β} and μ_{a, k_a} are Maslov indices and $\sigma_{z_{1,k}}(\beta, a)$ is the signature index as described in Sections C.1 and C.5.

The states in the inner product models will frequently feature common symmetry groups which manifest as higher-dimensional intersections of the two Lagrangian manifolds that support the WKB wavefunctions of the states. The intersections are interpreted as a set of disconnected group orbits of the common symmetry group. Let $G_{H,1}$ be the common symmetry group between the a - and β -manifolds in the target space model with group orbits of dimension s_1 . The common symmetry group may be made explicit by choosing a basis of the Lie algebras for \mathfrak{g}_A and \mathfrak{g}_β such that the first s_1 components of the momentum maps \mathbf{A} and β are identical [1]. The stationary phase approximation of Eq. 2.1.6 becomes

$$\frac{(2\pi i)^{(n_1 - s_1)/2}}{\sqrt{V_a V_\beta}} \sum_k V_{H_1, k} \left| \tilde{\Omega}^{(1)}(z_{1,k}) \right|^{1/2} e^{i\varphi_k^1}, \quad (2.1.38)$$

where k indexes group orbits of $G_{H,1} \in I^{(1)}$, $z_{1,k}$ is a point in the group orbit, $V_{H_1, k}$ is the volume of the group orbit with respect to the Haar measure on $G_{H,1}$. The phase is the same as in Eq. 2.1.37 but $\tilde{\Omega}^{(1)}(z_{1,k})$ is a ‘‘reduced’’ amplitude determinant involving an $(n_1 - s_1) \times (n_1 - s_1)$ -matrix of Poisson brackets of the last $(n_1 - s_1)$ components of \mathbf{A} and β (the components that are not common to both momentum maps).

Define $I^{(12)} \equiv \mathcal{L}_{ab} \cap \mathcal{L}_M$. The stationary phase evaluation of the product space model yields

$$\text{tr}(|a\rangle\langle b|)^\dagger \hat{M} = \frac{(2\pi i)^{(n_1 + n_2)/2}}{\sqrt{V_{ab} V_M}} \sum_k \left| \Omega^{(12)}(z_k) \right|^{1/2} e^{i\varphi_k^{12}}, \quad (2.1.39)$$

where k indexes points $z_k \in I^{(12)}$, $\Omega^{(12)}(z_k) = (\det \{\mathbf{P}_{AB, \alpha}, M_{\alpha'}\})^{-1}$ is the amplitude determinant evaluated at z_k , and φ_k^{12} is a phase. Let z_k be on the k_{ab} -th branch of \mathcal{L}_{ab} and the k_M -th branch of \mathcal{L}_M over representation point (x_k, y_k) . Then the phase φ_k^{12} is

$$S_{ab, k_{ab}}(x_k, y_k) - S_{M, k_M}(x_k, y_k) - (\mu_{ab, k_{ab}} - \mu_{M, k_M}) \frac{\pi}{2} + \sigma_{z_k}(M, ab) \frac{\pi}{4}. \quad (2.1.40)$$

If there is a common symmetry group $G_{H,12}$ with s_{12} -dimensional group orbits between \mathcal{L}_{ab} and \mathcal{L}_M then Eq. 2.1.39 becomes

$$\frac{(2\pi i)^{(n_1 + n_2 - s_{12})/2}}{\sqrt{V_{ab} V_M}} \sum_k V_{H_{12}, k} \left| \tilde{\Omega}^{(12)}(z_k) \right|^{1/2} e^{i\varphi_k^{12}}, \quad (2.1.41)$$

The rest of this chapter is devoted to exploring the remodeling algebra and geometry. We ultimately show that the pieces of the stationary phase results in Eqs. 2.1.38 and 2.1.41 agree. In particular the phases and amplitude determinants of the target space model are identical to the phase and amplitude determinant of the product space model. Thus we may carry out different pieces of the semi-classical evaluation of a matrix element in different models.

2.2 The Transport of a Manifold

The semiclassical evaluation of an inner product $\langle A|B\rangle$ as performed in Littlejohn [54] and Aquilanti *et al* [44, 1] involves expressing the inner product as an integral of WKB wavefunctions. The integral is then approximated using the stationary phase approximation. The stationary phase set is interpreted as the set of phase space points in the intersection of the Lagrangian manifolds associated with $|A\rangle$ and $|B\rangle$. Similarly, since $|\beta\rangle$ is defined to be $\hat{M}|b\rangle$, the WKB wavefunction for $\psi_\beta(x)$ in Eq. 2.1.13 can be approximated using a stationary phase approximation on the integral in Eq. 2.2.1, below. The stationary phase set is the set of product phase space points in the intersection of a Lagrangian manifold and a co-isotropic manifold. This is a generalization of the inner product procedure to acting a map on a vector. In this generalization the inner product is interpreted in a remodeling picture where the target Hilbert space is just \mathbf{C} and the target phase space is zero-dimensional.

In Section 2.2.1, we evaluate the wavefunction ψ_β using the stationary phase approximation and the WKB forms of ψ_M and ψ_b . The geometry of the stationary phase set inspires a geometric construction of a target space manifold $\mathcal{T}_M(\mathcal{L}_b) \subset \Phi_1$ from \mathcal{L}_M and \mathcal{L}_b . We call $\mathcal{T}_M(\mathcal{L}_b)$ the “transport” of \mathcal{L}_b through \mathcal{L}_M . We describe the geometric construction of the transported manifold and then show that $\mathcal{T}_M(\mathcal{L}_b)$ and \mathcal{L}_β are identical as manifolds in Section 2.2.2. In Section 2.2.3 we start to investigate the symplectic structure of the transported manifold in cases where \mathcal{L}_M and \mathcal{L}_b do not share a non-trivial common symmetry group and prove that the transport procedure generically results in a Lagrangian manifold. Finally we consider the transport of a manifold in the presence of a non-trivial common symmetry group in Section 2.2.4.

2.2.1 The Stationary Phase Approximation for $\psi_\beta(x)$.

Using Eq. 2.1.5, the wavefunction of $|\beta\rangle$ can be expressed as

$$\psi_\beta(x) = \langle x|\beta\rangle = \langle x|M|b\rangle = \int dy \langle x|M|y\rangle \langle y|b\rangle = \int dy \psi_M(x, y) \psi_b(y). \quad (2.2.1)$$

Plugging in the WKB forms Eq. 2.1.19 and 2.1.15 gives

$$\psi_\beta(x) = \sum_{\text{branches}} \int dy A_M(x, y) A_b(y) e^{iS_M(x, y) - i\mu_M \pi/2} e^{iS_b(y) - i\mu_b \pi/2}, \quad (2.2.2)$$

where the sum is taken over both the branches of $\psi_M(x, y)$ and the branches of $\psi_b(y)$. The stationary phase condition is

$$\frac{\partial S_M}{\partial y} + \frac{\partial S_b}{\partial y} = 0. \quad (2.2.3)$$

In terms of the momentum functions defined in Eq. 2.1.20 and 2.1.16, this implicitly defines the function $y_\beta(x)$,

$$-r_M(x, y_\beta(x)) + r_b(y_\beta(x)) = 0. \quad (2.2.4)$$

For a fixed x Eq. 2.2.4 is a set of n_2 equations for the n_2 unknowns y_β . This generically yields a discrete set of solutions which are labeled by a branch index for $y_\beta(x)$. In situations with symmetry such as those that occur in spin networks there will be a continuum of solutions. We will explore how to handle these situations in greater detail in Section 2.2.4. Therefore the phase in Eq. 2.1.13 can be expressed as

$$S_\beta(x) = S_M(x, y_\beta(x)) + S_b(y_\beta(x)). \quad (2.2.5)$$

The function $p_\beta(x)$ defined in Eq. 2.1.14 is therefore

$$p_\beta(x) = \frac{\partial S_M(x, y_\beta(x))}{\partial x} + \frac{\partial S_b(y_\beta(x))}{\partial x} = \frac{\partial S_M}{\partial x} + \left(\frac{\partial S_M}{\partial y} + \frac{\partial S_b}{\partial y} \right) \frac{\partial y_\beta}{\partial x}. \quad (2.2.6)$$

Replacing the derivatives with the momentum functions gives

$$p_M(x, y_\beta(x)) + (r_b(y_\beta(x)) - r_M(x, y_\beta(x))) \frac{\partial y_\beta}{\partial x}. \quad (2.2.7)$$

The last term vanishes by Eq. 2.2.4 and therefore the momentum function $p_\beta(x)$ for \mathcal{L}_β is

$$p_\beta(x) = p_M(x, y_\beta(x)). \quad (2.2.8)$$

Note that the branches of $p_\beta(x)$ that occur in Eq. 2.1.13 are indexed by the triplet of branches of $p_M(x, y)$, $r_b(y)$, and $y_\beta(x)$.

2.2.2 Geometric Construction of $\mathcal{T}_M(\mathcal{L}_b)$

We assume in this section that \mathcal{L}_b and \mathcal{L}_M do not share a non-trivial common symmetry group. Even though most of the spin-network examples will exhibit symmetry, it is worthwhile to study the generic case to illustrate the main features of the transport procedure.

We start with $\mathcal{L}_b \subset \Phi_2$ which is described locally by $(y, r_b(y)) \in \Phi_2$. The first stage in the transport is to push-forward \mathcal{L}_b into Φ_2^* using the dual map. As discussed in the previous section, this yields the dual- b -manifold $\mathcal{L}_{\bar{b}} = G_2(\mathcal{L}_b)$, described locally by coordinates $(y, r_b(y)) \in \Phi_2^*$. Since both \mathcal{L}_b and $\mathcal{L}_{\bar{b}}$ are Lagrangian submanifolds, they are both n_2 -dimensional.

The next stage in the transport is to form a manifold in the product phase space $\Phi_1 \times \Phi_2^*$ by taking the inverse image of $\mathcal{L}_{\bar{b}}$ under the projection map π_2 ,

$$\pi_2^{-1}\mathcal{L}_{\bar{b}} = \{(z_1, z_2) \in \Phi_{12} \mid z_2 \in \mathcal{L}_{\bar{b}}\}. \quad (2.2.9)$$

This is a $(2n_1 + n_2)$ co-isotropic submanifold of Φ_{12} . The inverse image is equal to the Cartesian product $\Phi_1 \times \mathcal{L}_{\bar{b}}$ and is described locally by coordinates $(x, p; y, r_b(y))$. Let \mathcal{L}_b be the fixed-point level set of momentum map \mathbf{B} as in Section 2.1.4. The inverse-image in Eq. 2.2.9 can then be described as the level set $\mathbf{B}^{-1}(\mu_b) \subset \Phi_{12}$ where, in an abuse of notation, $\mathbf{B} : \Phi_{12} \rightarrow \mathfrak{g}_B$ is interpreted as the pull-back of $\mathbf{B} : \Phi_2 \rightarrow \mathfrak{g}_B$ by $G_2^{-1} \circ \pi_2$. As discussed in

Section 2.1.4, the momentum map for the symplectic G_B action on Φ_{12} is $-\mathbf{B}$. The level set $\mathbf{B}^{-1}(\mu_b)$ can be described as the level set of the momentum map $-\mathbf{B}$ at fixed point $-\mu_b \in \mathfrak{g}_B^2$ and is therefore co-isotropic.

The third stage in the transport is to form the intersection manifold \mathcal{I} of the inverse image with the map manifold \mathcal{L}_M ,

$$\mathcal{I} \equiv \mathcal{L}_M \cap \pi_2^{-1}\mathcal{L}_{\bar{b}}. \quad (2.2.10)$$

As discussed in Sec. 2.1.3, points on the map manifold \mathcal{L}_M are locally described by coordinates $(x, p_M(x, y); y, r_M(x, y))$. The intersection occurs over points (x, y) satisfying $r_M(x, y) = r_b(y)$. This implicitly defines the function $y_I(x)$,

$$r_b(y_I(x)) = r_M(x, y_I(x)). \quad (2.2.11)$$

Points on \mathcal{I} are thus locally described by coordinates $(x, p_M(x, y_I(x)); y_I(x), r_b(y_I(x)))$. Comparing Eq. 2.2.11 with Eq. 2.2.4 shows that the set of stationary phase points of the integral in Eq. 2.2.1 is precisely the intersection manifold \mathcal{I} . The map manifold \mathcal{L}_M has co-dimension $(n_1 + n_2)$ and the inverse image has co-dimension n_1 , so the intersection manifold generically has co-dimension $(2n_1 + n_2)$, meaning that $\dim \mathcal{I}$ is generically n_1 . In cases of symmetry the intersection manifold \mathcal{I} may have a greater dimension, as will be discussed in Section 2.2.4. If \mathcal{L}_b and \mathcal{L}_M are both fixed-point level sets of momentum maps as in Section 2.1.4, the intersection manifold may be described as the simultaneous level set

$$\mathcal{I} = \left(\begin{array}{cc} \mathbf{B} & \mathbf{M} \\ \mu_b & \mu_m \end{array} \right). \quad (2.2.12)$$

The transport is concluded by projecting \mathcal{I} onto the target phase space Φ_1 using the projection map π_1 ,

$$\mathcal{T}_M(\mathcal{L}_b) \equiv \pi_1(\mathcal{L}_M \cap \pi_2^{-1}\mathcal{L}_{\bar{b}}). \quad (2.2.13)$$

Manifold $\mathcal{T}_M(\mathcal{L}_b)$ is therefore locally described by $(x, p_{\mathcal{T}}(x))$, where

$$p_{\mathcal{T}}(x) \equiv p_M(x, y_I(x)). \quad (2.2.14)$$

The branches of $p_{\mathcal{T}}$ are labeled by the three branch indices of r_b , p_M , and y_I . Generically this projection is full rank and yields an n_1 -dimensional submanifold of Φ_1 . In cases of symmetry the projection will not be full rank and there will be “vertical” directions of \mathcal{I} over Φ_1 , in which case the intersection manifold has a larger dimension than the transported manifold, $\dim \mathcal{I} > n_1$.

The definition of the transported momenta $p_{\mathcal{T}}(x)$ in Eq. 2.2.14 is the same as the stationary phase result for $p_{\beta}(x)$ in Eq. 2.2.8 since $y_I(x) = y_{\beta}(x)$. Therefore \mathcal{L}_{β} and $\mathcal{T}_M(\mathcal{L}_b)$ are described by the same set of points and we can conclude that the β -manifold and the transported manifold are identical submanifolds of the target phase space.

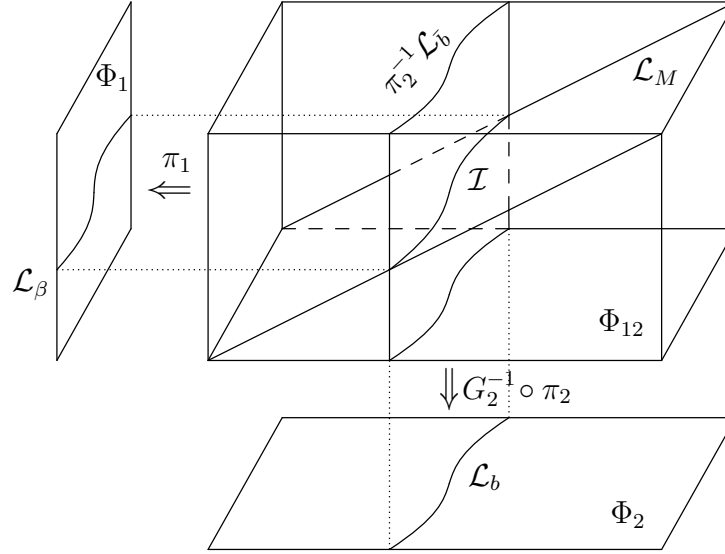


Figure 2.2.1: The geometric construction of the transport of the manifold \mathcal{L}_b through \mathcal{L}_M . The manifold \mathcal{I} is the intersection of the inverse image $\pi_2^{-1}\mathcal{L}_{\bar{b}}$ with \mathcal{L}_M . The transported manifold \mathcal{L}_β is the projection of \mathcal{I} onto the target phase space.

Manifold	Space	Dimension	Co-Dimension
\mathcal{L}_b	Φ_2	n_2	n_2
$\mathcal{L}_{\bar{b}}$	Φ_2^*	n_2	n_2
$\pi_2^{-1}\mathcal{L}_{\bar{b}}$	Φ_{12}	$2n_1 + n_2$	n_2
\mathcal{L}_M	Φ_{12}	$n_1 + n_2$	$n_1 + n_2$
\mathcal{I}	Φ_{12}	n_1	$n_1 + 2n_2$
$\mathcal{T}_M(\mathcal{L}_b)$	Φ_1	n_1	n_1

Table 2.3: Manifolds and spaces involved in forming the transport $\mathcal{T}_M(\mathcal{L}_b)$. The dimensions in the first four rows are exact while the dimensions for the last two rows are generic.

Figure 2.2.1 shows the transport of \mathcal{L}_b through \mathcal{L}_M to form the manifold \mathcal{L}_β using the geometric construction just discussed. Table 2.3 lists the manifolds described in the procedure above along with the spaces they belong to and their dimension and co-dimension. The dimensions listed for the first four rows are exact while the dimensions for \mathcal{I} and $\mathcal{T}_M(\mathcal{L}_b)$ are merely the dimensions that occur in cases without symmetry.

Consider a point $z_1 \in \mathcal{L}_\beta$. The transport procedure described above ensures that there exists at least one point $z \in \mathcal{I}$ such that $\pi_1(z) = z_1$. However the point z is in general not unique, even in cases without symmetry. Let $\pi_{\mathcal{I}} : \mathcal{I} \rightarrow \mathcal{T}_M(\mathcal{L}_b)$ be the projection map π_1 whose domain is restricted to the intersection manifold and whose range is restricted to the transported manifold. The inverse image $\pi_{\mathcal{I}}^{-1}(z_1)$ is the set of intersection points projecting to the same point of the transported manifold. In cases without symmetry this set will be the discrete set of points $\{z_\rho\}$ indexed by ρ . The intersection manifold \mathcal{I} thus becomes the

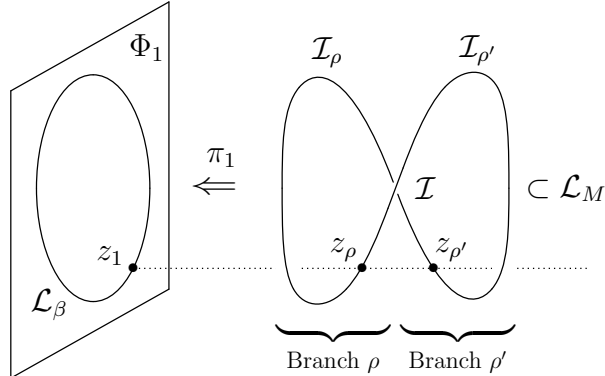


Figure 2.2.2: An example of the branches of the intersection manifold \mathcal{I} under the projection onto \mathcal{L}_β . The restriction of the projection map π_1 to the branch \mathcal{I}_ρ or $\mathcal{I}_{\rho'}$ of the intersection manifold is injective.

$$\begin{array}{ccc}
 T_{z_1} \Phi_1 & \xleftarrow{\pi_{1*}} & T_z \Phi_{12} \\
 & & \downarrow \pi_{2*} \\
 & & T_{z_2} \Phi_2^* \xrightarrow{G_2^{-1}} T_{z_2} \Phi_2
 \end{array}$$

Figure 2.2.3: Maps between tangent spaces in the remodeling geometry.

union of branches \mathcal{I}_ρ , as shown in Figure 2.2.2. The branches \mathcal{I}_ρ are connected submanifolds of \mathcal{I} such that the restricted projection map $\pi_1|_{\mathcal{I}_\rho}$ is injective.

The transport procedure as defined above results in a manifold that has all of the properties that are required to support the semi-classical approximation of a quantum state. For example, the transport of a Lagrangian manifold is itself a Lagrangian manifold, as proven in the next section. In addition we show explicitly in Section 2.5.6 that if \mathcal{L}_M and \mathcal{L}_b are a quantized manifolds, then so is the transported manifold.

2.2.3 The Transport of an Isotropic Manifold is Isotropic

Since the transport of \mathcal{L}_b is identical to the manifold \mathcal{L}_β it is a Lagrangian manifold. However we may show more generally that the transport procedure applied to an isotropic manifold always yields an isotropic manifold of the target phase space. Let $B \in \Phi_2$ be an isotropic submanifold of the source space and let $\mathcal{T}_M(B)$ be the transport of B under M , following the procedure of Section 2.2.2. Consider a point $z = (z_1, z_2) \in \mathcal{I}$ and the tangent spaces $T_z \Phi_{12}$, $T_{z_1} \Phi_1$, $T_{z_2} \Phi_2^*$, and $T_{z_2} \Phi_2$. These are all symplectic vector spaces since the phase spaces are symplectic manifolds. Also note that $T_z \Phi_{12} = T_{z_1} \Phi_1 \times T_{z_2} \Phi_2^*$. The maps in Fig. 2.1.2 are pushed-forward to become maps π_{1*} , π_{2*} , and G_2^{-1} between tangent spaces, as shown in Fig. 2.2.3.

Define \bar{B} to be the image of B under the dual map, $\bar{B} = G_2(B)$. Since B is an isotropic

manifold of Φ_2 , \bar{B} is an isotropic submanifold of Φ_2^* and the tangent space $T_{z_2}\bar{B}$ is an isotropic plane in $T_{z_2}\Phi_2^*$. Similarly, $T_z\mathcal{L}_M$ is a Lagrangian plane in $T_z\Phi_{12}$. The tangent space to the inverse image at z is given by $T_{z_1}\Phi_1 \times T_{z_2}\bar{B}$ and is a co-isotropic plane in $T_z\Phi_{12}$. The tangent space at z of the intersection manifold is given by $T_z\mathcal{I} = T_z(\pi_2^{-1}\bar{B}) \cap T_z\mathcal{L}_M$. Since this is a subspace of the Lagrangian plane $T_z\mathcal{L}_M$, $T_z\mathcal{I}$ will always be an isotropic plane in $T_z\Phi_{12}$. The dimension of $T_z\mathcal{I}$ is generically $(n_1 - n_2 + \dim B)$ but may be larger in cases of symmetry. Note that if B is Lagrangian then the dimension of $T_z\mathcal{I}$ is generically n_1 . Finally, the tangent space at z_1 of the transported manifold is $T_{z_1}(\mathcal{T}_M(B)) = \pi_{1*}(T_z\mathcal{I})$.

Consider an arbitrary point $z_1 \in \mathcal{T}_M(B)$ and let $z \in \pi_{\mathcal{I}}^{-1}(z_1)$ be some point in \mathcal{I} that projects onto z_1 . Let $X_\beta \in T_{z_1}(\mathcal{T}_M(B))$ be an arbitrary tangent vector to the transported manifold at z_1 . Since $T_{z_1}(\mathcal{T}_M(B)) = \pi_{1*}(T_z\mathcal{I})$, there must exist a vector $X_M \in T_z\mathcal{I}$ such that $\pi_{1*}X_M = X_\beta$. Note that since \mathcal{I} is a subspace of the tangent space to the inverse image of \bar{B} , the push-forward of any vector in $T_z\mathcal{I}$ by π_2 will be tangent to \bar{B} . Therefore $\pi_{2*}X_M \in T_{z_2}\bar{B}$.

Acting the symplectic form ω_1 on any pair of vectors in the tangent space $T_{z_1}(\mathcal{T}_M(B))$ therefore gives

$$\omega_1(X_{\beta_1}, X_{\beta_2}) = \omega_1(\pi_{1*}X_{M1}, \pi_{1*}X_{M2}) = \pi_{1*}\omega_1(X_{M1}, X_{M2}). \quad (2.2.15)$$

Since $\omega_{12} \equiv \pi_{1*}\omega_1 + \pi_{2*}\omega_2$, the last expression in Eq. 2.2.15 can be rewritten

$$\omega_{12}(X_{M1}, X_{M2}) - \pi_{2*}\omega_2(X_{M1}, X_{M2}). \quad (2.2.16)$$

The tangent space to \mathcal{I} is a subspace of the Lagrangian plane $T_z\mathcal{L}_M$, so the first term in Eq. 2.2.16 is zero. The second term is $-\omega_2(\pi_{2*}X_{M1}, \pi_{2*}X_{M2})$. The pushed-forward vectors are both elements of $T_{z_2}\bar{B}$ so this term also evaluates to zero since \bar{B} is isotropic. Thus, for any two vectors $X_{\beta_1}, X_{\beta_2} \in T_{z_1}(\mathcal{T}_M(B))$ in the tangent space for any point $z_1 \in \mathcal{T}_M(B)$,

$$\omega_1(X_{\beta_1}, X_{\beta_2}) = 0. \quad (2.2.17)$$

The transport of an isotropic manifold is therefore always an isotropic submanifold of Φ_1 . The transport of a Lagrangian manifold generically has dimension n_1 and will be generically Lagrangian. Even in non-generic cases the transport of a Lagrangian manifold will be isotropic and thus $\dim \mathcal{T}_M(\mathcal{L}_b) \leq n_1$, even when symmetries result in an intersection manifold that has a non-generic dimension greater than n_1 .

2.2.4 The Transport of a Manifold in Cases of Symmetry

When the M - and b -states share a non-trivial common symmetry group the intersection manifold \mathcal{I} in Eq. 2.2.10 will have a dimension greater than the generic dimension n_1 . Such symmetry groups occur often in spin networks. The symmetry group shared by a Lagrangian and co-isotropic manifold is determined in a manner similar to the determination of the symmetry group shared by a pair of Lagrangian manifolds described in Aquilanti *et al* [1].

Consider \mathcal{L}_M and $\pi_2^{-1}\mathcal{L}_b$, both co-isotropic submanifolds of Φ_{12} . Assume that \mathcal{L}_b and \mathcal{L}_M are fixed-point level sets of momentum maps as described in Section 2.1.4. As discussed in

Section 2.2.2, the inverse image $\pi_2^{-1}\mathcal{L}_b$ is the level set $\mathbf{B}^{-1}(\mu_b) \subset \Phi_{12}$ and is co-isotropic. As in Eq. 2.2.12, the intersection manifold \mathcal{I} is described as the simultaneous level set of \mathbf{M} and \mathbf{B} . Consider a point in the intersection $z \in \mathcal{I}$. As in Section B.3, let L be the level set $\mathbf{B}^{-1}(\mu_b)$ containing z and let B be the group orbit through z for the action of G_B on Φ_{12} . As discussed in Section 2.2.3, the tangent space $T_z\mathcal{I}$ is the intersection $T_z\mathcal{L}_M \cap T_zL$ and is an isotropic plane of $T_z\Phi_{12}$. The set of $(n_1 + n_2)$ Hamiltonian vector fields $\{X_\alpha^M\}$ span the entire Lagrangian plane $T_z\mathcal{L}_M$. The co-isotropic manifold L is the union of isotropic group orbits and T_zB is an isotropic sub-plane of T_zL . Each group orbit in L is isomorphic to \mathcal{L}_b and therefore n_2 -dimensional. The set of n_2 Hamiltonian vector fields $\{X_I^B\}$ span T_zB .

Let T_zH be the intersection $T_z\mathcal{L}_M \cap T_zB$ and let $\dim T_zH = s$. Rewrite the bases of \mathfrak{g}_M and \mathfrak{g}_B such that the first s basis vectors generate identical Hamiltonian vector fields X_τ^H , where $\tau = 1, \dots, s$ and the set of s vectors $\{X_\tau^H\}$ span T_zH . Since the action of groups G_M and G_B provide a Lie algebra anti-homomorphism between \mathfrak{g}_M and \mathfrak{g}_B and the Lie algebra of Hamiltonian vector fields on Φ_{12} , the first s basis vectors of \mathfrak{g}_M can be identified with the first s basis vectors of \mathfrak{g}_B . Call these vectors $\{\xi_\tau\}$ and let the span of these vectors be \mathfrak{g}_H . The space \mathfrak{g}_H is interpreted as the intersection of Lie algebras \mathfrak{g}_M and \mathfrak{g}_B and is therefore itself a Lie algebra. The group H generated by \mathfrak{g}_H is thus the “common symmetry group” of \mathcal{L}_M and $\pi_2^{-1}\mathcal{L}_b$.

With this new choice of bases, the first s components of \mathbf{M} are identical to the first s components of \mathbf{B} . These components form the s components for the momentum map $\mathbf{H} : \Phi_{12} \rightarrow \mathfrak{g}_H$. As in Eq. 2.2.12, \mathcal{I} can be expressed as the simultaneous level set of the $(n_1 + n_2)$ momentum map components M_α and the n_2 momentum map components B_I . The s components of \mathbf{H} each occur twice in this list of functions and \mathcal{I} is the simultaneous level set of $(n_1 + 2n_2 - s)$ “independent” functions. Therefore, in the case of an s -dimensional common symmetry group H , $\dim \mathcal{I} = (n_1 + s)$.

The Hamiltonian vector fields X_τ^H are all vertical over the target space and the H group action only affects the source space variables z_2 . Each of the s -dimensional group orbits of H is thus mapped to a single point in the target space Φ_1 under the projection π_1 . Therefore the projection of \mathcal{I} onto $\mathcal{T}_M(\mathcal{L}_b)$ has co-rank s and $\dim \mathcal{T}_M(\mathcal{L}_b) = \dim \mathcal{I} - s = n_1$. The extra dimensions of \mathcal{I} generated by the common symmetry group are eliminated under the projection.

The inverse image $\pi_1^{-1}(z_1)$ of a point $z_1 \in \mathcal{L}_b$ is the union of a set of H -group orbits, indexed by ρ . In cases without symmetry the group H is trivial and the inverse image is just a discrete set of points. As in Figure 2.2.2, the intersection manifold \mathcal{I} breaks up into the union of branches \mathcal{I}_ρ . The branches \mathcal{I}_ρ are connected submanifolds of \mathcal{I} such that the inverse image under the restricted projection map $\pi_1|_{\mathcal{I}_\rho}$ contains a single connected H -group orbit, as shown in Figure 2.2.4.

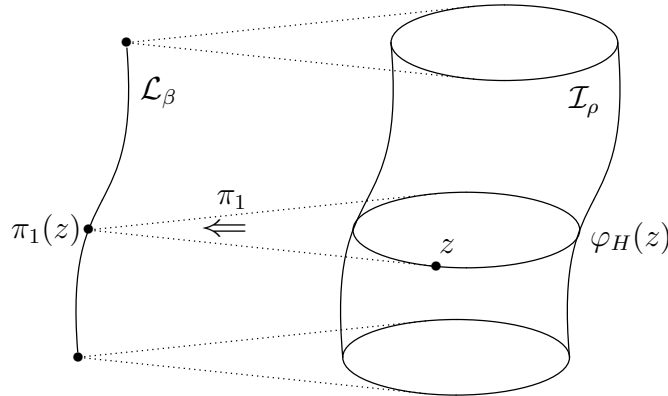


Figure 2.2.4: The projection of the ρ -th branch \mathcal{I}_ρ of the intersection manifold $\mathcal{I} = \mathcal{L}_M \cap \pi_2^{-1}(\mathcal{L}_b)$ to the source phase space when \mathcal{L}_M and \mathcal{L}_b share a non-trivial common symmetry group H . Each H -group orbit $\varphi_H(z)$ in \mathcal{I} is vertical over the source space and projects onto a single point of \mathcal{L}_β .

2.3 The Transport of the Density

As discussed in Sections C.1 and C.2, the WKB wavefunction of a state specifies a Lagrangian manifold and a density or volume form on that manifold. The definition of the β -state in Eq. 2.1.5 allows the density form on \mathcal{L}_β to be constructed from the WKB forms of ψ_M and ψ_b . The transport procedure outlined in Section 2.2.2 provides a second construction of a density form on \mathcal{L}_β , which is inherited from the structures associated with \mathcal{L}_M and \mathcal{L}_b . Finally, the description of \mathcal{L}_β as the level set of a momentum map as shown in Table 2.2 provides a third way of defining a density on \mathcal{L}_β . These three densities are the same. Analysis of the momentum map β describing \mathcal{L}_β and the associated density is discussed in greater detail in Section 2.4.

In Sections 2.3.1 and 2.3.2 we find the density form σ_β on \mathcal{L}_β that arises from the product space stationary phase evaluation of $|x\rangle\langle\beta| = \langle x|\hat{M}|b\rangle$, first in cases without symmetry and then in cases with a non-trivial common symmetry group. Then in Sections 2.3.3 and 2.3.4 we present a geometric construction of a density form $\sigma_\mathcal{T}$ on the transport of a Lagrangian manifold, first in cases without symmetry and then in cases with a non-trivial common symmetry group. Finally in Section 2.3.5 we show that the transported density is identical to the WKB density σ_β .

2.3.1 The WKB Amplitude of ψ_β

Consider the x -representation wavefunction $\psi_\beta(x)$ for the β -state, Eq. 2.1.13 and the Lagrangian manifold $\mathcal{L}_\beta \subset \Phi_1$ generated by the phase function. The wavefunction $\langle x|\beta\rangle$ can be interpreted as a target space inner product model for the matrix element $\langle x|\hat{M}|b\rangle$, just as Eq. 2.1.6 is a formulation of the matrix element 2.1.1. Here, the x -representation basis

states $|x\rangle \in \mathcal{H}_1$ serve as the a -states in Section 2.1.1. The product space model for the wavefunction is

$$\psi_\beta(x) = \langle x|\hat{M}|b\rangle = \text{tr} \left((|x\rangle\langle b|)^\dagger \hat{M} \right). \quad (2.3.1)$$

The semiclassical evaluation of this inner product involves Lagrangian manifolds \mathcal{L}_M and \mathcal{L}_{xb} in Φ_{12} . As in Section 2.1.4, \mathcal{L}_M is the level set of the $(n_1 + n_2)$ components M_α of momentum map \mathbf{M} . The product manifold \mathcal{L}_{xb} is the Cartesian product of the constant- x manifold $\mathcal{L}_x \subset \Phi_1$ and the \bar{b} -manifold $\mathcal{L}_{\bar{b}} \subset \Phi_2^*$. Interpret $x_i : \Phi_{12} \rightarrow \mathbb{R}$ as the pull-back of the n_1 functions $x_i : \Phi_1 \rightarrow \mathbb{R}$ by π_1 . Similarly, interpret $\mathbf{B} : \Phi_{12} \rightarrow \mathfrak{g}_B$ as the pull-back of the momentum map on Φ_2 by $\pi_2 \circ G_2^{-1}$. The momentum map for the symplectic action of G_B on Φ_{12} is $-\mathbf{B}$. Thus \mathcal{L}_{xb} is the simultaneous level set of the n_1 functions x_i and the n_2 components of momentum map $-\mathbf{B}$.

First consider the semiclassical evaluation of the inner product $\text{tr} \left((|x\rangle\langle b|)^\dagger \hat{M} \right)$ when the Lagrangian manifolds \mathcal{L}_{xb} and \mathcal{L}_M do not share a non-trivial common symmetry group. In particular, let $\{z_{\tilde{k}}\} \in \Phi_{12}$ be the discrete set of intersection points $\mathcal{L}_M \cap \mathcal{L}_{xb}$, which is semiclassically the stationary phase set for the WKB approximation in Eq. 2.3.1. The analysis in the presence of common symmetry groups is discussed in Section 2.3.2. The geometry of the transport discussed in Section 2.2.2 provides a map between $\mathcal{L}_M \cap \mathcal{L}_{xb}$ and points on \mathcal{L}_β over x -representation configuration point x . The projection $\pi_1(\mathcal{L}_M \cap \mathcal{L}_{xb})$ is a set of points $z_{1,k} \in \mathcal{L}_\beta$, where k indexes the x -representation branches of \mathcal{L}_β . This is the same branch index that appears in the WKB form for $\psi_\beta(x)$ in Eq. 2.1.13. As discussed in Section 2.2.2, there may be more than one point in $\mathcal{L}_M \cap \mathcal{L}_{xb}$ that projects onto a given point $z_{1,k}$. As in Figure 2.2.2, let ρ index these points. Thus the index \tilde{k} will be treated as a combined index for the pair of indices (k, ρ) . Note that $\mathcal{L}_M \cap \mathcal{L}_{xb}$ can be expressed as $\mathcal{I} \cap \mathbf{X}^{-1}(x) = \bigcup_\rho \mathcal{I}_\rho \cap \mathbf{X}^{-1}(x)$. A point $z_{\tilde{k}}$ can therefore be described as the unique point on the ρ -th branch of \mathcal{I} that projects onto the k -th x -representation branch of \mathcal{L}_β over configuration x , as shown in Figure 2.3.1.

The wavefunction at x is, to within an overall phase, the sum

$$\psi_\beta(x) = \sum_{\tilde{k}} A_{\beta, \tilde{k}}(x) e^{i\varphi_{\tilde{k}}(x)}, \quad (2.3.2)$$

where $\varphi_{\tilde{k}}(x)$ encodes the relative phases between intersection point $z_{\tilde{k}}$ and a reference intersection point. Let $z_1 \in \mathcal{L}_\beta$ be on the k -th x -representation branch of \mathcal{L}_β and lie over configuration point x and let $z_{\tilde{k}} \in \mathcal{I}$ be the ρ -th point in $\mathcal{L}_M \cap \mathcal{L}_{xb}$ such that $\pi_1(z_{\tilde{k}})$ as shown in Figure 2.3.1.

As summarized in Section C.4, the amplitudes for the product space evaluation Eq. 2.3.1 can be expressed using the determinant of an $(n_1 + n_2) \times (n_1 + n_2)$ matrix of Poisson brackets evaluated at $z_{\tilde{k}}$ [54],

$$A_{\beta, \tilde{k}}(x) = \left| \det \left[\begin{array}{c} \{x_i, M_\alpha\} \\ \{-B_I, M_\alpha\} \end{array} \right]_{z_{\tilde{k}}} \right|^{-1/2}. \quad (2.3.3)$$

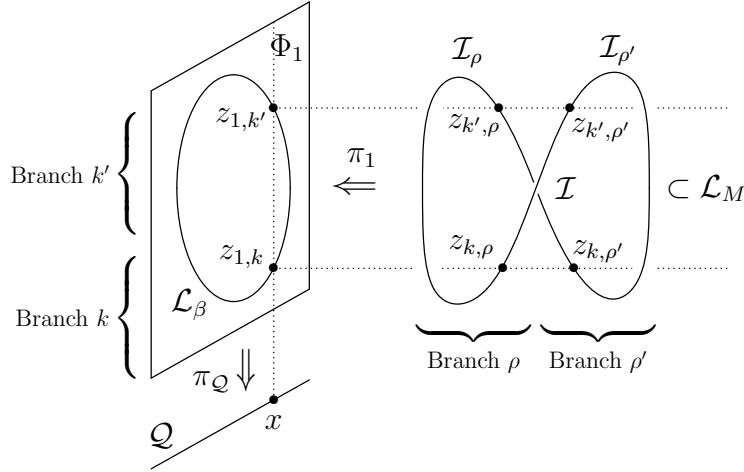


Figure 2.3.1: An example of the two types of branch indices that occur in constructing the x -representation wavefunction of a transported manifold. The branches of \mathcal{I} over the manifold \mathcal{L}_β are indexed by ρ as in Figure 2.2.2 and the branches of \mathcal{L}_β over configuration space \mathcal{Q} are indexed by k . The index \tilde{k} represents the pair of indices (k, ρ) .

We define a density $\sigma_{\beta,\rho}$ on \mathcal{L}_β for each ρ and for each \tilde{k} define a density function $\Omega_{\beta,\tilde{k}}$ so that $\sigma_\rho|_{z_1} = \Omega_{\beta,\tilde{k}}(x) dx_1 \wedge \cdots \wedge dx_{n_1}$. The density functions are related to the amplitude by $A_{\beta,\tilde{k}}(x) = |\Omega_{\beta,\tilde{k}}|^{1/2}$. Comparing the relationships between the amplitude, density function, and density with Eq. 2.3.3 yields

$$\Omega_{\beta,\tilde{k}}(x) = \left(\det \left[\begin{array}{c} \{x_i, M_\alpha\} \\ \{-B_I, M_\alpha\} \end{array} \right]_{z_{\tilde{k}}} \right)^{-1}, \quad (2.3.4)$$

$$\sigma_{\beta,\rho}|_{z_1} = (-1)^{n_2} \frac{dx_1 \wedge \cdots \wedge dx_{n_1}}{\det \left[\begin{array}{c} \{x_i, M_\alpha\} \\ \{B_I, M_\alpha\} \end{array} \right]_{z_{\tilde{k}}}}. \quad (2.3.5)$$

Note that since the sum in Eq. 2.3.2 is over both the x -representation branches of \mathcal{L}_β and the set of ρ -indexed points that project onto the same point in Φ_1 . Thus we get a set of amplitudes $A_{\beta,\tilde{k}}(x)$ and density functions $\Omega_{\beta,\tilde{k}}(x)$ indexed by $\tilde{k} = (k, \rho)$ which correspond to densities $\sigma_{\beta,\rho}$ indexed by ρ . The presence of the relative phases $\varphi_{\tilde{k}}$ in Eq. 2.3.2 prevents forming a single density on \mathcal{L}_β from the sum over ρ of the densities $\sigma_{\beta,\rho}$. However, if it is shown that in a specific application the relative phases between any two points $z_{\tilde{k}}$ over the same point z_1 are zero then we may make the simplification $A_{\beta,k}(x) = \sum_\rho A_{\beta,\tilde{k}}(x)$, in which case we may define $\Omega_{\beta,k}(x) = \sum_\rho \Omega_{\beta,\tilde{k}}(x)$ and $\sigma_\beta = \sum_\rho \sigma_{\beta,\rho}$.

2.3.2 The WKB Amplitude in Cases of Symmetry

Now consider the case when the M - and b -states share a non-trivial common symmetry group. Consider the bases of \mathfrak{g}_b and \mathfrak{g}_M constructed in Section 2.2.4. Recall that in this basis the first s basis vectors in both sets are identical and generate the Lie algebra \mathfrak{g}_H of the common symmetry Lie group H . The momentum maps \mathbf{B} and \mathbf{M} thus decompose into $(-\mathbf{H}, B_{\tilde{I}})$ ($\tilde{I} = s+1, \dots, n_2$) and $(\mathbf{H}, M_{\tilde{\alpha}})$, ($\tilde{\alpha} = s+1, \dots, n_1+n_2$), where \mathbf{H} is the momentum map for the subgroup G_H . Note that the momentum map for the action of G_H on Φ_2 is $-\mathbf{H}$ due to the fact that the construction of the basis relied on identical Hamiltonian flow vectors in $\Phi_1 \times \Phi_2^*$.

Evaluation of the WKB amplitude in the case of symmetry proceeds as in Section 2.3.1. However, naïve use of the momentum maps in the $(n_1 + n_2) \times (n_1 + n_2)$ -matrix of Poisson brackets of Eq. 2.3.3 yields

$$\left[\begin{array}{c} \{x_i, M_\alpha\} \\ \{-B_I, M_\alpha\} \end{array} \right]_{z_{\tilde{k}}} = \left[\begin{array}{c|c} \frac{\{x_i, H_\tau\}}{\{H_\tau, H_{\tau'}\}} & \frac{\{x_i, M_{\tilde{\alpha}}\}}{\{H_\tau, M_{\tilde{\alpha}}\}} \\ \hline \frac{\{-B_{\tilde{I}}, H_\tau\}}{\{-B_{\tilde{I}}, M_{\tilde{\alpha}}\}} & \frac{\{-B_{\tilde{I}}, M_{\tilde{\alpha}}\}}{\{-B_{\tilde{I}}, M_{\tilde{\alpha}}\}} \end{array} \right]_{z_{\tilde{k}}} = 0, \quad (2.3.6)$$

since the second row of the block matrix evaluates to zero on \mathcal{L}_M and $z_{\tilde{k}} \in \mathcal{I}$. Eq. 2.3.3 does not give the proper amplitude because in the case of symmetry the stationary phase set contains H -group orbits rather than just isolated points. In Section 11.2 of Aquilanti *et al* [44] it was shown that the stationary phase evaluation applied to the inner product of states whose Lagrangian manifolds are described as level sets of functions (C, D) and (C, E) yields the amplitude

$$A_k = \frac{V_I}{\sqrt{|\det \{D, E\}|}}. \quad (2.3.7)$$

In the above equation V_I is the volume of the intersection, which will be the volume of the common symmetry group with respect to the Haar measure divided by the cardinality of the isotropy subgroup. Note that the symmetry implies that the denominator of Eq. 2.3.7 is the same no matter where the evaluation occurs in a common symmetry group orbit. Thus the WKB amplitude functions Eq. 2.3.3 in the case of symmetry are

$$A_{\beta, \tilde{k}}(x) = \frac{V_H}{|H|} \sqrt{|\tilde{\Omega}_{\beta, \tilde{k}}(x)|}, \quad (2.3.8)$$

where $V_H/|H|$ is the volume of the H -group orbits in Φ_{12} and

$$\tilde{\Omega}_{\beta, \tilde{k}}(x) = (-1)^{\tilde{n}} \left(\det \left[\begin{array}{c} \{x_i, M_{\tilde{\alpha}}\} \\ \{B_{\tilde{I}}, M_{\tilde{\alpha}}\} \end{array} \right]_{z_{\tilde{k}}} \right)^{-1}. \quad (2.3.9)$$

The group orbits are parameterized by index \tilde{k} as in Figure 2.2.4. The matrix in Eq. 2.3.9 is now a smaller $(n_1 + n_2 - s) \times (n_1 + n_2 - s)$ -matrix of Poisson brackets.

2.3.3 The Transported Density on $\mathcal{T}_M(\mathcal{L}_b)$

The manifolds $\mathcal{L}_b \subset \Phi_2$ and $\mathcal{L}_M \subset \Phi_{12}$ and their defining momentum maps \mathbf{B} and \mathbf{M} allow a form $\sigma_{\mathcal{I}}$ to be constructed on the intersection manifold \mathcal{I} defined in Eq. 2.2.10, called the “induced form on \mathcal{I} .” The induced form then defines an n_1 -form on the transported manifold $\mathcal{T}_M(\mathcal{L}_b) = \mathcal{L}_\beta$. This “transported density” is identical to the density form defined by Eq. 2.3.5 and Eq. 2.3.4. In this section we describe the construction of $\sigma_{\mathcal{I}}$ in the generic case when \mathcal{L}_b and \mathcal{L}_M do not share a non-trivial common symmetry group, in which case $\sigma_{\mathcal{I}}$ is an n_1 -form on \mathcal{I} . Construction of the induced form on \mathcal{I} in the presence of symmetry is discussed in Section 2.3.4.

Construction of $\sigma_{\mathcal{I}}$ requires a form that annihilates spaces that are tangent to momentum map level sets. We first show how to construct such a form for a general momentum map. Let Φ be a $2n$ -dimensional phase space with a symplectic G -action and an Ad^* -equivariant momentum map $\mathbf{P} : \Phi \rightarrow \mathfrak{g}^*$. Let $m = \dim G \leq n$ and let the Hamiltonian vector fields X_i be linearly independent. Given an ordered choice of basis $\{\xi_i\}$ of \mathfrak{g} , an m -form Π_P on Φ can be constructed,

$$\Pi_P \equiv \bigwedge_{i=1}^m \langle d\mathbf{P}, \xi_i \rangle = dP_1 \wedge \cdots \wedge dP_m \in \Omega^m(\Phi). \quad (2.3.10)$$

A different choice of ordered basis will yield the same form up to a multiplicative constant. By construction the one-forms dP_i restricted to any level set $\mathbf{P}^{-1}(\mu)$ are zero and Π_P annihilates any tangent plane to any level set $\mathbf{P}^{-1}(\mu)$,

$$\Pi_P(X_1, \cdots, X_n) = \det [dP_i(X_j)] = \det [\omega(X_i, X_j)] = 0. \quad (2.3.11)$$

For most points $z \in \Phi$, the level set of \mathbf{P} passing through z is generically $(2n-m)$ -dimensional and the phase space is locally foliated into an m -dimensional family of level sets in the neighborhood of z parameterized by $\mu \in \mathfrak{g}$.

The form $\Pi_B \in \Omega^{n_2}(\Phi_{12})$ associated with momentum map $-\mathbf{B}$ on Φ_{12} is thus

$$\Pi_B \equiv (-1)^{n_2} \bigwedge_{I=1}^{n_2} dB_I \in \Omega^{n_2}(\Phi_{12}). \quad (2.3.12)$$

The n_1 -form $\sigma_{\mathcal{I}}$ on \mathcal{I} is constructed from the $(n_1 + n_2)$ -form σ_M on \mathcal{L}_M and the n_2 -form Π_B on Φ_{12} by a “division of forms” procedure. Consider a set of n_1 vectors $\Xi_i \in T_z\mathcal{I}$ and n_2 vectors $Y_I \in T_z\mathcal{L}_M$ such that $\{\Xi_i; Y_I\}$ span $T_z\mathcal{L}_M$. Implicitly define $\sigma_{\mathcal{I}}$ so that

$$\sigma_M(\Xi_1, \cdots, \Xi_{n_1}, Y_1, \cdots, Y_{n_2}) = (\sigma_{\mathcal{I}} \wedge \Pi_B)(\Xi_1, \cdots, \Xi_{n_1}, Y_1, \cdots, Y_{n_2}). \quad (2.3.13)$$

Since Ξ_i is a vector in the tangent space of the intersection \mathcal{I} , it is also tangent to the level set $\mathbf{B}^{-1}(\mu_b)$. Therefore, $dB_I(\Xi_j) = 0$ and any term in the expansion of the wedge product that involves one of the Ξ_i being acted on by Π_B will vanish. Thus the wedge product on the right-hand side of Eq. 2.3.13 factors into $\sigma_{\mathcal{I}}(\Xi_1, \cdots, \Xi_{n_1})\Pi_B(Y_1, \cdots, Y_{n_2})$. By Eq. 2.3.12 and

the definition of the wedge product, the action of Π_B on the n_2 vectors Y_I can be re-expressed as an $n_2 \times n_2$ determinant of 1-forms acting on vectors,

$$\Pi_B(Y_1, \dots, Y_{n_2}) = \det[-dB_I(Y_J)] = (-1)^{n_2} \det[dB_I(Y_J)]. \quad (2.3.14)$$

Solving for $\sigma_{\mathcal{I}}$ gives

$$\sigma_{\mathcal{I}}(\Xi_1, \dots, \Xi_{n_1}) = (-1)^{n_2} \frac{\sigma_M(\Xi_1, \dots, \Xi_{n_1}, Y_1, \dots, Y_{n_2})}{\det[dB_I(Y_J)]}. \quad (2.3.15)$$

We now show that the expression on the right-hand side of Eq. 2.3.15 is independent of the choice of vectors Y_I used (as long as the determinant in Eq. 2.3.14 does not vanish) and thus that $\sigma_{\mathcal{I}}$ is well-defined. Consider the quotient vector space $T_z\mathcal{L}_M/T_z\mathcal{I}$ and let $[Y_I] \in T_z\mathcal{L}_M/T_z\mathcal{I}$ be the equivalence class with representative Y_I . The matrix $dB_I(Y_J)$ evaluated at z is non-singular if and only if the set of vectors $\{[Y_I]\}$ are linearly independent. Another way of expressing this is to say that $\{[Y_I]\}$ forms a basis of $T_z\mathcal{L}_M/T_z\mathcal{I}$. Let Y_I and Y'_I be two elements of the same equivalence class. There exists a $\xi_I \in T_z\mathcal{I}$ such that $Y'_I = Y_I + \xi_I$. Since dB_I annihilates vectors in the tangent plane to $\mathbf{B}^{-1}(\mu_b)$ and by definition $\mathcal{I} \subset \mathbf{B}^{-1}(\mu_b)$, $dB_I(\xi_J) = 0$ for all I and J . Thus $dB_I(Y'_J) = dB_I(Y_J)$. The set of vectors $\{\Xi_i\}$ span $T_z\mathcal{I}$ by construction and thus any ξ_I is a linear combination of the Ξ_i . Since the n_1 Ξ_i vectors are used in the first n_1 slots of σ_M , any ξ_I appearing in a later slot results in the form evaluating to zero. Therefore $\sigma_M(\Xi_i, Y'_I) = \sigma_M(\Xi_i, Y_I + \xi_I) = \sigma_M(\Xi_i, Y_I)$. Thus, given a basis $\{[Y_I]\}$, $\sigma_{\mathcal{I}}$ in Eq. 2.3.15 is independent of which representative vector in $[Y_I]$ is used in Eq. 2.3.15.

Let $\{[Y_I]\}$ and $\{[Y'_I]\}$ be separate bases of $T_z\mathcal{L}_M/T_z\mathcal{I}$ and let Z_I^J be the non-singular $n_2 \times n_2$ transformation matrix, so $[Y'_I] = Z_I^J [Y_J]$. Let Y_I and Y'_I be representative elements $[Y_I]$ and $[Y'_I]$ such that $Y'_I = Z_I^J Y_J$. The numerator of Eq. 2.3.15 transforms as $\sigma_M(\Xi_i, Y'_I) = \sigma_M(\Xi_i, Z_I^J Y_J) = (\det Z) \sigma_M(\Xi_i, Y_I)$ and the matrix elements in the denominator transforms as $dB_I(Y'_J) = Z_J^K dB_I(Y_K)$. Thus $\det[dB_I(Y'_J)] = (\det Z) \det[dB_I(Y_J)]$. Therefore,

$$\frac{\sigma_M(\Xi_i, Y'_I)}{\det[dB_I(Y'_J)]} = \frac{(\det Z) \sigma_M(\Xi_i, Y_J)}{(\det Z) \det[dB_I(Y_J)]} = \frac{\sigma_M(\Xi_i, Y_J)}{\det[dB_I(Y_J)]}. \quad (2.3.16)$$

The definition 2.3.15 of $\sigma_{\mathcal{I}}$ is thus independent of the set of vectors Y_I chosen and is well-defined.

As shown in Figure 2.3.1, there are a set of points indexed by ρ that project onto the same point in \mathcal{L}_β and thus \mathcal{I} breaks up into branches \mathcal{I}_ρ . Define a set of n_1 -forms $\sigma_{\mathcal{T}, \rho}$ on the transported manifold $\mathcal{T}_M(\mathcal{L}_b)$ such that $\sigma_{\mathcal{I}}$ is the pullback of $\sigma_{\mathcal{T}, \rho}$ by π_1 . Here ρ is used as in Section 2.3.1 to index the set of points in \mathcal{I} that project onto the same point on the transported manifold. Given a ρ , the projection map from \mathcal{I}_ρ to $\mathcal{T}_M(\mathcal{L}_b)$ is invertible and thus $\sigma_{\mathcal{T}, \rho}$ is defined to be the pullback of $\sigma_{\mathcal{I}}$ under the inverse of the projection. Thus, given a point $z_{\bar{k}}$ on the ρ -th branch of \mathcal{I} that projects onto z_1 as shown in Figure 2.3.1 and a set of vectors $\Xi_i \in T_{z_{\bar{k}}}\mathcal{I}$,

$$\sigma_{\mathcal{T}, \rho}|_{z_1}(\pi_{1*}\Xi_i) = \left. \frac{\sigma_M(\Xi_i, Y_I)}{\det[dB_I(Y_J)]} \right|_{z_{\bar{k}}}, \quad (2.3.17)$$

$$\sigma_{\mathcal{T},\rho} = \Omega_{\mathcal{T},\tilde{k}}(x) dx_1 \wedge \cdots \wedge dx_{n_1}. \quad (2.3.18)$$

It remains to be shown that Eq. 2.3.17 is equal to the expression given in Eq. 2.3.5.

2.3.4 The Transported Density in Cases of Symmetry

Now we construct the density form on \mathcal{L}_β in the case where there is a common symmetry group G_H . Using the Lie algebra bases and momentum maps of Section 2.3.2 we may express the form Π_B defined in Eq. 2.3.12 as $\Pi_B \equiv \Pi_H \wedge \Pi_{\tilde{B}}$, where Π_H is the analogous form for \mathbf{H} and $\Pi_{\tilde{B}}$ is defined as

$$\Pi_{\tilde{B}} \equiv (-1)^{n_2-s} \bigwedge_{\tilde{I}=1}^{n_2-s} dB_{\tilde{I}} \in \Omega^{n_2-s}(\Phi_{12}). \quad (2.3.19)$$

Similarly, the density on \mathcal{L}_M may be expressed as $\sigma_M = \sigma_H \wedge \sigma_{\tilde{M}}$, where $\sigma_H = \bigwedge_{\alpha=1}^s \lambda_\alpha$ and $\sigma_{\tilde{M}} = \bigwedge_{\alpha=s+1}^{n_1+n_2} \lambda_\alpha$ and the 1-forms λ_α are dual to the Hamiltonian vector fields X_α on \mathcal{L}_M as in Section C.2. Note that by construction $\sigma_{\tilde{M}}$ acting on any of the Hamiltonian vector fields generated by the momentum map \mathbf{H} of the subgroup G_H is zero.

As discussed in Section 2.2.4 the intersection manifold \mathcal{I} has dimension $(n_1 + s)$ so the density $\sigma_{\mathcal{I}}$ must be defined as an $(n_1 + s)$ -form on \mathcal{I} . Following Eq. 2.3.13, we implicitly define $\sigma_{\mathcal{I}}$ in the case of symmetry as

$$\sigma_M(\Xi_{\tilde{i}}, Y_{\tilde{I}}) = (\sigma_{\mathcal{I}} \wedge \Pi_{\tilde{B}})(\Xi_{\tilde{i}}, Y_{\tilde{I}}), \quad (2.3.20)$$

where vectors $\Xi_{\tilde{i}}$ ($\tilde{i} = 1, \dots, n_1 + s$) span $T_z\mathcal{I}$ and $\{\Xi_{\tilde{i}}, Y_{\tilde{I}}\}$ span $T_z\mathcal{L}_M$. Similarly we may define an n_1 -form $\sigma_{\tilde{\mathcal{I}}}$ by

$$\sigma_{\tilde{M}}(\Xi'_{\tilde{i}}, Y_{\tilde{I}}) = (\sigma_{\tilde{\mathcal{I}}} \wedge \Pi_{\tilde{B}})(\Xi'_{\tilde{i}}, Y_{\tilde{I}}), \quad (2.3.21)$$

where $\{\Xi'_{\tilde{i}}\}$ are a subset of n_1 vectors of $\{\Xi_{\tilde{i}}\}$. We may perform the division of forms procedure as in Section 2.3.3 to define $\sigma_{\mathcal{I}}$ and $\sigma_{\tilde{\mathcal{I}}}$,

$$\sigma_{\mathcal{I}}(\Xi_{\tilde{i}}) = (-1)^{n_2-s} \frac{\sigma_M(\Xi_{\tilde{i}}, Y_{\tilde{I}})}{\det [dB_{\tilde{I}}(Y_{\tilde{J}})]}, \quad \sigma_{\tilde{\mathcal{I}}}(\Xi'_{\tilde{i}}) = (-1)^{n_2-s} \frac{\sigma_{\tilde{M}}(\Xi'_{\tilde{i}}, Y_{\tilde{I}})}{\det [dB_{\tilde{I}}(Y_{\tilde{J}})]}. \quad (2.3.22)$$

Next we shown that $\sigma_{\mathcal{I}} = \sigma_H \wedge \sigma_{\tilde{\mathcal{I}}}$. By definition of the set $\{\Xi_{\tilde{i}}\}$ we may always construct an invertible linear transformation Z such that first s vectors in $\{\Xi_{\tilde{i}}\}$ are mapped to the Hamiltonian vector fields X_m^H generated by the components of \mathbf{H} . Acting either of the $n_1 + s$ -forms $\sigma_{\mathcal{I}}$ or $\sigma_H \wedge \sigma_{\tilde{\mathcal{I}}}$ on $\{\Xi_{\tilde{i}}\}$ is the same as $(\det Z)$ times the forms acting on the transformed set and thus we may show that the forms are equal by showing that their evaluation on the spanning set of $n_1 + s$ vectors $\{X_m^H, \Xi'_{\tilde{i}}\}$ are equal. Since $\sigma_M = \sigma_H \wedge \sigma_{\tilde{M}}$, $\sigma_{\tilde{M}}$ acting on any of the X_m^H is zero, and $\sigma_H(X_1^H, \dots, X_s^H) = 1$,

$$\sigma_{\mathcal{I}}(X_m^H, \Xi'_{\tilde{i}}) = (-1)^{n_2-s} \frac{\sigma_{\tilde{M}}(X'_i, Y_{\tilde{I}})}{\det [dB_{\tilde{I}}(Y_{\tilde{J}})]} = \sigma_{\tilde{\mathcal{I}}}(X'_i). \quad (2.3.23)$$

Similarly, $\sigma_{\tilde{\mathcal{I}}}$ acting on any of the X_m^H is zero and thus $(\sigma_H \wedge \sigma_{\tilde{\mathcal{I}}})(X_m^H, \Xi'_i) = \sigma_{\tilde{\mathcal{I}}}(X'_i)$. Comparing this result with Eq. 2.3.23 shows that $\sigma_{\mathcal{I}} = \sigma_H \wedge \sigma_{\tilde{\mathcal{I}}}$. Another perspective on this result is that $\sigma_{\mathcal{I}}$ is the wedge product of the density σ_H on the H -group orbits with the pull-back of the density $\sigma_{\mathcal{I}}$ on the reduced intersection manifold when a symplectic reduction by \mathbf{H} is performed. Symplectic reductions are discussed in Section B.4 and Sections 2.4.3 and 2.4.4 provide a full discussion of the role of symplectic reduction in the remodeling geometry.

Since G_H is the common symmetry group between G_M and G_b , the G_H group action on Φ_{12} is purely vertical over the target phase space Φ_1 and thus any G_H -group orbit projects to a single point of Φ_1 . In cases of symmetry the points shown in Figure 2.3.1 all become G_H group orbits and project onto the same point in \mathcal{L}_β . The different group orbits are disconnected and thus \mathcal{I} breaks up into branches \mathcal{I}_ρ , as in Section 2.3.1. The s -form density σ_H naturally lives on these group orbits and the n_1 -form $\sigma_{\tilde{\mathcal{I}}}$ is invariant under the flows generated by \mathbf{H} .

Let $z_{\tilde{k}}$ be a point on the ρ -th branch of \mathcal{I} that projects onto z_1 , a point on the k -th x -representation branch of \mathcal{L}_β and let $\{\Xi_i\}$ be a set of n_1 vectors in $T_{z_{\tilde{k}}}\mathcal{I}$ such that $\pi_{1*}\Xi_i \neq 0$. Then the density $\sigma_{\mathcal{T},\rho}$ on the transported manifold $\mathcal{T}_M(\mathcal{L}_b)$ is defined through

$$\sigma_{\mathcal{T},\rho}|_{z_1}(\pi_{1*}\Xi_i) = \int_{\varphi^H(z_{\tilde{k}})} \sigma_{\tilde{\mathcal{I}}}(\Xi_i, \cdot). \quad (2.3.24)$$

We may “sum” the densities over points on the same group orbit because the relative phase between any two points on the same group orbit will be zero. Note that this reproduces the definition of $\sigma_{\mathcal{T},\rho}$ in Eq. 2.3.17 in the case where the common symmetry group is trivial. The density functions $\Omega_{\mathcal{T},\tilde{k}}(x)$ are then defined as in Eq. 2.3.18.

2.3.5 Equality of the WKB and Transported Densities

To show that the WKB densities $\sigma_{\beta,\rho}$ are identical to the transported densities $\sigma_{\mathcal{T},\rho}$ we show that the density functions $\Omega_{\beta,\tilde{k}}$ defined in Eq. 2.3.4 are equal to the density functions $\Omega_{\mathcal{T},\rho}$ defined in Eq. 2.3.18.

Consider $\sigma_{\mathcal{T},\rho}$ evaluated at a point $z_{1,k}$ on the k -th x -representation branch of \mathcal{L}_β and let $z_{\tilde{k}} \in \mathcal{I}$ be the point on the ρ -th branch of \mathcal{I} that projects onto $z_{1,k}$ as in Figure 2.3.1. Let $X_\alpha^M \in T_{z_{\tilde{k}}}\mathcal{L}_M$ be the $(n_1 + n_2)$ Hamiltonian flow vectors for the momentum map components M_α . Consider a non-singular linear transformation matrix, Z_α^β such that Z acting on the first n_1 flow vectors X_α^M gives vectors in the subspace $T_z\mathcal{I}$. Define $\Xi_i \equiv Z_i^\alpha X_\alpha^M \in T_{z_{\tilde{k}}}\mathcal{I}$ as the first n_1 transformed vectors and define $Y_I \equiv Z_{(n_1+I)}^\alpha X_\alpha^M \in T_{z_{\tilde{k}}}\mathcal{L}_M$. Since the matrix Z is non-singular, the set of vectors $\{\Xi_i, Y_I\}$ span $T_{z_{\tilde{k}}}\mathcal{L}_M$. Furthermore the first n_1 vectors span $T_{z_{\tilde{k}}}\mathcal{I}$. The vectors Ξ_i can be pushed-forward by π_1 into $T_{z_1}\mathcal{L}_\beta$ and the set $\{[Y_I]\}$ are linearly independent in $T_{z_{\tilde{k}}}\mathcal{L}_M/T_z\mathcal{I}$. The transformed vectors can therefore be used in Eq. 2.3.17.

We now evaluate $\sigma_{\mathcal{T},\rho}$ on the pushed-forward vectors $\pi_{1*}\Xi_i$. Consider first the evaluation of $\sigma_{\mathcal{T},\rho}$ using the x -representation expression in Eq. 2.3.18,

$$\sigma_{\mathcal{T},\rho}(\pi_{1*}\Xi_i) = \Omega_{\mathcal{T},\tilde{k}}(x) (dx_1 \wedge \cdots \wedge dx_{n_1})(\pi_{1*}\Xi_i). \quad (2.3.25)$$

The wedge product on the right-hand side of the above equation evaluates to $\det [dx_i(\pi_{1*}\Xi_j)] = \det [(\pi_1^* dx_i)(\Xi_j)]$. The pull-back of the forms dx_i on Φ_1 are the forms dx_i on Φ_{12} . Solving for $\Omega_{\mathcal{T},\tilde{k}}$ in Eq. 2.3.25 therefore gives

$$\Omega_{\mathcal{T},\tilde{k}}(x) = \frac{(\sigma_{\mathcal{T}}(\pi_{1*}\Xi_i))_{z_{1,k}}}{\det [dx_i(\Xi_j)]_{z_{\tilde{k}}}}. \quad (2.3.26)$$

We now evaluate $\sigma_{\mathcal{T},\rho}$ on the pushed-forward vectors $\pi_{1*}\Xi_i$ using Eq. 2.3.17. The numerator $\sigma_M(\Xi_i, Y_I)$ expressed in terms of the Hamiltonian flow vectors is $\sigma_M(Z_\beta^\alpha X_\alpha^M) = (\det Z) \sigma_M(X_\alpha^M)$. By Eq. C.2.3, $\sigma_M(X_\alpha^M) = 1$ and thus $\sigma_M(\Xi_i, Y_i) = \det Z$. Therefore,

$$\Omega_{\mathcal{T},\tilde{k}}(x) = (-1)^{n_2} \frac{\det Z}{\det [dx_i(\Xi_j)] \det [dB_I(Y_J)]}, \quad (2.3.27)$$

where all forms and vectors on the right-hand side are evaluated at point $z_{\tilde{k}} \in \mathcal{I}$.

Let A be an $n_1 \times n_1$ matrix and let D be an $n_2 \times n_2$ matrix. The product of the determinants of A and D can be expressed as a single $(n_1 + n_2) \times (n_1 + n_2)$ -determinant,

$$(\det A)(\det D) = \det \left[\begin{array}{c|c} A & B \\ \hline 0 & D \end{array} \right], \quad (2.3.28)$$

where B is an arbitrary $n_1 \times n_2$ matrix. The denominator of Eq. 2.3.27 can thus be combined into the $(n_1 + n_2) \times (n_1 + n_2)$ -determinant

$$\det \left[\begin{array}{c|c} dx_i(\Xi_j) & dx_i(Y_J) \\ \hline 0 & dB_I(Y_J) \end{array} \right], \quad (2.3.29)$$

where the matrix $dx_i(Y_J)$ is used as the arbitrary matrix in the upper-right block. Since the Ξ_i lie in the tangent space to the intersection and thus are tangent to the \mathbf{B} level sets, the matrix $dB_I(\Xi_j)$ evaluates to the $n_2 \times n_1$ zero matrix and Eq. 2.3.29 can be written

$$\det \left[\begin{array}{c|c} dx_i(\Xi_j) & dx_i(Y_J) \\ \hline dB_I(\Xi_j) & dB_I(Y_J) \end{array} \right] = \det \left[\begin{array}{c} dx_i(Z_\beta^\alpha X_\alpha^M) \\ dB_I(Z_\beta^\alpha X_\alpha^M) \end{array} \right], \quad (2.3.30)$$

where the transformation matrix Z has been used to express all vectors in terms of the Hamiltonian flow vectors X_α^M . The transformation matrix comes out of the determinant and the forms acting on Hamiltonian flow vectors become Poisson brackets, yielding

$$\det [dx_i(\Xi_j)] \det [dB_I(Y_J)] = (\det Z) \det \left[\begin{array}{c} \{x_i, M_\alpha\} \\ \{B_I, M_\alpha\} \end{array} \right]. \quad (2.3.31)$$

The determinant of Z cancels when using the above in Eq. 2.3.27 and therefore

$$\Omega_{\mathcal{T},\tilde{k}}(x) = (-1)^{n_2} \left(\det \left[\begin{array}{c} \{x_i, M_\alpha\} \\ \{B_I, M_\alpha\} \end{array} \right]_{z_{\tilde{k}}} \right)^{-1}. \quad (2.3.32)$$

The expression in Eq. 2.3.32 for the transported density functions is equal to the expression in Eq. 2.3.4 for the density functions resulting from the WKB evaluation and thus the transported densities $\sigma_{\mathcal{T},\rho}$ of Eq. 2.3.17 are equal to the WKB densities $\sigma_{\beta,\rho}$ of Eq. 2.3.5. A similar analysis holds with the same result when a non-trivial common symmetry group is present.

2.4 The Transport of a Momentum Map

The transport procedure that generates \mathcal{L}_β from \mathcal{L}_M and \mathcal{L}_b allows the level set conditions defining \mathcal{L}_β to be expressed in terms of the momentum maps \mathbf{M} and \mathbf{B} that define \mathcal{L}_M and \mathcal{L}_b . At the heart of this construction is the “core isomorphism” generated by \hat{M} which defines a “core symplectomorphism” \mathcal{M} between certain symplectic reductions of the source and target spaces.

We start in Sections 2.4.1 and 2.4.2 by looking at the linear algebra description of the β -state. First we construct a “core isomorphism” for \hat{M} between subspaces of \mathcal{H}_2 and \mathcal{H}_1 and then use this core isomorphism to construct the observables that describe $|\beta\rangle$. Then we turn to symplectic geometry. In Section 2.4.3 we explore the two geometric objects that are the classical analogues of Hilbert subspaces, which allows us to construct a “core symplectomorphism” between symplectic reductions of Φ_2 and Φ_1 in Section 2.4.4. In Section 2.4.5 we describe how the core symplectomorphism in the geometric construction of a momentum map on Φ_1 for which the β -manifold is a level set. Finally in Section 2.4.6 we show that the density functions that arise from this new momentum map are equal to the density functions found via the WKB method in the previous section.

2.4.1 The Core Isomorphism of \hat{M}

Consider two Hilbert spaces \mathcal{H}_1 and \mathcal{H}_2 and a linear map $\hat{M} : \mathcal{H}_2 \rightarrow \mathcal{H}_1$. The first isomorphism theorem of linear algebra [57] says that the quotient space $\mathcal{H}_2/(\ker \hat{M})$, is isomorphic to the image of \hat{M} . This quotient space is called the coimage of \hat{M} . Furthermore, the inner product structure on \mathcal{H}_2 provides a natural isomorphism between the coimage of \hat{M} and the orthogonal complement of $\ker \hat{M}$, $(\ker \hat{M})_\perp$. Since $\text{img } \hat{M}$ and $(\ker \hat{M})_\perp$ are vector subspaces of \mathcal{H}_1 and \mathcal{H}_2 they inherit an inner product structure. Thus we may treat $\text{img } \hat{M}$ and $(\ker \hat{M})_\perp$ as either subspaces or as Hilbert spaces in their own right. We write $\text{img } \hat{M}$ and $(\ker \hat{M})_\perp$ as \mathcal{H}_{img} and \mathcal{H}_{ker} when explicitly treating them as separate Hilbert spaces. Let $\hat{\Pi}_{\text{img}} : \mathcal{H}_1 \rightarrow \text{img } \hat{M}$ and $\hat{\Pi}_{\text{ker}} : \mathcal{H}_2 \rightarrow (\ker \hat{M})_\perp$ be projection operators. Note that we may also treat the projections as linear maps $\hat{\Pi}_{\text{img}} : \mathcal{H}_1 \rightarrow \mathcal{H}_{\text{img}}$ and $\hat{\Pi}_{\text{ker}} : \mathcal{H}_2 \rightarrow \mathcal{H}_{\text{ker}}$. We also define the inclusion maps $\hat{\mathcal{I}}_{\text{img}} : \mathcal{H}_{\text{img}} \rightarrow \mathcal{H}_1$ and $\hat{\mathcal{I}}_{\text{ker}} : \mathcal{H}_{\text{ker}} \rightarrow \mathcal{H}_2$. Note that the composition $\hat{\Pi}_{\text{img}} \circ \hat{\mathcal{I}}_{\text{img}}$ is the identity on \mathcal{H}_{img} , with a similar statement for \mathcal{H}_{ker} .

We define the “core isomorphism” $\hat{M}_C : \mathcal{H}_{\text{ker}} \rightarrow \mathcal{H}_{\text{img}}$ associated with \hat{M} by

$$\hat{M}_C = \hat{\Pi}_{\text{img}} \circ \hat{M} \circ \hat{\mathcal{I}}_{\text{ker}}. \quad (2.4.1)$$

$$\begin{array}{ccc}
 \mathcal{H}_2 & \xrightarrow{\hat{M}} & \mathcal{H}_1 \\
 \hat{\Pi}_{\ker} \updownarrow \hat{\mathcal{I}}_{\ker} & & \hat{\Pi}_{\text{img}} \updownarrow \hat{\mathcal{I}}_{\text{img}} \\
 \mathcal{H}_{\ker} & \xrightarrow{\hat{M}_C} & \mathcal{H}_{\text{img}}
 \end{array}$$

 Figure 2.4.1: The core isomorphism $\hat{M}_C : \mathcal{H}_{\ker} \rightarrow \mathcal{H}_{\text{img}}$.

We include $\hat{\Pi}_{\text{img}}$ in the above composition so that \hat{M}_C is explicitly a map onto the Hilbert space \mathcal{H}_{img} . In terms of the core isomorphism, the map \hat{M} is

$$\hat{M} = \hat{\mathcal{I}}_{\text{img}} \circ \hat{M}_C \circ \hat{\Pi}_{\ker}, \quad (2.4.2)$$

where $\hat{\Pi}_{\ker}$ is needed in the composition because \hat{M}_C acts on the Hilbert space \mathcal{H}_{\ker} . We may also treat \hat{M}_C as a map $:(\ker \hat{M})_{\perp} \rightarrow \text{img } \hat{M}$ whose range and domain are treated as subsets of \mathcal{H}_2 and \mathcal{H}_1 rather than independent Hilbert spaces. The spaces and maps involved in forming the core isomorphism are shown in Figure 2.4.1.

Consider the subspace $(\text{img } \hat{M}) \otimes (\ker \hat{M})_{\perp}^*$ of the product Hilbert space \mathcal{H}_{12} . By construction $\hat{M} \in (\text{img } \hat{M}) \otimes (\ker \hat{M})_{\perp}^*$. As with $\text{img } \hat{M}$ and $(\ker \hat{M})_{\perp}$, $(\text{img } \hat{M}) \otimes (\ker \hat{M})_{\perp}^*$ inherits an inner product structure from \mathcal{H}_{12} and we may treat it as a Hilbert space. We write $(\text{img } \hat{M}) \otimes (\ker \hat{M})_{\perp}^*$ as \mathcal{H}_{rp} when explicitly treating it as a separate Hilbert space (the subscript “rp” stands for “reduced product”). This space is the product Hilbert space $\mathcal{H}_{\text{img}} \otimes \mathcal{H}_{\ker}^*$, whose elements are linear maps $:\mathcal{H}_{\ker} \rightarrow \mathcal{H}_{\text{img}}$, so $\hat{M}_C \in \mathcal{H}_{\text{rp}}$. We may also define the “core Hilbert space” $\mathcal{H}_{\text{core}} \cong \mathcal{H}_{\text{img}} \cong \mathcal{H}_{\ker}$ so that $\mathcal{H}_{\text{rp}} \cong \mathcal{H}_{\text{core}} \otimes \mathcal{H}_{\text{core}}^*$. The core isomorphism is thus an operator on $\mathcal{H}_{\text{core}}$.

In many spin network examples the map \hat{M} is an $SU(2)$ intertwiner. In such cases we may express \hat{M} in terms of a set of unitary maps between the irreducible subspaces of $(\ker \hat{M})_{\perp}$ and $\text{img } \hat{M}$. We call these maps the “unitary core” of the intertwiner. Intertwiners and their unitary cores will be discussed in more detail in Section 3.1.3.

Describe $\text{img } \hat{M}$ as the simultaneous eigenspace of a set of observables $\hat{C}_a : \mathcal{H}_1 \rightarrow \mathcal{H}_1$ at eigenvalues $\mu_{c,a}$,

$$\hat{C}_a |\psi\rangle = \mu_{c,a} |\psi\rangle \quad \forall |\psi\rangle \in \text{img } \hat{M}, \quad (2.4.3)$$

where the observables \hat{C}_a must all mutually commute on $\text{img } \hat{M}$,

$$[\hat{C}_a, \hat{C}_b] |\psi\rangle = 0 \quad \forall a, b, |\psi\rangle \in \text{img } \hat{M}. \quad (2.4.4)$$

The number of observables needed to specify $\text{img } \hat{M}$ is, at most, n_1 (since a set of n_1 mutually commuting observables will uniquely specify a one-dimensional subspace of \mathcal{H}_1). Define \tilde{n} so that index a runs from 1 to $n_1 - \tilde{n}$ and thus $\text{img } \hat{M}$ is described as the simultaneous eigenspace of a set of $(n_1 - \tilde{n})$ observables. A state in $\text{img } \hat{M}$ may be specified as a non-degenerate eigenstate of a set of n_1 independent observables, $(n_1 - \tilde{n})$ of which are \hat{C}_a . Thus an additional

\tilde{n} observables are needed to specify a state within $\text{img } \hat{M}$. Alternatively, a complete set of observables in the Hilbert space \mathcal{H}_{img} must consist of \tilde{n} independent operators.

Similarly, describe $(\ker \hat{M})_{\perp}$ as the simultaneous eigenspace of a set of observables $\hat{D}_A : \mathcal{H}_2 \rightarrow \mathcal{H}_2$ at eigenvalues $\mu_{d,A}$,

$$\hat{D}_A|\phi\rangle = \mu_{d,A}|\phi\rangle \quad \forall |\phi\rangle \in (\ker \hat{M})_{\perp}, \quad (2.4.5)$$

where the observables \hat{D}_A must all mutually commute on $(\ker \hat{M})_{\perp}$,

$$[\hat{D}_A, \hat{D}_B]|\phi\rangle = 0 \quad \forall |\phi\rangle \in (\ker \hat{M})_{\perp}. \quad (2.4.6)$$

Since $\text{img } \hat{M}$ and $(\ker \hat{M})_{\perp}$ are isomorphic, a complete set of observables in the Hilbert space \mathcal{H}_{\ker} must consist of \tilde{n} operators. A complete set of observables in \mathcal{H}_2 contains n_2 independent operators so it must require an additional $(n_2 - \tilde{n})$ independent operators to specify $(\ker \hat{M})_{\perp}$ as an eigenspace of \mathcal{H}_2 . Index A runs from 1 to $(n_2 - \tilde{n})$.

As in Section 2.1.1, the operators \hat{C}_a and \hat{D}_A can be promoted to operators $\hat{C}_a^{(12)}$ and $\hat{D}_A^{(12)}$ on $\mathcal{H}_1 \otimes \mathcal{H}_2^*$. These operators naturally commute in the product space, $[\hat{C}_a^{(12)}, \hat{D}_A^{(12)}] = 0$. The subspace $(\text{img } \hat{M}) \otimes (\ker \hat{M})_{\perp}^*$ is the simultaneous eigenspace of the set of $(n_1 + n_2 - 2\tilde{n})$ observables $\hat{C}_a^{(12)}$ and $\hat{D}_A^{(12)}$ with eigenvalues $(\mu_{c,a}, \mu_{d,A}^*)$. Note that since operators \hat{D}_A are assumed to be observables, the eigenvalues $\mu_{d,A}$ are real and thus the complex conjugation can be dropped.

2.4.2 Observables of the β -State

In most spin network applications we have some choice as to how to define the b - and M -states when setting up the remodeling algebra. In particular, if $|b\rangle \notin (\ker \hat{M})_{\perp}$ then we make the replacement $|b\rangle \mapsto \hat{\Pi}_{\ker}|b\rangle$. If such a replacement is made then a new set of operators \hat{B}_A and eigenvalues $\mu_{b,A}$ must be used in Eq. 2.1.4 and these operators define a new Lie algebra \mathfrak{g}_B^* . Since $|b\rangle$ is now an element of $(\ker \hat{M})_{\perp}$ by construction, it is a simultaneous eigenstate of all $(n_2 - \tilde{n})$ observables \hat{D}_A . Thus a basis of \mathfrak{g}_B^* may be chosen such that the first $(n_2 - \tilde{n})$ components of the \mathfrak{g}_B^* -valued operator $\hat{\mathbf{B}}$ on \mathcal{H}_2 are \hat{D}_A . Call the remaining \tilde{n} components \hat{B}_{ℓ} ($\ell = 1 \cdots \tilde{n}$). In this basis the generalized momentum μ_b has components $(\mu_{d,A}, \mu_{b,\ell}^R)$ and $|b\rangle$ may be expressed as

$$|b\rangle = \left| \begin{array}{cccccc} \hat{D}_1 & \cdots & \hat{D}_{n_2-\tilde{n}} & \hat{B}_1 & \cdots & \hat{B}_{\tilde{n}} \\ \mu_{d,1} & & \mu_{d,n_2-\tilde{n}} & \mu_{b,1}^R & & \mu_{b,\tilde{n}}^R \end{array} \right\rangle. \quad (2.4.7)$$

Note that $[\hat{D}_A, \hat{B}_{\ell}]|b\rangle = 0$ and $[\hat{B}_{\ell}, \hat{B}_{\ell'}]|b\rangle = 0$ for all A, ℓ, ℓ' . We make the stricter assumption that operators \hat{D}_A and \hat{B}_{ℓ} commute on the entire subspace $(\ker \hat{M})_{\perp}$, $[\hat{D}_A, \hat{B}_{\ell}]|\psi\rangle = 0$ for all $|\psi\rangle \in (\ker \hat{M})_{\perp}$. This assumption is met in all of our spin network applications and guarantees that operators \hat{B}_{ℓ} leave the subspace $(\ker \hat{M})_{\perp}$ invariant. Therefore the \tilde{n} operators \hat{B}_{ℓ} may be restricted to observables $\hat{B}_{\ell} : \mathcal{H}_{\ker} \rightarrow \mathcal{H}_{\ker}$ and moreover the \tilde{n} observables are enough to completely characterize a non-degenerate eigenstate on \mathcal{H}_{\ker} .

We define the “transported operators” $\hat{\beta}_\ell : \mathcal{H}_{\text{img}} \rightarrow \mathcal{H}_{\text{img}}$ as the operators \hat{B}_ℓ conjugated by the core isomorphism \hat{M}_C ,

$$\hat{\beta}_\ell \equiv \hat{M}_C \circ \hat{B}_\ell \circ \hat{M}_C^{-1}. \quad (2.4.8)$$

Since $|\beta\rangle \in \text{img } \hat{M}$ by definition, the β -state is a simultaneous eigenstate of all $(n_1 - \tilde{n})$ observables \hat{C}_a . We now show that $|\beta\rangle$ is also an eigenstate of the transported operators. By Eq. 2.4.8 and 2.1.5,

$$\hat{\beta}_\ell |\beta\rangle = \hat{M}_C \circ \hat{B}_\ell \circ \hat{M}_C^{-1} \circ \hat{M} |b\rangle. \quad (2.4.9)$$

Since $|b\rangle$ was chosen to be an element of $(\ker \hat{M})_\perp$ we may interpret $|b\rangle$ as an element of \mathcal{H}_{ker} and use the relation $\hat{M}|b\rangle = \hat{M}_C|b\rangle$ to express the right-hand side of Eq. 2.4.9 as

$$\hat{M}_C \circ \hat{B}_\ell \circ \hat{M}_C^{-1} \circ \hat{M}_C |b\rangle = \hat{M}_C \circ \hat{B}_\ell |b\rangle. \quad (2.4.10)$$

By construction, $\hat{B}_\ell |b\rangle = \mu_{b,\ell} |b\rangle$ and thus 2.4.10 simplifies to $\mu_{b,\ell} \hat{M}_C |b\rangle$, or

$$\hat{\beta}_\ell |\beta\rangle = \mu_{b,\ell} |\beta\rangle. \quad (2.4.11)$$

Since \hat{M}_C is an isomorphism between $(\ker \hat{M})_\perp$ and $\text{img } \hat{M}$, and \hat{B}_ℓ form a complete set of observables on $(\ker \hat{M})_\perp$, operators $\hat{\beta}_\ell$ form a complete set of observables in the subspace $\text{img } \hat{M}$. Furthermore, these operators commute with \hat{C}_a on $\text{img } \hat{M}$ and thus we may express $|\beta\rangle$ as

$$|\beta\rangle = \left| \begin{array}{cccccc} \hat{C}_a & \dots & \hat{C}_{n_1-\tilde{n}} & \hat{\beta}_1 & \dots & \hat{\beta}_{\tilde{n}} \\ \mu_{c,a} & & \mu_{c,n_1-\tilde{n}} & \mu_{b,1} & & \mu_{b,\tilde{n}} \end{array} \right\rangle. \quad (2.4.12)$$

2.4.3 Subspaces and Symplectic Reduction

In this section we adopt a general notation, independent of the notation of the remodeling algebra and geometry. In particular the operators \hat{A} bear no relation to the operators defined in Section 2.1.1.

We now turn to general semiclassical considerations and expand the “semi-classical dictionary” presented in Chapter 2 of Bates and Weinstein [58] to include subspaces. As noted in Sections 2.1.2 and 2.1.4, a Hilbert space \mathcal{H} may be represented semiclassically by a symplectic manifold Φ and individual states in the Hilbert space may be represented by Lagrangian submanifolds of Φ . If a state is presented as the simultaneous non-degenerate eigenstate of a set of operators \hat{A}_i at eigenvalues μ_i ($i = 1 \dots n$) then the Lagrangian manifold that supports the semiclassical approximation to the state is described as the simultaneous level set of the Weyl symbols A_i at contour values μ_i . Now let $\{\hat{A}_i\}$ ($i = 1 \dots m < n$) be an incomplete set of independent operators and consider the simultaneous μ_i -eigenspace $\mathcal{H}_\mu \subset \mathcal{H}$. In other words the simultaneous eigenstates of operators \hat{A}_i are degenerate and the set of such eigenstates form the eigenspace \mathcal{H}_μ . The existence of such an eigenspace requires $[\hat{A}_i, \hat{A}_j]|\psi\rangle = 0$ for all $|\psi\rangle \in \mathcal{H}_\mu$. The obvious classical manifold corresponding to this subspace is the simultaneous level set of the Weyl symbols A_i at contour values μ_i ,

$$\mathcal{H}_\mu \subset \mathcal{H} \implies \left(\begin{array}{ccc} A_1 & \dots & A_m \\ \mu_1 & & \mu_m \end{array} \right) \subset \Phi. \quad (2.4.13)$$

The commutation of the operators \hat{A}_i on \mathcal{H}_μ semiclassically becomes the statement that the functions A_i Poisson commute on this level set and thus the level set is a co-isotropic manifold. The subspace \mathcal{H}_μ contains all states $|\psi\rangle$ that satisfy $\hat{A}_i|\psi\rangle = \mu_i|\psi\rangle$ for all i . The set of Lagrangian manifolds supporting the semi-classical approximations for these states are therefore contained in the simultaneous $A_i = \mu_i$ level set ($i = 1, \dots, m$). Thus, in the semi-classical dictionary, a basis of a subspace corresponds to a Lagrangian foliation of the co-isotropic level set.

As in Section 2.1.1 we assume the set of operators $\{\hat{A}_i\}$ form a Lie algebra under the commutator so that they may be the generators of a Lie group G on \mathcal{H} . Once again this assumption will be valid for all spin network applications. The operators \hat{A}_i can be considered the components of the \mathfrak{g}^* -valued operator $\hat{\mathbf{A}} : \mathcal{H} \rightarrow \mathfrak{g}^* \times \mathcal{H}$ and the eigenvalues μ_i can be considered the components of a generalized momentum $\mu \in \mathfrak{g}^*$ with respect to some basis. A simultaneous eigenspace of $\hat{\mathbf{A}}$ will exist when μ is a fixed point under the co-adjoint action of G on \mathfrak{g}^* . In this case the level set in Eq. 2.4.13 may be written $\mathbf{A}^{-1}(\mu)$. The Poisson bracket conditions on the components A_i are equivalent to requiring that μ be a fixed point in \mathfrak{g}^* .

The eigenspace \mathcal{H}_μ inherits an inner product structure from \mathcal{H} and thus may be considered a Hilbert space in its own right and thus there should be an associated phase space Φ_μ corresponding to \mathcal{H}_μ . Since the Hilbert space \mathcal{H}_μ is constructed by considering the μ -eigenspace of $\hat{\mathbf{A}}$ in \mathcal{H} , we should be able to construct the phase space Φ_μ from the level set $\mathbf{A}^{-1}(\mu)$ in Φ . If \mathbf{A} is an Ad^* -equivariant momentum map then this may be achieved by performing a symplectic reduction of Φ . As discussed in Abraham and Marsden [56], symplectic reduction is a way of constructing a new, smaller phase space from an old one by exploiting a symmetry of the old phase space. As summarized in Section B.4, the first step in the reduction is to form an equivalence relation on the level set $\mathbf{A}^{-1}(\mu)$, where two points are equivalent if they lie on the same isotropy subgroup orbit. This divides the level set into a union of isotropic submanifolds. In this example μ is a fixed point and thus the isotropy subgroup is the entire group G . The reduced manifold Φ_μ is then the set of equivalence classes $\mathbf{A}^{-1}(\mu)/G_\mu$. Let ω be the symplectic form on Φ , $\pi_\mu : \mathbf{A}^{-1}(\mu) \rightarrow \Phi_\mu$ be the natural projection of the quotient operation and $\iota_\mu : \mathbf{A}^{-1}(\mu) \rightarrow \Phi$ be the inclusion map of the level set. Then the symplectic form ω_μ on Φ_μ is uniquely defined by $\pi_\mu^*\omega_\mu = \iota_\mu^*\omega$. As in Section B.4 we write the symplectic reduction of Φ by \mathbf{A} at μ as $\Phi//(\mathbf{A}=\mu)$.

We assume that the momentum map components A_i are independent on the level set so that the set of Hamiltonian flow vectors $\{X_i\}$ has full rank at points $z \in \mathbf{A}^{-1}(\mu)$. Thus the co-dimension of the level set is m , the number of components of \mathbf{A} and thus the dimension of the Lie group G . The group orbits will generically be m -dimensional as well, though isolated orbits may in the level set may have lower dimensions. The reduced space thus has m fewer dimensions than the $(2n - m)$ -dimensional level set, $\dim \Phi_\mu = 2(n - m)$.

In summary, let \mathcal{H} be a Hilbert space with associated phase space (Φ, ω) , let G be a group with generators $\hat{\mathbf{A}}$ on \mathcal{H} and a symplectic action on Φ with momentum map \mathbf{A} , and let $\mu \in \mathfrak{g}^*$ be a fixed point under the co-adjoint action. The μ -eigenspace of $\hat{\mathbf{A}}$ in \mathcal{H}_μ is

associated with two semiclassical manifolds. If \mathcal{H}_μ is interpreted as a subspace of \mathcal{H} then the associated semiclassical object is a co-isotropic manifold, $\mathbf{A}^{-1}(\mu)$. If \mathcal{H}_μ is interpreted as a Hilbert space then the associated semiclassical object is the phase space Φ_μ obtained by the symplectic reduction $\Phi//(\mathbf{A}=\mu)$.

2.4.4 The Core Geometry and Symplectomorphism

We now apply the results of the previous section to define the spaces on which a “core symplectomorphism” may be defined, which will allow construction of the defining momentum map of \mathcal{L}_β .

As in Section 2.1.1 we assume the sets of operators $\{\hat{C}_a\}$ and $\{\hat{D}_A\}$ introduced in Section 2.4.1 form Lie algebras under the commutator so that they may be the generators of group G_{img} on \mathcal{H}_1 and G_{ker} on \mathcal{H}_2 , respectively. Since the operators are assumed to be independent, $\dim G_{\text{img}} = (n_1 - \tilde{n})$ and $\dim G_{\text{ker}} = (n_2 - \tilde{n})$. Define dual algebra valued operators $\hat{\mathbf{C}} : \mathcal{H}_1 \rightarrow \mathfrak{g}_{\text{img}}^* \times \mathcal{H}_1$ and $\hat{\mathbf{D}} : \mathcal{H}_2 \rightarrow \mathfrak{g}_{\text{ker}}^* \times \mathcal{H}_2$ whose components with respect to some basis are \hat{C}_a and \hat{D}_A . For conditions 2.4.4 and 2.4.6 to be satisfied we require that μ_c and μ_d are Ad^* -fixed points of $\mathfrak{g}_{\text{img}}^*$ and $\mathfrak{g}_{\text{ker}}^*$. Using these definitions we may express the subspaces from Section 2.4.1 as

$$\text{img } \hat{M} = \left\{ |\psi\rangle \in \mathcal{H}_1 \mid \hat{\mathbf{C}}|\psi\rangle = \mu_c|\psi\rangle \right\}, \quad (2.4.14)$$

$$(\text{ker } \hat{M})_\perp = \left\{ |\phi\rangle \in \mathcal{H}_2 \mid \hat{\mathbf{D}}|\phi\rangle = \mu_d|\phi\rangle \right\}. \quad (2.4.15)$$

The co-isotropic submanifolds corresponding to these subspaces are

$$\mathbf{C}^{-1}(\mu_c) = \begin{pmatrix} \mathbf{C} \\ \mu_c \end{pmatrix} \subset \Phi_1, \quad \mathbf{D}^{-1}(\mu_d) = \begin{pmatrix} \mathbf{D} \\ \mu_d \end{pmatrix} \subset \Phi_2, \quad (2.4.16)$$

with $\dim \mathbf{C}^{-1}(\mu_c) = (n_1 + \tilde{n})$ and $\dim \mathbf{D}^{-1}(\mu_d) = (n_2 + \tilde{n})$.

Following the discussion in Section 2.4.3, we may interpret the subspaces $\text{img } \hat{M}$ and $(\text{ker } \hat{M})_\perp$ as Hilbert spaces \mathcal{H}_{img} and \mathcal{H}_{ker} . We form the associated phase spaces Φ_{img} and Φ_{ker} by symplectic reduction,

$$\Phi_{\text{img}} \equiv \Phi_1//(\mathbf{C}=\mu_c), \quad \Phi_{\text{ker}} \equiv \Phi_2//(\mathbf{D}=\mu_d). \quad (2.4.17)$$

We call Φ_{img} the “reduced target phase space” and Φ_{ker} the “reduced source phase space.” Let ι_{img} , ι_{ker} , π_{img} , and π_{ker} be the inclusion and projection maps of the reductions, as shown in Figure 2.4.2. The groups G_{img} and G_{ker} are $(n_1 - \tilde{n})$ - and $(n_2 - \tilde{n})$ -dimensional so the reduced phase spaces both have dimension $2\tilde{n}$.

The Lagrangian manifold \mathcal{L}_β is a submanifold of $\mathbf{C}^{-1}(\mu_c)$ and thus the projection $\mathcal{L}_\beta^R \equiv \pi_{\text{img}}\mathcal{L}_\beta$ is a Lagrangian manifold of the reduced target phase space Φ_{img} . We may consider \mathcal{L}_β^R to be the Lagrangian manifold that supports the semiclassical approximation of $\hat{\Pi}_{\text{img}}|\beta\rangle \in \mathcal{H}_{\text{img}}$. Similarly, we specified that $|b\rangle \in (\text{ker } \hat{M})_\perp$ so the Lagrangian manifold \mathcal{L}_b

is a submanifold of $\mathbf{D}^{-1}(\mu_d)$ and thus the projection $\mathcal{L}_b^R \equiv \pi_{\ker} \mathcal{L}_b$ is a Lagrangian manifold of the reduced source phase space Φ_{\ker} .

Now we turn to the product space. We lift operators \hat{C}_a and \hat{D}_A into operators on the product Hilbert space as in Section 2.1.1. In particular, $(\hat{C}_a^{(12)}(\hat{M}))(|\psi\rangle) = \hat{C}_a \hat{M} |\psi\rangle$ and $(\hat{D}_A^{(12)}(\hat{M}))(|\psi\rangle) = \hat{M} \hat{D}_A |\psi\rangle$ for all $|\psi\rangle \in \mathcal{H}_2$. Since $\text{img } \hat{M}$ and $(\ker \hat{M})_\perp$ are eigenspaces of \hat{C}_a and \hat{D}_A , respectively, \hat{M} is a simultaneous eigenstate of operators $\hat{C}_a^{(12)}$ and $\hat{D}_A^{(12)}$ at eigenvalues μ_c and μ_d . In Section 2.1.1 we expressed the map \hat{M} as the simultaneous eigenstate of a \mathfrak{g}_M^* -valued operator $\hat{\mathbf{O}}_M$ on \mathcal{H}_{12} . We choose a basis of \mathfrak{g}_M^* such that the first $(n_1 - \tilde{n})$ components of $\hat{\mathbf{O}}_M$ are the operators $\hat{C}_a^{(12)}$ and the next $(n_2 - \tilde{n})$ components are the operators $-\hat{D}_A^{(12)}$. We choose to add the negative sign to ensure that the Lie algebra generated by $-\hat{\mathbf{D}}^{(12)}$ on \mathcal{H}_{12} is identical to the Lie algebra generated by $\hat{\mathbf{D}}$ on \mathcal{H}_2 . Thus the operators $\hat{\mathbf{C}}^{(12)}$ and $-\hat{\mathbf{D}}^{(12)}$ generate the Lie group $G_{\text{img}} \times G_{\ker}$ on \mathcal{H}_{12} which is a subgroup of G_M . We express the subspace $(\text{img } \hat{M}) \otimes (\ker \hat{M})_\perp^* \subset \mathcal{H}_{12}$ as the simultaneous eigenspace of $\hat{\mathbf{C}}^{(12)}$ and $-\hat{\mathbf{D}}^{(12)}$ with eigenvalues μ_c and $-\mu_d$,

$$(\text{img } \hat{M}) \otimes (\ker \hat{M})_\perp^* = \left\{ \hat{\mathbf{O}} \in \mathcal{H}_{12} \mid \hat{\mathbf{C}}^{(12)}(\hat{\mathbf{O}}) = \mu_c \hat{\mathbf{O}}, -\hat{\mathbf{D}}^{(12)}(\hat{\mathbf{O}}) = -\mu_d \hat{\mathbf{O}} \right\}. \quad (2.4.18)$$

As in Section 2.1.4, we may lift momentum maps \mathbf{C} and \mathbf{D} to the momentum map $(\mathbf{C}, -\mathbf{D})$ for the group $G_{\text{img}} \times G_{\ker}$ on the product phase space $\Phi_1 \times \Phi_2^*$. The eigenspace conditions in Eq. 2.4.18 translate to level set conditions defining the co-isotropic submanifold of Φ_{12} corresponding to $(\text{img } \hat{M}) \otimes (\ker \hat{M})_\perp^*$,

$$L_{\text{rp}} \equiv \left(\begin{array}{cc} \mathbf{C} & -\mathbf{D} \\ \mu_c & -\mu_d \end{array} \right) \subset \Phi_{12}, \quad (2.4.19)$$

which has dimension $(n_1 + n_2 + 2\tilde{n})$. This is guaranteed to be a co-isotropic manifold since $(\mu_c, -\mu_d)$ is a fixed point of $\mathfrak{g}_{\text{img}}^* \oplus \mathfrak{g}_{\ker}^*$ under the co-adjoint action. We may also consider L_{rp} to be the intersection of the inverse images of $\mathbf{C}^{-1}(\mu_c)$ and $\mathbf{D}^{-1}(\mu_d)$ according the remodeling geometry.

As above, we treat the subspaces $(\text{img } \hat{M}) \otimes (\ker \hat{M})_\perp^*$ as the Hilbert spaces \mathcal{H}_{rp} and form the associated phase spaces Φ_{rp} by symplectic reduction,

$$\Phi_{\text{rp}} \equiv \Phi_1 \times \Phi_2^* // ((\mathbf{C}, -\mathbf{D}) = (\mu_c, -\mu_d)), \quad (2.4.20)$$

where rp stands for ‘‘reduced product.’’ We call Φ_{rp} the ‘‘reduced product phase space’’ and define ι_{rp} and π_{rp} to be the inclusion and projection maps of the reductions, as shown in Figure 2.4.2. The reduced product phase space has dimension $4\tilde{n}$. We may carry out the reduction in two steps, first reducing by \mathbf{C} , which only affects the Φ_1 variables, and then by \mathbf{D} , which only affects the Φ_2 variables. Thus the reduced product phase space is the product space of the reduced phase spaces,

$$\Phi_{\text{rp}} = \Phi_{\text{img}} \times \Phi_{\ker}^*, \quad (2.4.21)$$

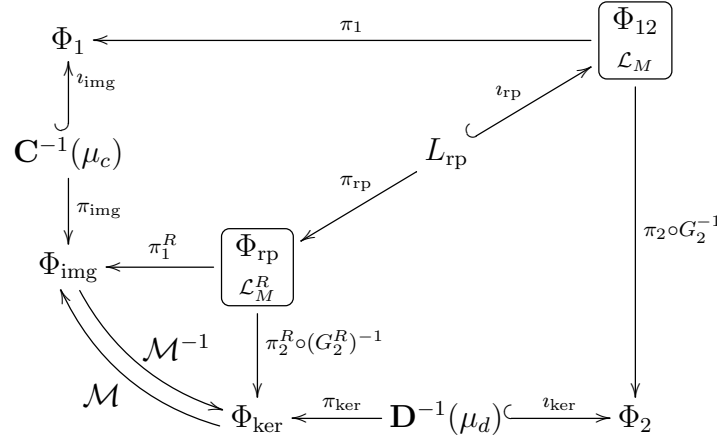


Figure 2.4.2: The core geometry and core symplectomorphism $\mathcal{M} : \Phi_{\text{ker}} \rightarrow \Phi_{\text{img}}$, with $\Phi_{\text{rp}} \equiv \Phi_{\text{img}} \times \Phi_{\text{ker}}^*$ and $L_{\text{rp}} \equiv \mathbf{C}^{-1}(\mu_c) \cap \mathbf{D}^{-1}(\mu_d)$. The left column, bottom row, and diagonal show the symplectic reductions of Φ_1 , Φ_2 , and Φ_{12} , respectively.

with projectors $\pi_1^R : \Phi_{\text{rp}} \rightarrow \Phi_{\text{img}}$ and $\pi_2^R : \Phi_{\text{rp}} \rightarrow \Phi_{\text{ker}}^*$.

The Lagrangian manifold \mathcal{L}_M is a submanifold of L_{rp} and thus the projection $\mathcal{L}_M^R \equiv \pi_{\text{rp}} \mathcal{L}_M$ is a Lagrangian manifold of the reduced product phase space Φ_{img} . We may consider \mathcal{L}_M^R to be the Lagrangian manifold that supports the semiclassical approximation of the core isomorphism \hat{M}_C .

As discussed in Section B.1, the graph of a symplectomorphism is a Lagrangian manifold in a product phase space and furthermore this Lagrangian manifold supports the semiclassical approximation to a unitary operator on the associated Hilbert space. In such a case the transport procedure described in Section 2.2.2 applied to a single point of the source phase space results in a single point of the target phase space, the image of the source phase space point under the symplectomorphism. In fact, it was this observation in Miller [39] that led to our development of the remodeling geometry. Scaling the unitary operator affects structures such as the density that live on the Lagrangian manifold but does not affect the manifold itself. In order to proceed we make the assumption that \hat{M}_C is proportional to an isometry of $\mathcal{H}_{\text{core}}$ and thus $\hat{M}_C = a \hat{U}$ for some constant a and unitary operator \hat{U} . This will be the case for all spin network applications discussed. Under this assumption the reduced Lagrangian manifold \mathcal{L}_M^R associated with the core isomorphism \hat{M}_C may be interpreted as the graph of some symplectic map $\mathcal{M} : \Phi_{\text{ker}} \rightarrow \Phi_{\text{img}}$ which we call the “core symplectomorphism.” Geometrically, given a point $\tilde{z}_2 \in \Phi_{\text{ker}}$, there is a unique point $\tilde{z}_1 \in \Phi_{\text{img}}^R$ such that $(\tilde{z}_1, \tilde{z}_2) \in \mathcal{L}_M^R$. This unique point defines the symplectomorphism, $\tilde{z}_1 = \mathcal{M}(\tilde{z}_2)$. Note that \mathcal{L}_M^R itself is isomorphic as a manifold to Φ_{img} and Φ_{ker} , with the projection maps π_1^R and π_2^R providing the isomorphism.

We collectively refer to the spaces, reductions, and maps described above that are used to form the core symplectomorphism as the “core geometry” associated with \hat{M} . The spaces and maps in the core geometry are shown in Figure 2.4.2.

2.4.5 Momentum Maps in the Core Geometry

For the following discussion we define local Darboux coordinates $\tilde{z}_1 = (q_\ell, p_\ell)$ on Φ_{img} and $\tilde{z}_2 = (Q_\ell, P_\ell)$ on Φ_{ker} . These provide coordinates $\tilde{z}_{12} = (\tilde{z}_1, \tilde{z}_2) = (q_\ell, p_\ell; Q_\ell, P_\ell)$ on Φ_{rp} in which the symplectic form is $\omega_{\text{rp}} = \sum_\ell dp_\ell \wedge dq_\ell - dP_\ell \wedge dQ_\ell$. Treating q_ℓ and p_ℓ as coordinate functions $:\Phi_{\text{img}} \rightarrow \mathbb{R}$, we may use the symplectic core to define the $2\tilde{n}$ functions

$$M_{q,\ell}^R : \Phi_{\text{rp}} \rightarrow \mathbb{R} : (\tilde{z}_1, \tilde{z}_2) \mapsto q_\ell(\tilde{z}_1) - q_\ell(\mathcal{M}(\tilde{z}_2)), \quad (2.4.22)$$

$$M_{p,\ell}^R : \Phi_{\text{rp}} \rightarrow \mathbb{R} : (\tilde{z}_1, \tilde{z}_2) \mapsto p_\ell(\tilde{z}_1) - p_\ell(\mathcal{M}(\tilde{z}_2)), \quad (2.4.23)$$

These may be combined into the two \tilde{n} -component functions $\mathbf{M}_q^R, \mathbf{M}_p^R : \Phi_{\text{rp}} \rightarrow \mathbb{R}^{\tilde{n}}$. Since \mathcal{L}_M^R was defined to be the graph of the symplectomorphism \mathcal{M} , it is the simultaneous level set,

$$\mathcal{L}_M^R = \begin{pmatrix} \mathbf{M}_q^R & \mathbf{M}_p^R \\ \mathbf{0} & \mathbf{0} \end{pmatrix}. \quad (2.4.24)$$

The symplectic nature of \mathcal{M} ensures that these $2\tilde{n}$ functions all mutually Poisson commute on Φ_{rp} .

In Eq. 2.4.7, a basis of \mathfrak{g}_B^* was chosen that split the operators $\hat{\mathbf{B}}$ into the ordered set $\{\hat{\mathbf{D}}, \hat{B}_\ell\}$. We assume that the Lie algebra G_B may be expressed as a Cartesian product $G_{\text{ker}} \times G_{\text{core}}$ and choose a basis so that the functions \hat{B}_ℓ generate the Lie group G_{core} on \mathcal{H}_2 . This assumption will be true for our spin network applications. Let $\hat{\mathbf{B}}' : \mathcal{H}_2 \rightarrow \mathfrak{g}_{\text{core}} \times \mathcal{H}_2$ be the $\mathfrak{g}_{\text{core}}$ -valued operator on the source space whose \tilde{n} components are \hat{B}_ℓ . The prime on $\hat{\mathbf{B}}'$ is used to distinguish it from the full \mathfrak{g}_B^* -valued operator defined in Eq. 2.1.4. The momentum map \mathbf{B} on Φ_2 splits into component functions \mathbf{D} and B_ℓ ($\ell = 1 \cdots \tilde{n}$) and the generalized momentum μ_b splits into $(\mu_d, \mu_{b,\ell})$. The \tilde{n} functions B_ℓ are components of a G_{core} momentum map \mathbf{B}' and the values $\mu_{b,\ell}$ are components of the generalized momentum $\mu_b^R \in \mathfrak{g}_{\text{core}}$ so that the b -manifold may be expressed as the level set

$$\mathcal{L}_b = \begin{pmatrix} \mathbf{D} & \mathbf{B}' \\ \mu_d & \mu_b^R \end{pmatrix}. \quad (2.4.25)$$

The Cartesian product decomposition of G_B ensures that the momentum map \mathbf{B}' is constant under the flows generated by \mathbf{D} and thus projects down under the reduction to \mathbf{B}^R on Φ_{ker} . Alternatively, we may define the functions B_ℓ^R as the Weyl symbols of operators \hat{B}_ℓ on \mathcal{H}_{ker} and then let B_ℓ be the local extension of B_ℓ^R into a neighborhood of $\mathbf{D}^{-1}(\mu_d)$ as discussed later on. In terms of these functions,

$$\mathcal{L}_b^R = \begin{pmatrix} \mathbf{B}^R \\ \mu_b^R \end{pmatrix} \quad (2.4.26)$$

The core symplectomorphism \mathcal{M} induces a symplectic action φ^{img} of G_{core} on Φ_{img} by conjugation of the symplectic action φ^{ker} of G_{core} on Φ_{ker} ,

$$\varphi_g^{\text{img}} \equiv \mathcal{M} \circ \varphi_g^{\text{ker}} \circ \mathcal{M}^{-1}, \quad \forall g \in G_{\text{core}}. \quad (2.4.27)$$

Let X_ℓ^{img} be the infinitesimal generators of φ^{img} corresponding to the basis vectors ξ_ℓ of $\mathfrak{g}_{\text{core}}^*$. Since \mathcal{M} is a symplectomorphism it preserves the symplectic structure, $\omega_{\text{img}} = \mathcal{M}^* \omega_{\text{ker}}$ and $X_\ell^{\text{img}} = \mathcal{M}_* X_\ell^{\text{ker}}$. Therefore the momentum map β^R is the pull-back of \mathbf{B}^R ,

$$\beta^R \equiv \mathbf{B}^R \circ \mathcal{M}^{-1} : \Phi_{\text{img}} \rightarrow \mathfrak{g}_{\text{core}}^*. \quad (2.4.28)$$

We now show that the level set $[\beta^R]^{-1}(\mu_b^R)$ is identical to the reduced β -manifold \mathcal{L}_β^R . Since \mathcal{L}_β may be obtained by transporting \mathcal{L}_b using \mathcal{L}_M , the reduced manifold \mathcal{L}_β^R may be obtained by transporting \mathcal{L}_b^R using \mathcal{L}_M^R . Since \mathcal{L}_M^R is the graph of \mathcal{M} , the transport procedure implies that the points of \mathcal{L}_β^R and \mathcal{L}_b^R are in one-to-one correspondence and $\mathcal{M}(\mathcal{L}_b^R) = \mathcal{L}_\beta^R$. Let $\tilde{z}_1 \in \mathcal{L}_\beta^R$. Then $\beta^R(\tilde{z}_1) = \mathbf{B}^R(\mathcal{M}^{-1}(\tilde{z}_1)) = \mathbf{B}^R(\tilde{z}_2)$. Since \tilde{z}_2 must be in \mathcal{L}_b^R , $\mathbf{B}^R(\tilde{z}_2) = \mu_b^R$ and thus \mathcal{L}_β^R is a subset of the level set $[\beta^R]^{-1}(\mu_b^R)$. Conversely, consider a point $\tilde{z}_1 \in [\beta^R]^{-1}(\mu_b^R)$. By Eq 2.4.28, $\mathbf{B}^R(\mathcal{M}^{-1}(\tilde{z}_1)) = \mu_b^R$. Therefore $\mathcal{M}^{-1}(\tilde{z}_1)$ is in the level set $[\mathbf{B}^R]^{-1}(\mu_b^R)$ which is the manifold \mathcal{L}_b^R . We may then conclude that \tilde{z}_1 is point of \mathcal{L}_β^R since $\mathcal{M}(\tilde{z}_2) \in \mathcal{L}_\beta^R$ for all $\tilde{z}_2 \in \mathcal{L}_b^R$. Thus the level set is both a subset and a superset of \mathcal{L}_β^R and we may conclude

$$\mathcal{L}_\beta^R = \left(\begin{array}{c} \beta^R \\ \mu_b^R \end{array} \right). \quad (2.4.29)$$

Now we construct the extensions of functions in the core geometry into neighborhoods of the level sets of the reduction. The main reason we need to do this is so that we can take Poisson brackets of these functions in the next section. First consider some phase space Φ with a symplectic group action under group G with an Ad^* -equivariant momentum map \mathbf{P} and the symplectic reduction $\Phi^R = \Phi // (\mathbf{P} = \mu)$ for some generalized momentum $\mu \in \mathfrak{g}^*$. A function A on Φ may be projected down to Φ^R if it is constant on the isotropy subgroup orbits of G in the level set $\mathbf{P}^{-1}(\mu)$. Conversely, we may lift a function A^R from the reduced space into $\mathbf{P}^{-1}(\mu)$ by demanding that the lifted function be constant along the isotropy subgroup orbits. We actually consider a broader definition of the lift and demand that the lifted function A be fully G -invariant in the space of G -orbits that intersect $\mathbf{P}^{-1}(\mu)$. In terms of Poisson brackets this means that $\{A, \mathbf{P}\} = 0$. Consider two functions G -invariant functions A_i and A_j on $\mathbf{P}^{-1}(\mu)$. The Poisson bracket $\{A_i, A_j\}$ is then also a G -invariant function as a result of the Jacobi identity. Since A_i , A_j , and $\{A_i, A_j\}$ are G -invariant, they may be projected down to the reduced space functions A_i^R , A_j^R , and $\{A_i, A_j\}^R$. The projection of the Poisson bracket is then the Poisson bracket of the projection, $\{A_i, A_j\}^R = \{A_i^R, A_j^R\}$ [56]. Thus the lifting procedure described above ensures that, when evaluated on the level set, the Poisson bracket of lifted functions is identical to the Poisson bracket of the functions on the reduced space.

Consider the reduced space Φ_{img} with local Darboux coordinates (q_ℓ, p_ℓ) . Lift these coordinates into $\mathbf{C}^{-1}(\mu_c)$ as defined above. We may then locally define new Darboux coordinates $(q_\ell, p_\ell; \tilde{q}_a, \tilde{p}_a)$ in Φ_1 for points on $\mathbf{C}^{-1}(\mu_c)$. If G_{img} is an Abelian group, as it will be in spin network applications, then these extra coordinates may be taken to be the momentum map components $\mu_{c,a}$ and their conjugate angles $\vartheta_{c,a}$. We define the lift of a function into a

neighborhood of $\mathbf{C}^{-1}(\mu_c)$ so that the function is locally independent of these new coordinates on $\mathbf{C}^{-1}(\mu_c)$. For an Abelian group the lift as defined earlier is already independent of the conjugate angles $\vartheta_{c,a}$. We may construct similar lifts for the source space and product space. Again, the reduction groups for these spaces are Abelian in our spin network applications.

Let $M_{q,\ell}$ and $M_{p,\ell}$ be the extensions of functions $M_{q,\ell}^R$ and $M_{p,\ell}^R$ defined in a neighborhood of L_{rp} . The $2\tilde{n}$ functions $M_{q,\ell}$ and $M_{p,\ell}$ all mutually Poisson commute on L_{rp} and furthermore Poisson commute with \mathbf{C} and \mathbf{D} on L_{rp} . Therefore we may choose a basis of \mathfrak{g}_M^* such that the components of the momentum map \mathbf{M} are the ordered set $\{C_a, D_A, M_{q,\ell}, M_{p,\ell}\}$ and express \mathcal{L}_M as

$$\mathcal{L}_M = \begin{pmatrix} \mathbf{C} & \mathbf{D} & \mathbf{M}_q & \mathbf{M}_p \\ \mu_c & \mu_d & \mathbf{0} & \mathbf{0} \end{pmatrix}. \quad (2.4.30)$$

Similarly, we construct the extension β' in a neighborhood of $\mathbf{C}^{-1}(\mu_c)$ whose components are the extensions of the components of β^R . In terms of β' we may express the β -manifold as

$$\mathcal{L}_\beta = \begin{pmatrix} \mathbf{C} & \beta' \\ \mu_c & \mu_b^R \end{pmatrix}. \quad (2.4.31)$$

The component functions β_ℓ correspond to the observables $\hat{\beta}_\ell$ and Eq. 2.4.31 is the semi-classical version of Eq. 2.4.12.

2.4.6 The Density on \mathcal{L}_β Using β

Consider the x -representation wavefunction for the β -state $\psi_\beta(x)$ defined in Eq. 2.1.13. As discussed in Section 2.1.3, the phase function $S_\beta(x)$ of $\psi_\beta(x)$ generates the Lagrangian manifold $\mathcal{L}_\beta \subset \Phi_1$. Let \mathcal{L}_β be described as the level set of momentum map β as discussed in Section 2.1.4 and construct the density $\sigma_\beta \in \Omega^{n_1}(\mathcal{L}_\beta)$ as in Eq. C.2.2. Each x -representation branch (indexed by k) of \mathcal{L}_β carries a density function $\Omega_{\beta,k}(x)$ defined by

$$\sigma_\beta|_z = \Omega_{\beta,k}(x) dx_1 \wedge \cdots \wedge dx_{n_1}, \quad (2.4.32)$$

where x is a point of configuration space (with coordinates x_1, \cdots, x_{n_1}) and $z_1 \in \mathcal{L}_\beta$ is the point on the k -th branch of \mathcal{L}_β over point x . The density functions are expressed in terms of an $n_1 \times n_1$ -matrix of Poisson brackets,

$$\Omega_{\beta,k}(x) = \left(\det [\{x_i, \beta_j\}]_{z_1} \right)^{-1}. \quad (2.4.33)$$

Choose an ordered bases of \mathfrak{g}_b , \mathfrak{g}_M , and \mathfrak{g}_β such that the components of the momentum maps \mathbf{B} , \mathbf{M} , and β decompose into the ordered sets (D_A, B_ℓ) , $(C_a, -D_A, M_{q,\ell}, M_{p,\ell})$, and (C_a, β_ℓ) , respectively. The manifolds \mathcal{L}_b , \mathcal{L}_M , and \mathcal{L}_β are thus expressed in terms of the level sets 2.4.25, 2.4.30, and 2.4.31 and the density functions on \mathcal{L}_β are

$$\Omega_{\beta,k}(x) = \frac{1}{\det [\{x_i, C_a\} | \{x_i, \beta_\ell\}]_{z_1}}. \quad (2.4.34)$$

We want to show that Eq. 2.4.34 is the same as the result from the WKB evaluation. The manifolds \mathcal{L}_b and \mathcal{L}_M share a common symmetry group G_{\ker} and thus the analysis of Section 2.3.2 must be used to find the WKB density functions. Comparing with the notation of that section, $-\mathbf{D}$ serves as the common symmetry group momentum map \mathbf{H} , functions B_ℓ serve as the other components $B_{\tilde{I}}$ of momentum map \mathbf{B} and $(C_a, M_{q,\ell}, M_{p,\ell})$ serve as the other components $M_{\tilde{\alpha}}$ of momentum map \mathbf{M} . Therefore the matrix of Poisson brackets in Eq. 2.3.9 becomes the $(n_1 + \tilde{n}) \times (n_1 + \tilde{n})$ -matrix W ,

$$W = \left[\begin{array}{c|c|c} \{x_i, C_a\} & \{x_i, M_{q,\ell}\} & \{x_i, M_{p,\ell}\} \\ \hline \{-B_\ell, C_a\} & \{-B_\ell, M_{q,\ell'}\} & \{-B_\ell, M_{p,\ell'}\} \end{array} \right], \quad (2.4.35)$$

where the double lines separate the rows and columns of the matrix into sets of n_1 and \tilde{n} entries and the single line separates the first n_1 rows into $(n_1 - \tilde{n})$ and \tilde{n} rows. The Poisson brackets in 2.4.35 are all to be evaluated at a point $z_{\tilde{k}}$ of the intersection manifold $\mathcal{I} \in \Phi_{12}$. The intersection manifold is naturally subset of the level set L_{rp} and so we evaluate these brackets using the local coordinates $(q_\ell, p_\ell; \tilde{q}_a, \tilde{p}_a; Q_\ell, P_\ell; \tilde{Q}_A, \tilde{P}_A)$, where (q_ℓ, p_ℓ) and (Q_ℓ, P_ℓ) on L_{rp} project to Darboux coordinates on the reduced spaces Φ_{img} and Φ_{\ker} . In these coordinates the symplectic form on Φ_{12} near L_{rp} is

$$\omega_{12} = \sum_{\ell=1}^{\tilde{n}} (dp_\ell \wedge dq_\ell - dP_\ell \wedge dQ_\ell) + \sum_{a=1}^{n_1-\tilde{n}} d\tilde{p}_a \wedge d\tilde{q}_a - \sum_{A=1}^{n_2-\tilde{n}} d\tilde{P}_A \wedge d\tilde{Q}_A. \quad (2.4.36)$$

We now start evaluating the Poisson brackets in the block matrix W to show that $\det W$ is equal to the determinant in Eq. 2.4.34. The functions C_a only depend on the Φ_1 -coordinates and the functions B_i only depend on the Φ_2 -coordinates, so the Poisson brackets $\{-B_\ell, C_a\}$ are all zero. Next we consider the Poisson brackets $\{x_i, M_{q,\ell}\}$ evaluated at points $z_{\tilde{k}}$. By the choice of extension of functions $M_{q,\ell}^R$ into $M_{p,\ell}$, the partial derivatives of $M_{q,\ell}$ with respect to variables $\tilde{q}_a, \tilde{p}_a, \tilde{Q}_A$, and \tilde{P}_A at $z_{\tilde{k}}$ are all zero. Furthermore, the functions x_i are independent of all Φ_2 variables so the bracket simplifies to

$$\{x_i, M_{q,\ell}\} = \frac{\partial x_i}{\partial q_{\ell'}} \frac{\partial M_{q,\ell}}{\partial p_{\ell'}} - \frac{\partial x_i}{\partial p_{\ell'}} \frac{\partial M_{q,\ell}}{\partial q_{\ell'}}. \quad (2.4.37)$$

The definition of $M_{q,\ell}$ ensures that the partial derivatives $\partial M_{q,\ell}/\partial q_{\ell'}$ and $\partial M_{q,\ell}/\partial p_{\ell'}$ when evaluated at points $z_{\tilde{k}} \in \mathcal{I}$ are equal to the partial derivatives $\partial M_{q,\ell}^R/\partial q_{\ell'}$ and $\partial M_{q,\ell}^R/\partial p_{\ell'}$ of the reduced functions on Φ_{rp} evaluated at $\pi_{\text{rp}}(z_{\tilde{k}})$. Using Eq. 2.4.22 for the definition of $M_{q,\ell}^R$ gives $\partial M_{q,\ell}/\partial p_{\ell'} = \partial q_\ell/\partial p_{\ell'} = 0$ and $\partial M_{q,\ell}/\partial q_{\ell'} = \partial q_\ell/\partial q_{\ell'} = \delta_{\ell\ell'}$. Therefore Eq. 2.4.37 simplifies to $\{x_i, M_{q,\ell}\} = -\partial x_i/\partial p_\ell$. A similar calculation shows $\{x_i, M_{p,\ell}\} = \partial x_i/\partial q_\ell$.

The functions B_ℓ and M_ℓ^q are lifts from the reduced space so their Poisson bracket in the product space at $z_{\tilde{k}}$ is equal to the Poisson bracket in the reduced space,

$$\{B_\ell, M_{q,\ell'}\} = \{B_\ell^R, M_{q,\ell'}^R\} = -\frac{\partial B_\ell}{\partial Q_{\ell''}} \frac{\partial M_{q,\ell'}}{\partial P_{\ell''}} + \frac{\partial B_\ell}{\partial P_{\ell''}} \frac{\partial M_{q,\ell'}}{\partial Q_{\ell''}}. \quad (2.4.38)$$

By Eq. 2.4.28 the functions B_ℓ^R may be expressed as $\beta_\ell^R \circ \mathcal{M}$ so by the chain rule,

$$\frac{\partial B_\ell^R}{\partial Q_{\ell''}} = \frac{\partial \beta_\ell^R}{\partial q_{\tilde{\ell}}} \frac{\partial (q_\ell \circ \mathcal{M})}{\partial Q_{\ell''}} + \frac{\partial \beta_\ell^R}{\partial p_{\tilde{\ell}}} \frac{\partial (p_\ell \circ \mathcal{M})}{\partial Q_{\ell''}}, \quad (2.4.39)$$

where q_ℓ and p_ℓ are considered to be coordinate functions on Φ_{img} . By Eqs. 2.4.22 and 2.4.23 we may express the partial derivatives of the coordinate components of $\partial(q_\ell \circ \mathcal{M})/\partial Q_{\ell''}$ and $\partial(p_\ell \circ \mathcal{M})/\partial Q_{\ell''}$ as $-\partial M_{q,\ell}^R/\partial Q_{\ell''}$ and $-\partial M_{p,\ell}^R/\partial Q_{\ell''}$. Similar expressions hold for derivative with respect to P_ℓ . Therefore the right-hand side of Eq. 2.4.38 becomes

$$+ \left(\frac{\partial \beta_\ell^R}{\partial q_{\tilde{\ell}}} \frac{\partial M_{q,\ell}^R}{\partial Q_{\ell''}} + \frac{\partial \beta_\ell^R}{\partial p_{\tilde{\ell}}} \frac{\partial M_{p,\ell}^R}{\partial Q_{\ell''}} \right) \frac{\partial M_{q,\ell'}^R}{\partial P_{\ell''}} - \left(\frac{\partial \beta_\ell^R}{\partial q_{\tilde{\ell}}} \frac{\partial M_{q,\ell}^R}{\partial P_{\ell''}} + \frac{\partial \beta_\ell^R}{\partial p_{\tilde{\ell}}} \frac{\partial M_{p,\ell}^R}{\partial P_{\ell''}} \right) \frac{\partial M_{q,\ell'}^R}{\partial Q_{\ell''}}. \quad (2.4.40)$$

Consider the coefficients of $\partial \beta_\ell^R / \partial q_{\tilde{\ell}}$,

$$\frac{\partial M_{q,\ell}^R}{\partial Q_{\ell''}} \frac{\partial M_{q,\ell'}^R}{\partial P_{\ell''}} - \frac{\partial M_{q,\ell}^R}{\partial P_{\ell''}} \frac{\partial M_{q,\ell'}^R}{\partial Q_{\ell''}}. \quad (2.4.41)$$

Using the fact that the Poisson brackets $\{M_{q,\ell}^R, M_{q,\ell'}^R\}$ vanish at the relevant evaluation points we may re-express 2.4.41 as,

$$\frac{\partial M_{q,\ell}^R}{\partial q_{\ell''}} \frac{\partial M_{q,\ell'}^R}{\partial p_{\ell''}} - \frac{\partial M_{q,\ell}^R}{\partial p_{\ell''}} \frac{\partial M_{q,\ell'}^R}{\partial q_{\ell''}}. \quad (2.4.42)$$

Since $\frac{\partial M_{q,\ell}^R}{\partial p_{\ell''}} = 0$ the terms of 2.4.40 containing $\partial \beta_\ell^R / \partial q_{\tilde{\ell}}$ cancel out. The coefficients of $\partial \beta_\ell^R / \partial p_{\tilde{\ell}}$ similarly may be expressed as

$$\frac{\partial M_{p,\ell}^R}{\partial q_{\ell''}} \frac{\partial M_{q,\ell'}^R}{\partial p_{\ell''}} - \frac{\partial M_{p,\ell}^R}{\partial p_{\ell''}} \frac{\partial M_{q,\ell'}^R}{\partial q_{\ell''}}. \quad (2.4.43)$$

The first term vanishes but $\partial M_{q,\ell}^R / \partial q_{\ell''} = \partial M_{p,\ell}^R / \partial p_{\ell''} = \delta_{\ell\ell''}$ and thus the second term becomes $\delta_{\tilde{\ell}\ell''} \delta_{\ell'\ell''}$. Therefore Eq. 2.4.38 evaluates to

$$\{B_\ell, M_{q,\ell'}\} = -\frac{\partial \beta_\ell^R}{\partial p_{\ell'}}. \quad (2.4.44)$$

A similar calculation shows

$$\{B_\ell, M_{p,\ell'}\} = \frac{\partial \beta_\ell^R}{\partial q_{\ell'}}. \quad (2.4.45)$$

Therefore the matrix of Poisson brackets 2.4.35 simplifies to

$$\left[\begin{array}{c|c|c} \{x_i, C_a\} & -\frac{\partial x_i}{\partial p_\ell} & +\frac{\partial x_i}{\partial q_\ell} \\ \hline 0 & \frac{\partial \beta_\ell^R}{\partial p_{\ell'}} & -\frac{\partial \beta_\ell^R}{\partial q_{\ell'}} \end{array} \right]. \quad (2.4.46)$$

The top block of rows contains n_1 rows and the bottom block contains \tilde{n} rows. From left to right, the three blocks of columns contain $n_1 - \tilde{n}$, \tilde{n} , and \tilde{n} columns. To simplify this matrix, consider the determinant of the following similar block matrix,

$$W = \left[\begin{array}{c|c|c} A & E & B \\ \hline 0 & -C & -D \end{array} \right], \quad (2.4.47)$$

where we will assume that D is an invertible matrix. First we decompose 2.4.47 into the product of two block matrices,

$$W = \left[\begin{array}{c|c} Id_{n_1} & B \\ \hline 0 & -D \end{array} \right] \left[\begin{array}{c|c|c} A & E - BD^{-1}C & 0 \\ \hline 0 & D^{-1}C & Id_{\tilde{n}} \end{array} \right]. \quad (2.4.48)$$

Since both matrices are block-triangular the determinant $\det W$ simplifies to

$$\det W = (-1)^{\tilde{n}} (\det D) \det [A \mid E - BD^{-1}C] \quad (2.4.49)$$

We interpret $\det D$ as the determinant of an $n_1 \times n_1$ -matrix

$$\det D = \left[\begin{array}{c|c} Id_{n_1 - \tilde{n}} & 0 \\ \hline 0 & D^\top \end{array} \right]. \quad (2.4.50)$$

Eq. 2.4.50 may be used in 2.4.49 to express $\det W$ as the determinant of the single $\tilde{n} \times \tilde{n}$ -matrix

$$[A \mid E - BD^{-1}C] \det \left[\begin{array}{c|c} Id_{n_1 - \tilde{n}} & 0 \\ \hline 0 & D^\top \end{array} \right] = [A \mid ED^\top - BD^{-1}CD^\top]. \quad (2.4.51)$$

The matrix CD^\top is the product of partial derivative matrices $\frac{\partial \beta_\ell^R}{\partial p_{\ell''}} \frac{\partial \beta_{\ell'}^R}{\partial q_{\ell''}}$. Since the functions β_ℓ^R all mutually Poisson commute the order of the $p_{\ell''}$ and $q_{\ell''}$ derivatives may be flipped and thus $CD^\top = DC^\top$. Therefore the matrix $BD^{-1}CD^\top$ in 2.4.51 simplifies to BC^\top .

The above results allow the determinant of matrix 2.4.46 to be expressed as

$$\det W = (-1)^{\tilde{n}} \det \left[\{x_i, C_a\} \mid -\frac{\partial x_i}{\partial p_\ell} \frac{\partial \beta_{\ell'}^R}{\partial q_\ell} + \frac{\partial x_i}{\partial q_\ell} \frac{\partial \beta_{\ell'}^R}{\partial p_\ell} \right], \quad (2.4.52)$$

By definition of the extension of β^R on Φ_{img} into β' in a neighborhood of $\mathbf{C}^{-1}(\mu_c)$, the right-hand block in the above matrix is equal to the matrix of Poisson brackets $\{x_i, \beta_\ell\}$ on the target phase space Φ_1 . Similarly we may interpret $\{x_i, C_a\}$ as a matrix of Poisson brackets on Φ_1 rather than Φ_{12} . Thus the density functions 2.3.9 are

$$\tilde{\Omega}_{\beta, \tilde{k}}(x) = \frac{(-1)^{\tilde{n}}}{\det \left[\begin{array}{c} \{x_i, M_{\tilde{\alpha}}\} \\ \{B_{\tilde{I}}, M_{\tilde{\alpha}}\} \end{array} \right]_{z_{\tilde{k}}}} = \frac{1}{\left[\{x_i, C_a\} \mid \{x_i, \beta_\ell\} \right]_{z_1}}, \quad (2.4.53)$$

where the Poisson brackets in the first expression are evaluated in the product space at $z_{\tilde{k}}$ and the Poisson brackets in the second expression are evaluated in the target space at z_1 . The density functions $\tilde{\Omega}_{\beta, \tilde{k}}(x)$ determined from the WKB approximation of the matrix element $\langle x | \hat{M} | b \rangle$ are identical to the density functions $\Omega_{\beta, k}(x)$ in Eq. 2.4.34 from the WKB approximation of the inner product $\langle x | \beta \rangle$ using the observables $\hat{\beta}$ and momentum maps β defined in Sections 2.4.2 and 2.4.5. Note that Eq. 2.4.53 is true for all \mathcal{I} branches ρ and thus the density functions on the target space are independent of the index ρ and only need to be indexed by the x -representation branch index k . Thus the combined index \tilde{k} on the amplitudes A_β and density functions Ω_β defined in Eqs. 2.3.3 and 2.3.4 may be replaced by the single branch index k and the \mathcal{I} branch index on the density σ_β in Eq. 2.3.5 may be dropped.

The above analysis hold when the x -representation momentum map components x_i are replaced with the components of \mathbf{A} ,

$$\frac{(-1)^{\tilde{n}}}{\det \left[\begin{array}{c} \{A_i, M_{\tilde{\alpha}}\} \\ \{B_{\tilde{I}}, M_{\tilde{\alpha}}\} \end{array} \right]_{z_{\tilde{k}}}} = \frac{1}{\left[\{A_i, C_a\} \mid \{A_i, \beta_\ell\} \right]_{z_1}}. \quad (2.4.54)$$

The amplitude determinants in the stationary phase evaluation of the inner products 2.1.36 and 2.1.41 may be considered to be the amplitude functions in the local “ \mathbf{A} ” representation [54]. The amplitude determinants, assuming no non-trivial common symmetry group in the target space model, are

$$\Omega^{(1)}(z_{1,k}) = \frac{1}{\left[\{A_i, C_a\} \mid \{A_i, \beta_\ell\} \right]_{z_{1,k}}}, \quad (2.4.55)$$

$$\tilde{\Omega}^{(12)}(z_{\tilde{k}}) = \frac{(-1)^{\tilde{n}}}{\det \left[\begin{array}{c} \{A_i, M_{\tilde{\alpha}}\} \\ \{B_{\tilde{I}}, M_{\tilde{\alpha}}\} \end{array} \right]_{z_{\tilde{k}}}}, \quad (2.4.56)$$

where $z_{1,k} = \pi_1(z_{\tilde{k}})$. By Eq. 2.4.54, $\Omega^{(1)}(z_{1,k}) = \tilde{\Omega}^{(12)}(z_{\tilde{k}})$. A similar analysis holds when there is a non-trivial common symmetry group in the target space model, which requires the elimination of the momentum map components for the common symmetry group in both Eq. 2.4.55 and Eq. 2.4.56. Therefore we may conclude that the target space amplitude determinants are identical to the product space amplitude determinants,

$$\tilde{\Omega}^{(1)}(z_{1,k}) = \tilde{\Omega}^{(12)}(z_{\tilde{k}}). \quad (2.4.57)$$

2.5 Phases in the Remodeling Geometry

Now we turn to a calculation of the phases φ^1 and φ^{12} that occur in the stationary phase results in Eqs. 2.1.36 and 2.1.39. The goal of this section is to demonstrate that the relative phases that occur in terms of these stationary phase evaluations are equal.

In Section 2.5.1 the relative phases and stationary phase sets for the models in the remodeling geometry are defined. The relative phases calculations depend on closed paths, which are defined in Section 2.5.2. The relative phases contain three main terms, an action integral, a Maslov index, and a signature index. We show that the difference in relative phases between the two models is zero in three steps. First in Section 2.5.3 we show that the action integrals around the paths defined in Section 2.5.2 are equal. Then the Maslov indices are analyzed in Section 2.5.4 and ultimately combined and re-expressed as a single signature index. Finally in Section 2.5.5 the signature indices are all combined into a single term which evaluates to zero. Once the equality of the target and product space relative phases is proven we prove in Section 2.5.6 that, if \mathcal{L}_M is a quantized manifold, then the transport of a quantized Lagrangian manifold is itself a quantized manifold.

In the following we assume that the source and target phase space manifolds Φ_1 and Φ_2 are isomorphic to \mathbb{R}^{2n} for some n and thus $\Phi_1 \cong \mathbb{R}^{2n_1}$, $\Phi_2 \cong \mathbb{R}^{2n_2}$, and $\Phi_{12} \cong \mathbb{R}^{2(n_1+n_2)}$. This is certainly the case in spin network applications, where the target, source, and product spaces are products of the Schwinger phase spaces defined in Section A.2, which are isomorphic to \mathbb{R}^4 . It is worth noting that symplectic reductions of these phase spaces will, in general, have other topologies. However, this will not affect the analysis in this section.

2.5.1 Relative Phases

Let $I^{(12)}$ and $I^{(1)}$ be the stationary phase sets of the product and target phase space models in the remodeling geometry as discussed in Section 2.1.5,

$$I^{(12)} = \mathcal{L}_{ab} \cap \mathcal{L}_M, \quad I^{(1)} = \mathcal{L}_a \cap \mathcal{L}_\beta. \quad (2.5.1)$$

The target model stationary phase set $I^{(1)}$ is the projection of the product model stationary phase set $I^{(12)}$, as we now demonstrate. Since \mathcal{L}_{ab} is a subset of the inverse image $\pi_2^{-1}(\mathcal{L}_b)$, $I^{(12)}$ is a subset of the intersection manifold of the transport \mathcal{I} defined in Eq. 2.2.10. By the geometric construction of the transported manifold in Eq. 2.2.13, the projection $\pi_1(I^{(12)})$ is a subset of \mathcal{L}_β . Similarly, since $\pi_1(\mathcal{L}_{ab}) = \mathcal{L}_a$, the projection $\pi_1(I^{(12)})$ is a subset of \mathcal{L}_a . Therefore $\pi_1(I^{(12)}) \subset I^{(1)}$. Conversely, consider a point $z_1 \in I^{(1)}$. Since $z_1 \in \mathcal{L}_\beta$, the transport procedure ensures that there exists at least one point $z_{12} \in \mathcal{I}$ such that $\pi_1(z_{12}) = z_1$. By definition of \mathcal{I} , $z_{12} \in \mathcal{L}_M$ and $z_{12} \in \pi_2^{-1}(\mathcal{L}_b)$. Furthermore, since $z_1 \in \mathcal{L}_a$, this z_{12} lies in $\pi_1^{-1}\mathcal{L}_a$ and therefore $z_{12} \in \pi_1^{-1}(\mathcal{L}_a) \cap \pi_2^{-1}(\mathcal{L}_b) = \mathcal{L}_{ab}$. Thus $I^{(1)} \subset \pi_1(I^{(12)})$ and we may conclude that $\pi_1(I^{(12)}) = I^{(1)}$.

For the following analysis we use indices i and j to label points in the stationary phase sets. Let $z_i \in I^{(12)}$ and define $z_{1,i} = \pi_1(z_i)$ and $z_{2,i} = \pi_2(z_i)$. We use a subscript ‘1’ and ‘2’ to refer to target and source phase space points and assume that z without a subscript is a product phase space point. Let φ_i^{12} be the phase of the term in Eq. 2.1.39 for stationary phase point z_i in the product space and let φ_i^1 be the phase of the term in Eq. 2.1.36 for stationary phase point $z_{1,i}$ in the target space. Given a pair of points z_i and z_j in $I^{(12)}$, define the relative phase in the product space as $\Delta\varphi_{ij}^{12} \equiv \varphi_j^{12} - \varphi_i^{12}$ and the relative phase in the target space as $\Delta\varphi_{ij}^1 \equiv \varphi_j^1 - \varphi_i^1$.

Let Γ_{ij}^{12} be a closed path required to start at $z_i \in I^{(12)}$, travel along the M -manifold to $z_j \in I^{(12)}$, and then travel back to z_i along the ab -manifold. Similarly, let the path Γ_{ij}^1 be a closed path required to start at $z_{1,i} \in I^{(1)}$, travel along the β -manifold to $z_{1,j} \in I^{(1)}$, and then travel back to $z_{1,i}$ along the a -manifold. Then the relative phases may be computed as in Eq. C.5.7,

$$\Delta\varphi_{ij}^{12} = \oint_{\Gamma_{ij}^{12}} \theta_{12} - \mu(\Gamma_{ij}^{12}) \frac{\pi}{2} + \Delta\sigma(M, ab) \frac{\pi}{4}, \quad (2.5.2)$$

$$\Delta\varphi_{ij}^1 = \oint_{\Gamma_{ij}^1} \theta_1 - \mu(\Gamma_{ij}^1) \frac{\pi}{2} + \Delta\sigma(\beta, a) \frac{\pi}{4}, \quad (2.5.3)$$

where in both equations the first term is the action integral around the closed path, the second term is the Maslov index that is accumulated around the path, and the last term is the difference in the signature index between the two stationary phase points.

2.5.2 Paths in the Remodeling Geometry

To show the relationship between $\Delta\varphi_{ij}^1$ and $\Delta\varphi_{ij}^{12}$ we first need to construct the target and product space paths that are used in Eqs. 2.5.3 and 2.5.2. We start with a given target space path and use that path to construct a related product space path. We then show that the relative phases are equal for these related paths. Once we have that result, we may use the quantization conditions on the manifolds in the remodeling geometry to argue that $\Delta\varphi_{ij}^{12} = \Delta\varphi_{ij}^1 \bmod 2\pi$ for *any* path Γ_{ij}^{12} that starts at z_i , travels to z_j along \mathcal{L}_M , and then travels back to z_i along \mathcal{L}_{ab} .

Let $\Gamma_{ij}^{(a)} \subset \mathcal{L}_a$ be a path from $z_{1,i}$ to $z_{1,j}$ on \mathcal{L}_a . Similarly let $\Gamma_{ij}^{(\beta)} \subset \mathcal{L}_\beta$ be a path from $z_{1,i}$ to $z_{1,j}$ on \mathcal{L}_β . Define the closed path Γ_{ij}^1 to be the concatenation of $\Gamma_{ij}^{(\beta)}$ with the inverse of $\Gamma_{ij}^{(a)}$, which we write as

$$\Gamma_{ij}^1 \equiv \Gamma_{ij}^{(\beta)} - \Gamma_{ij}^{(a)}. \quad (2.5.4)$$

This target space path satisfies all of the conditions required for use in Eq. 2.5.3 by construction.

We use the geometry of the transport described in Section 2.2.2 to lift $\Gamma_{ij}^{(\beta)}$ into a path $\Gamma_{ij}^{(M)} \in \mathcal{L}_M$. Recall that for every point in \mathcal{L}_β there exists at least one point in the intersection \mathcal{I} defined in Eq. 2.2.10. Define $\Gamma_{ij}^{(M)}$ to be a path in \mathcal{I} such that $\Gamma_{ij}^{(M)}$ starts at z_i , ends at z_j , and projects onto $\Gamma_{ij}^{(\beta)}$. For such a path to be continuous we require that the points z_i and z_j lie on the same connected piece of \mathcal{I} . Define the path $\Gamma_{ij}^{(b)}$ to be the projection of \mathcal{L}_M onto the dual source space so that $\Gamma_{ij}^{(M)}$ satisfies

$$\pi_1(\Gamma_{ij}^{(M)}) = \Gamma_{ij}^{(a)}, \quad \pi_2(\Gamma_{ij}^{(M)}) = \Gamma_{ij}^{(b)}. \quad (2.5.5)$$

By the geometry of the transport procedure, $\Gamma_{ij}^{(b)}$ is a path on $\mathcal{L}_{\bar{b}}$ from $z_{2,i}$ to $z_{2,j}$. Figure 2.5.1 shows the construction of $\Gamma_{ij}^{(M)}$ and $\Gamma_{ij}^{(b)}$ from $\Gamma_{ij}^{(\beta)}$ using the transport procedure.

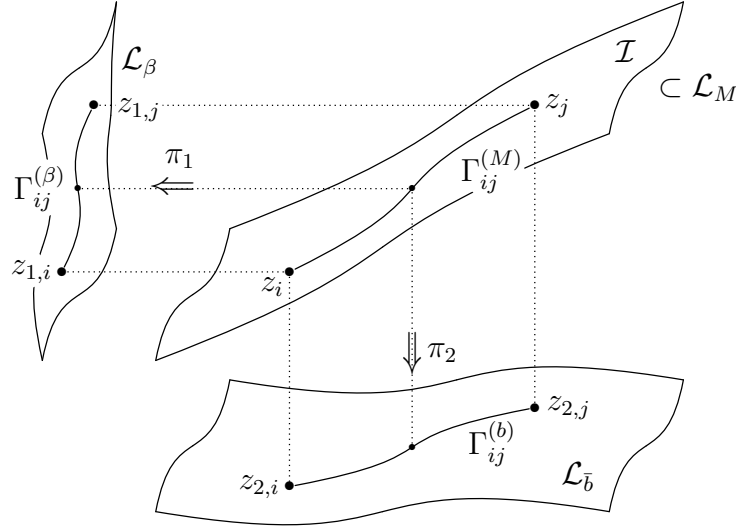


Figure 2.5.1: The path $\Gamma_{ij}^{(\beta)}$ on the β -manifold \mathcal{L}_β lifts to a path $\Gamma_{ij}^{(M)}$ on a connected piece of the intersection submanifold \mathcal{I} of the M -manifold \mathcal{L}_M . The path $\Gamma_{ij}^{(b)}$ on the dual b -manifold $\mathcal{L}_{\bar{b}}$ is the projection of $\Gamma_{ij}^{(M)}$ by π_2 .

Next define the auxiliary point $z_{\text{aux}} \equiv (\pi_1(z_i), \pi_2(z_j)) \in \Phi_{12}$ so that $\pi_1(z_{\text{aux}}) = z_{1,i}$ and $\pi_2(z_{\text{aux}}) = z_{2,j}$. Since $z_{1,i} \in \mathcal{L}_a$ by definition and $z_{2,j} \in \mathcal{L}_{\bar{b}}$ by construction, z_{aux} is a point on the product manifold \mathcal{L}_{ab} . Define path $\Gamma_{a,i}^{(ab)}$ to be the lift of $\Gamma_{ij}^{(a)}$ into \mathcal{L}_{ab} such that $\Gamma_{a,i}^{(ab)}$ starts at z_i and is vertical over Φ_2^* and similarly define $\Gamma_{b,j}^{(ab)}$ to be the lift of $\Gamma_{ij}^{(b)}$ into \mathcal{L}_{ab} such that $\Gamma_{b,j}^{(ab)}$ ends at z_j and is vertical over Φ_1 . These paths satisfy

$$\pi_1(\Gamma_{a,i}^{(ab)}) = \Gamma_{ij}^{(a)}, \quad \pi_2(\Gamma_{a,i}^{(ab)}) = z_{2,i}, \quad (2.5.6)$$

$$\pi_1(\Gamma_{b,j}^{(ab)}) = z_{1,j}, \quad \pi_2(\Gamma_{b,j}^{(ab)}) = \Gamma_{ij}^{(b)}. \quad (2.5.7)$$

By construction the end point of $\Gamma_{a,i}^{(ab)}$ is z_{aux} , as is the initial point of $\Gamma_{b,j}^{(ab)}$. Therefore we may concatenate the paths to create a path from z_i to z_j on \mathcal{L}_{ab} ,

$$\Gamma_{ij}^{(ab)} \equiv \Gamma_{a,i}^{(ab)} + \Gamma_{b,j}^{(ab)}. \quad (2.5.8)$$

Figure 2.5.1 shows the construction of $\Gamma_{a,i}^{(ab)}$, $\Gamma_{b,j}^{(ab)}$, and $\Gamma_{ij}^{(ab)}$ from $\Gamma_{ij}^{(a)}$ and $\Gamma_{ij}^{(b)}$.

Finally, define the closed path Γ_{ij}^{12} to be the concatenation of $\Gamma_{ij}^{(M)}$ with the inverse of $\Gamma_{ij}^{(ab)}$,

$$\Gamma_{ij}^{12} \equiv \Gamma_{ij}^{(M)} - \Gamma_{ij}^{(ab)}. \quad (2.5.9)$$

This product space path satisfies all of the conditions required for use in Eq. 2.5.2 by construction. Note that the construction of Γ_{ij}^{12} from Γ_{ij}^1 is not unique but depends on how we choose to lift the portion of the path along \mathcal{L}_β onto the intersection manifold.

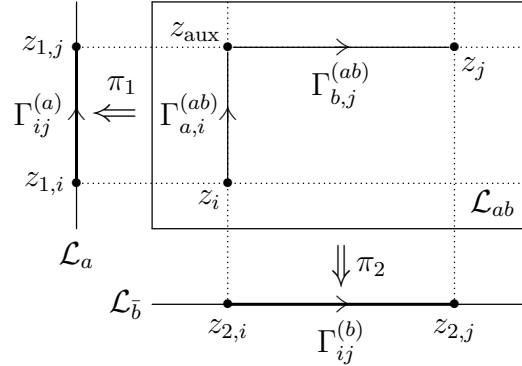


Figure 2.5.2: That paths $\Gamma_{ij}^{(a)}$ on the a -manifold \mathcal{L}_a and $\Gamma_{ij}^{(b)}$ on the dual b -manifold $\mathcal{L}_{\bar{b}}$ define the paths $\Gamma_{a,i}^{(ab)}$ and $\Gamma_{b,j}^{(ab)}$ on the product manifold \mathcal{L}_{ab} . The path $\Gamma_{ij}^{(ab)}$ on \mathcal{L}_{ab} is the concatenation of $\Gamma_{a,i}^{(ab)}$ with $\Gamma_{b,j}^{(ab)}$.

2.5.3 The Action Integrals

Given the paths defined in Eqs. 2.5.4 and 2.5.9, the action integral parts of the relative phase expressions 2.5.3 and 2.5.2 are equal, as we now demonstrate. We work in the x -representation of Φ_1 , the y -representation of Φ_2 , and the xy -representation of Φ_{12} , as described in Section 2.1.2.

The form of the product space symplectic potential in Eq. 2.1.10 allows the action integral of an arbitrary path Γ in the product phase space to be expressed as integrals over the projected paths $\pi_1(\Gamma)$ and $\pi_2(\Gamma)$ in the target and dual source phase spaces,

$$\int_{\Gamma} \theta_{12} = \int_{\Gamma} \pi_1^* \theta_1 + \int_{\Gamma} \pi_2^* \theta_2 = \int_{\pi_1(\Gamma)} \theta_1 + \int_{\pi_2(\Gamma)} \theta_2. \quad (2.5.10)$$

Eq. 2.5.10 can be used to evaluate the product space action integral over Γ_{ij}^{12} , which we do piece by piece. First evaluate the action integral over path $\Gamma_{a,i}^{(ab)}$,

$$\int_{\Gamma_{ij}^{(ab)}} \theta_{12} = \int_{\Gamma_{ij}^{(a)}} \theta_1 + \int_{\Gamma_{ij}^{(b)}} \theta_2, \quad (2.5.11)$$

where Eqs. 2.5.6 and 2.5.7 have been used to write the projections of $\Gamma_{ij}^{(ab)}$ in terms of target and dual source space paths. Similarly, evaluating the action integral over $\Gamma_{ij}^{(M)}$ using Eqs. 2.5.10 and 2.5.5 yields

$$\int_{\Gamma_{ij}^{(M)}} \theta_{12} = \int_{\Gamma_{ij}^{(\beta)}} \theta_1 + \int_{\Gamma_{ij}^{(b)}} \theta_2. \quad (2.5.12)$$

By definition 2.5.9 of closed path $\Gamma_{ij}^{(12)}$ the product space action integral contribution to the relative phase is

$$\oint_{\Gamma^{12}} \theta_{12} = \int_{\Gamma_{ij}^{(M)}} \theta_{12} - \int_{\Gamma_{ij}^{(ab)}} \theta_{12}. \quad (2.5.13)$$

Using results 2.5.11 and 2.5.12, Eq. 2.5.13 simplifies to

$$\oint_{\Gamma_{ij}^{12}} \theta_{12} = \int_{\Gamma_{ij}^{(\beta)}} \theta_1 - \int_{\Gamma_{ij}^{(a)}} \theta_1, \quad (2.5.14)$$

where the two dual source space integrals over $\Gamma_{ij}^{(b)}$ cancel each other out. The terms in Eq. 2.5.14 can be combined into a single integral over path $\Gamma_{ij}^{(\beta)} - \Gamma_{ij}^{(a)}$, which is the definition of the closed target space path Γ_{ij}^1 . Therefore it may be concluded that the product and target space action integrals are identical,

$$\oint_{\Gamma_{ij}^{12}} \theta_{12} = \oint_{\Gamma_{ij}^1} \theta_1, \quad (2.5.15)$$

This result is independent of the choice of lift of $\Gamma^{(\beta)}$ into the intersection manifold \mathcal{I} . Moreover, since the final result is a relationship between integrals of the symplectic potential over closed paths, the statement 2.5.15 is independent of representation.

2.5.4 Maslov Indices

We now turn our attention to the Maslov indices $\mu(\Gamma_{ij}^1)$ and $\mu(\Gamma_{ij}^{12})$ of the relative phases. The Maslov index along a path is additive by definition [59] and therefore we may express the total Maslov indices as sums over open-path Maslov indices,

$$\mu(\Gamma_{ij}^1) = \mu(\Gamma_{ij}^{(\beta)}) - \mu(\Gamma_{ij}^{(a)}), \quad (2.5.16)$$

$$\mu(\Gamma_{ij}^{12}) = \mu(\Gamma_{ij}^{(M)}) - \mu(\Gamma_{b,j}^{(ab)}) - \mu(\Gamma_{a,i}^{(ab)}). \quad (2.5.17)$$

As described in Section C.1, the Maslov index along a path Γ on \mathcal{L} computed in the x -representation tracks the change of the matrix signature of the Hessian matrix $\partial^2 T(p)$, where $T(p)$ is the action of the conjugate p -representation WKB wavefunction. The actions on any given branch of the product manifold \mathcal{L}_{ab} decomposes in the (p, r) -representation as a sum of target and dual source space actions, $T_{ab}(p, r) = T_a(p) + T_b(r)$. Therefore, the Hessian matrix $\partial^2 T_{ab}(p, r)$ is block-diagonal and the matrix signature of the product space Hessian becomes the sum of the target and dual source space Hessians,

$$\text{sgn } \partial^2 T_{ab}(p, r) = \text{sgn } \partial^2 T_a(p) + \text{sgn } \partial^2 T_b(r). \quad (2.5.18)$$

The second signature in Eq. 2.5.18 remains constant along path $\Gamma_{a,i}^{(ab)}$ since the z_2 -coordinate is fixed. Similarly, the first signature remains constant along $\Gamma_{b,j}^{(ab)}$. The Maslov index

contributions along the product manifold \mathcal{L}_{ab} thus are equal to the Maslov indices on \mathcal{L}_a and $\mathcal{L}_{\bar{b}}$,

$$\mu(\Gamma_{a,i}^{(ab)}) = \mu(\Gamma_{ij}^{(a)}), \quad \mu(\Gamma_{b,j}^{(ab)}) = \mu(\Gamma_{ij}^{(b)}). \quad (2.5.19)$$

The difference in Maslov indices between the product and target space paths is therefore

$$\mu(\Gamma_{ij}^{12}) - \mu(\Gamma_{ij}^1) = \mu(\Gamma_{ij}^{(M)}) - \mu(\Gamma_{ij}^{(b)}) - \mu(\Gamma_{ij}^{(\beta)}). \quad (2.5.20)$$

The Maslov indices occurring in equation 2.5.20 can be re-expressed in terms of the signature index through the analysis of the matrix element

$$\langle \beta | \hat{M} | b \rangle = \text{tr} \left((|\beta\rangle\langle b|)^\dagger \hat{M} \right) = \langle \beta | \beta \rangle = |N|^2, \quad (2.5.21)$$

where $|\beta\rangle\langle b| \in \mathcal{H}_1 \otimes \mathcal{H}_2^*$. Consider the remodeling geometry for matrix element 2.5.21. The Lagrangian manifolds in the product phase space are \mathcal{L}_M and the product manifold $\mathcal{L}_{\beta b} = \mathcal{L}_\beta \times \mathcal{L}_b$. Recall that \mathcal{I} , defined by Eq. 2.2.10, is the intersection of the inverse image of $\mathcal{L}_{\bar{b}}$ under the projection π_2 and the manifold \mathcal{L}_M . By the geometric construction of Section 2.2.2, $\pi_1(\mathcal{I}) = \mathcal{L}_\beta$ and $\pi_2(\mathcal{I}) \subset \mathcal{L}_{\bar{b}}$. Therefore $\mathcal{I} \subset \mathcal{L}_{\beta b}$. Since by definition $\mathcal{I} \subset \mathcal{L}_M$, this implies that $\mathcal{I} \subset \tilde{I}^{(12)}$, where $\tilde{I}^{(12)} \equiv \mathcal{L}_M \cap \mathcal{L}_{\beta b}$, the set of stationary phase points in the product space evaluation of 2.5.21. Moreover, $\mathcal{L}_M \cap \mathcal{L}_{\beta b}$ is a subset of \mathcal{I} since $\mathcal{L}_{\beta b} \subset \pi_2^{-1}(\mathcal{L}_{\bar{b}})$. Therefore $\mathcal{I} = \tilde{I}^{(12)}$ and the stationary phase set for the WKB evaluation of the product space model of 2.5.21 is the entire intersection manifold \mathcal{I} . The intersection manifold reflects that there is at least an n_1 -dimensional common symmetry group between \mathcal{L}_M and $\mathcal{L}_{\beta b}$. The relative phase between two points on the same common symmetry group orbit is zero. Since we assumed that z_i and z_j were on the same connected piece of \mathcal{I} we may thus conclude that $\Delta\tilde{\varphi}_{ij}^{12}$, the relative phase between these two points in the product space WKB evaluation of $\langle \beta | \hat{M} | b \rangle$, is zero.

Consider the target space closed path $\tilde{\Gamma}_{ij}^1 \equiv \Gamma_{ij}^{(\beta)} - \Gamma_{ij}^{(\beta)}$. Note that the action integral, Maslov index, and signature indices are all trivially zero for this path. Create a product space closed path $\tilde{\Gamma}_{ij}^{12}$ from this by the same method as in Section 2.5.2, where $\Gamma_{ij}^{(a)} = \Gamma_{ij}^{(\beta)}$. As shown in Section 2.5.3 the action integral around $\tilde{\Gamma}_{ij}^{12}$ is identical to the action integral around $\tilde{\Gamma}_{ij}^1$ and thus vanishes. By the analysis of Section 2.5.4, the Maslov index $\mu(\tilde{\Gamma}_{ij}^{12})$ is equal to the difference of Maslov indices in Eq. 2.5.20. Since the total relative phase between points z_i and z_j is zero, we may conclude from an equation like Eq. 2.5.2 for matrix element 2.5.21 that

$$\left(\mu(\Gamma_{ij}^{(M)}) - \mu(\Gamma_{ij}^{(b)}) - \mu(\Gamma_{ij}^{(\beta)}) \right) \frac{\pi}{2} = \Delta\sigma(M, \beta b) \frac{\pi}{4}. \quad (2.5.22)$$

Applying Eq. 2.5.22 to Eq. 2.5.20 yields

$$\mu(\Gamma_{ij}^{12}) - \mu(\Gamma_{ij}^1) = \frac{1}{2} \Delta\sigma(M, \beta b). \quad (2.5.23)$$

2.5.5 The Signature Index

Eqs. 2.5.15 and 2.5.23 allows the difference in relative phases 2.5.2 and 2.5.2 in the two models to be expressed entirely in terms of signature indices,

$$\Delta\varphi_{ij}^{12} - \Delta\varphi_{ij}^1 = (\Delta\sigma(M, ab) - \Delta\sigma(\beta, a) - \Delta\sigma(M, \beta b)) \frac{\pi}{4}. \quad (2.5.24)$$

We now shown that the combination of signature indices in Eq. 2.5.24 evaluates to zero.

The target space signature index $\sigma_i(\beta, a)$ at intersection point $z_{1,i}$ is identical to the product space signature index $\sigma_i(\beta b, ab)$ at z_i , as we now show. As described in Section C.5, the target space signature index is the matrix signature of the Hessian $\partial^2(S_{\beta, k_\beta} - S_{a, k_a}) / \partial x_i \partial x_j$, where $S_a(x)$ and $S_\beta(x)$ are the WKB phase functions for the a - and β -states and z_i is on the k_a -th and k_β -th x -representation branch of \mathcal{L}_a and \mathcal{L}_β over point x . As discussed in Section 2.1.3, the phase function for the product manifold \mathcal{L}_{ab} is $S_{ab}(x, y) = S_a(x) + S_{\bar{b}}(y)$. Therefore $S_{\beta b}(x, y) - S_{ab}(x, y) = S_\beta(x) - S_a(x)$ and thus the product space Hessian is

$$\frac{\partial^2(S_{\beta b} - S_{ab})}{\partial Q_\alpha \partial Q_\beta} = \left[\begin{array}{c|c} \frac{\partial^2(S_\beta - S_a)}{\partial x_i \partial x_j} & 0 \\ \hline 0 & 0 \end{array} \right], \quad (2.5.25)$$

where $Q_\alpha = (x_i, y_I)$. The matrix signature of the product space Hessian is thus equal to the matrix signature of the target space Hessian and we may conclude that $\sigma_i(\beta, a) = \sigma_i(\beta b, ab)$. This allows us to express all of the signature indices in Eq. 2.5.24 as signature indices in the product phase space.

As discussed in Section B.5, the Lagrangian signature [59] is a map from a triplet of Lagrangian planes to \mathbb{Z} . By Eq. C.5.4, the signature index in a given representation of a pair of Lagrangian manifolds at an intersection point is equal to the Lagrangian signature of the Lagrangian plane defining the representation and the two planes tangent to the Lagrangian manifolds. Applying this to Eq. 2.5.24 lets the signature indices be expressed as

$$\sigma(\Lambda_{xy}, \Lambda_M, \Lambda_{ab}) - \sigma(\Lambda_{xy}, \Lambda_{\beta b}, \Lambda_{ab}) - \sigma(\Lambda_{xy}, \Lambda_M, \Lambda_{\beta b}), \quad (2.5.26)$$

where Λ_{xy} is the Lagrangian plane defining the xy -representation at z_i and Λ_M , Λ_{ab} , and $\Lambda_{\beta b}$ are the tangent planes to Lagrangian manifolds \mathcal{L}_M , \mathcal{L}_{ab} , and $\mathcal{L}_{\beta b}$ at z_i . The Lagrangian signature is a 2-cocycle and thus obeys the cocycle property Eq. B.5.6 [60, 61]. Thus expression 2.5.26 may be expressed as a single Lagrangian signature $\sigma(\Lambda_M, \Lambda_{ab}, \Lambda_{\beta b})$ and the difference in relative phases is

$$\Delta\varphi_{ij}^{12} - \Delta\varphi_{ij}^1 = \Delta\sigma(\Lambda_M, \Lambda_{ab}, \Lambda_{\beta b}) \frac{\pi}{4}. \quad (2.5.27)$$

Note that the above equation is now independent of representation, since the representation plane Λ_{xy} no longer appears.

The intersection of tangent planes Λ_{ab} and $\Lambda_{\beta b}$ minimally contains the isotropic plane $\{0\} \times \Lambda_b$ and the intersection of tangent planes $\Lambda_M \cap \Lambda_{\beta b}$ minimally contains the isotropic plane $\Lambda_\beta \times \{0\}$. Since $\Lambda_{\beta b} = \Lambda_\beta \times \Lambda_b$, we can conclude

$$\Lambda_{\beta b} \subset (\Lambda_{\beta b} \cap \Lambda_M) \oplus (\Lambda_{\beta b} \cap \Lambda_{ab}). \quad (2.5.28)$$

Therefore, by the discussion leading up to Eq. B.5.10,

$$\sigma(\Lambda_M, \Lambda_{ab}, \Lambda_{\beta b}) = 0, \quad (2.5.29)$$

for tangent planes Λ_M , Λ_{ab} , and $\Lambda_{\beta b}$ to any intersection point in $I^{(12)}$.

Applying Eq. 2.5.29 to Eq. 2.5.27 yields

$$\Delta\varphi^{12} = \Delta\varphi^1. \quad (2.5.30)$$

Therefore the phase difference between related pairs of intersection points in the product space model and the target space model are equal when the product space path Γ_{ij}^{12} is constructed from the target space path Γ_{ij}^1 as in Section 2.5.2. This statement is independent of representation, up to the requirement that the product space representation contains the target space representation.

2.5.6 Quantization

As discussed in Section C.1, a Lagrangian manifold \mathcal{L} is said to be quantized if, for all closed paths Γ on \mathcal{L} ,

$$\oint_{\Gamma} \theta - \mu(\Gamma) \frac{\pi}{2} = 0 \pmod{2\pi}, \quad (2.5.31)$$

which comes from the requirement that the WKB wavefunction be single-valued. In this section we demonstrate two results relating to quantization in the remodeling geometry. The first result involves deforming the product space path from the path constructed in Section 2.5.2 and the second result demonstrates that the transport procedure described in Section 2.2.2 results in a quantized manifold as long as \mathcal{L}_M and \mathcal{L}_b are also quantized.

Consider the open paths $\Gamma_{ij}^{(M)}$ and $\Gamma_{ij}^{(ab)}$ defined in Eqs. 2.5.5 and 2.5.8, and the closed path Γ_{ij}^{12} defined in Eq. 2.5.9. Let $\gamma_{ij}^{(M)} \subset \mathcal{L}_M$ and $\gamma_{ij}^{(ab)} \subset \mathcal{L}_{ab}$ be any other paths that start at z_i , end at z_j and form the closed path $\gamma_{ij}^{12} = \gamma_{ij}^{(M)} - \gamma_{ij}^{(ab)}$. Let $\Delta\varphi(\Gamma_{ij}^{12})$ and $\Delta\varphi(\gamma_{ij}^{12})$ be the relative phases for these two paths as in Eq. 2.5.2. The signature index pieces of both relative phases will be equal since the intersection points z_i and z_j used to define the paths are the same for both Γ_{ij}^{12} and γ_{ij}^{12} . Therefore,

$$\Delta\varphi(\Gamma_{ij}^{12}) - \Delta\varphi(\gamma_{ij}^{12}) = \oint_{\Gamma_{ij}^{12}} \theta_{12} - \oint_{\gamma_{ij}^{12}} \theta_{12} - (\mu(\Gamma_{ij}^{12}) - \mu(\gamma_{ij}^{12})) \frac{\pi}{2}. \quad (2.5.32)$$

Since the action integral and Maslov index are both additive this expression may be rewritten

$$\begin{aligned} \Delta\varphi(\Gamma_{ij}^{12}) - \Delta\varphi(\gamma_{ij}^{12}) &= \left(\oint_{\Gamma_{ij}^{(M)} - \gamma_{ij}^{(M)}} \theta_{12} - \mu(\Gamma_{ij}^{(M)} - \gamma_{ij}^{(M)}) \frac{\pi}{2} \right) \\ &\quad - \left(\oint_{\Gamma_{ij}^{(ab)} - \gamma_{ij}^{(ab)}} \theta_{12} - \mu(\Gamma_{ij}^{(ab)} - \gamma_{ij}^{(ab)}) \frac{\pi}{2} \right). \end{aligned} \quad (2.5.33)$$

Since $\Gamma_{ij}^{(M)}$ and $\gamma_{ij}^{(M)}$ are both paths in \mathcal{L}_M and share the same starting and ending points, the concatenation $\Gamma_{ij}^{(M)} - \gamma_{ij}^{(M)}$ is a closed path on \mathcal{L}_M . Similarly, $\Gamma_{ij}^{(ab)} - \gamma_{ij}^{(ab)}$ is a closed

path on \mathcal{L}_{ab} . Both \mathcal{L}_M and \mathcal{L}_{ab} are quantized manifolds so, by Eq. 2.5.31, each of the two parenthetical expressions in Eq. 2.5.33 equals 0 modulo 2π . Thus

$$\Delta\varphi(\gamma_{ij}^{12}) = \Delta\varphi(\Gamma_{ij}^{12}) \pmod{2\pi}. \quad (2.5.34)$$

As was shown in the previous sections, the relative phase for the path Γ_{ij}^{12} is equal to the relative phase for the target space path Γ_{ij}^1 . Thus the relative phase for any product space path that starts at z_i , travels along \mathcal{L}_M to z_j , and then returns to z_i along \mathcal{L}_{ab} is equal modulo 2π to any target space path that starts at $z_{1,i}$, travels along \mathcal{L}_β to $z_{1,j}$, and then returns to z_i along \mathcal{L}_a .

Next we turn to the β manifold and the remodeling geometry for $\langle\beta|\hat{M}|b\rangle$. Since every point on \mathcal{L}_β is a stationary phase point in $\tilde{T}^{(1)}$ we may proceed as above and consider the relative phase around any closed loop starting at an arbitrary point $z_\beta \in \mathcal{L}_\beta$. Let $\Gamma^{(\beta)}$ in \mathcal{L}_β be a closed loop starting at z_β , and lift it to a closed path $\Gamma^{(M)}$ in \mathcal{I} . Let the starting point of $\Gamma^{(M)}$ be $z_{\mathcal{I}}$ so $\pi_1(z_{\mathcal{I}}) = z_\beta$. These paths act like the open paths $\Gamma_{ij}^{(\beta)}$ and $\Gamma_{ij}^{(M)}$ defined in Section 2.5.2 with $z_\beta = z_{i,1} = z_{j,1}$ and $z_{\mathcal{I}} = z_i = z_j$. Define $\Gamma^{(a)}$ to be the trivial path that starts and remains at z_i . Then the target space closed path is simply $\Gamma^1 = \Gamma^{(\beta)}$, the path $\Gamma^{(b)}$ is a closed loop on $\mathcal{L}_{\bar{b}}$. The auxiliary point z_{aux} is the same as $z_{\mathcal{I}}$, and thus the path $\Gamma_{a,i}^{(ab)}$ is the trivial path at $z_{\mathcal{I}}$ and $\Gamma_{b,j}^{(ab)}$ is the lift of $\Gamma^{(b)}$ onto the $z_1 = z_\beta$ plane of Φ_{12} , which we write as $\tilde{\Gamma}^{(b)}$. Thus the product space closed path is the concatenation $\Gamma^{12} = \Gamma^{(M)} - \tilde{\Gamma}^{(b)}$.

We first turn our attention to the relative phase $\Delta\varphi^1$ for the target space closed path Γ^1 . The signature index $\sigma_i(\beta, \beta)$ in the x -representation is equal to the Lagrangian signature $\sigma(\Lambda_x, \Lambda_\beta, \Lambda_\beta)$, where Λ_x is the Lagrangian plane defining the x -representation at the base point z_β and Λ_β is the tangent plane to \mathcal{L}_β at z_β . Since the Lagrangian signature is defined to be antisymmetric, $\sigma(\Lambda_x, \Lambda_\beta, \Lambda_\beta) = 0$ and thus Eq. 2.5.3 becomes

$$\Delta\varphi^1 = \oint_{\Gamma^1} \theta_1 - \mu(\Gamma^1) \frac{\pi}{2}. \quad (2.5.35)$$

Next we analyze the relative phase $\Delta\varphi^{12}$ for the product space closed path Γ^{12} . Since both component paths $\Gamma^{(M)}$ and $\tilde{\Gamma}^{(b)}$ are closed paths the relative phase Eq. 2.5.2 may be written

$$\Delta\varphi^{12} = \oint_{\Gamma^{(M)}} \theta_{12} - \oint_{\tilde{\Gamma}^{(b)}} \theta_{12} - \mu(\Gamma^{(M)}) \frac{\pi}{2} + \mu(\tilde{\Gamma}^{(b)}) \frac{\pi}{2} + \Delta\sigma(M, \beta b) \frac{\pi}{4}. \quad (2.5.36)$$

Since $z_{\mathcal{I}}$ serves as both stationary phase points in the above analysis the difference in signature index between the two points is zero. The two terms in Eq. 2.5.36 that depend on $\tilde{\Gamma}^{(b)}$ can be expressed in terms of the dual source space path $\Gamma^{(b)}$. Therefore,

$$\Delta\varphi^{12} = \left(\oint_{\Gamma^{(M)}} \theta_{12} - \mu(\Gamma^{(M)}) \frac{\pi}{2} \right) - \left(\oint_{\Gamma^{(b)}} \theta_{\bar{2}} - \mu(\Gamma^{(b)}) \frac{\pi}{2} \right). \quad (2.5.37)$$

As discussed in Section C.1, the requirement that the WKB wavefunction be single-valued is what defines the quantization condition on the Lagrangian manifold generated by

the wavefunction. According to Eq. 2.5.31, each of the two terms in Eq. 2.5.37 is 0 mod 2π since \mathcal{L}_M and $\mathcal{L}_{\bar{b}}$ are both quantized manifolds and thus $\Delta\varphi^{12} = 0 \text{ mod } 2\pi$. Applying this result to Eqs. 2.5.30 and 2.5.35 yields

$$\oint_{\Gamma^1} \theta_1 - \mu(\Gamma^1) \frac{\pi}{2} = 0 \text{ mod } 2\pi, \quad (2.5.38)$$

for all closed paths Γ^1 on \mathcal{L}_β . Therefore, by Eq. 2.5.31, the transported manifold \mathcal{L}_β is quantized if \mathcal{L}_M and \mathcal{L}_b are.

2.6 Summary

In this chapter we introduced the linear algebra and semiclassical geometry involved in the remodeling of an inner product. The core idea was that a linear map between Hilbert spaces may itself be interpreted as an element of a product Hilbert space. The Lagrangian manifold that supports the semiclassical approximation to this state allows the Lagrangian manifolds that correspond to source space states to be mapped to Lagrangian manifolds that correspond to target space states. The transport was achieved geometrically by taking the inverse image of the dual of the source Lagrangian manifold under the canonical projection $:\Phi_1 \times \Phi_2^* \rightarrow \Phi_2^*$, forming the intersection with the manifold corresponding to the map, and projecting onto the target space. We found that this geometric procedure indeed gave the same manifold as the stationary phase approximation applied to the WKB wavefunctions. Moreover, we showed how the momentum maps that define the source space manifolds get transported to become the momentum maps that define the transported manifold. Then we showed that the amplitude and phase calculations for the target and product space inner product models are equal in the remodeling geometry.

The remodeling of an inner product ultimately is a general procedure that creates two models of the same matrix element, one in a larger product space and one in a smaller target space. The amplitude determinant, action integral, and combined Maslov and signature index pieces that occur in the stationary phase approximations of these models are identical so that, once the remodeling geometry is set up, the action integral can be evaluated in the product space and the amplitude and Maslov index can be computed in the target space. When the remodeling geometry connects a one degree of freedom model with a two degree of freedom model, as in our first concrete example, the evaluation of the $3j$ -symbol in Chapter 3, the advantages of the remodeling of an inner product may not be apparent. However in the evaluation of more complicated spin networks, such as the $6j$ - or $9j$ -symbols, the ability to take determinants in a low-dimensional space becomes important. Moreover the product space models of such symbols tend to be symmetric and treat all of the angular momenta involved on the same footing, a feature which the target space models lack. Given this symmetry, paths are easier to construct from Hamiltonian flows along the relevant manifolds and the action integrals become much easier to evaluate.

The main example for comparing the advantages of different models is the $6j$ -symbol which was studied in a symmetric $12j$ -model by Roberts [2] and in an asymmetric $4j$ -model by Aquilanti *et al* [1]. The phase calculation in the $12j$ -model is elegant and clean and easily reproduces the expected result of Ponzano and Regge [27]. However, the computation of the amplitude involved taking the determinant of a complicated 9×9 matrix and the Maslov correction not even attempted. In contrast, the amplitude in the $4j$ -model is a single Poisson bracket, essentially the determinant of a 1×1 matrix on the phase space S^2 . Moreover the amplitude has a clear geometric meaning, being proportional to the volume of a tetrahedron. We developed and applied a method for the calculation of the Maslov index to the $4j$ -model of the $6j$ -symbol in Esterlis *et al* [55]. Again, the low dimensionality of the $4j$ -model made this calculation much more tractable. The path in this model is less intuitive, however, and is more computationally involved. As we will see in Chapter 4, we can easily set up the remodeling geometry and then cherry-pick where we want to perform certain calculations, transforming potentially tedious calculations into simple exercises in symplectic geometry. First, however, we turn our attention to the simpler $3j$ -symbol in Chapter 3 and use it as an example to demonstrate the various features and ideas involved in the remodeling of an inner product.

Chapter 3

Models of the $3j$ -Symbol

The Wigner $3j$ -symbol and the closely related Clebsch-Gordan coefficients are some of the central objects of standard angular momentum theory. The semiclassical behavior of the $3j$ -symbol has been studied extensively (Ponzano and Regge [27], Neville [38], Miller [39], Schulten and Gordon [40, 41], Biedenharn and Louck [42], Aquilanti *et al* [44]) since it is one of the simplest nontrivial objects in angular momentum theory. It also provides one of the simplest nontrivial spin networks. In the notation explained in Aquilanti *et al* [1], the $3j$ -symbol is

$$\begin{pmatrix} j_1 & j_2 & j_3 \\ m_1 & m_2 & m_3 \end{pmatrix} = \begin{array}{c} *m_1 \\ \uparrow j_1 \\ \bullet \\ \swarrow j_2 \quad \searrow j_3 \\ *m_2 \quad *m_3 \end{array} . \quad (3.0.1)$$

This is the spin network representing the “completely contravariant components” of the $3j$ -intertwiner as shown in Figure 28 of Aquilanti *et al* [1]. We use this version rather than the conjugate because it involves fewer dual Schwinger Hilbert spaces.

For given values of the three j 's and m 's, the $3j$ -symbol is just a number, but to study its semiclassical limit it is useful to write it as a scalar product $\langle A|B\rangle$ of wavefunctions in some Hilbert space. This can be done in many different ways, with different choices of Hilbert space corresponding to different “models”. There are two models for the $3j$ -symbol, called the “ $3j$ -model” and the “ $2j$ -model.”

The $3j$ -model is an inner product in a Hilbert space formed by taking the tensor product of three copies of the Schwinger Hilbert space discussed in Section A.1. The advantage of the $3j$ -model is that it is the most symmetric way of expressing the $3j$ -symbol. The analysis of Aquilanti *et al* [44] used the $3j$ -model of the $3j$ -symbol. The $2j$ -model is an inner product in a Hilbert space formed by taking the tensor product of two copies of the Schwinger Hilbert space. The $2j$ -model is not as symmetric as the $3j$ -model, but has the advantage of living in a smaller Hilbert space. The Clebsch-Gordan coefficients are usually expressed as an inner product on a space very closely related to the $2j$ -Hilbert space which makes their connection to the $3j$ -symbol more apparent than in the $3j$ -model.

The relationship between the $2j$ - and $3j$ -models provides our first example of the remodeling of an inner product discussed in Chapter 2. In Section 3.1 the remodeling algebra for the $3j$ -symbol is constructed and the connections between the states in the two different models is explored. Then in Section 3.2 the remodeling geometry will be constructed, which sets the stage for the comparison of the semiclassical evaluations of the $2j$ - and $3j$ -models of the $3j$ -symbol in Section 3.3. Throughout this chapter the various concepts and relationships described abstractly in Chapter 2 will be demonstrated explicitly.

3.1 Linear Algebra of the $3j$ -Symbol

The $2j$ - and $3j$ -models of the $3j$ -symbol may be interpreted as the target- and product-space models for a remodel of the spin network in Eq. 3.0.1. The “operator” at the heart of the $3j$ -symbol is the Wigner intertwiner, which is defined and discussed in Section 3.1.1. Then in section 3.1.2 the Hilbert spaces, states, and inner product models of the $3j$ -symbol are constructed. We explore Schur’s Lemma as it applies to intertwiners between different carrier spaces of (potentially reducible) representations in Section 3.1.3 in order to more fully understand the core isomorphism in spin network applications. The core isomorphism for the $3j$ -remodeling geometry turns out to be proportional to a $2j$ -intertwiner, which we define and explore in Section 3.1.4. In Section 3.1.5 we define all of the states and the subspaces $\text{img } \hat{W}$ and $(\ker \hat{W})_{\perp}$ as simultaneous eigenspaces of sets of observables and show how the core isomorphism is used to derive the observables for the β -state from the observables from the b -state. Finally in Section 3.1.6 we show how the $2j$ -model of the $3j$ -symbol is related to the Clebsch-Gordan coefficients.

3.1.1 The Wigner Intertwiner and the $3j$ -Symbol

Consider a triplet of irreps (j_1, j_2, j_3) and the tensor product of carrier spaces $\mathcal{C}_{j_1} \otimes \mathcal{C}_{j_2} \otimes \mathcal{C}_{j_3}$, as described in Section A.1. This space contains a nontrivial, $SU(2)$ -invariant vector iff (j_1, j_2, j_3) satisfy the triangle inequalities and $j_1 + j_2 + j_3$ is an integer, in which case the vector is unique up to a phase and normalization. Using the standard angular momentum basis discussed in Section A.1 (due to Schwinger [62] and Bargmann [63]) and the standard notation and definition for the Wigner $3j$ -symbol [28, 64], we construct an invariant reference vector,

$$|W\rangle = \sum_{m_1 m_2 m_3} |j_1 m_1\rangle \otimes |j_2 m_2\rangle \otimes |j_3 m_3\rangle \begin{pmatrix} j_1 & j_2 & j_3 \\ m_1 & m_2 & m_3 \end{pmatrix}. \quad (3.1.1)$$

Under this construction, the vector $|W\rangle$ is normalized, $\langle W|W\rangle = 1$ (see Eq. (3.7.8) in Edmonds [28]). The vector $|W\rangle$ is the “Wigner state” discussed from a semiclassical standpoint in Aquilanti *et al* [44].

The Wigner state can be considered a map $:\mathcal{C}_{j_1}^* \otimes \mathcal{C}_{j_2}^* \otimes \mathcal{C}_{j_3}^* \rightarrow \mathbb{C}$ via the inner product. Since the state $|W\rangle$ is invariant under the action of the group $SU(2)$, the map is an $SU(2)$

intertwiner. In general, an $SU(2)$ intertwiner is a linear map between vector spaces that commutes with the actions of $SU(2)$ on the two spaces. The Wigner state is closely associated with several other intertwiners, such as the dual of the Wigner state, $\langle W| : \mathcal{C}_{j_1} \otimes \mathcal{C}_{j_2} \otimes \mathcal{C}_{j_3} \rightarrow \mathbb{C}$, and the map $\hat{W} : \mathcal{C}_{j_3}^* \rightarrow \mathcal{C}_{j_1} \otimes \mathcal{C}_{j_2}$ which is defined by the action of $\hat{W}(\langle \psi_3|)$ on dual vectors in $\mathcal{C}_{j_1}^* \otimes \mathcal{C}_{j_2}^*$ via

$$\hat{W}(\langle \psi_3|) : \langle \psi_{12}| \mapsto (\langle \psi_{12}| \otimes \langle \psi_3|) |W\rangle. \quad (3.1.2)$$

These intertwiners will all be called $3j$ -intertwiners since the vector spaces involved are composed from three $SU(2)$ carrier spaces.

The various $3j$ -intertwiners are all unique up to a normalization and phase. By Eq. 3.1.1, the $3j$ -symbol forms the contravariant components of the $3j$ -intertwiner associated with the Wigner state in the standard angular momentum basis,

$$\langle j_1 j_2 j_3 m_1 m_2 m_3 | W \rangle = \begin{pmatrix} j_1 & j_2 & j_3 \\ m_1 & m_2 & m_3 \end{pmatrix}. \quad (3.1.3)$$

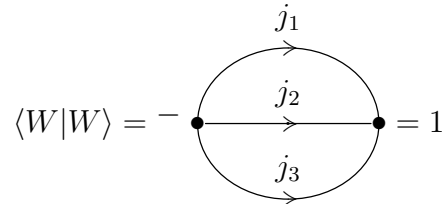
Thus the normalization and phase conventions for the $3j$ -symbol fix a conventional normalization and phase for the $3j$ -intertwiners.

In spin network language the Wigner vector in Eq. 3.1.1 is written



$$\quad (3.1.4)$$

This is also the spin network for the map \hat{W} as in Eq. 3.1.2. The normalization of the various $3j$ -intertwiners is expressed using the “theta graph”,



$$\langle W|W \rangle = - \quad = 1, \quad (3.1.5)$$

where the minus sign on the left node indicates an inverted orientation in the ordering of the three legs following the notation used in Yutsis [7] and Stedman [8].

3.1.2 The Remodeling Algebra of the $3j$ -Symbol

The different inner product models of the $3j$ -symbol are constructed by interpreting the $3j$ -symbol as a matrix element and then forming the remodeling algebra as in Section 2.1.1

of Chapter 2. This is accomplished by “cutting” the network in Eq. 3.0.1 into three pieces,

$$(3.1.6)$$

These pieces represent the dual of the a -state, the b -state, and the operator \hat{M} of the matrix element 2.1.1.

We take the dual of the a -state to be the subnetwork of network 3.1.6 consisting of the two legs ending in labels “ $*m_1$ ” and “ $*m_2$.” These legs end in bra chevrons and the subnetwork is an element of $\mathcal{S}_1^* \otimes \mathcal{S}_2^*$. The a -state is the conjugate of this subnetwork and is an element of the $2j$ -Hilbert space $\mathcal{S}_1 \otimes \mathcal{S}_2$, which serves as the target Hilbert space \mathcal{H}_1 in the language of Chapter 2. The Schwinger Hilbert spaces and operators used to describe angular momenta are defined and described in detail in Section A.1. The $2j$ -Hilbert space may be described in the Schwinger model by four degrees of freedom and thus $n_1 = 4$. The a -state is a standard basis ket in the $2j$ -Hilbert space and is the simultaneous eigenstate of observables \hat{I}_1 , \hat{I}_2 , \hat{J}_{1z} , and \hat{J}_{2z} ,

$$\text{“}a\text{-state”} = \left| \begin{array}{cccc} \hat{I}_1 & \hat{I}_2 & \hat{J}_{1z} & \hat{J}_{2z} \\ j_1 & j_2 & m_1 & m_2 \end{array} \right\rangle = \begin{array}{c} m_1 \xrightarrow{j_1} \\ m_2 \xrightarrow{j_2} \end{array} \in \mathcal{S}_1 \otimes \mathcal{S}_2. \quad (3.1.7)$$

The group G_A is therefore $U(1)^4$ since these four operators all mutually commute on all of the target Hilbert space and thus form a $U(1)^4$ Lie algebra under the commutator. The basis of $\mathfrak{g}_A \cong \mathbb{R}^4$ is chosen so that the components of the \mathbb{R}^4 -valued operator $\hat{\mathbf{A}}$ are $\{\hat{I}_1, \hat{I}_2, \hat{J}_{1z}, \hat{J}_{2z}\}$. We write the a -state in this chapter as either $|a\rangle$ or $|j_1 j_2 m_1 m_2\rangle$. We may also call the a -state the “ $2jm$ -state” since it is the standard basis vector in the $2j$ -Hilbert space.

The b -state is taken to be to be the subnetwork of 3.1.6 consisting of the leg ending in label “ $*m_3$.” This leg ends in a bra chevron and the subnetwork is an element of \mathcal{S}_3^* . The source Hilbert space \mathcal{H}_2 is thus the space of bras \mathcal{S}_3^* . A complete set on the Schwinger Hilbert space consists of two operators so $n_2 = 2$. The b -state is a standard basis bra in the Schwinger Hilbert space,

$$\text{“}b\text{-state”} = \left\langle \begin{array}{cc} \hat{I}_3 & \hat{J}_{3z} \\ j_3 & m_3 \end{array} \right| = *m_3 \xleftarrow{j_3} \in \mathcal{S}_3^*. \quad (3.1.8)$$

The group G_B is $U(1)^2$ and the basis of $\mathfrak{g}_B \cong \mathbb{R}^2$ is chosen so that the components of the \mathbb{R}^2 -valued operator $\hat{\mathbf{B}}$ are $\{\hat{I}_3^\top, \hat{J}_{3z}^\top\}$ where, as discussed in Section A.1, \hat{I}_3^\top is the natural action of \hat{I}_3 on dual vectors from the right. We write the b -state in this chapter as either $\langle b|$ or $\langle j_3 m_3|$.

The product Hilbert space of this remodeling algebra is $(\mathcal{S}_1 \otimes \mathcal{S}_2) \otimes (\mathcal{S}_3^*)^* = \mathcal{S}_1 \otimes \mathcal{S}_2 \otimes \mathcal{S}_3$. We call this space the $3j$ -Hilbert space \mathcal{H}_{3j} . The last piece of network 3.1.6 is a subnetwork

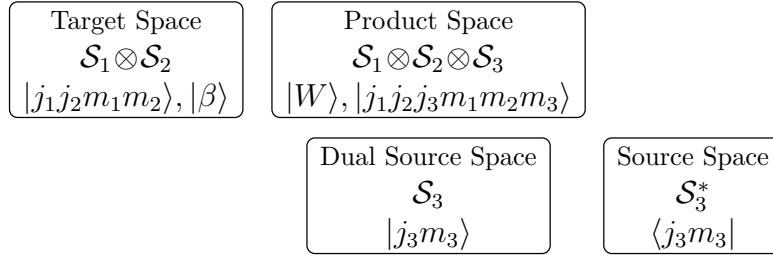


Figure 3.1.1: Spaces and states in the remodeling algebra for the 3j-symbol.

This spin network illustrates the multiple roles that elements can play, an advantage of the spin network notation over the standard Dirac notation. As expected, the two open ket chevrons that are left in the network after the contraction demonstrate that $|\beta\rangle \in \mathcal{S}_1 \otimes \mathcal{S}_2$. The action of this Wigner map in Dirac notation can be extracted by adding a resolution of the identity to each of the open chevrons, yielding

$$\hat{W} : \langle j'_3 m_3| \mapsto \sum_{m_1 m_2} |j_1 j_2 m_1 m_2\rangle \delta_{j_3 j'_3} \begin{pmatrix} j_1 & j_2 & j_3 \\ m_1 & m_2 & m_3 \end{pmatrix}. \quad (3.1.12)$$

The four operators \hat{I}_1 , \hat{I}_2 , $\hat{\mathbf{J}}_{12}^2$, and J_{12z} all mutually commute and therefore G_β is $U(1)^4$. The basis of $\mathfrak{g}_\beta \cong \mathbb{R}^4$ is chosen so that the components of the \mathbb{R}^4 -valued operator $\hat{\beta}$ are $\{\hat{I}_1, \hat{I}_2, \hat{\mathbf{J}}_{12}^2, \hat{J}_{12z}\}$. To avoid confusion with the coupled basis states we write the β -state in this chapter as simply $|\beta\rangle$. Since the β -state involves the coupling of two angular momenta into a third we may refer to $|\beta\rangle$ as the “coupled state”, though this is understood to be distinct from the standard coupled basis states of Φ_{2j} .

The identification of the spaces and states of the remodeling algebra for the 3j-symbol are summarized in Figure 3.1.1.

The product space model of this remodeling algebra is the 3j-model of the 3j-symbol and takes place in the Hilbert space \mathcal{H}_{3j} . The two states involved are the product state in Eq. 3.1.10 and the Wigner state in Eq. 3.1.9,

$$\begin{pmatrix} j_1 & j_2 & j_3 \\ m_1 & m_2 & m_3 \end{pmatrix} = \langle ab|W\rangle = \begin{array}{c} *m_1 \\ | \\ \overleftarrow{\leftarrow} j_1 \\ \bullet \\ \swarrow \leftarrow j_2 \quad \searrow \leftarrow j_3 \\ *m_2 \quad \quad *m_3 \end{array}. \quad (3.1.13)$$

This is precisely the inner product presented in Eq. (22) of Aquilanti *et al* [44]. The target space model is the 2j-model of the 3j-symbol and takes place in the Hilbert space $\mathcal{H}_{2j} =$

$\mathcal{S}_1 \otimes \mathcal{S}_2$. The two states involved are the a -state in Eq. 3.1.7 and the β -state in Eq. 3.1.11,

$$\begin{pmatrix} j_1 & j_2 & j_3 \\ m_1 & m_2 & m_3 \end{pmatrix} = \langle a | \beta \rangle = \begin{array}{c} *m_1 \\ | \\ \text{---} j_1 \\ | \\ \bullet \\ / \quad \backslash \\ j_2 \quad j_3 \\ / \quad \backslash \\ *m_2 \quad *m_3 \end{array} . \quad (3.1.14)$$

3.1.3 Schur's Lemma and the 3j-Intertwiner

To construct observables for $|\beta\rangle$ as in Section 2.4.2 we need to construct the core isomorphism for the Wigner state as in Section 2.4.1. As discussed in Section 3.1.1, the Wigner state is an example of an intertwiner. The linear map in the remodeling algebra for all of our spin network examples will be intertwiners, in fact. Therefore we turn our attention in this section to the more general consideration of how to construct the core isomorphism for an intertwiner.

Schur's lemma [65] allows any intertwiner between two vector spaces carrying unitary representations of a group to be expressed in terms of unitary maps between invariant subspaces. We will only be interested in unitary representations in the work. These unitary maps will be called the “unitary core of the intertwiner.” The core isomorphism for an intertwiner will ultimately be expressed in terms of this unitary core.

Consider two vector spaces \mathcal{E} and \mathcal{F} and a linear map $\hat{A} : \mathcal{E} \rightarrow \mathcal{F}$. As in Section 2.4.1, the core isomorphism is the map $\hat{A}_C = \hat{\Pi}_F \circ \hat{A} \circ \hat{\mathcal{I}}_E : (\ker \hat{A})_\perp \rightarrow \text{img } \hat{A}$, where the range and domain spaces are treated as vector spaces in their own right, $\hat{\mathcal{I}}_E : (\ker \hat{A})_\perp \rightarrow \mathcal{E}$ is the inclusion map and $\hat{\Pi}_F : \mathcal{F} \rightarrow \text{img } \hat{A}$ is a projection map. Conversely, $\hat{A} = \hat{\mathcal{I}}_F \circ \hat{A}_C \circ \hat{\Pi}_E$.

Now let \mathcal{E} and \mathcal{F} be two carrier spaces for unitary representations $\hat{U}(g)$ and $\hat{V}(g)$ of $SU(2)$, respectively. Define the vector space of intertwiners \mathcal{Z} to be the subspace of linear maps $: \mathcal{E} \rightarrow \mathcal{F}$ that commute with $SU(2)$,

$$\mathcal{Z} = \left\{ \hat{M} : \mathcal{E} \rightarrow \mathcal{F} \mid \hat{M} \circ \hat{U}(g) = \hat{V}(g) \circ \hat{M}, \forall g \in SU(2) \right\}. \quad (3.1.15)$$

The space \mathcal{Z} is isomorphic to the space of intertwiners $: \mathcal{E} \otimes \mathcal{F}^* \rightarrow \mathbb{C}$ and the subspace of $SU(2)$ -invariant elements of the product vector space $\mathcal{F} \otimes \mathcal{E}^*$.

The representations \hat{U} and \hat{V} are called equivalent if there exists some invertible map $\hat{A} : \mathcal{E} \rightarrow \mathcal{F}$ such that

$$\hat{A} \circ \hat{U}(g) \circ \hat{A}^{-1} = \hat{V}(g), \quad \forall g \in SU(2). \quad (3.1.16)$$

Thus $\hat{U}(g)$ and $\hat{V}(g)$ are equivalent representations if there exists an *invertible* intertwiner between the carrier spaces. If no such intertwiner exists, then $\hat{U}(g)$ and $\hat{V}(g)$ are inequivalent. This terminology will be used for reducible as well as irreducible representations.

In the following subsections we analyze how Schur's lemma applies to cases where both \mathcal{E} and \mathcal{F} are carrier spaces for irreducible representations, where either \mathcal{E} or \mathcal{F} carries a

reducible representation but the other carries an irreducible representation, and where both \mathcal{E} and \mathcal{F} carry reducible representations.

3.1.3.1 Case I - Both $\hat{U}(g)$ and $\hat{V}(g)$ Irreducible

The traditional form of Schur's lemmas deals with the case where both \mathcal{E} and \mathcal{F} are carrier spaces for finite-dimensional irreducible representations. If $\hat{U}(g)$ and $\hat{V}(g)$ are inequivalent representations then Schur's lemma says that $\hat{M} = 0$ is the only intertwiner between \mathcal{E} and \mathcal{F} , so \mathcal{Z} is a zero-dimensional vector space. On the other hand, if $\hat{U}(g)$ and $\hat{V}(g)$ are equivalent irreducible representations then Schur's lemma states that any non-zero intertwiner between \mathcal{E} and \mathcal{F} is invertible and all such intertwiners are proportional. Furthermore, if $\hat{U}(g)$ and $\hat{V}(g)$ are both unitary representations, then there exists a *unitary* intertwiner $\hat{A} \in \mathcal{Z}$ which is unique up to a phase. Thus every nontrivial intertwiner $\hat{M} \in \mathcal{Z}$ from a finite-dimensional irreducible carrier space to a finite-dimensional irreducible carrier space can be decomposed as

$$\hat{M} = c\hat{A}, \quad (3.1.17)$$

where $c \in \mathbb{C}$ and $\hat{A} : \mathcal{E} \rightarrow \mathcal{F}$ is a unitary map. As a result, \mathcal{Z} is at most one-dimensional, with $\dim \mathcal{Z} = 0$ if \mathcal{E} and \mathcal{F} carry inequivalent irreducible representations and $\dim \mathcal{Z} = 1$ if \mathcal{E} and \mathcal{F} carry equivalent irreducible representations. Given a non-zero intertwiner \hat{M} in this case, $(\ker \hat{M})_\perp$ and $\text{img } \hat{M}$ are the entire spaces \mathcal{E} and \mathcal{F} and \hat{M} itself is the core isomorphism. If \mathcal{E} and \mathcal{F} are Hilbert spaces then the unitary core \hat{A} in Eq. 3.1.17 is an isometry. In the theory of angular momenta, the carrier spaces of irreducible representations \mathcal{C}_j are parameterized by $j = 0, 1/2, 1, \dots$, with $\dim \mathcal{C}_j = 2j + 1$. The space of intertwiners $:\mathcal{C}_j \rightarrow \mathcal{C}_{j'}$ therefore has dimension $\delta_{jj'}$.

3.1.3.2 General Considerations for the Other Cases

The spaces \mathcal{E} and \mathcal{F} may carry reducible representations in which case the results of Schur's lemma can be generalized. Suppose $\hat{U}(g)$ and $\hat{V}(g)$ are unitary, potentially reducible representations and let $\hat{M} : \mathcal{E} \rightarrow \mathcal{F}$ be an intertwiner in \mathcal{Z} . For any $y \in \text{img } \hat{M}$ there exists some $x \in \mathcal{E}$ such that $y = \hat{M}x$. By the intertwiner property, $\hat{V}(y) = \hat{V}(\hat{M}(x)) = \hat{M}(\hat{U}(x)) \in \text{img } \hat{M}$. Thus, $\text{img } \hat{M} \subset \mathcal{F}$ is an invariant subspace of \mathcal{F} . Similarly, let $x \in \ker \hat{M}$ so $\hat{M}x = 0$. By the intertwiner property, $0 = \hat{V}(\hat{M}(x)) = \hat{M}(\hat{U}(x))$ so $\hat{U}x \in \ker \hat{M}$ which means $\ker \hat{M}$ is an invariant subspace of \mathcal{E} . Since $\hat{U}(g)$ is a unitary action, the invariant subspaces of \mathcal{E} are orthogonal and thus $(\ker \hat{M})_\perp \subset \mathcal{E}$ is an invariant subspace. Since $(\ker \hat{M})_\perp$ and $\text{img } \hat{M}$ are invariant subspaces of \mathcal{E} and \mathcal{F} , they can be considered carrier spaces for the restricted representations $\hat{U}_R(g)$ and $\hat{V}_R(g)$, respectively.

Let $\hat{M}_C = \hat{\Pi}_{\text{img}} \circ \hat{M} \circ \hat{\mathcal{I}}_{\ker} : (\ker \hat{M})_\perp \rightarrow \text{img } \hat{M}$ be the isomorphic core of the intertwiner \hat{M} . Since $\text{img } \hat{M}$ and $(\ker \hat{M})_\perp$ are invariant subspaces, the restricted map \hat{M}_C inherits the intertwiner property from \hat{M} and

$$\hat{M}_C \circ \hat{U}_R(g) \circ \hat{M}_C^{-1} = \hat{V}_R(g), \quad \forall g \in SU(2). \quad (3.1.18)$$

Thus $(\ker \hat{M})_\perp$ and $\text{img } \hat{M}$ are not only isomorphic but carry equivalent representations \hat{U}_R and \hat{V}_R .

In summary, the core isomorphism of *any* intertwiner is an intertwiner between subspaces carrying equivalent representations.

3.1.3.3 Case II - $\hat{U}(g)$ Reducible and $\hat{V}(g)$ Irreducible

Now consider the case where $\hat{U}(g)$ is a reducible representation and $\hat{V}(g)$ is a finite-dimensional irreducible representation. Since \mathcal{F} is a carrier space for an irreducible representation there are no proper invariant subspaces of \mathcal{F} and any non-zero intertwiner $\hat{M} \in \mathcal{Z}$ must have $\text{img } \hat{M} = \mathcal{F}$. The “restricted” representation $\hat{V}_R(g)$ in Eq. 3.1.18 is therefore just the original representation $\hat{V}(g)$. By Eq. 3.1.18, representation $\hat{V}(g)$ on \mathcal{F} is equivalent to the restricted representation $\hat{U}_R(g)$ on $(\ker \hat{M})_\perp$. The core isomorphism $\hat{M}_C : (\ker \hat{M})_\perp \rightarrow \mathcal{F}$ is thus an intertwiner between two equivalent irreducible representations. By the discussion leading up to Eq. 3.1.17, $\hat{M}_C = c\hat{A}$ for some unitary $\hat{A} : (\ker \hat{M})_\perp \rightarrow \mathcal{F}$ and scalar $c \in \mathbb{C}$. If \mathcal{E} and \mathcal{F} are Hilbert spaces then this says that the core isomorphism is proportional to an isometry.

Let the space \mathcal{E} be decomposed into a direct sum of invariant subspaces $\mathcal{E} = \bigoplus \mathcal{E}_i$. Any intertwiner \hat{M} then decomposes as

$$\hat{M} = \sum c_i \hat{A}_i \circ \hat{\Pi}_i, \quad (3.1.19)$$

where $c_i \in \mathbb{C}$, $\hat{A}_i : \mathcal{E}_i \rightarrow \mathcal{F}$ is either a unitary map or zero depending on whether \mathcal{E}_i is equivalent to \mathcal{F} or not, and $\hat{\Pi}_i : \mathcal{E} \rightarrow \mathcal{E}_i$ is a projection map. The direct sum decomposition of \mathcal{E} is not unique if it contains multiple copies of a single irrep carrier space. If there are multiple copies of an irrep carrier space that is equivalent to \mathcal{F} then the set of unitary core maps \hat{A}_i is not unique. The set of non-zero maps $\hat{A}_i \circ \hat{\Pi}_i$ acts as a basis for the space of intertwiners \mathcal{Z} . Choosing a different basis in \mathcal{Z} corresponds to a different choice of maps and a different direct-sum decomposition of \mathcal{E} .

The space of \mathcal{Z} of $SU(2)$ intertwiners $: \mathcal{E} \rightarrow \mathcal{F}$ is isomorphic to the space $\tilde{\mathcal{Z}}$ of intertwiners $: \mathcal{E} \otimes \mathcal{F}^* \rightarrow \mathbb{C}$. The space \mathbb{C} , considered as a one-dimensional vector space, is invariant under $SU(2)$ and thus is an irreducible carrier space for the $j = 0$ representation of $SU(2)$. We may therefore apply Eq. 3.1.19 to intertwiners in $\tilde{\mathcal{Z}}$, making the replacements $\mathcal{E} \mapsto \mathcal{E} \otimes \mathcal{F}^*$ and $\mathcal{F} \mapsto \mathbb{C}$. The only non-zero terms of Eq. 3.1.19 are the those corresponding to the $j = 0$ irreps that occur in the direct-sum decomposition of $\mathcal{E} \otimes \mathcal{F}^*$, so $\tilde{\mathcal{Z}}$ is spanned by $\{\hat{A}_i \circ \hat{\Pi}_i\}$, where i indexes the $j = 0$ irreps in the direct-sum decomposition. Since \mathcal{Z} is isomorphic to $\tilde{\mathcal{Z}}$, and the dimension of space of intertwiners \mathcal{Z} is thus equal to the number of $j = 0$ irreps that occur in a direct-sum decomposition of $\mathcal{E} \otimes \mathcal{F}^*$. Conversely, every element of \mathcal{Z} picks out a $j = 0$ irreducible subspace of $\mathcal{E} \otimes \mathcal{F}^*$. For example, let $\mathcal{E} = \mathcal{C}_{j_1} \otimes \mathcal{C}_{j_2} \otimes \mathcal{C}_{j_3}$ and consider the space of intertwiners $\mathcal{E} \rightarrow \mathbb{C}$. If (j_1, j_2, j_3) is a triangle-allowed triplet, then there is a unique (up to a phase) normalized invariant vector in $\mathcal{C}_{j_1} \otimes \mathcal{C}_{j_2} \otimes \mathcal{C}_{j_3}$, $|W\rangle$. The dual of the Wigner state $\langle W|$ forms the basis of \mathcal{Z} and thus \mathcal{Z} is one-dimensional in this case. The

core isomorphism for any intertwiner \hat{M} with $(\ker \hat{M})_\perp \cong \mathcal{C}_{j_1} \otimes \mathcal{C}_{j_2} \otimes \mathcal{C}_{j_3}$ and $\text{img } \hat{M} \cong \mathbb{C}$ is therefore proportional to the Wigner state $\langle W |$. If (j_1, j_2, j_3) are not triangle-allowed, then there does not exist an invariant vector in \mathcal{E} and \mathcal{Z} is zero-dimensional.

3.1.3.4 Case III - $\hat{U}(g)$ Irreducible and $\hat{V}(g)$ Reducible

Next consider the case where $\hat{U}(g)$ is a finite-dimensional irreducible representation and $\hat{V}(g)$ is a reducible representation. Since \mathcal{E} is a carrier space for an irreducible representation, there are no proper invariant subspaces of \mathcal{E} . Thus any non-zero intertwiner $\hat{M} \in \mathcal{Z}$ must have $\ker \hat{M} = 0$ and $(\ker \hat{M})_\perp = \mathcal{E}$. The representation $\hat{U}(g)$ is therefore the same as the restricted representation $\hat{U}_R(g)$ and, by Eq. 3.1.18, is equivalent to the restricted representation $\hat{V}_R(g)$ on $\text{img } \hat{M}$. The core isomorphism $\hat{M}_C : \mathcal{E} \rightarrow \text{img } \hat{M}$ is thus an intertwiner between two equivalent irreducible representations. By the discussion leading up to Eq. 3.1.17, $\hat{M}_C = c\hat{A}$ for some unitary $\hat{A} : \mathcal{E} \rightarrow \text{img } \hat{M}$ and scalar $c \in \mathbb{C}$. If \mathcal{E} and \mathcal{F} are Hilbert spaces then this says that the core isomorphism is proportional to an isometry.

Let the space \mathcal{F} be decomposed into a direct sum of invariant subspaces $\mathcal{F} = \bigoplus \mathcal{F}_i$. Any intertwiner \hat{M} then decomposed as

$$\hat{M} = \sum c_i \hat{\mathcal{I}}_i \circ \hat{A}_i, \quad (3.1.20)$$

where $c \in \mathbb{C}$, $\hat{A}_i : \mathcal{E} \rightarrow \mathcal{F}_i$ is either a unitary map or zero depending on whether \mathcal{F}_i is equivalent to \mathcal{E} or not, and $\hat{\mathcal{I}}_i$ is the inclusion map $\mathcal{F}_i \rightarrow \mathcal{F}$. The direct sum decomposition of \mathcal{F} is not unique if it contains multiple copies of a single irrep carrier space. If there are multiple copies of an irrep carrier space that is equivalent to \mathcal{E} then the set of unitary core maps \hat{A}_i is not unique. The set of non-zero maps $\hat{\mathcal{I}}_i \circ \hat{A}_i$ acts as a basis for the space of intertwiners \mathcal{Z} . Choosing a different basis in \mathcal{Z} corresponds to a different choice of maps and a different direct-sum decomposition of \mathcal{F} .

The Wigner map $\hat{W} : \mathcal{C}_{j_3}^* \rightarrow \mathcal{C}_{j_1} \otimes \mathcal{C}_{j_2}$ defined in Eq. 3.1.2 is an example of an intertwiner from an irreducible to a reducible carrier space. If the triplet (j_1, j_2, j_3) is triangle-allowed then the intertwiner will be nontrivial and Eq. 3.1.20 can be applied. A familiar result from standard angular momentum theory says that the target space $\mathcal{C}_{j_1} \otimes \mathcal{C}_{j_2}$ breaks into a direct sum of irreducible subspaces as

$$\mathcal{C}_{j_1} \otimes \mathcal{C}_{j_2} = \bigoplus_{J=|j_1-j_2|}^{j_1+j_2} \mathcal{C}_J. \quad (3.1.21)$$

The image of the Wigner map must carry a representation equivalent to the representation on $\mathcal{C}_{j_3}^*$. A simple dimension count implies that $\text{img } \hat{W}$ must be \mathcal{C}_{j_3} . The restricted intertwiner is therefore a map $\mathcal{C}_{j_3}^* \rightarrow \mathcal{C}_{j_3}$. Let $\hat{\mathcal{I}}_{j_3} : \mathcal{C}_{j_3} \rightarrow \mathcal{C}_{j_1} \otimes \mathcal{C}_{j_2}$ be the inclusion map of the j_3 -subspace in the direct sum decomposition Eq. 3.1.21. Then, by Eq. 3.1.20, the Wigner map can be written as

$$\hat{W} = c\hat{\mathcal{I}}_{j_3} \circ \hat{A}, \quad (3.1.22)$$

where $\hat{A} : \mathcal{C}_{j_3}^* \rightarrow \mathcal{C}_{j_3}$ is the unitary core of the Wigner map. This map is closely related to the $2j$ intertwiner that will be explored more fully in the context of the $2j$ -symbol, in section 3.1.4. The prefactor c can be determined by considering the operator $\hat{W} \circ \hat{W}^\dagger$. By the orthogonality of the $3j$ -symbol (Eq. (3.7.7) of Edmonds [28]),

$$\hat{W} \circ \hat{W}^\dagger = \left\langle \begin{array}{c} j_2 \\ \leftarrow j_3 \bullet \begin{array}{c} \curvearrowright \\ j_1 \\ \curvearrowleft \end{array} \bullet j_3 \rightarrow \end{array} \right\rangle = \frac{1}{2j_3 + 1} \left\langle \begin{array}{c} j_3 \\ \leftarrow \bullet \rightarrow \end{array} \right\rangle. \quad (3.1.23)$$

On the other hand, the decomposition in Eq. 3.1.22 says

$$\hat{W} \circ \hat{W}^\dagger = |c|^2 \hat{A}^\dagger \circ \hat{\mathcal{I}}_{j_3}^\dagger \circ \hat{\mathcal{I}}_{j_3} \circ \hat{A} = |c|^2 \hat{I}_{d_{j_3}} = |c|^2 \left\langle \begin{array}{c} j_3 \\ \leftarrow \bullet \rightarrow \end{array} \right\rangle. \quad (3.1.24)$$

Therefore, the Wigner operator is determined (up to a phase) to be

$$\hat{W} = \frac{1}{\sqrt{2j_3 + 1}} \hat{\mathcal{I}}_{j_3} \circ \hat{A}. \quad (3.1.25)$$

3.1.3.5 Case IV - Both $\hat{U}(g)$ and $\hat{V}(g)$ Reducible

Finally consider the case where both $\hat{U}(g)$ and $\hat{V}(g)$ are reducible representations. Let $\hat{M} \in \mathcal{Z}$ be a particular intertwiner and create the restricted intertwiner $\hat{M}_R : (\ker \hat{M})_\perp \rightarrow \text{img } \hat{M}$. This restricted map is an isomorphism but the restricted representations $\hat{U}_R(g)$ and $\hat{V}_R(g)$ are still potentially reducible so Eq. 3.1.17 can't be directly applied. Let the invariant subspace $(\ker \hat{M})_\perp$ be decomposed into irreducible subspaces $\mathcal{E}_i \subset (\ker \hat{M})_\perp \subset \mathcal{E}$ such that $(\ker \hat{M})_\perp = \bigoplus \mathcal{E}_i$. The intertwiner \hat{M}_R can be block-diagonalized in this decomposition. Each block on the diagonal corresponds to a map $\hat{M}_i : \mathcal{E}_i \rightarrow \text{img } \hat{M}$. Since by definition \mathcal{E}_i is irreducible, the decomposition in Eq. 3.1.20 can be applied. Thus every nontrivial intertwiner $\hat{M} \in \mathcal{Z}$ from a reducible carrier space to a reducible carrier space can be decomposed as

$$\hat{M} = \sum_{ij} c_{ij} \hat{\mathcal{I}}_j \circ \hat{A}_{ij} \circ \hat{\Pi}_i, \quad (3.1.26)$$

where $c_{ij} \in \mathbb{C}$, $\hat{\Pi}_i : \mathcal{E} \rightarrow \mathcal{E}_i$ are projection maps onto the irreducible subspaces of \mathcal{E} , $\hat{\mathcal{I}}_j : \mathcal{F}_j \rightarrow \mathcal{F}$ are inclusion maps, and $\hat{A}_{ij} : \mathcal{E}_i \rightarrow \mathcal{F}_j$ are unitary maps.

For example, we may apply Eq. 3.1.26 to the operator $\hat{W} : \mathcal{S}_3^* \rightarrow \mathcal{S}_1 \otimes \mathcal{S}_2$ defined in Eqs. 3.1.9 and 3.1.12. Both domain and target spaces are infinite-dimensional reducible carrier spaces. We first identify the relevant invariant subspaces of the target and domain space. The dual Schwinger Hilbert space decomposes into the direct sum of irreducible carrier spaces, $\mathcal{S}_3^* = \bigoplus_J \mathcal{C}_J^*$, where each of the carrier spaces is considered a vector subspace of \mathcal{S}_3^* . The Wigner map annihilates any vector outside of the j_3 subspace so

$$\ker \hat{W} = \bigoplus_{J \neq j_3} \mathcal{C}_J^*, \quad (\ker \hat{W})_\perp = \mathcal{C}_{j_3}^*. \quad (3.1.27)$$

Thus $(\ker \hat{W})_\perp$ is a carrier space for a finite-dimensional irreducible representation and there is only a single term in the sum over index i in Eq. 3.1.26. Restricting the domain of the Wigner map to $(\ker \hat{W})_\perp$ yields an intertwiner $\hat{W}' : \mathcal{C}_{j_3}^* \rightarrow \mathcal{S}_1 \otimes \mathcal{S}_2$ from a finite-dimensional irreducible carrier space to a reducible carrier space and so Eq. 3.1.20 can be applied. By definition, $\text{img } \hat{W}$ is a subspace of $\mathcal{C}_{j_1} \otimes \mathcal{C}_{j_2} \subset \mathcal{S}_1 \otimes \mathcal{S}_2$ and thus Eq. 3.1.22 can be applied, yielding

$$\hat{W} = \frac{1}{\sqrt{2j_3 + 1}} \hat{\mathcal{I}}_{j_3} \circ \hat{A} \circ \hat{\Pi}_{j_3}. \quad (3.1.28)$$

Note that all versions of the Wigner map encountered in this section share the same unitary core $\hat{A} : \mathcal{C}_{j_3}^* \rightarrow \mathcal{C}_{j_3}$.

3.1.4 The $2j$ -Intertwiner State

As shown in the previous section, the core isomorphism of the Wigner intertwiner is partially constructed from a “ $2j$ -intertwiner” $: \mathcal{C}_j^* \rightarrow \mathcal{C}_j$, which we explore in this section.

Consider the space \mathcal{Z}_{2j} of $2j$ -intertwiners $: \mathcal{C}_j \otimes \mathcal{C}'_j \rightarrow \mathbb{C}$, where the domain is the tensor product of two identical irrep carrier spaces. The prime on the second copy of \mathcal{C}_j is used to distinguish the second carrier space from the first. This space is isomorphic to the space of $2j$ -intertwiners $: \mathcal{C}'_j \rightarrow \mathcal{C}_j^*$ which, by Schur’s lemma, is one-dimensional. According to the discussion following Eq. 3.1.19, any non-zero $SU(2)$ -invariant element in $\mathcal{C}_j^* \otimes \mathcal{C}'_j$ spans \mathcal{Z} . The components of such an element can be expressed in terms of the “ $2j$ -symbol” (a terminology found in Stedman [8] and Aquilanti *et al* [1]), which is defined in terms of the $3j$ -symbol as

$$\begin{pmatrix} j & j \\ m & m' \end{pmatrix} = \begin{pmatrix} j & j & 0 \\ m & m' & 0 \end{pmatrix} = \frac{(-1)^{j-m}}{\sqrt{2j+1}} \delta_{m,-m'}. \quad (3.1.29)$$

Thus the $2j$ -symbol is seen as a special case of the $3j$ -symbol. The $2j$ -symbol represents the covariant components of the $2j$ -intertwiner $\langle K | \in \mathcal{C}_j^* \otimes \mathcal{C}'_j$ in the standard basis,

$$\langle K | = \sum_{mm'} \sqrt{2j+1} \begin{pmatrix} j & j \\ m & m' \end{pmatrix} \langle jm | \otimes \langle jm' |. \quad (3.1.30)$$

The prefactor $\sqrt{2j+1}$ is due to the normalization convention $\langle K | K \rangle = 2j+1$. The phase convention for $\langle K |$ is tied to the phase convention of the $2j$ -symbol which ultimately derives from the phase convention for the $3j$ -symbol. The spin network notation for the $2j$ -intertwiner $\langle K | \in \mathcal{C}_j^* \otimes \mathcal{C}'_j$ is given by

$$\langle K | = \left\langle \begin{array}{c} \hat{I} \\ j \end{array} \quad \begin{array}{c} \hat{\mathbf{J}} + \hat{\mathbf{J}}' \\ \mathbf{0} \end{array} \right| = \rangle \text{---} \text{---} \text{---} \langle, \quad (3.1.31)$$

where by convention the chevron counterclockwise of the stub corresponds to the first (unprimed) carrier space. The “stub” notation for the $2j$ -intertwiner is further explained in

Stedman [8] and Aquilanti *et al* [1]. Since $\langle K | (\hat{\mathbf{J}} + \hat{\mathbf{J}}') = \mathbf{0}$ the operator identity Eq. A.1.3 implies that $\langle K |$ is also an eigenstate of \hat{I}' with eigenvalue j .

It follows from Eq. 3.1.30 that the components of the $2j$ -intertwiner are proportional to the $2j$ -symbol,

$$m \rightarrow \begin{array}{c} | \\ \leftarrow \\ j \end{array} \leftarrow m' = \sqrt{2j+1} \begin{pmatrix} j & j \\ m & m' \end{pmatrix} = (-1)^{j-m} \delta_{m,-m'}. \quad (3.1.32)$$

The spin network in Eq. 3.1.31 can also be interpreted as a map $\hat{K}_j : \mathcal{C}_j \rightarrow \mathcal{C}_j^*$, where an input \mathcal{C}_j ket is contracted against the right bra chevron. This is a *unitary* map from kets to bras and is thus distinct from Hermitian conjugation, which is anti-unitary. The inverse map is given by

$$\hat{K}_j^{-1} : \mathcal{C}_j^* \rightarrow \mathcal{C}_j = \left\langle \begin{array}{c} | \\ \leftarrow \\ j \end{array} \right\rangle, \quad (3.1.33)$$

where an input \mathcal{C}_j^* bra is contracted against the left ket chevron. The spin network in Eq. 3.1.33 can also be interpreted as the ket $|K\rangle \in \mathcal{C}_j \otimes \mathcal{C}_j'^*$, where by convention the first and second chevrons correspond to the first and second (unprimed and primed) carrier spaces. As in Eq. (3.27) of Aquilanti *et al* [1], the action of \hat{K}_j and \hat{K}_j^{-1} on the standard basis kets gives

$$\hat{K}_j(|jm\rangle) = (-1)^{j-m} \langle j, -m|, \quad \hat{K}_j^{-1}(\langle jm|) = (-1)^{j+m} |j, -m\rangle. \quad (3.1.34)$$

The $2j$ intertwiner is closely related to the time-reversal operator. The time reversal operator $\hat{\Theta}$ on a carrier space \mathcal{C}_j is an anti-linear map $: \mathcal{C}_j \rightarrow \mathcal{C}_j : |jm\rangle \mapsto (-1)^{j-m} |j, -m\rangle$ [66]. Note that the square of time reversal is $\hat{\Theta}^2 = (-1)^{2j}$ when acting on \mathcal{C}_j and therefore $\hat{\Theta}^{-1} = (-1)^{2j} \hat{\Theta}$. The time reversal operator is $\hat{\Theta} = \hat{K}_j^{-1} \circ \hat{G}$ [1] and so the $2j$ -intertwiner may be expressed as

$$\hat{K}_j^{-1} = \hat{\Theta} \circ \hat{G}^{-1}, \quad \hat{K}_j = (-1)^{2j} \hat{G} \circ \hat{\Theta}. \quad (3.1.35)$$

3.1.5 Observables of $3j$ -Remodeling Algebra

Eqs. 3.1.7, 3.1.8, 3.1.10, 3.1.9, and 3.1.11 express the states of the remodeling algebra as non-degenerate eigenstates of sets of observables. In this section we find the sets of observables that define the core Hilbert spaces for the Wigner intertwiner and show how the method in Section 2.4.2 reproduces the β -list of observables in Eq. 3.1.11.

Consider the operator $\hat{W} : \mathcal{S}_3^* \rightarrow \mathcal{S}_1 \otimes \mathcal{S}_2$ defined in Eqs. 3.1.9 and 3.1.12. As already stated in Eq. 3.1.27, $(\ker \hat{W})_\perp = \mathcal{C}_{j_3}^* \subset \mathcal{S}_{j_3}^*$. The set of operators $\{\hat{D}_A\}$ that define $(\ker \hat{W})_\perp$ through Eq. 2.4.5 thus contains a single entry (the index A only takes on a single value),

$$\hat{D}_A = \hat{I}_3^\top, \quad \mu_{d,A} = j_3. \quad (3.1.36)$$

Since $\mathcal{S}_{j_3}^*$ is the Hilbert space for a system described by two classical degrees of freedom, $n_2 = 2$. Since only a single operator is needed to classify $(\ker \hat{W})_\perp$, $n_2 - \tilde{n} = 1$ and thus

$\tilde{n} = 1$ for the 3j-symbol remodeling algebra. Note that since there is only one entry in the “D-list” of operators, Eq. 2.4.6 is automatically satisfied. Furthermore, \hat{I}_3^\top generates the group $U(1)$ on $\mathcal{S}_{j_3}^*$ so $G_D = U(1)$ and $\mathfrak{g}_D \cong \mathbb{R}$. The “B-list” of operators is chosen to be $\{\hat{I}_3^\top, \hat{J}_{3z}^\top\}$ as in Eq. 3.1.8. Note that the b -state is an element of $(\ker \hat{W})_\perp$, as required by Section 2.4.2. This B-list is already written in the form of Eq. 2.4.7 and thus the single operator (since $\tilde{n} = 1$) \hat{B}_ℓ can be read off as

$$\hat{B}_\ell = \hat{J}_{3z}^\top, \quad \mu_{b,\ell} = m_3. \quad (3.1.37)$$

As already discussed in Section 3.1.3, $\text{img } \hat{W}$ is the invariant subspace \mathcal{C}_{j_3} contained in $\mathcal{C}_{j_1} \otimes \mathcal{C}_{j_2} \subset \mathcal{S}_1 \otimes \mathcal{S}_2$. The $\mathcal{C}_{j_1} \otimes \mathcal{C}_{j_2}$ subspace is the simultaneous eigenspace of operators \hat{I}_1 and \hat{I}_2 at eigenvalues j_1 and j_2 . The \mathcal{C}_{j_3} subspace is further specified as the eigenspace of operator $\hat{\mathbf{J}}_{12}^2$ at eigenvalue $j_3(j_3 + 1)$, as can be seen by the following analysis. Recall that the Wigner state in the product space (which serves as the map \hat{W}) is in the simultaneous eigenspace of operators \hat{I}_3 and $\hat{\mathbf{J}}_T$ at eigenvalues j_3 and $\mathbf{0}$. By the operator identity A.1.3, the eigenvalue condition $\hat{I}_3|W\rangle = j_3|W\rangle$ may be replaced by $\hat{\mathbf{J}}_3^2|W\rangle = \hat{I}_3(\hat{I}_3 + 1)|W\rangle = j_3(j_3 + 1)|W\rangle$. Moreover, $\hat{\mathbf{J}}_T|W\rangle = \mathbf{0}|W\rangle$ implies that $\hat{\mathbf{J}}_3|W\rangle = -\hat{\mathbf{J}}_{12}|W\rangle$. Therefore,

$$\hat{\mathbf{J}}_{12}^2|W\rangle = j_3(j_3 + 1)|W\rangle, \quad (3.1.38)$$

where $\hat{\mathbf{J}}_{12} \equiv \hat{\mathbf{J}}_1 + \hat{\mathbf{J}}_2$. Since $\hat{\mathbf{J}}_{12}$ only acts on the target space component of the product Hilbert space, $\text{img } \hat{W}$ is a subset of the $j_3(j_3 + 1)$ -eigenspace of $\hat{\mathbf{J}}_{12}$. The set of operators $\{\hat{C}_a\}$ that define $\text{img } \hat{W}$ through Eq. 2.4.3 thus contains three entries,

$$\{\hat{C}_a\} = \{\hat{I}_1, \hat{I}_2, \hat{\mathbf{J}}_{12}^2\}, \quad \mu_{c,a} = j_1, j_2, j_3(j_3 + 1). \quad (3.1.39)$$

The target Hilbert space $\mathcal{S}_{j_1} \otimes \mathcal{S}_{j_2}$ is the Hilbert space for a system described by four classical degrees of freedom, $n_1 = 4$. Thus $n_1 - \tilde{n} = 3$ is the appropriate number of operators needed to define $\text{img } \hat{W}$. The “C-list” of operators are easily shown to commute on the entire target space so Eq. 2.4.4 is satisfied. These operators generate a group $U(1)^3$ on $\mathcal{S}_1 \otimes \mathcal{S}_2$ so $G_C = U(1)^3$ and $\mathfrak{g}_C \cong \mathbb{R}^3$.

In Section 3.1.3 the core isomorphism of \hat{W} was determined to be an intertwiner $:\mathcal{C}_{j_3}^* \rightarrow \mathcal{C}_{j_3}$. By Schur’s lemma, this intertwiner must be proportional to the (unitary) $2j$ -intertwiner $\hat{K}_{j_3}^{-1}$ defined in Eq. 3.1.33. Applying this to Eq. 3.1.28 yields

$$\hat{W} = \frac{1}{\sqrt{2j_3 + 1}} \hat{\mathcal{I}}_{j_3} \circ \hat{K}_{j_3}^{-1} \circ \hat{\Pi}_{j_3}, \quad \hat{W}_C = \frac{1}{\sqrt{2j_3 + 1}} \hat{K}_{j_3}^{-1}. \quad (3.1.40)$$

By Eq. 2.4.12, $|\beta\rangle$ may be described using the three operators in Eq. 3.1.39 and the single operator $\hat{\beta}$ which is defined via Eq. 2.4.8 to be

$$\hat{\beta} \equiv \hat{W}_C \circ \hat{B} \circ \hat{W}_C^{-1} = \hat{K}_{j_3}^{-1} \circ \hat{J}_{3z}^\top \circ \hat{K}_{j_3}, \quad (3.1.41)$$

where \hat{K}_{j_3} is understood in this context to be a map from the \mathcal{C}_{j_3} subspace of $\mathcal{C}_1 \otimes \mathcal{C}_2$ to the space $\mathcal{C}_{j_3}^*$ subspace on which \hat{J}_{3z}^\top acts. Operator $\hat{\beta}$ is equal to $-\hat{J}_{12z} \equiv -(\hat{J}_{1z} + \hat{J}_{2z})$, which

may be shown by analyzing the action of the operator on the coupled angular momentum basis vectors in $\mathcal{C}_{j_3} \subset \mathcal{C}_1 \otimes \mathcal{C}_2$,

$$\hat{\beta}|j_1 j_2; JM\rangle = \hat{K}_{j_3}^{-1} \circ \hat{J}_{3z}^\top \circ \hat{K}_{j_3}|j_1 j_2; JM\rangle. \quad (3.1.42)$$

By Eq. 3.1.34, the left-hand side of Eq. 3.1.42 becomes

$$(-1)^{j_3-M} \hat{K}_{j_3}^{-1} \circ \hat{J}_{3z}^\top (\langle j_3, -M |). \quad (3.1.43)$$

The bra $\langle j_3, -M |$ is an eigenbra of \hat{J}_{3z}^\top with eigenvalue $-M$. Applying this and Eq. 3.1.34 once again yields

$$\hat{\beta}|j_1 j_2; JM\rangle = -M|j_1 j_2; j_3 M\rangle = -\hat{J}_{12z}|j_1 j_2; j_3 M\rangle, \quad \forall M. \quad (3.1.44)$$

This operator is naturally expanded to an operator \hat{J}_{12z} on all of $\mathcal{S}_1 \otimes \mathcal{S}_2$. Thus, in agreement with Eq. 2.4.11,

$$\hat{\beta}_\ell = -\hat{J}_{12z}, \quad \hat{\beta}_\ell |\beta\rangle = \mu_{b,\ell} |\beta\rangle, \quad (3.1.45)$$

where $\mu_{b,\ell} = m_3$ as in Eq. 3.1.37.

Combining the results in this section with Eq. 2.4.12 yields

$$|\beta\rangle = \frac{1}{\sqrt{2j_3+1}} \left| \begin{array}{ccc} \hat{I}_1 & \hat{I}_2 & \hat{\mathbf{J}}_{12}^2 \\ j_1 & j_2 & j_3(j_3+1) \end{array} \right. \left. \begin{array}{c} -\hat{J}_{12z} \\ m_3 \end{array} \right\rangle, \quad (3.1.46)$$

where $|\beta\rangle$ is assumed normalized and an explicit normalization factor has been included. Note that \hat{J}_{12z} does indeed commute with all operators in the C -list on all of the target space as required by Section 2.4.2. Moreover, the “ β -list” of operators $\{\hat{I}_1, \hat{I}_2, \hat{\mathbf{J}}_{12}^2, \hat{J}_{12z}\}$ agrees with the expected list from Eq 3.1.11. Note that the state $|\beta\rangle$ as written in Eq. 3.1.46 differs from the standard coupled basis vector $|j_1 j_2; j_3, -m_3\rangle$ of angular momentum theory by a normalization and a phase factor.

We summarize the operator lists and eigenvalues for the various states and subspaces of interest in the $3j$ -symbol remodeling algebra in Table 3.1.

3.1.6 The Clebsch-Gordan Coefficients and Map

Related to the $3j$ -symbol are the Clebsch-Gordan coefficients, which may be considered the components of an intertwiner between a space of two angular momenta to a space of one angular momentum (the coefficients are used to “couple” two angular momenta into a third). This intertwiner is distinct from the Wigner intertwiners explored in Section 3.1.3, however, since both the domain and the range Hilbert spaces are considered to be spaces of kets. The Clebsch-Gordan coefficients *are* related to the $3j$ -symbol through the $2j$ -intertwiner of Section 3.1.4 and are naturally analyzed using a $2j$ -model (as was carried out in Miller [39]).

The Clebsch-Gordan intertwiner is the map $\hat{C} : \mathcal{C}_{j_1} \otimes \mathcal{C}_{j_2} \rightarrow \mathcal{C}_J$,

$$\hat{C} = \sum_{m_1 m_2 M} |JM\rangle \mathcal{C}_{j_1 j_2 m_1 m_2}^{JM} \langle j_1 m_1 | \otimes \langle j_2 m_2 |, \quad (3.1.47)$$

State or Subspace	Group	Operators	Eigenvalues
$\langle b $	$U(1)^2$	$\hat{I}_3^\dagger, \hat{J}_{3z}^\dagger$	j_3, m_3
$(\ker \hat{W})_\perp$	$U(1)$	\hat{I}_3^\dagger	j_3
$ a\rangle$	$U(1)^4$	$\hat{I}_1, \hat{I}_2, \hat{J}_{1z}, \hat{J}_{2z}$	j_1, j_2, m_1, m_2
$ \beta\rangle$	$U(1)^4$	$\hat{I}_1, \hat{I}_2, \hat{\mathbf{J}}_{12}^2, -\hat{J}_{12z}$	$j_1, j_2, j_3(j_3 + 1), m_3$
$\text{img } \hat{W}$	$U(1)^3$	$\hat{I}_1, \hat{I}_2, \hat{\mathbf{J}}_{12}^2$	$j_1, j_2, j_3(j_3 + 1)$
$ ab\rangle$	$U(1)^6$	$\hat{I}_1, \hat{I}_2, \hat{I}_3, \hat{J}_{1z}, \hat{J}_{2z}, \hat{J}_{3z}$	$j_1, j_2, j_3, m_1, m_2, m_3$
$ W\rangle$	$U(1)^3 \times SU(2)$	$\hat{I}_1, \hat{I}_2, \hat{I}_3, \hat{\mathbf{J}}_T$	$j_1, j_2, j_3, \mathbf{0}$
$\text{img } \hat{W} \otimes (\ker \hat{W})_\perp^*$	$U(1)^4$	$\hat{I}_1, \hat{I}_2, \hat{I}_3, \hat{\mathbf{J}}_{12}^2$	$j_1, j_2, j_3, j_3(j_3 + 1)$

Table 3.1: Subspaces and states in the remodeling algebra for the 3j-symbol. The first two rows are source space subspaces, the next three are target space subspaces, and the last three are product space subspaces.

where $\mathcal{C}_{j_1 j_2 m_1 m_2}^{JM}$ are the standard Clebsch-Gordan coefficients. It is related to the 3j- and 2j-intertwiners by

$$\hat{C} = (-1)^{j_1 - j_2 - J} \sqrt{2J + 1} \hat{K}_J^{-1} \circ \hat{W}^\dagger, \quad (3.1.48)$$

where \hat{W}^\dagger is the Hermitian conjugate of the 3j-intertwiner, interpreted as a map : $\mathcal{C}_{j_1} \otimes \mathcal{C}_{j_2} \rightarrow \mathcal{C}_J^*$.

In spin network language, the Clebsch-Gordan map is expressed as

$$\hat{C} = (-1)^{j_1 - j_2 - J} \sqrt{2J + 1} \left\langle \begin{array}{c} \text{---} \\ \text{---} \\ \text{---} \end{array} \leftarrow \begin{array}{c} \text{---} \\ \text{---} \\ \text{---} \end{array} \right\rangle, \quad (3.1.49)$$

where the rules for converting bras to kets covered in Aquilanti *et al* [1] have been used to remove the stub and internal arrow that arise when the \hat{K}^{-1} network is contracted with the \hat{W}^\dagger network. The Clebsch-Gordan coefficients are then found as the components of this map in the standard angular momentum basis,

$$\mathcal{C}_{j_1 j_2 m_1 m_2}^{JM} = (-1)^{j_1 - j_2 - J} \sqrt{2J + 1} *M \left\langle \begin{array}{c} \text{---} \\ \text{---} \\ \text{---} \end{array} \leftarrow \begin{array}{c} \text{---} \\ \text{---} \\ \text{---} \end{array} \right\rangle. \quad (3.1.50)$$

Flipping the internal arrow on the J -leg by replacing the stub that was removed in Eq. 3.1.49 and inserting a resolution of the identity expresses the Clebsch-Gordan coefficients in terms

of the components of the $2j$ - and $3j$ -intertwiners,

$$(-1)^{j_1-j_2-J} \sqrt{2J+1} \sum_{m_3} *M \begin{array}{c} \leftarrow \\ \text{---} \\ \rightarrow \end{array} \begin{array}{c} \text{---} \\ \text{---} \\ \text{---} \end{array} *m_3 \begin{array}{c} \xrightarrow{J} \\ \nearrow^{j_2} \\ \searrow_{j_1} \\ \xrightarrow{m_1} \end{array} \begin{array}{c} m_2 \\ \nearrow \\ \searrow \\ m_1 \end{array} . \quad (3.1.51)$$

The first spin network in the above equation evaluates to $(-1)^{J-m_3} \delta_{M,-m_3}$ by Eq. 3.1.32 and the second network gives the $3j$ -symbol. Summing over m_3 yields the standard result for the relationship between the Clebsch-Gordan coefficients and the $3j$ -symbol [28],

$$C_{j_1 j_2 m_1 m_2}^{JM} = (-1)^{j_1-j_2+M} \sqrt{2J+1} \begin{pmatrix} j_1 & j_2 & J \\ m_1 & m_2 & -M \end{pmatrix} . \quad (3.1.52)$$

3.2 Remodeling Geometry for the $3j$ -Symbol

In this section we construct the remodeling geometry for the $3j$ -symbol and explore the various aspects of transport in the remodeling geometry discussed in Chapter 2. First in Section 3.2.1 we set up the phase spaces for the $3j$ -remodeling geometry and then in Section 3.2.2 define the Lagrangian manifolds that will support the semiclassical approximations to all of the states defined in Section 3.1.2. Then in Section 3.2.3 we see how the transport procedure of Section 2.2.2 applies to the b -manifold to give the β -manifold. In Section 3.2.4 the core geometry associated with the Wigner manifold is described. Once the core geometry has been established, in Section 3.2.5 the core symplectomorphism is constructed and we show how the B -momentum map gets transported to the β -momentum map.

3.2.1 Phase Spaces

Each of the Hilbert spaces \mathcal{S} in the remodeling algebra corresponds semiclassically to a copy of the Schwinger phase space Σ . Let Σ_r be the Schwinger phase space for angular momentum r with the standard symplectic form ω_r as in Section A.2. The dual phase space Σ_r^* is the same manifold but with the opposite symplectic form and is the classical analogue of the dual Hilbert space \mathcal{S}_r .

The source Hilbert space is \mathcal{S}_3^* so $\Phi_2 = \Sigma_3^*$ in the remodeling geometry of Section 2.1.2. This space is 4-dimensional and carries the symplectic form $-\omega_3$. The dual source phase space is $\Phi_2^* = \mathcal{S}_3$, which is also 4-dimensional and carries the symplectic form ω_3 .

The semiclassical analysis of the $2j$ -model of the $3j$ -symbol (Eq. 3.1.14) takes place in the 8-dimensional target phase space $\Phi_{2j} = \Sigma_1 \times \Sigma_2$, which carries the symplectic form $\omega_{2j} = \omega_1 + \omega_2$ as described in Section A.2. We visualize a point of Φ_{2j} as a pair of spinors (z_1, z_2) . These spinors project onto the product of two copies of angular momentum space,

$$\begin{array}{ccc}
 \Phi_{2j} & \xleftarrow{\pi_{12}} & \Phi_{3j} \\
 & & \downarrow \pi_3 \\
 & & \Sigma_3 \xrightleftharpoons[G_3]{G_3^{-1}} \Sigma_3^*
 \end{array}$$

Figure 3.2.1: Phase spaces and the maps between them in the remodeling geometry for the $3j$ -symbol.

Name	Phase Space	Dimension
Source Space	Σ_3^*	$2n_2 = 4$
Dual Source Space	Σ_3	$2n_2 = 4$
Target Space	$\Phi_{2j} = \Sigma_1 \times \Sigma_2$	$2n_1 = 8$
Product Space	$\Phi_{3j} = \Sigma_1 \times \Sigma_2 \times \Sigma_3$	$2(n_1 + n_2) = 12$

Table 3.2: Phase spaces in the remodeling geometry for the $3j$ -symbol.

$\Lambda_{2j} = \mathbb{R}^6$, via the map $(z_1, z_2) \mapsto (\mathbf{J}_1(z_1), \mathbf{J}_2(z_2))$. The “ $2j$ -angular momentum space” may also be considered the Poisson reduction of Φ_{2j} by the pair of momentum maps I_1 and I_2 .

Similarly, the semiclassical analysis of the $3j$ -model of the $3j$ -symbol (Eq. 3.1.13) takes place in the 12-dimensional product phase space $\Phi_{3j} = \Sigma_1 \times \Sigma_2 \times \Sigma_3$, which carries the symplectic form $\omega_{3j} = \omega_1 + \omega_2 + \omega_3$. We visualize a point of Φ_{3j} as a set of three spinors z_i . The triplet of maps $(\mathbf{J}_1, \mathbf{J}_2, \mathbf{J}_3)$ act as a Poisson map onto three copies of angular momentum space, $\Lambda_{3j} = (\mathbb{R}^3)^3$. A point of Λ_{3j} may be visualized as a set of three vectors in \mathbb{R}^3 . Angular momentum space is constructed by doing a Poisson reduction on Φ_{3j} by the three momentum maps I_i , as discussed in Section A.2.

Figure 3.2.1 shows the phase spaces in the $3j$ -remodeling geometry and the relevant maps between these spaces and Table 3.2 lists the phase spaces and their dimensions. Note that the subscripts on the maps are referring to which of the three angular momenta the map is concerned with, in contrast to the general notation used in Section 2.1.2.

3.2.2 Lagrangian Manifolds

Before describing the Lagrangian manifolds in the remodeling geometry, we describe a general “ $1jm$ -state” $|jm\rangle$ in an Schwinger Hilbert space \mathcal{S} and the Lagrangian manifold \mathcal{L}_{1jm} in the Schwinger phase space Σ that supports its semiclassical approximation. This state is the simultaneous eigenstate of operators \hat{I} and \hat{J}_z with eigenvalues j and m . As discussed in Littlejohn [54], the Lagrangian manifold that supports the semiclassical approximation to this state is the level set of the list of classical observables, with appropriate quantized contour values. The Lagrangian manifold in the Schwinger phase space Σ corresponding to

this state is described as the level set,

$$\mathcal{L}_{1jm} = \left(\begin{array}{cc} I & J_z \\ J & m \end{array} \right) \subset \Sigma, \quad (3.2.1)$$

where the classical contour value J is related to the quantum eigenvalue j via $J \equiv j + 1/2$. The functions I and J_z serve as the two components of a $U(1)^2$ momentum map. As described in Section A.3, the Hamiltonian function I generates a $U(1)$ phase rotation $z \mapsto \exp(-i\psi/2)$ of period 4π and J_z generates an $SU(2)$ rotation about the z -axis $z \mapsto \exp(-i\phi\sigma_z/2)z$, which is a $U(1)$ subgroup of $SU(2)$ with period 4π . The manifold \mathcal{L}_{1jm} is also a $U(1)^2$ group orbit. Let (ψ, ϕ) be the 4π -periodic coordinates on $U(1)^2$ so that we can take Haar measure on $U(1)^2$ to be $d\psi \wedge d\phi$. The forms $d\psi$ and $d\phi$ may be locally pulled back to \mathcal{L}_{1jm} . The pull-backs of these forms are dual to the Hamiltonian vector fields X_I and X_{J_z} on \mathcal{L}_{1jm} . Therefore by Eq. C.2.2 the density σ on \mathcal{L}_{1jm} is the pull-back of $d\psi \wedge d\phi$. This density is the pullback of the Haar measure on $U(1)^2$, as expected.

Since $U(1)^2$ is a compact Abelian group, the Liouville-Arnold theorem [67] says that the manifold \mathcal{L}_{1jm} has the topology of a torus. In coordinates (ψ, ϕ) on $U(1)^2$, the isotropy subgroup is generically generated by a single element, $(2\pi, 2\pi)$. The isotropy subgroup becomes larger if $I = 0$ (in which case the isotropy subgroup is all of $U(1)^2$) or if $J_z = \pm I$ (in which case the isotropy subgroup is the group $U(1)$ generated by J_z). If the observables are constrained to take on quantized values, $j \geq 0$ implies $I \geq 1/2$ and $j - m \in \mathbb{Z}$ prevents the situation where $J_z = \pm I = \pm(j + 1/2)$. Therefore, the quantized torus has the topology $U(1)^2/\mathbb{Z}_2$. The volume of \mathcal{L}_{1jm} with respect to density σ is thus $(4\pi)^2/2 = 2^3\pi^2$.

Now we turn to the Lagrangian manifolds associated with the states described in Section 3.1.2. First consider the b -state Eq. 3.1.8, which is an element of the Schwinger Hilbert space \mathcal{S}_3^* and is the simultaneous eigenstate of operators \hat{I}_3^\top and \hat{J}_{3z}^\top with eigenvalues j_3 and m_3 . The Lagrangian manifold \mathcal{L}_b in the source phase space Σ_3^* corresponding to the b -state is a $1jm$ -Lagrangian manifold in a dual Schwinger space and is generated by the group $G_B = U(1)^2$. The symplectic action of $U(1)^2$ on the dual Schwinger space is defined to be the action in Σ_3 conjugated by the dual map, as in Eq. 2.1.27. Thus the momentum map defining \mathcal{L}_b is the negative of the pull-back of the momentum map defining the $1jm$ -manifold,

$$\mathcal{L}_b = \left(\begin{array}{cc} -I_3 & -J_{3z} \\ -(j_3 + 1/2) & -m_3 \end{array} \right) \subset \Sigma_3^*. \quad (3.2.2)$$

This manifold is the image of a $1jm$ -Lagrangian manifold under the dual map G_3 and thus has the topology $U(1)^2/\mathbb{Z}_2$ and volume $2^3\pi^2$. Because of the antisymplectic nature of the dual map, the conjugate angles to $-I_3$ and $-J_{3z}$ on the source phase space Σ_3^* are again ψ_3 and ϕ_3 and thus the pull-back of the Haar measure to \mathcal{L}_b is $\sigma_b = d\psi_3 \wedge d\phi_3$. Since $\mathcal{L}_{\bar{b}} = G_3^{-1}(\mathcal{L}_b)$, and the dual map only affects the symplectic structure of the phase space the topology and volume of $\mathcal{L}_{\bar{b}}$ and \mathcal{L}_b are identical.

The a -state of Eq. 3.1.7 in the target Hilbert space \mathcal{H}_{2j} is the simultaneous eigenstate of operators \hat{I}_1 , \hat{I}_2 , \hat{J}_{1z} , and \hat{J}_{2z} with eigenvalues j_1 , j_2 , m_1 , and m_2 . The Lagrangian manifold

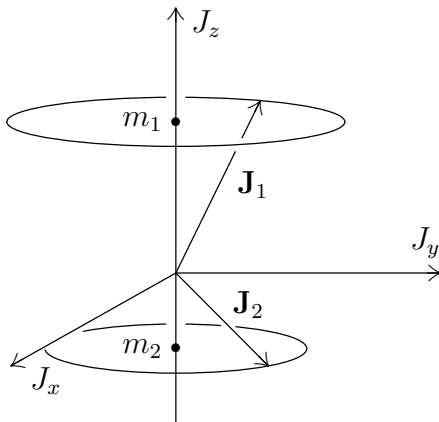


Figure 3.2.2: A point on the $2jm$ -manifold \mathcal{L}_{2jm} projected onto a pair of vectors in \mathbb{R}^3 of fixed lengths $|\mathbf{J}_1| = J_1$ and $|\mathbf{J}_2| = J_2$ and fixed z -components $J_{1,z} = m_1$ and $J_{2,z} = m_2$. The two azimuthal angles are independent.

in the target phase space Φ_{2j} corresponding to the a -state is described as the level set,

$$\mathcal{L}_a = \left(\begin{array}{cccc} I_1 & I_2 & J_{1z} & J_{2z} \\ J_1 & J_2 & m_1 & m_2 \end{array} \right) \subset \Sigma_1 \times \Sigma_2, \quad (3.2.3)$$

where the classical contour values J_r are related to the quantum eigenvalues j_r via $J_r \equiv j_r + 1/2$ ($r = 1, 2$). The maps I_1 , I_2 , J_{1z} , and J_{2z} serve as the four components of a $G_A = U(1)^4$ momentum map, comprised of two copies of the $U(1)^2$ group described earlier for the $1jm$ -manifold. The topology and volume of the a -manifold is given by

$$\mathcal{L}_a \cong \left[\frac{U(1)^2}{\mathbb{Z}_2} \right]^2, \quad V_a = \left(\frac{(4\pi)^2}{2} \right)^2 = 2^6 \pi^4, \quad (3.2.4)$$

where the volume is taken with respect to the measure $d\psi_1 \wedge d\psi_2 \wedge d\phi_1 \wedge d\phi_2$. The projection of \mathcal{L}_a onto the $2j$ -angular momentum space Λ_{2j} consists of the pair of vectors in \mathbb{R}^3 of fixed lengths $j_1 + 1/2$ and $j_2 + 1/2$ and fixed z -components m_1 and m_2 , as illustrated in Fig. 3.2.2. The quantization conditions ensure that neither of the vectors is aligned with the z -axis so the projection is topologically a 2-torus, formed by rotating each of the vectors independently about the z -axis. The $2jm$ -manifold can then be considered a T^2 bundle over T^2 .

The ab -state of Eq. 3.1.10 in the product Hilbert space \mathcal{H}_{3j} is the simultaneous eigenstate of operators \hat{I}_r and \hat{J}_{rz} with eigenvalues j_r and m_r for $r = 1, 2, 3$. The Lagrangian manifold in Φ_{3j} corresponding to the $3jm$ -state is described as the level set,

$$\mathcal{L}_{ab} = \left(\begin{array}{cccccc} I_1 & I_2 & I_3 & J_{1z} & J_{2z} & J_{3z} \\ J_1 & J_2 & J_3 & m_1 & m_2 & m_3 \end{array} \right) \subset \Sigma_1 \times \Sigma_2 \times \Sigma_3. \quad (3.2.5)$$

Note that this level set may arise directly as the list of classical functions corresponding to the “ ab -list” of operators or as the combination of the conditions for \mathcal{L}_a and $\mathcal{L}_{\bar{j}}$, as in

Section 2.1.4. The group generating \mathcal{L}_{ab} is $G_A \times G_B = U(1)^4 \times U(1)^2 = U(1)^6$, which may be interpreted as three copies of the $U(1)^2$ group generating the $1jm$ manifold. The functions I_r and J_{rz} are the six components of a $G_A \times G_B$ momentum map. The topology and volume of the a -manifold is given by

$$\mathcal{L}_{ab} \cong \left[\frac{U(1)^2}{\mathbb{Z}_2} \right]^3, \quad V_{ab} = \left(\frac{(4\pi)^2}{2} \right)^3 = 2^9 \pi^6, \quad (3.2.6)$$

where the volume is taken with respect to the measure $d\psi_1 \wedge d\psi_2 \wedge d\psi_3 \wedge d\phi_1 \wedge d\phi_2 \wedge d\phi_3$. The projection of \mathcal{L}_{ab} onto the $3j$ -angular momentum space Λ_{3j} consists of a triplet of vectors in \mathbb{R}^3 of fixed lengths $j_r + 1/2$ and fixed z -components m_r . The quantization conditions ensure that none of the vectors is aligned with the z -axis so the projection is topologically a 3-torus, formed by rotating each of the vectors independently about the z -axis. The $3jm$ -manifold can then be considered a T^3 bundle over T^3 .

The Wigner state of Fig. 3.1.9 is the simultaneous eigenstate of operators \hat{I}_r ($r = 1, 2, 3$) and $\hat{\mathbf{J}}_T$ with eigenvalues j_r and $\mathbf{0}$. The Lagrangian manifold $\mathcal{L}_W \subset \Phi_{3j}$ corresponding to the Wigner state is described as the level set,

$$\mathcal{L}_W = \left(\begin{array}{cccc} I_1 & I_2 & I_3 & \mathbf{J}_T \\ J_1 & J_2 & J_3 & \mathbf{0} \end{array} \right) \subset \Sigma_1 \times \Sigma_2 \times \Sigma_3, \quad (3.2.7)$$

where the classical function \mathbf{J}_T is the sum of the three classical angular momenta, $\mathbf{J}_1 + \mathbf{J}_2 + \mathbf{J}_3$.

The Wigner manifold is generated by the group $G_M = U(1)^3 \times SU(2)$, where each of the I_r generates a $U(1)$ rotation and \mathbf{J}_T generates a diagonal $SU(2)$ rotation on all three spinors. If we denote coordinates on $U(1)^3 \times SU(2)$ by $(\psi_1, \psi_2, \psi_3, g)$, where $g \in SU(2)$ and where the three angles are the 4π -periodic evolution variables conjugate to (I_1, I_2, I_3) , respectively, then the isotropy subgroup is generated by a single element, $(2\pi, 2\pi, 2\pi, -1)$. Therefore, the Wigner manifold has the topology and volume

$$\mathcal{L}_W \cong \frac{U(1)^3 \times SU(2)}{\mathbb{Z}_2}, \quad V_W = \frac{1}{2} (4\pi)^3 (16\pi^2) = 2^9 \pi^5, \quad (3.2.8)$$

where the volume is taken with respect to the Haar measure on the group $U(1)^3 \times SU(2)$ and the $1/2$ compensates for the 2-element isotropy subgroup. Explicitly, the Haar measure on G_M may be written $d\psi_1 \wedge d\psi_2 \wedge d\psi_3 \wedge d\alpha \wedge \sin \beta d\beta \wedge d\gamma$, where α , β , and γ are the $SU(2)$ Euler angles.

The projection of \mathcal{L}_W onto Λ_{3j} consists of the set of three vectors \mathbf{J}_r in \mathbb{R}^3 of fixed lengths $j_r + 1/2$ such that the vectors sum to zero. This allows the three angular momentum vectors to fit together into a triangle as in Fig. 3.2.3. We choose to place the three vectors end-to-end in the order $(\mathbf{J}_1, \mathbf{J}_2, \mathbf{J}_3)$. This choice of ordering fixes the orientation of the area vector $\mathbf{\Delta} = (\mathbf{J}_1 \times \mathbf{J}_2)/2$ and the unit vector $\mathbf{n} = \mathbf{\Delta}/|\mathbf{\Delta}|$ normal to the triangle. Note that even though we have asymmetrically chosen two of the three vectors making up the triangle, the condition $\mathbf{J}_T = 0$ allows any pair to define $\mathbf{\Delta}$, up to an overall sign. The area of the triangle

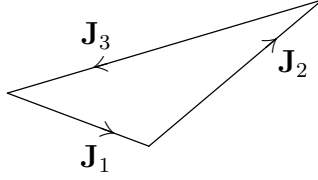


Figure 3.2.3: A point on the Wigner manifold \mathcal{L}_W projected onto a triplet of vectors in \mathbb{R}^3 of fixed lengths $|\mathbf{J}_r| = J_r$ ($r = 1, 2, 3$). The three vectors satisfy the condition $\mathbf{J}_1 + \mathbf{J}_2 + \mathbf{J}_3 = \mathbf{0}$ and can therefore be arranged into a closed chain to form a triangle.

is a fixed value based on the three parameters j_r and can be written in a symmetric fashion using Heron's formula,

$$|\Delta| = \frac{1}{4} \sqrt{j_{123}(j_{123} - 2j_1)(j_{123} - 2j_2)(j_{123} - 2j_3)}, \quad (3.2.9)$$

where $j_{123} \equiv j_1 + j_2 + j_3$. The set of orientations $SO(3)$ of Δ parametrizes the projection of \mathcal{L}_W onto Λ_{3j} and thus the Wigner manifold may be seen as a T^3 bundle over $SO(3)$.

Finally we turn to the β -state of Eq. 3.1.11. We first provide a direct analysis of \mathcal{L}_β based on the β -list of operators in Eq. 3.1.11. In Section 3.2.3 we demonstrate how the transport procedure of Sections 2.2.2 and 2.4.5 reproduces these results. The β -state is the simultaneous eigenstate of operators \hat{I}_1 , \hat{I}_2 , $\hat{\mathbf{J}}_{12}^2$, and $-\hat{J}_{12z}$ with eigenvalues j_i , $j_3(j_3 + 1)$, and m_3 , respectively. The Lagrangian manifold in Φ_{2j} corresponding to this state is described as the level set,

$$\mathcal{L}_\beta = \left(\begin{array}{cccc} I_1 & I_2 & \mathbf{J}_{12}^2 & -J_{12z} \\ J_1 & J_2 & J_3^2 & m_3 \end{array} \right). \quad (3.2.10)$$

As discussed in Section C.3, the Weyl symbol for operator $\hat{\mathbf{J}}_{12}^2$ is $\mathbf{J}_{12}^2 - 3/4$ [1]. Since the eigenvalue of $\hat{\mathbf{J}}_{12}^2$ on $|\beta\rangle$ is $j_3(j_3 + 1)$, the classical contour value for \mathbf{J}_{12}^2 may naively be expected to be $j_3(j_3 + 1) + 3/4 = (j_3 + 1/2)^2 + 1/2$. However, the appropriate quantized contour value is in fact just J_3^2 , where $J_3 \equiv j_3 + 1/2$. This mismatch in contour values occurs because $\hat{\mathbf{J}}_{12}^2$ is a quartic polynomial in the fundamental \hat{x} 's and \hat{p} 's defining the Schwinger Hilbert space and so the Weyl quantization is not exact. This is in contrast to all of the other operators considered so far, which are *quadratic* in the fundamental operators. However, the error is of relative order \hbar^2 (or $1/j^2$), which is the expected error for the semiclassical approximations we are performing. As we will see in Section 3.2.3, this contour value is naturally reproduced by the transport of \mathcal{L}_b through \mathcal{L}_W .

The β -manifold is generated by a $G_\beta = U(1)^4$ symmetry group whose momentum map components are $(I_1, I_2, \mathbf{J}_{12}^2, -J_{12z})$. Components I_1 and I_2 generate phase rotations of z_1 and z_2 , \mathbf{J}_{12}^2 generates a $U(1)$ subgroup of the diagonal $SU(2)$ group consisting of rotations about the axis \mathbf{J}_{12} and J_{12z} generates a $U(1)$ subgroup of the diagonal $SU(2)$ group consisting of rotations about the z -axis. Let coordinates on $U(1)^4$ be $(\psi_1, \psi_2, \theta_{12}, \phi_{12})$, where the angles are the 4π -periodic evolution variables corresponding to the four momentum map components. The isotropy subgroup is generically generated by two elements, say, $x = (2\pi, 2\pi, 2\pi, 0)$ and

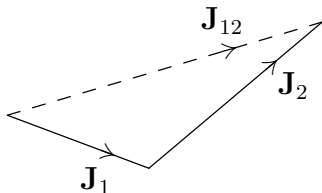


Figure 3.2.4: A point on the “coupled” manifold \mathcal{L}_β projected onto a pair of vectors in \mathbb{R}^3 of fixed lengths $|\mathbf{J}_1| = J_1$ and $|\mathbf{J}_2| = J_2$ arranged into a chain. The length of the sum of the two vectors is constrained to be $|\mathbf{J}_1 + \mathbf{J}_2| = J_3$. A triangle is formed by including vector $\mathbf{J}_{12} \equiv \mathbf{J}_1 + \mathbf{J}_2$ in the diagram.

Lagrangian Manifold	Space	Topology	Volume
\mathcal{L}_b	Σ_3^*	$U(1)^2/\mathbb{Z}_2$	$2^3\pi^2$
$\mathcal{L}_{\bar{b}}$	Σ_3	$U(1)^2/\mathbb{Z}_2$	$2^3\pi^2$
\mathcal{L}_{ab}	Φ_{3j}	$[U(1)^2/\mathbb{Z}_2]^3$	$2^9\pi^6$
\mathcal{L}_W	Φ_{3j}	$(U(1)^3 \times SU(2))/\mathbb{Z}_2$	$2^9\pi^5$
\mathcal{L}_a	Φ_{2j}	$[U(1)^2/\mathbb{Z}_2]^2$	$2^6\pi^4$
\mathcal{L}_β	Φ_{2j}	$U(1)^4/(\mathbb{Z}_2)^2$	$2^6\pi^4$

Table 3.3: Lagrangian manifolds in the remodeling geometry for the 3j-symbol.

$y = (2\pi, 2\pi, 0, 2\pi)$. This isotropy subgroup becomes larger if either $I_1 = 0$, $I_2 = 0$, $|\mathbf{J}_{12}| = 0$, or if \mathbf{J}_{12} is parallel to the z -axis. The quantization conditions rule out all of these conditions except the possibility that $\mathbf{J}_{12} = 0$. Such a situation arises in the analysis of the 2j-symbol of Eq. 3.1.29. We proceed explicitly ruling out this situation. We may therefore conclude that the isotropy subgroup is the 4-element group $(\mathbb{Z}_2)^2$ and the coupled manifold has the topology and volume

$$\mathcal{L}_\beta \cong \frac{U(1)^4}{(\mathbb{Z}_2)^2}, \quad V_\beta = \frac{1}{4}(4\pi)^4 = 2^6\pi^4, \quad (3.2.11)$$

where the volume is taken with respect to the Haar measure $d\psi_1 \wedge d\psi_2 \wedge d\theta_{12} \wedge d\phi_{12}$ and the 1/4 compensates for the 4-element isotropy subgroup.

The projection of \mathcal{L}_β onto Λ_{2j} consists of the set of two vectors \mathbf{J}_1 and \mathbf{J}_2 in \mathbb{R}^3 of fixed lengths such that the vector sum \mathbf{J}_{12} has length J_3 and z -component $-m_3$ as in Fig. 3.2.4. For future use we may again define the vector $\mathbf{\Delta} = (\mathbf{J}_1 \times \mathbf{J}_2)/2$ for points on \mathcal{L}_β which is the area vector for the oriented triangle formed by the triplet of vectors $(\mathbf{J}_1, \mathbf{J}_2, -\mathbf{J}_{12})$. The projection is topologically a 2-torus, formed by simultaneously rotating the pair of vector about the z -axis and then about the axis defined by \mathbf{J}_{12} . The β -manifold is then seen as a T^2 bundle over T^2 .

A summary of the topologies and volumes of the Lagrangian manifolds in the 3j-remodeling geometry is given in Table 3.3.

3.2.3 The Transport of \mathcal{L}_b Through \mathcal{L}_W

Now we show how the transport procedure of Section 2.2.2 applies to the 3j-remodeling geometry to produce \mathcal{L}_β . We start with \mathcal{L}_b as described by Eq. 3.2.2. Step one of the transport procedure is to form the manifold $\mathcal{L}_{\bar{b}}$ using the dual map. Since the source space is Σ_3^* , the appropriate map from the source space to the dual source space is G_3^{-1} , as shown in Figure 3.2.1. The dual b -manifold obeys the same level set conditions as \mathcal{L}_b , with the functions interpreted as functions on the dual source space. Therefore,

$$\mathcal{L}_{\bar{b}} = \left(\begin{array}{cc} I_3 & J_{3z} \\ J_3 & m_3 \end{array} \right) \subset \Sigma_3. \quad (3.2.12)$$

This is a Lagrangian manifold of Σ_3 and has $\dim \mathcal{L}_{\bar{b}} = \dim \Sigma_3/2 = 2$. Alternatively, Eq. 3.2.12 contains two independent conditions on a four-dimensional space and so specifies a two-dimensional manifold.

The next step of the transport procedure, Eq. 2.2.9, is to take the inverse image of $\mathcal{L}_{\bar{b}}$ under the projection map $\pi_3 : \Phi_{3j} \rightarrow \Sigma_3$,

$$\pi_3^{-1}(\mathcal{L}_{\bar{b}}) = \left(\begin{array}{cc} I_3 & J_{3z} \\ J_3 & m_3 \end{array} \right) \subset \Phi_{3j}. \quad (3.2.13)$$

As discussed in Section 2.2.2, the inverse image obeys the same level set conditions as $\mathcal{L}_{\bar{b}}$, but in a larger space. This manifold is the Cartesian product $\Phi_{2j} \times \mathcal{L}_{\bar{b}}$. Once again the level set conditions represent two independent conditions and thus $\pi_3^{-1}(\mathcal{L}_{\bar{b}})$ has co-dimension 2. Since the product space is 12-dimensional, $\dim \pi_3^{-1}(\mathcal{L}_{\bar{b}}) = 10$.

Next we form the intersection manifold \mathcal{I} between the inverse image and the Wigner map, as in Eq. 2.2.10. This may be expressed as the combination of the level set conditions in Eq. 3.2.13 for $\pi_3^{-1}(\mathcal{L}_{\bar{b}})$ and in Eq. 3.2.7 for \mathcal{L}_W . This amounts to eight conditions. However, these conditions are not all independent, as can be seen by the fact that I_3 occurs in *both* sets of conditions. This is because the Wigner state and b -state share a non-trivial common symmetry group and thus the analysis of Section 2.2.4 must be used. In particular, the Hamiltonian vector X_{I_3} is in both the tangent plane to \mathcal{L}_M and in the tangent plane to the G_B group orbits at points on \mathcal{I} . The intersection of these tangent planes is only one-dimensional ($s = 1$ in the notation of Section 2.2.4) since the group orbits of G_B are only two-dimensional and the flow under J_{3z} takes one off \mathcal{L}_W . Therefore the common symmetry group H is the group $U(1)$ generated by I_3 . The intersection manifold is thus written as the simultaneous level set of $n_1 + 2n_2 - s = 7$ independent functions,

$$\mathcal{I} = \left(\begin{array}{ccccc} I_1 & I_2 & I_3 & \mathbf{J}_T & J_{3z} \\ J_1 & J_2 & J_3 & \mathbf{0} & m_3 \end{array} \right) \subset \Phi_{3j}. \quad (3.2.14)$$

Since $\dim \Phi_{3j} = 12$, the intersection manifold is five-dimensional, one greater dimension than generically expected.

The last step Eq. 2.2.13 in the transport procedure is the projection of \mathcal{I} onto the target space. Note that the $U(1)$ orbits of the common symmetry group are purely vertical over

Manifold	Space	Momentum Map Components	Co-Dimension	Dimension
\mathcal{L}_b	Σ_3^*	$-I_3, -J_{3z}$	2	2
$\mathcal{L}_{\bar{b}}$	Σ_3	I_3, J_{3z}	2	2
$\pi_3^{-1}\mathcal{L}_{\bar{b}}$	Φ_{3j}	I_3, J_{3z}	2	10
\mathcal{L}_M	Φ_{3j}	$I_1, I_2, I_3, \mathbf{J}_T$	6	6
\mathcal{I}	Φ_{3j}	$I_1, I_2, I_3, \mathbf{J}_T, J_{3z}$	7	5
$\mathcal{T}_W(\mathcal{L}_b)$	Φ_{2j}	$I_1, I_2, \mathbf{J}_{12}^2, -J_{12z}$	4	4

Table 3.4: Manifolds, spaces, and momentum maps involved in the construction of the transport $\mathcal{T}_W(\mathcal{L}_b)$.

Φ_{2j} and thus the projection will eliminate one dimension from the intersection manifold. We construct the projected manifold by looking at how the seven level set conditions in Eq. 3.2.14 combine to form four level set conditions on Φ_{2j} . Conditions $I_1 = J_1$ and $I_2 = J_2$ only depend on target-space variables and thus are still valid for the projected manifold. As discussed in Section 3.2.4, conditions $\mathbf{J}_T = \mathbf{0}$ and $I_3 = J_3$ combine to form the condition $\mathbf{J}_{12}^2 = J_3^2$ on the projection. Finally, z -component of the condition $\mathbf{J}_T = \mathbf{0}$ may be re-expressed as $J_{12z} = -J_{3z}$ thus the condition $J_{3z} = m_3$ becomes the target-space condition $J_{12z} = -m_3$. Thus we have four independent conditions for a four-dimensional manifold in Φ_{2j} and we may conclude that the transported manifold is

$$\mathcal{T}_W(\mathcal{L}_b) = \left(\begin{array}{cccc} I_1 & I_2 & \mathbf{J}_{12}^2 & J_{12z} \\ J_1 & J_2 & J_3^2 & -m_3 \end{array} \right). \quad (3.2.15)$$

These are the same level set conditions as in Eq. 3.2.10 for \mathcal{L}_β and thus we see that the transported manifold is the β -manifold as promised.

Table 3.4 lists the manifolds, spaces, and momentum maps involved in the transport of \mathcal{L}_b by \mathcal{L}_W .

3.2.4 The Core Geometry

Next we study the core geometry associated with the Wigner manifold \mathcal{L}_W as described in Section 2.4.4. As discussed in Section 3.1.5, the D -list of operators defining $(\ker \hat{W})_\perp$ as a subspace of \mathcal{S}_3^* is the single operator \hat{I}_3^\top , with $(\ker \hat{W})_\perp$ the j_3 eigenspace. This operator generates a $G_{\ker} = U(1)$ Lie group. The co-isotropic manifold in Σ_3^* corresponding to this subspace is the level set

$$(\ker \hat{W})_\perp \implies \left(\begin{array}{c} -I_3 \\ -J_3 \end{array} \right) \subset \Sigma_3^*, \quad (3.2.16)$$

where $J_3 = j_3 + 1/2$ as usual and the momentum map $-I_3$ is used so that the symplectic flow under $-I_3$ on Σ_3^* maps to the symplectic flow of I_3 on Σ_3 under the dual map. This level set is a 3-sphere $S^3 \subset \mathbb{C}^2$. The projection of the level set onto angular momentum

space \mathbb{R}^3 is the set of all vectors $-\mathbf{J}_3$ of fixed length J_3 and is thus a 2-sphere. The level set itself may then be interpreted as an S^1 bundle over S^2 , with the fibers being G_{\ker} group orbits. Note that since G_{\ker} is an abelian group the group orbits lie entirely in the level set. This foliation of S^3 into S^1 group orbits is the Hopf fibration [68]. The phase space Φ_{\ker} associated with $(\ker \hat{W})_{\perp}$ treated as a Hilbert space is the symplectic reduction of Σ_3^* by G_{\ker} . The reduced space $\Phi_{\ker} \equiv \Sigma_3^* // (I_3^{\top} = J_3)$ is precisely the 2-sphere of radius J_3 in angular momentum space, which is a symplectic leaf of angular momentum space, a Poisson manifold. The projection map for the reduction is the Hopf map $: S^3 \rightarrow S^2$, as discussed in Aquilanti *et al* [1]. The symplectic form on Φ_{\ker} is $\omega_{\ker} = -J_3 d\Omega$, where $d\Omega$ is the solid angle element. This may also be expressed as $-dJ_{3z} \wedge d\phi_3$, where ϕ_3 is defined to be the azimuthal angle with respect to the z -axis in angular momentum space.

The C -list of operators defining $\text{img } \hat{W}$ as a subspace of \mathcal{H}_{2j} are the three mutually commuting operators \hat{I}_1 , \hat{I}_2 , and $\hat{\mathbf{J}}_{12}^2$, with $\text{img } \hat{W}$ the simultaneous $(j_1, j_2, j_3(j_3 + 1))$ -eigenspace of these operators. These operators are the generators of a $G_{\text{img}} = U(1)^3$ Lie group. The co-isotropic manifold in Σ_3^* corresponding to this subspace is the level set

$$\text{img } \hat{W} \implies \left(\begin{array}{ccc} I_1 & I_2 & \mathbf{J}_{12}^2 \\ J_1 & J_2 & J_3^2 \end{array} \right) \subset \Sigma_1 \times \Sigma_2. \quad (3.2.17)$$

As discussed earlier, the contour value J_3^2 for \mathbf{J}_{12}^2 ultimately derives from the Weyl symbol correspondence and the quantization condition for Lagrangian manifold \mathcal{L}_{β} . We now demonstrate a more geometric determination of this value. First consider the Wigner manifold as described by Eq. 3.2.7. The condition $\mathbf{J}_T = \mathbf{0}$ for points on \mathcal{L}_W may be re-expressed as $\mathbf{J}_{12} = -\mathbf{J}_3$ which implies

$$\mathbf{J}_{12}^2(z) = \mathbf{J}_3^2(z) = I_3^2(z) = J_3^2, \quad \forall z \in \mathcal{L}_W, \quad (3.2.18)$$

where the identity in Eq. A.2.3 is used in the second equality. The projection $\pi_{12}(\mathcal{L}_W)$ of the Wigner manifold onto the target space will therefore lie in the level set $\mathbf{J}_{12}^2 = J_3^2$ and thus the appropriate contour value for \mathbf{J}_{12}^2 in Eqs. 3.2.10 and 3.2.17 is indeed J_3^2 .

The projection of the co-isotropic manifold in Eq. 3.2.17 onto the $2j$ -angular momentum space $\Lambda_{2j} = (\mathbb{R}^3)^2$ is the pair of vectors \mathbf{J}_1 and \mathbf{J}_2 such that \mathbf{J}_1 and \mathbf{J}_2 have fixed lengths J_1 and J_2 and the vector sum $\mathbf{J}_1 + \mathbf{J}_2$ has fixed length J_3 . This projection generated by simultaneous $SO(3)$ rotations of vectors \mathbf{J}_1 and \mathbf{J}_2 and is thus topologically $SO(3)$ (as long as \mathbf{J}_1 and \mathbf{J}_2 are not collinear, in which case the triangle formed by \mathbf{J}_1 , \mathbf{J}_2 , and $-\mathbf{J}_{12}$ has zero area). Thus the level set is a T^2 bundle over $SO(3)$ with the fibers being group orbits generated by I_1 and I_2 . This $SO(3)$ manifold is the level set $(\mathbf{J}_{12}^2)^{-1}(J_3^2)$ in the symplectic leaf $S^2 \times S^2$ of Λ_{2j} , which is the symplectic reduction of Φ_{2j} under the $U(1)^2$ subgroup of G_{img} generated by I_1 and I_2 . The symplectic form on this reduced space is $\omega_{j_1 j_2} = dJ_{1z} \wedge \phi_1 + dJ_{2z} \wedge \phi_2$. The reduced phase space Φ_{img} is formed by the symplectic reduction of $S^2 \times S^2$ by the remaining $U(1)$ group generated by \mathbf{J}_{12}^2 . This group generates $SO(2)$ rotations about the \mathbf{J}_{12} -axis which foliate $SO(3)$. This forms another Hopf fibration and the projection map of the final symplectic reduction is the Hopf map $\pi : SO(3) \rightarrow S^2$.

Thus the reduced space Φ_{img} is a two-sphere. This is what was expected since \mathcal{H}_{img} is isomorphic to \mathcal{H}_{ker} and therefore Φ_{img} should be topologically identical to Φ_{ker} . Note that the function \mathbf{J}_{12} is invariant under these $SO(2)$ rotations and thus may be projected down to Φ_{img} . Points on Φ_{img} give the orientation of the vector \mathbf{J}_{12} and the symplectic form may be expressed as $\omega_{\text{img}} = dJ_{12z} \wedge d\phi_{12}$, where $J_{12z} = J_{1z} + J_{2z}$ and ϕ_{12} is defined to be the azimuthal angle of \mathbf{J}_{12} with respect to the z -axis.

The product Hilbert space subspace $(\text{img } \hat{W}) \otimes (\text{ker } \hat{W})_{\perp}^*$ is the simultaneous eigenspace of the combined list of operators \hat{I}_1 , \hat{I}_2 , $\hat{\mathbf{J}}_{12}^2$, and \hat{I}_3 at eigenvalues (J_1, J_2, J_3^2, J_3) . These operators generate a Lie algebra for the group $G_{\text{img}} \times G_{\text{ker}} = U(1)^4$. Following Eq. 2.4.19, the co-isotropic manifold $L_{\text{rp}} \subset \Phi_{3j}$ corresponding to this subspace is the level set

$$(\text{img } \hat{W}) \otimes (\text{ker } \hat{W})_{\perp}^* \implies \left(\begin{array}{cccc} I_1 & I_2 & I_3 & \mathbf{J}_{12}^2 \\ J_1 & J_2 & J_3 & J_3^2 \end{array} \right) \subset \Sigma_1 \times \Sigma_2 \times \Sigma_3. \quad (3.2.19)$$

The projection of L_{rp} onto the $3j$ -angular momentum space $\Lambda_{3j} = (\mathbb{R}^3)^3$ is the triplet of vectors \mathbf{J}_1 , \mathbf{J}_2 , and \mathbf{J}_3 with fixed lengths J_1 , J_2 , and J_3 such that the vector sum $\mathbf{J}_1 + \mathbf{J}_2$ also has fixed length J_3 . Symplectic reduction by I_1 , I_2 , and \mathbf{J}_{12}^2 only affects the target space component of Φ_{3j} and symplectic reduction by I_3 only affects the dual source space component so the reduced product phase space is $\Phi_{\text{rp}} = \Phi_{\text{img}} \times \Phi_{\text{ker}}^*$. This is the manifold $S^2 \times S^2$ with symplectic form $\omega_{\text{rp}} = dJ_{12z} \wedge d\phi_{12} + dJ_{3z} \wedge d\phi_3$.

3.2.5 The Core Symplectomorphism

Now we turn to the core symplectomorphism $\mathcal{M} : \Phi_{\text{ker}} \rightarrow \Phi_{\text{img}}$, where $\Phi_{\text{ker}} = (S^2, -dJ_{3z} \wedge d\phi_3)$ and $\Phi_{\text{img}} = (S^2, dJ_{12z} \wedge d\phi_{12})$ as in Section 3.2.4. First consider the projection of the Wigner manifold \mathcal{L}_W onto the reduced product space Φ_{rp} . By construction of the core geometry the Wigner manifold is a submanifold of the level set L_{rp} defined in Eq. 3.2.19 and projects onto a Lagrangian manifold \mathcal{L}_W^R in Φ_{rp} . Since target and dual source space functions \mathbf{J}_{12} and \mathbf{J}_3 are invariant under the reduction group $U(1)^4$ of the reduction they may be considered functions on the reduced space as well and the reduced Wigner manifold may be expressed as the level set

$$\mathcal{L}_W^R = \left(\begin{array}{c} \mathbf{J}_T \\ \mathbf{0} \end{array} \right) \subset \Phi_{\text{rp}} = \Phi_{\text{img}} \times \Phi_{\text{ker}}^*, \quad (3.2.20)$$

where \mathbf{J}_T is interpreted as the sum $\mathbf{J}_{12} + \mathbf{J}_3$ on the reduced space. This is three conditions on a four-dimensional phase space but only two of these conditions are independent. In particular, the two vectors \mathbf{J}_{12} and \mathbf{J}_3 are already constrained to have the same length by the reduction so $\mathbf{J}_T = \mathbf{0}$ really just constrains the unit vectors \mathbf{j}_{12} and \mathbf{j}_3 to be equal and opposite, which amounts to two conditions.

Another interpretation is to consider \mathbf{J}_T as the momentum map for a $SO(3)$ group on Φ_{rp} . The two S^2 components of Φ_{rp} may be interpreted as giving the orientation of vectors

\mathbf{J}_{12} and \mathbf{J}_3 and so the isotropy subgroup of $SO(3)$ is the rotations that leave these orientations unchanged. At every point on the level set \mathcal{L}_W^R there is an $SO(2)$ isotropy subgroup, consisting of rotations about the axis defined by \mathbf{J}_{12} or \mathbf{J}_3 . Thus the $SO(3)$ group orbit in Φ_{rp} is only 2-dimensional. The topology of \mathcal{L}_W^R is given by the quotient $SO(3)/SO(2)$ which is another occurrence of the Hopf map. Thus \mathcal{L}_W^R has the topology of a two-sphere on the reduced product space. This is exactly what we would expect since we now wish to interpret \mathcal{L}_W^R as the graph of a symplectomorphism $S^2 \rightarrow S^2$ and thus must have the same topology as the reduced source and reduced target space.

Next we show that \mathcal{L}_W^R is indeed the graph of the symplectomorphism associated with the core isomorphism for the Wigner map. As discussed in Section 3.1.5, the core isomorphism for the Wigner map is proportional to the inverse of the $2j$ -intertwiner $\hat{K}_{j_3}^{-1} : \mathcal{C}_{j_3}^* \rightarrow \mathcal{C}_{j_3}$, where the domain $\mathcal{C}_{j_3}^*$ is $(\ker \hat{W})_{\perp}$ and the range \mathcal{C}_{j_3} is $\text{img } \hat{W}$, the j_3 -irrep carrier space in the decomposition of Eq. 3.1.21. The proportionality $1/(2j_3 + 1)$ in Eq. 3.1.28 will only affect the overall scale of the density on the manifold that supports the semi-classical approximation of \hat{W} so the core symplectomorphism for \hat{W}_C is the classical map associated with the isometry $\hat{K}_{j_3}^{-1}$. The classical phase space associated with the carrier space for representation j is an S^2 of radius $j + 1/2$ which is constructed via symplectic reduction by $I = j + 1/2$ from the Schwinger phase space. The source and target phase spaces for the semiclassical version of $\hat{K}_{j_3}^{-1}$ are thus both two-spheres of radius $j_3 + 1/2$ and have symplectic forms $-dJ_{3z} \wedge d\phi_3$ and $+dJ_{3z} \wedge d\phi_3$, respectively. These are exactly the reduced source and target spaces that occur in the core geometry, with J_{12z} and ϕ_{12} taking the role of the target space coordinates J_{3z} and ϕ_3 . We use the subscript ‘12’ in the following to distinguish the target carrier space from the source carrier space. Since $\hat{K}_{j_3}^{-1}$ is an $SU(2)$ intertwiner, it may be treated as an $SU(2)$ -invariant element of the product Hilbert space $\mathcal{C}_{j_{12}} \otimes \mathcal{C}_{j_3}$. The Lagrangian manifold supporting the semiclassical approximation to this vector is thus invariant under the group $SU(2)$ and must obey the level set condition $\mathbf{J}_{12} + \mathbf{J}_3 = \mathbf{0}$. This is exactly the condition given for \mathcal{L}_W^R in Eq. 3.2.20 and therefore the reduced Wigner manifold is the manifold supporting the semiclassical approximation of the core isomorphism, as expected.

As in Eq. 3.1.35, the operator $\hat{K}_{j_3}^{-1}$ may be expressed in terms of the time reversal operator as $\hat{\Theta} \circ \hat{G}^{-1}$, where $\hat{G}^{-1} : \mathcal{C}_{j_3}^* \rightarrow \mathcal{C}_{j_3}$ is the dual map. The core symplectomorphism \mathcal{M} may therefore be expressed as the composition of the classical time reversal map $\theta : \mathcal{C}_{j_3} \rightarrow \mathcal{C}_{j_3}$ with the classical dual metric map $G^{-1} : \mathcal{C}_{j_3}^{-1} \rightarrow \mathcal{C}_{j_3}$. Consider first the action of time reversal and the dual metric on the full Schwinger space. As in Eq. A.2.7, the classical metric and dual metric leave coordinates z and \bar{z} unchanged, with the antisymplectic nature of the metric coming solely from the change in sign of the symplectic form. The classical time reversal map is $\theta : z \mapsto \exp(-i\sigma_2\pi/2)\bar{z}$ [1]. This has the effect of mapping \mathbf{J} into $-\mathbf{J}$, which is what is expected of a time reversal map. Therefore, the classical version of $\hat{K}_{j_3}^{-1}$ maps \mathbf{J}_3 into $-\mathbf{J}_3$ and the core symplectomorphism is

$$\mathcal{M} : S^{2*} \rightarrow S^2 : \mathbf{J}_3 \mapsto -\mathbf{J}_3, \quad (3.2.21)$$

where both spheres are interpreted as the symplectic leaves of radius $j_3 + 1/2$ in some

angular momentum space \mathbb{R}^3 and the star indicates that the source space carries the opposite symplectic form. The graph of this map is the manifold satisfying $\mathbf{J}_{12} - \mathcal{M}(\mathbf{J}_3) = \mathbf{0}$ on Φ_{rp} which is again identical to the condition $\mathbf{J}_{12} + \mathbf{J}_3 = 0$ given in Eq. 3.2.20.

Let canonical coordinates on the reduced target space be ϕ_{12} and J_{12z} . The functions M_q^R and M_p^R from Eqs. 2.4.22 and 2.4.23 are then

$$M_q^R = \phi_{12} - (\phi_3 + \pi), \quad M_p^R = J_{12z} + J_{3z}. \quad (3.2.22)$$

Note that $\{M_q^R, M_p^R\} = \{\phi_{12}, J_{12z}\} - \{\phi_3, J_{3z}\} = 1 - 1 = 0$ as expected. In terms of these functions the reduced Wigner manifold is expressed as

$$\mathcal{L}_W^R = \left(\begin{array}{cc} M_q^R & M_p^R \\ 0 & 0 \end{array} \right) = \left(\begin{array}{cc} \phi_{12} - \phi_3 & J_{12z} + J_{3z} \\ -\pi & 0 \end{array} \right) \subset \Phi_{\text{rp}}. \quad (3.2.23)$$

The functions on M_q^R and M_p^R on the reduced space are easily lifted to the full Φ_{3j} phase space in a way consistent with Section 2.4.5. The coordinates involved are all well-defined on the full $3j$ -angular momentum space, with J_{12z} and J_{3z} the z -components of $\mathbf{J}_1 + \mathbf{J}_2$ and \mathbf{J}_3 and ϕ_{12} and ϕ_3 the azimuthal angles of $\mathbf{J}_1 + \mathbf{J}_2$ and \mathbf{J}_3 with respect to the z -axis. Angular momentum space Λ_{3j} is the Poisson reduction of Φ_{3j} , so these functions are lifted into the full $3j$ -Schwinger phase space by requiring that they are constant on the $U(1)^3$ orbits generated by I_1 , I_2 , and I_3 that define the reduction. In particular, this lift leaves the functions $(G_{\text{ker}} \times G_{\text{img}})$ -invariant. In terms of the lifted functions $M_q \equiv \phi_{12} - \phi_3$ and $M_p \equiv J_{12z} + J_{3z} = J_{Tz}$ Eq. 3.2.7 is rewritten in the form Eq. 2.4.30 as

$$\mathcal{L}_W = \left(\begin{array}{cccccc} I_1 & I_2 & \mathbf{J}_{12}^2 & I_3 & \phi_{12} - \phi_3 & J_{Tz} \\ J_1 & J_2 & J_3^2 & J_3 & -\pi & 0 \end{array} \right) \subset \Sigma_1 \times \Sigma_2 \times \Sigma_3, \quad (3.2.24)$$

with the first three columns acting as the C -list, the fourth column acting as the D -list, and the last two columns the lifted version of the core symplectomorphism graph conditions.

Now we show how the momentum map conditions Eq. 3.2.2 for \mathcal{L}_b are transported via the core symplectomorphism Eq. 3.2.21 to the momentum map conditions Eq. 3.2.10 for \mathcal{L}_β . Note that Eq. 3.2.2 is already in the form Eq. 2.4.25, with $\mathbf{D} = -I_3$ (as in Eq. 3.2.16) and $\mathbf{B}' = -J_{3z}$. The transported function β' on the reduced target space Φ_{img} is the pullback of the reduced B -list (which will be the single function $-J_{3z}$) under the core symplectomorphism as in Eq. 2.4.28. Therefore $\beta' = J_{12z}$, which may be interpreted as a function on just the reduced target space or on the full target space Φ_{2j} . Thus the β manifold expressed in the form of Eq. 2.4.31 is

$$\mathcal{L}_\beta = \left(\begin{array}{cccc} I_1 & I_2 & \mathbf{J}_{12}^2 & J_{12z} \\ J_1 & J_2 & J_3^2 & -m_3 \end{array} \right), \quad (3.2.25)$$

which is exactly the expected result as described in Eqs. 3.2.10 and 3.2.15.

3.3 Analysis of the Inner Product Models

Now that the remodeling geometry has been determined we turn our attention to the various aspects of the semiclassical approximations to the $2j$ - and $3j$ -models of the $3j$ -symbol. As mentioned in the introduction these approximations have been studied extensively [27, 38, 39, 40, 41, 42, 44], so the main focus of the rest of this chapter is comparing the calculations for the two models to demonstrate the results claimed in Chapter 2.

In this section we determine the various pieces of the stationary phase approximation for the $3j$ -symbol in the $3j$ -model and the $2j$ -model. In Section 3.3.1 the stationary phase sets for the $3j$ - and $2j$ -models of the $3j$ -symbol are determined and we show that the stationary phase set in the target-space model is indeed the projection of the stationary phase set in the product space model. Then in Section 3.3.2 the amplitude determinants in the two models are computed and compared. In Section 3.3.3 we review the calculation of the action integral piece of the phase in the $3j$ -model and in Section 3.3.4 with a calculation of the Maslov index and signature index pieces of the phase in the $2j$ -model. Combining these results yields the standard formula for the asymptotics of the $3j$ -symbol.

3.3.1 Stationary Phase Sets

Now we construct the stationary phase sets for the $3j$ - and $2j$ -models of the $3j$ -symbol and show that, as discussed in Section 2.5.1, the $2j$ -stationary phase set $I^{(2j)}$ is the projection of the $3j$ -stationary phase set $I^{(3j)}$ under π_{12} . We fix the values $J_r > 0$ and treat all other variables as continuous. We also assume that the parameters are in the classically allowed region so that at least one real intersection point exists. This implies the constraint $m_1 + m_2 + m_3 = 0$ and restricts (J_1, J_2, J_3) to triangle-allowed triplets.

As in Eq. 2.5.1 the stationary phase set for the $3j$ -model is the intersection $I^{(3j)} = \mathcal{L}_{ab} \cap \mathcal{L}_W$. The intersection will be comprised of group orbits of the common symmetry group shared by the $U(1)^6$ group that generates \mathcal{L}_{ab} and the $U(1)^3 \times SU(2)$ group that generates \mathcal{L}_W . Comparing the lists in Eqs. 3.2.5 and 3.2.7 shows that the momentum map components I_1, I_2, I_3 , and J_{Tz} occur as generators in both groups. In particular, the Hamiltonian vector field $X_{J_{Tz}} = X_{J_{1z}} + X_{J_{2z}} + X_{J_{3z}}$ is tangent to both \mathcal{L}_{ab} and \mathcal{L}_W . Thus the stationary phase set is generated by the common symmetry group $H_{3j} = U(1)^4$ and is the simultaneous level set

$$I^{(3j)} = \left(\begin{array}{ccccccccc} I_1 & I_2 & I_3 & J_{Tz} & J_{2z} & J_{3z} & J_{Tx} & J_{Ty} \\ J_1 & J_2 & J_3 & 0 & m_2 & m_3 & 0 & 0 \end{array} \right) \subset \Phi_{3j}, \quad (3.3.1)$$

where the four common symmetry group momentum map components are listed first and all eight conditions are independent so $\dim I^{(3j)} = 12 - 8 = 4$. Note that the condition $J_{1z} = m_1$ is implied by the three conditions $J_{Tz} = 0$, $J_{2z} = m_2$, $J_{3z} = m_3$, and the initial constraint $m_1 + m_2 + m_3 = 0$. Since $U(1)^4$ is Abelian every point of the dual Lie algebra $\mathfrak{u}(1)$ is a fixed point of the co-adjoint action and thus the level set L_I defined by $I_r = J_r$, $J_{Tz} = 0$ is a co-isotropic submanifold of Φ_{3j} . This level set includes not only the intersections $I^{(3j)}$ but the full Lagrangian manifolds \mathcal{L}_{ab} and \mathcal{L}_W .

Since both manifolds are invariant under the group orbits defining the Poisson reduction onto angular momentum space, the stationary phase set may be interpreted as a $U(1)^3$ bundle over the intersection of the projections of the product and Wigner manifolds in Λ_{3j} . Following Section 3.2.2, the intersection in angular momentum space consists of all triplets of vectors $(\mathbf{J}_1, \mathbf{J}_2, \mathbf{J}_3)$ of fixed lengths (J_1, J_2, J_3) such that $J_{rz} = m_r$ and $\mathbf{J}_T = \mathbf{0}$. Rotation of all three vectors about the z -axis leaves all nine of these conditions invariant and so the intersection will be foliated by $SO(2)$ group orbits. The full intersection manifold in angular momentum space is one-dimensional and consists of two disconnected group orbits [44]. For example, we may use a rotation generated by J_{Tz} to orient the vector \mathbf{J}_3 in the xz -plane with $J_{3x} > 0$, in which case reflection through the xz -plane maps one intersection point into another. This operation reverses parity and so the two points lie on different $SO(2)$ group orbits. Label the two group orbits comprising the intersection in angular momentum space S^1_{\pm} , where the subscript indicates the sign of J_{1y} when \mathbf{J}_3 lies in the xz -plane with $J_{3x} > 0$. Each of the $SO(2)$ orbits in Λ_{3j} lifts to a $U(1)^3$ bundle over S^1 in Φ_{3j} . Let \mathcal{I}_{\pm} label the two disconnected pieces of the intersection manifold so $I^{(3j)}$ is the disjoint union $I_+^{(3j)} \cup I_-^{(3j)}$. Let $(\psi_1, \psi_2, \psi_3, \phi_T)$ be the 4π -periodic coordinates on the common symmetry group H_{3j} . The isotropy subgroup on $I^{(3j)}$ consists of only one nontrivial element, $(2\pi, 2\pi, 2\pi, 2\pi)$. Therefore each of the two connected pieces of the intersection manifold have the properties

$$I_{\pm}^{(3j)} \cong \frac{U(1)^4}{\mathbb{Z}_2}, \quad V_{\pm}^{3j} = \frac{1}{2}(4\pi)^4 = 2^7\pi^4, \quad (3.3.2)$$

where the volume is taken with respect to the Haar measure on the group, $d\psi_1 \wedge d\psi_2 \wedge d\psi_3 \wedge d\phi_T$ and the $1/2$ compensates for the 2-element isotropy subgroup.

Next we turn our attention to the $2j$ -model. As in Eq. 2.5.1 the stationary phase set for the $2j$ -model is the intersection $I^{(2j)} = \mathcal{L}_a \cap \mathcal{L}_\beta$ and will be comprised of group orbits of the common symmetry group shared by the two $U(1)^4$ groups that generate \mathcal{L}_a and \mathcal{L}_β . The common symmetry group in this case is $H_{2j} = U(1)^3$, where the $U(1)^3$ subgroup of G_A and G_β is generated by the momentum map components I_1, I_2 , and J_{12z} . The $2j$ stationary phase set is thus the simultaneous level set

$$I^{(2j)} = \left(\begin{array}{ccccc} I_1 & I_2 & J_{12z} & J_{2z} & \mathbf{J}_{12}^2 \\ J_1 & J_2 & -m_3 & m_2 & J_3^2 \end{array} \right) \subset \Phi_{2j}, \quad (3.3.3)$$

where the three common symmetry group momentum map components are listed first and all five conditions are independent so $\dim I^{(3j)} = 8 - 5 = 3$. Again the conditions $J_{12z} = -m_3$ and $J_{2z} = m_2$ combined with the initial constraint $m_1 + m_2 + m_3 = 0$ imply the condition $J_{1z} = m_1$. The Abelian nature of H_{2j} means that the level set L_I defined by $I_1 = J_1, I_2 = J_2$, and $J_{12z} = 0$ is a co-isotropic submanifold of Φ_{2j} . This level set includes not only the stationary phase set $I^{(2j)}$ but the full Lagrangian manifolds \mathcal{L}_a and \mathcal{L}_β .

The topology of $I^{(2j)}$ is determined by looking at the projection onto the $2j$ -angular momentum space Λ_{2j} . Since both manifolds are invariant under the group orbits defining the Poisson reduction, the stationary phase set is a $U(1)^2$ bundle over the intersection manifold

in angular momentum space. The intersection in angular momentum space consists of all pairs of vectors $(\mathbf{J}_1, \mathbf{J}_2)$ of fixed lengths (J_1, J_2) such that $J_{1z} = m_1$, $J_{2z} = m_2$, and $\mathbf{J}_{12}^2 = J_3^2$. As in the $3j$ -model, these conditions are all invariant under the $SO(2)$ group or rotations about the z -axis so the projection of $I^{(2j)}$ will be foliated into $SO(2)$ group orbits. Again the intersection is comprised of two disconnected group orbits, which can be seen by using this $U(1)$ freedom to fix the vector \mathbf{J}_{12} in the xz -plane with $J_{12x} > 0$ and then reflecting through the xz -plane, which maps from one group orbit to a different group orbit. Let the two circles of intersection in angular momentum space be labeled S_{\pm}^1 as in the $3j$ -model. Each circle lifts to a $U(1)^2$ bundle over $U(1)$. Let $I_{\pm}^{(2j)}$ label the two intersection manifolds in Φ_{2j} so $I^{(2j)}$ is the disjoint union $I_{+}^{(2j)} \cup I_{-}^{(2j)}$. Let $(\psi_1, \psi_2, \phi_{12})$ parameterize H_{2j} , with ϕ_{12} parametrizing group flows under the $U(1)$ subgroup generated by J_{12z} . The isotropy subgroup consists of only one nontrivial element, $(2\pi, 2\pi, 2\pi)$, and thus the connected pieces of the intersection manifold have the properties

$$I_{\pm}^{(2j)} \cong \frac{U(1)^3}{\mathbb{Z}_2}, \quad V_{\pm}^{2j} = \frac{1}{2}(4\pi)^3 = 2^5\pi^3, \quad (3.3.4)$$

where the volume is taken with respect to the Haar measure on the group, $d\psi_1 \wedge d\psi_2 \wedge d\phi_{12}$ and the $1/2$ compensates for the 2-element isotropy subgroup.

Finally, consider the projection of $I^{(3j)}$ onto the target space. The equality of the projection of the product space stationary phase set and the target space stationary phase set was proved in Section 2.5.1 so we just demonstrate here that $\pi_{12}(I^{(3j)})$ satisfies the same level set conditions as $I^{(2j)}$ to support the equality. As shown in Section 3.2.3 the conditions $\mathbf{J}_T = \mathbf{0}$ and $I_3 = J_3$ on $I^{(3j)}$ imply the condition $\mathbf{J}_{12}^2 = J_3^2$. Similarly, the conditions $J_{Tz} = 0$ and $J_{3z} = m_3$ imply $J_{12z} = -m_3$. Therefore the eight conditions in Eq. 3.3.1 imply five independent conditions on target space variables, with I_1 , I_2 , and J_{2z} already expressed only in terms of the target space. The projection therefore satisfies

$$\pi_{12}(I^{(3j)}) \subset \left(\begin{array}{ccccc} I_1 & I_2 & J_{2z} & \mathbf{J}_{12}^2 & J_{12z} \\ J_1 & J_2 & m_2 & J_3^2 & -m_3 \end{array} \right) \subset \Phi_{2j}, \quad (3.3.5)$$

which is exactly the same conditions as in Eq. 3.3.3.

With the intersections understood the results from Section 2.1.5 for the stationary phase approximations for the $3j$ - and $2j$ -models can be set up. The semiclassical approximation of the $3j$ -model is given by the product space stationary phase expression Eq. 2.1.41,

$$\langle ab|W \rangle \approx \frac{(2\pi i)^{(n_1+n_2-s_{12})/2}}{\sqrt{V_{ab}V_W}} \sum_{\pm} V_{\pm}^{3j} \left| \tilde{\Omega}_{\pm}^{3j} \right|^{1/2} e^{i\varphi_{\pm}^{3j}}. \quad (3.3.6)$$

In the $3j$ -model the phase space contains $n_1+n_2 = 6$ degrees of freedom and the common symmetry group is $s_{12} = 4$ -dimensional. Plugging in the volumes determined in Eqs. 3.2.6, 3.2.8, and 3.3.2 simplifies Eq. 3.3.6 to

$$\frac{1}{\sqrt{4\pi}} \sum_{\pm} \left| \tilde{\Omega}_{\pm}^{3j} \right|^{1/2} e^{i\varphi_{\pm}^{3j}}, \quad (3.3.7)$$

where a prefactor of i has been left out of the above expression because we are unconcerned with the overall phase of the answer, which depends on various phase conventions of the states and manifolds. Similarly, the semiclassical approximation of the $2j$ -model is given by the target space stationary phase expression Eq. 2.1.38,

$$\langle a|\beta\rangle \approx \frac{(2\pi i)^{(n_1-s_1)/2}}{\sqrt{V_a V_\beta}} \sum_{\pm} V_{\pm}^{2j} \left| \tilde{\Omega}_{\pm}^{2j} \right|^{1/2} e^{i\varphi_{\pm}^{2j}}. \quad (3.3.8)$$

The target space contains $n_1 = 4$ degrees of freedom and the common symmetry group is $s_1 = 3$ -dimensional. Plugging in the volumes determined in Eqs. 3.2.4, 3.2.11, and 3.3.4 simplifies Eq. 3.3.8 to

$$\frac{1}{\sqrt{2\pi}} \sum_{\pm} \left| \tilde{\Omega}_{\pm}^{2j} \right|^{1/2} e^{i\varphi_{\pm}^{2j}}, \quad (3.3.9)$$

where again an overall phase factor of \sqrt{i} has been left out of the above expression.

3.3.2 Amplitude Determinants

The amplitude of the $3j$ -symbol in the $3j$ -model is found by taking the determinant of the appropriate matrix of Poisson brackets. Since the two manifolds \mathcal{L}_{3jm} and \mathcal{L}_W share a common symmetry group, the matrix of brackets of the defining momentum map components is singular. This is dealt with as in Aquilanti *et al* [44] and Section 2.3.4 by first performing a symplectic reduction by the momentum map of the common symmetry group and then finding the amplitude determinant in the reduced space. In practice this just involves removing the shared momentum map components from \mathcal{L}_{3jm} and \mathcal{L}_W and taking the determinant of the matrix of Poisson brackets among the remaining momentum map components.

As discussed in the previous section, the common symmetry group in the $3j$ -model is $H_{3j} = U(1)^4$ whose momentum map contains the four shared components $I_1, I_2, I_3,$ and J_{Tz} . Points on the reduced $3jm$ -phase space Φ_{3j}^R represent equivalence classes of the level set L_I where two points are said to be equivalent on L_I if they are connected by a group flow of the common $U(1)^4$ symmetry. The level set is a co-dimension four manifold of Φ_{3j} and the group orbits are generically four-dimensional tori. Thus the reduced phase space has dimension $\dim \Phi_{3j}^R = \dim \Phi_{3j} - 8 = 4$, which is a phase space with two degrees of freedom. The amplitude determinant thus is reduced from a singular 6×6 matrix to a non-singular 2×2 matrix.

Let Φ_{3j}^R be the symplectic reduction of Φ_{3j} by the intersection group H_{3j} . The reduction is performed in two steps, a reduction by the $U(1)^3$ group generated by the three I_r at contour values J_r followed by a reduction by the diagonal $U(1)$ group generated by J_{Tz} at contour value 0. As discussed in Section 3.2.4 the reduction by $U(1)^3$ yields the reduced phase space $(S^2 \times S^2 \times S^2, \sum_r dJ_{rz} \wedge d\phi_r)$, where the r -th sphere has radius $j_r + 1/2$ and ϕ_r is the azimuthal angle with respect to the z -axis. This reduced space can also be interpreted as a symplectic leaf of the Poisson reduction onto the $3j$ -angular momentum space Λ_{3j} . Restricting to the

symplectic leaf given by the level set $I_r = j_r + 1/2$ is equivalent to individually fixing the lengths of the three vectors. Under this reduction the ab -manifold reduces to a three-torus T^3 given by the level set $J_{rz} = m_r$ and the Wigner manifold reduces to the level set $\mathbf{J}_T = \mathbf{0}$, which is isomorphic to the manifold of triangle-orientations $SO(3)$. The intersection of these two manifolds in this reduced space is a pair of circles generated by the $U(1)$ action of J_{Tz} .

A canonical transformation may be performed to express the symplectic form after the first stage of this reduction as $dJ_{1z} \wedge d\tilde{\phi}_{13} + dJ_{2z} \wedge d\tilde{\phi}_{23} + dJ_{Tz} \wedge d\phi_3$, where $\tilde{\phi}_{r3} \equiv \phi_r - \phi_3$. In these coordinates the group orbits of the rotations generated by J_{Tz} are parameterized by ϕ_3 and the other five coordinates are invariant. The level set $J_{Tz} = 0$ is a four-dimensional region foliated by these group orbits. Even though we will not determine the topology of the reduced space we can give the reduced symplectic form, $\omega_{3j}^R = dJ_{1z} \wedge \tilde{\phi}_{13} + dJ_{2z} \wedge \tilde{\phi}_{23}$.

In Φ_{3j}^R the reduced ab - and Wigner manifolds are the level sets

$$\mathcal{L}_{ab}^R = \begin{pmatrix} J_{1z} & J_{2z} \\ m_1 & m_2 \end{pmatrix}, \quad \mathcal{L}_W^R = \begin{pmatrix} J_{Tz} & J_{Ty} \\ 0 & 0 \end{pmatrix}. \quad (3.3.10)$$

The reduced $3j$ -model amplitude determinant is thus given by the determinant of the 2×2 -matrix of Poisson brackets

$$\begin{bmatrix} \{J_{1z}, J_{Tx}\} & \{J_{1z}, J_{Ty}\} \\ \{J_{2z}, J_{Tx}\} & \{J_{2z}, J_{Ty}\} \end{bmatrix}. \quad (3.3.11)$$

Evaluating the Poisson brackets at the two intersection points yields the determinant for the two terms in the WKB expansion,

$$\tilde{\Omega}_{\pm}^{3j} = \left(\det \begin{bmatrix} J_{1y} & -J_{1x} \\ J_{2y} & -J_{2x} \end{bmatrix} \right)_{\pm}^{-1} = [\mathbf{z} \cdot (\mathbf{J}_1 \times \mathbf{J}_2)]_{\pm}^{-1} = \frac{1}{2\Delta_z|_{\pm}}, \quad (3.3.12)$$

where Δ_z is the z -component of the area vector $\mathbf{\Delta}$ defined in Section 3.2.2. Note that this expression is invariant under the common symmetry group H_{3j} and thus may be evaluated in the unreduced product space Φ_{3j} at any point on the group orbits $I_{\pm}^{(3j)}$. Similarly, given the point on $I_+^{(3j)}$ with \mathbf{J}_3 oriented in the xz -plane, reflection through the xz -plane generates a point on $I_-^{(3j)}$. This reflection leaves the z -component of $\mathbf{\Delta}$ invariant and thus $\tilde{\Omega}_+^{3j} = \tilde{\Omega}_-^{3j} = (2\Delta_z)^{-1}$ and expression 3.3.7 becomes

$$\frac{1}{2\sqrt{2\pi|\Delta_z|}} \sum_{\pm} e^{i\varphi_{\pm}^{3j}}. \quad (3.3.13)$$

Removing a common phase of $\exp(i(\varphi_+^{3j} + \varphi_-^{3j})/2)$ lets the sum over phase factors be re-expressed as a cosine so the semi-classical approximation of the $3j$ -symbol in the $3j$ -model becomes, up to an overall phase,

$$\langle ab|W\rangle \approx \frac{\cos(\Delta\varphi^{3j}/2)}{\sqrt{2\pi|\Delta_z|}}, \quad (3.3.14)$$

where $\Delta\varphi^{3j}$ is the relative phase between points on $I_+^{(3j)}$ and $I_-^{(3j)}$.

Now we turn to the evaluation of the amplitude determinant in the $2j$ -model. The two manifolds \mathcal{L}_a and \mathcal{L}_β in the target space share a common symmetry group $H_{2j} = U(1)^3$ that generates the intersection $I^{(2j)}$. Let Φ_2^R be the symplectic reduction of Φ_{2j} by H_{2j} . The momentum map for H_{2j} consists of the three components I_1 , I_2 , and J_{12z} . The level set of this momentum map is a co-dimension three manifold of Φ_{2j} and the group orbits are generically three-dimensional tori so the reduced phase space has dimension $\dim \Phi_{2j}^R = \dim \Phi_{2j} - 6 = 2$, which is a phase space of one degree of freedom. The amplitude determinant thus is reduced from a singular 4×4 matrix to a single Poisson bracket.

As in the $3j$ -model, the reduced space is best explored by taking the symplectic reduction in steps, first by the $U(1)^2$ group generated by I_1 and I_2 and then by the diagonal $U(1)$ group generated by J_{12z} . The first stage of the reduction yields the reduced space $(S^2 \times S^2, dJ_{1z} \wedge d\phi_1 + dJ_{2z} \wedge d\phi_2)$, where the two spheres have radii $j_1 + 1/2$ and $j_2 + 1/2$, respectively. This reduced space can also be interpreted as a symplectic leaf of the Poisson reduction onto the $2j$ -angular momentum space Λ_{2j} . Restricting to the symplectic leaf given by the level set $I_1 = J_1$ and $I_2 = J_2$ is equivalent to individually fixing the lengths of the pair of vectors. Under this reduction the a -manifold reduces to a two-torus T^2 satisfying $J_{1z} = m_1$ and $J_{2z} = m_2$ and the β -manifold reduces to a two-torus T^2 satisfying $\mathbf{J}_{12}^2 = J_3^2$ and $J_{12z} = -m_3$. The intersection of these two manifolds in this reduced space is a pair of circles generated by the $U(1)$ action of J_{12z} .

A canonical transformation may be performed to express the symplectic form after the first stage of this reduction as $dJ_{1z} \wedge d\tilde{\phi}_{12} + dJ_{12z} \wedge d\phi_2$, where $\tilde{\phi}_{12} \equiv \phi_1 - \phi_2$. In these coordinates the group orbits of the rotations generated by J_{12z} are parameterized by ϕ_2 and the other three coordinates are invariant. The level set $J_{12z} = -m_3$ is a two-dimensional region foliated by these group orbits. The reduced space has the topology of a two-sphere and carries the reduced symplectic form $\omega_{2j}^R = dJ_{1z} \wedge \tilde{\phi}_{12}$.

In Φ_{2j}^R the reduced a - and β -manifolds are the level sets

$$\mathcal{L}_a^R = \left(\begin{array}{c} J_{1z} \\ m_1 \end{array} \right), \quad \mathcal{L}_\beta^R = \left(\begin{array}{c} \mathbf{J}_{12}^2 \\ J_3^2 \end{array} \right). \quad (3.3.15)$$

The reduced $3j$ -model amplitude determinant is thus given by the Poisson bracket $\{J_{1z}, \mathbf{J}_{12}^2\}$. Expressing \mathbf{J}_{12}^2 as $\mathbf{J}_1^2 + \mathbf{J}_2^2 + 2\mathbf{J}_1 \cdot \mathbf{J}_2$ simplifies this bracket to $2\{J_{1z}, \mathbf{J}_1\} \cdot \mathbf{J}_2$ and therefore

$$\tilde{\Omega}_\pm^{2j} = [-2(\mathbf{z} \times \mathbf{J}_1) \cdot \mathbf{J}_2]_\pm^{-1} = [-2\mathbf{z} \cdot (\mathbf{J}_1 \times \mathbf{J}_2)]_\pm^{-1} = \frac{1}{-4\Delta_z|_\pm}. \quad (3.3.16)$$

The amplitude in Eq. 3.3.16 is invariant under the common symmetry group H_{2j} and thus may be evaluated in the unreduced product space Φ_{2j} at any point on the group orbits $I_\pm^{(2j)}$. Once again points on $I_+^{(2j)}$ and $I_-^{(2j)}$ may be related by a reflection through a plane containing the z -axis so Δ_z is the same on both orbits and expression 3.3.9 becomes

$$\langle a|\beta \rangle \approx \frac{\cos(\Delta\varphi^{2j}/2)}{\sqrt{2\pi} |\Delta_z|}, \quad (3.3.17)$$

where the sum of the two phase factors has been replaced by a cosine involving the relative phase $\Delta\varphi^{2j}$ between points on $I_+^{(2j)}$ and $I_-^{(2j)}$ and an overall phase factor has been removed.

Note that, by Eqs. 3.3.12 and 3.3.16, $\tilde{\Omega}_\pm^{3j} = -2\tilde{\Omega}_\pm^{2j}$. In Section 2.4.6 we showed that these two amplitudes will be the same *when* the momentum map components of the M -manifold are expressed in terms of the core symplectomorphism functions M_q and M_p . Since we used the components in Eq. 3.2.7 rather than in Eq. 3.2.24 the amplitudes differ by a factor. (Use of the list in Eq. 3.2.24 would result in the reduced W -list of functions \mathbf{J}_{12}^2 and $\phi_{12} - \phi_3$. Brackets involving ϕ_{12} are particularly messy to compute, unfortunately.) However, we see that this discrepancy doesn't affect the final equality of the overall pre-factors in Eqs. 3.3.14 and 3.3.17. This is because the choice of momentum map components M_α *also* affects the Hamiltonian vector fields X_α . This in turn affects the dual forms λ_α and ultimately the density form σ_W on \mathcal{L}_W . Since σ_W is constructed to be invariant under the group flows, the different choice in momentum map components scales σ_W by a constant factor. The scaling of σ_W affects the amplitude determinant, as we see here, *and* the expressed volume of the manifold. In general this means that if we compute the amplitude determinant in the target space model, we need to use the target space model volume factors in the stationary phase approximation expressions.

3.3.3 The Action Integral

Now we turn to the calculation of the phase $\Delta\varphi$ that occurs in Eqs. 3.3.14 and 3.3.17. As in Eqs. 2.5.2 and 2.5.3, the relative phase consists of an action integral, a Maslov index, and a signature index,

$$\Delta\varphi = \oint_\Gamma \theta - \mu(\Gamma)\frac{\pi}{2} + \Delta\sigma\frac{\pi}{4}, \tag{3.3.18}$$

where Γ is a closed path that starts at one of the connected pieces of the stationary phase set, traverses one Lagrangian manifold to the other connected piece, and returns along the other Lagrangian manifold. In Section 2.5.3 we showed that the action integrals in the two models of a remodeling geometry are equal and in Section 2.5.5 we showed that the combined Maslov and signature index pieces in the two models of a remodeling geometry are equal.

The phase calculations in the various models of the 3j-symbol are more complicated than similar calculations in the analysis of the 6j-symbol. Therefore we defer a comparison of the phase calculations in different models of a remodeling geometry to the analysis of the 6j-symbol in Chapter 4. Instead we present here a summary of the path and phase calculation that was calculated in the 3j-model in Aquilanti *et al* [44] and in Section 3.3.4 find the Maslov and signature index in the 2j-model. By the results of Section 2.5 we may combine these in Eq. 3.3.18 to create the relative phase and complete the derivation of the asymptotics of the 3j-symbol.

To compute the action integral in the 3j-model we need to construct an appropriate path in Φ_{3j} . To help construct this path we will utilize the 3j-angular momentum space Λ_{3j} and consider Φ_{3j} a $U(1)^3$ bundle over this space. For the start of the path we choose a standard

reference point $z_+ = (z_{1+}, z_{2+}, z_{3+})$ on $I_+^{(3j)}$ such that the vector \mathbf{J}_3 in angular momentum space lies within the xz -plane with $J_{3x} \geq 0$,

$$z_{r+} = \sqrt{2J_r} \begin{pmatrix} \cos(\theta_r/2)e^{-i\zeta_r/2} \\ \sin(\theta_r/2)e^{+i\zeta_r/2} \end{pmatrix}, \quad \mathbf{J}_{r+} = \begin{pmatrix} \sqrt{J_r^2 - m_r^2} \cos \zeta_r \\ \sqrt{J_r^2 - m_r^2} \sin \zeta_r \\ m_r \end{pmatrix}, \quad (3.3.19)$$

where θ_r is defined such that $J_r \cos \theta_r = m_r$ and $J_r \sin \theta_r = +\sqrt{J_r^2 - m_r^2}$ and ζ_r is the azimuthal angle of \mathbf{J}_r with respect to the z -axis. Let \mathbf{j}_3 be the unit vector for \mathbf{J}_3 at z_+ and let $\mathbf{\Delta}$ as the area vector for the triangle formed by the three vectors at z_+ as in Section 3.2.2. In addition, consider a reference fiber in $I_-^{(3j)}$ over the reflection of \mathbf{J}_{r+} through the xz -plane in angular momentum space,

$$\mathbf{J}_{r-} = \begin{pmatrix} \sqrt{J_r^2 - m_r^2} \cos \zeta_r \\ -\sqrt{J_r^2 - m_r^2} \sin \zeta_r \\ m_r \end{pmatrix}. \quad (3.3.20)$$

Let $\Gamma = \Gamma_W + \Gamma_{ab} + \Gamma_I$ be the path for the computation of the relative phase between $I_+^{(3j)}$ and $I_-^{(3j)}$, where $\Gamma_W \subset \mathcal{L}_W$, $\Gamma_{ab} \subset \mathcal{L}_{ab}$, and $\Gamma_I \subset I_+^{(3j)}$. The projection of Γ_W onto angular momentum space is a path that maps vectors \mathbf{J}_{r+} to \mathbf{J}_{r-} and the projection of Γ_{ab} is a path that maps vectors \mathbf{J}_{r-} back to \mathbf{J}_{r+} . The path Γ_I lies in the fiber over \mathbf{J}_{r+} and closes the path.

Path Γ_W is chosen to follow the Hamiltonian flow of $\mathbf{j}_3 \cdot \mathbf{J}_T$, which generates simultaneous $SU(2)$ rotations of all three angular momenta about the \mathbf{j}_3 -axis. The path on \mathcal{L}_{ab} is chosen to follow the Hamiltonian flows of J_{1z} and J_{2z} by angles $-\phi_1$, and $-\phi_2$ which generate rotations of vectors \mathbf{J}_1 and \mathbf{J}_2 about the z -axis. The path is closed by following the Hamiltonian flows of I_r by angles $-\psi_r$, for $r = 1, 2, 3$. The angles ϕ_1 , ϕ_2 , and ψ_r were computed in Aquilanti *et al* citeAquilanti2007 to be

$$\phi_1 = \cos^{-1} \left(\frac{-J_1^2 + J_2^2 - J_3^2 - 2m_1m_3}{2\sqrt{J_1^2 - m_1^2}\sqrt{J_3^2 - m_3^2}} \right), \quad (3.3.21)$$

$$\phi_2 = -\cos^{-1} \left(\frac{J_1^2 - J_2^2 - J_3^2 - 2m_2m_3}{2\sqrt{J_2^2 - m_2^2}\sqrt{J_3^2 - m_3^2}} \right), \quad (3.3.22)$$

$$\psi_1 = \cos^{-1} \left(\frac{J_1^2(m_3 - m_2) + m_1(J_3^2 - J_2^2)}{4|\mathbf{\Delta}|\sqrt{J_1^2 - m_1^2}} \right), \quad (3.3.23)$$

with ψ_2 and ψ_3 found by cyclicly permuting the indices 1, 2, 3.

The action integral for this path is evaluated using Eqs. A.4.7 and A.4.4,

$$\int_{\Gamma_W} \theta = \sum_{r=1}^3 (\mathbf{j}_3 \cdot \mathbf{J}_{r+}) \Delta\phi = (\mathbf{j}_3 \cdot \mathbf{J}_{T+}) \Delta\phi, \quad (3.3.24)$$

$$\int_{\Gamma_{ab}} \theta = -J_{1-,z} \phi_1 - J_{2-,z} \phi_2, \quad (3.3.25)$$

$$\int_{\Gamma_I} \theta = -\sum_{r=1}^3 I_r \psi, \quad (3.3.26)$$

where $\Delta\phi$ is the total angle of evolution for the Wigner manifold. On the Wigner manifold $\mathbf{J}_T = \mathbf{0}$ so the action integral in Eq. 3.3.24 evaluates to zero. The remaining segments of the path are along the $3jm$ -manifold \mathcal{L}_{ab} and thus $J_{rz} = m_r$ and $I_r = J_r = j_r + 1/2$ on this path. Therefore the total action integral along the closed path Γ is

$$\oint_{\Gamma} \theta = -S_{3j} \equiv -\sum_r (J_r \psi_r + m_r \phi_r), \quad (3.3.27)$$

where we define $\phi_3 \equiv 0$ for symmetry and ϕ_1 , ϕ_2 , and ψ_r are given by Eqs. 3.3.24, 3.3.25, and 3.3.26. This is the phase function found, for example, in Ponzano and Regge [27], and Miller [39], among others.

3.3.4 Maslov and Signature Indices

Now we turn our attention to the Maslov and signature indices μ and σ . We compute the Maslov index in Φ_{2j}^R , the two-dimensional phase space of the symplectic reduction of the $2j$ -model. As determined in Section 3.3.2, coordinates on Φ_{2j}^R are J_{1z} and ϕ_{12} , where $\phi_{12} = \phi_1 - \phi_2$, the difference in the azimuthal angles of vectors \mathbf{J}_1 and \mathbf{J}_2 in angular momentum space. The symplectic reduction of Φ_{2j} by I_1 and I_2 may be considered the symplectic leaf in the $2j$ -angular momentum space satisfying constraints $\mathbf{J}_1^2 = J_1^2$ and $\mathbf{J}_2^2 = J_2^2$. The reduction by J_{12z} is accomplished by restricting to the level set $J_{1z} + J_{2z} = -m_3$ and dividing by the group orbits of J_{12z} . These group orbits are simultaneous rotations of \mathbf{J}_1 and \mathbf{J}_2 about the z -axis. We may therefore choose a representative point on each group orbit where the vector sum \mathbf{J}_{12} lies in the xz -plane with $J_{12x} > 0$. Thus we may interpret the space Φ_{2j}^R as the space of pairs of vectors \mathbf{J}_1 and \mathbf{J}_2 in angular momentum space of fixed lengths J_1 and J_2 such that $J_{12x} > 0$, $J_{12y} = 0$ and $J_{12z} = -m_3$, as shown in Figure 3.3.1. Given this interpretation the projection of the stationary phase set $I^{(2j)}$ onto the reduced space are precisely the points where vectors $\mathbf{J}_{1\pm}$ and $\mathbf{J}_{2\pm}$ agree with the vectors in Eqs. 3.3.19 and 3.3.20. Note that, in this interpretation of Φ_{2j}^R , the projections of $I_+^{(2j)}$ and $I_-^{(2j)}$ satisfy $J_{1y} > 0$ and $J_{1y} < 0$, respectively.

To calculate the Maslov index we need to again construct a path in the reduced space and choose a fixed representation to work in. The two manifolds in the reduced space are

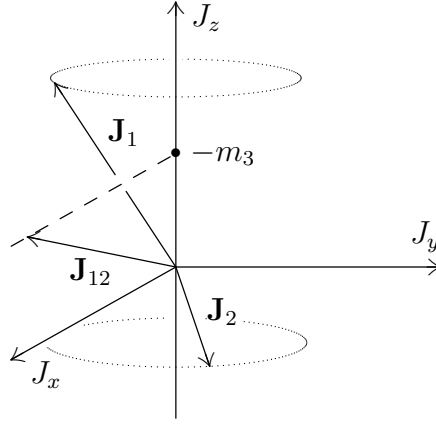


Figure 3.3.1: A point on the reduced $2j$ -phase space Φ_{2j}^R interpreted as a pair of vectors in \mathbb{R}^3 of fixed lengths $|\mathbf{J}_1| = J_1$ and $|\mathbf{J}_2| = J_2$ with the tip of the vector \mathbf{J}_{12} constrained to lie on the dashed line ($J_{12,x} > 0$, $J_{12,y} = 0$, and $J_{12,z} = -m_3$).

\mathcal{L}_a^R and \mathcal{L}_β^R , which were defined in Eq. 3.3.15. Let the path be $\Gamma = \Gamma_\beta + \Gamma_a$, where Γ_β starts at the projection of $I_+^{(2j)}$ and follows the flow of \mathbf{J}_{12}^2 along \mathcal{L}_β^R to the projection of $I_-^{(2j)}$ and Γ_a starts at the projection of $I_-^{(2j)}$ and follows the flow of J_{1z} back to the projection of $I_+^{(2j)}$ along \mathcal{L}_a^R . We choose to work in the J_{1z} -representation of Φ_{2j}^R , in which case J_{1z} is the configuration coordinate and $-\phi_{12}$ is conjugate momentum coordinate. In this representation the symplectic potential is $\theta = -\phi_{12}dJ_{1z}$. In terms of these coordinates the Hamiltonian \mathbf{J}_{12}^2 that defines \mathcal{L}_β^R is

$$\mathbf{J}_{12}^2 = J_1^2 + J_2^2 + 2J_{1z}J_{2z} + 2J_{1\perp}J_{2\perp}\cos\phi_{12}, \quad (3.3.28)$$

where $J_{2z} = -m_3 - J_{1z}$ and $J_{r\perp} \equiv \sqrt{J_r^2 - J_{rz}^2}$.

Consider a one degree-of-freedom phase space Φ . Let H be a Hamiltonian and let \mathcal{L} be a level set of this Hamiltonian, let x define the representation, and let p be the conjugate momentum to x . The caustics occur at points on \mathcal{L} where the function $e \equiv \{x, H\}$ is zero. This condition specifies where \mathcal{L} becomes tangent to one of the constant- x manifolds that defines the Lagrangian foliation for the representation. As in Esterlis *et al* [55], we define $f \equiv \{p, H\}$ and express the Maslov index accumulated by a path that crosses through the caustic point as

$$\mu = \frac{1}{2}\Delta\text{sgn } fe. \quad (3.3.29)$$

That is, the Maslov index in one degree-of-freedom tracks how the sign of fe changes upon passing through the caustic.

Since \mathcal{L}_a^R is one of the manifolds in the Lagrangian foliation of the J_{1z} -representation there is no Maslov contribution from Γ_a . In particular, $x = H = J_{1z}$ so $e = 0$ (every point on Γ_a is a caustic) and thus $\text{sgn } fe = 0$ at all points on \mathcal{L}_a^R so $\mu = 0$ for Γ_a . For Γ_β we still have $x = J_{1z}$ but now $H = \mathbf{J}_{12}^2$. Thus on the reduced β -manifold, $e = \{J_{1z}, \mathbf{J}_{12}^2\} = -4\Delta_z$,

where Δ_z is the z -component of $(\mathbf{J}_1 \times \mathbf{J}_2)/2$. The caustics on \mathcal{L}_β^R are therefore points where $\Delta_z = 0$. In the interpretation of Φ_{2j}^R from earlier, this is when $J_{1y} = 0$ (or, equivalently, when $J_{2y} = 0$). Since \mathbf{J}_{r+} and \mathbf{J}_{r-} are related by reflection through the xz -plane and the flow of \mathbf{J}_{12}^2 leaves \mathbf{J}_{12} invariant and in the xz -plane, Γ_β crosses a caustic exactly once. The entirety of the Maslov index for the $2j$ -model, then, occurs at the single point where the path crosses a caustic on the β -manifold. We defer performing a complete calculation of a Maslov index to the analysis of the $6j$ -symbol in Chapter 4, which may be analyzed simply using the method we developed in Esterlis *et al* [55]. Here we simply quote the result that $\mu = +1$ for this caustic point. The determination of the Maslov correction to the phase for the $3j$ -symbol was found numerically by Ponzano and Regge [27] and analytically using a different one degree-of-freedom phase space model by Schulten and Gordon [41].

Finally, we turn our attention to the signature index. We wish to compute $\sigma(\beta, a)$ at the two intersection points in Φ_{2j}^R in the J_{1z} -representation. As in Cappell, Lee, and Miller [59] and Section C.5, we may express this signature index in terms of the Lagrangian signature,

$$\sigma(\beta, a) = \sigma(\Lambda_x, \Lambda_\beta, \Lambda_a), \quad (3.3.30)$$

where Λ_β and Λ_a are the tangent planes to \mathcal{L}_β^R and \mathcal{L}_a^R at the stationary phase points and Λ_x is the plane tangent to the Lagrangian manifold in the Lagrangian foliation that defines the representation. Since \mathcal{L}_a^R is itself part of the representation-defining foliation Λ_x and Λ_a are equal and, due to the antisymmetry of the Lagrangian signature, Eq. 3.3.30 evaluates to zero at both stationary phase points.

Using the fact that the action integral piece of the phase and the Maslov and signature index pieces of the phase in the $3j$ - and $2j$ -models are separately equal gives that the total phase difference between the two connected pieces of the stationary phase set in the $2j$ -model of the $3j$ -symbol is

$$\Delta\varphi = -S_{3j} - \frac{\pi}{2}, \quad (3.3.31)$$

where S_{3j} is defined by Eq. 3.3.27. Combining everything yields the well-established result [27, 64, 44] for the asymptotics of the $3j$ -symbol,

$$\left(\begin{array}{ccc} j_1 & j_2 & j_3 \\ m_1 & m_2 & m_3 \end{array} \right) = \langle a|\beta \rangle = \langle ab|W \rangle \approx \frac{\cos(S_{3j}/2 + \pi/4)}{\sqrt{2\pi |\Delta_z|}}. \quad (3.3.32)$$

3.4 Summary

In this chapter we saw how the remodeling of an inner product generated two models of the Wigner $3j$ -symbol. In particular the product space model was a $3j$ -model of three angular momenta and the target space model was a $2j$ -model of two angular momenta. The $3j$ -model treats all three angular momenta symmetrically. It is a model where we consider how three angular momenta of fixed lengths and z -components couple to zero. The $2j$ -model involves three angular momenta as well, but two of the angular momenta are treated on a different

footing than the third. It is a model where we consider how two angular momenta of fixed lengths and z -components couple to create a third angular momentum of fixed length and z -component and is closely related to the Clebsch-Gordan coefficients. We analyzed the linear algebra and phase space geometry of the two models and saw how they were related by the remodeling procedure developed in Chapter 2. In particular we saw how the transport of a manifold geometrically plays out and demonstrated how the transport of a momentum map yields the appropriate functions to describe the transported manifold. We demonstrated how the amplitude determinant calculations play out in the two models and saw the advantages of the target-space model in computing such determinants. Finally, we presented an overview of the phase calculation, utilizing both models to simplify the work necessary. The action integral was calculated in the $3j$ -model following Aquilanti *et al* [44] and the Maslov and signature indices were computed in the reduced $2j$ -model.

Since the models of the $3j$ -symbol do not involve many degrees of freedom the advantages of using an inner product remodeling are not readily apparent. In particular, the simplification of a 2×2 matrix of Poisson brackets to a single Poisson bracket is not very dramatic and the geometry involved in the phase calculation is fairly involved in both $2j$ - and $3j$ -models. However, the $3j$ -symbol provided a very simple playground to demonstrate how the remodeling procedure plays out. In practice we do not need to tediously construct the core symplectomorphism or analyze in detail the transport of a manifold. It is enough to know that given a remodeling geometry setup the relevant manifolds *are* connected in such a manner. Thus we turn our attention in the next chapter to seeing how the remodeling procedure *does* simplify calculations in the case of the $6j$ -symbol. In fact, most of the work in that chapter will be in setting up the remodeling algebras and geometries. Once the playground has been constructed the actual analysis of the asymptotics of the $6j$ -symbol will be straightforward. We will be able to avoid the headaches involved in the calculation of a 9×9 determinant, instead calculating a single Poisson bracket. We will also be able to take advantage of the symmetry of the product space model to simplify the calculation of the action integral in the phase. Since we did not do so in this chapter, the action integral calculation will be performed in both relevant models to demonstrate that they are equal.

Chapter 4

Models of the $6j$ -Symbol

Now we turn to the Wigner $6j$ -symbol (which is related to the Racah W -coefficient by a phase). The $6j$ -symbol is a central object in angular momentum theory with applications wherever three angular momenta are coupled together, such as in molecular, atomic, and nuclear physics. Traditionally the $6j$ -symbol is considered as the unitary matrix elements involved in a change-of-basis between the various recoupling schemes of three angular momenta [28]. These basis vectors involve four angular momenta (the three original angular momenta and the coupled angular momentum) and we call such interpretations of the $6j$ -symbol “ $4j$ -models.” The asymptotic (large j or small \hbar) expression for the $6j$ -symbol was first obtained by Ponzano and Regge [27], though rigorous derivations of the formula did not come until later.

The Ponzano-Regge formula has since been derived by many different methods. Neville [38] presented the first derivation of the asymptotic formula, using the recursion relations of the $6j$ -symbol and a discrete form of WKB theory. Schulten and Gordon [40, 41] provided another proof along similar lines. Biedenharn and Louck [42] proved a proof of the Ponzano-Regge formula by showing that the formula satisfied all of the defining properties of the $6j$ -symbol. Roberts [2] presented a derivation of the Ponzano-Regge formula by introducing a “ $12j$ -model” of the $6j$ -symbol, which involves twelve angular momenta all treated on the same footing. Aquilanti *et al* [1] similarly used symplectic geometry of the sort used extensively in this work to derive the asymptotics in the $4j$ -model. Charles [43] derived the formula using the formalism of geometric quantization [69, 70, 71]. Dupuis and Livine [72, 73] expanded on the previous works and analytically presented a next-to-leading order approximation for the $6j$ -symbol.

The “Ponzano-Regge phase” that occurs in the asymptotic expression of the $6j$ -symbol is precisely the three-dimensional Einstein-Hilbert action integrated over a tetrahedron in the Regge calculus approach to quantum gravity [74]. In fact, the “Ponzano-Regge model” presented in Ponzano and Regge [27], a state-sum model for $3d$ -Euclidean quantum gravity treated as an $SU(2)$ gauge theory, is the first spin-foam model ever presented and uses the $6j$ -symbol as a fundamental building block. The $6j$ -symbol enters because the Ponzano-Regge model uses a triangulation of $3d$ -Euclidean spacetime into tetrahedra with $SU(2)$ -

irreps labeling the edges of the triangulation. A tetrahedron whose edges carry $SU(2)$ representations is one of the ways of interpreting the spin network for the 6j-symbol,

$$\left\{ \begin{array}{ccc} j_1 & j_2 & j_3 \\ j_4 & j_5 & j_6 \end{array} \right\} = \begin{array}{c} \bullet \\ \begin{array}{ccc} \nearrow 6 & \uparrow 1 & \nwarrow 5 \\ \searrow 2 & \bullet & \nearrow 3 \\ \leftarrow 4 & & \rightarrow \end{array} \\ \bullet \end{array} . \quad (4.0.1)$$

Turaev and Viro [29], unaware of the previous work by Ponzano and Regge, defined a similar state sum. They also expanded the formalism and created a state sum using the 6j-symbol for the Hopf algebra $SL_q(2)$. This naturally provides a cutoff for the values of j that characterize the irreps and thus provides a regularized version of the Ponzano-Regge model. Turaev [75] and Roberts [34], among others, also showed that the Turaev-Viro state sum for the “ q -deformed” 6j-symbol is a model for 3d-Euclidean quantum gravity with cosmological constant.

In this chapter we explore how the various models of the 6j-symbol fit in to the remodeling of an inner product presented in Chapter 2. The two treatments that are most applicable to this work are the symplectic derivations of the asymptotics of the 6j-symbol in the 12j-model [2] and 4j-model [1], which are connected by two applications of an inner product remodel. We choose to use a “symmetric” labeling of the in this work, where each of the six angular momenta in Eq. 4.0.1 are treated on an equal footing. In many of the works listed above, an “asymmetric” or “coupled” labeling scheme is preferred, where the angular momenta j_1, \dots, j_6 are instead written $j_1, j_2, j_{12}, j_3, j_4, j_{23}$. This labeling emphasizes the different coupling schemes used in the 4j-model but are inconvenient to use in the remodeling algebras that will be set up in this chapter.

We start in Section 4.1 by discussing the 2j-, 3j-, and 4j-intertwiner states that are the building blocks of the various models of the 6j-symbol. Then in Section 4.2 we build the two remodeling algebras that connect the 12j-model with the 4j-model. We discuss the classical phase spaces and Lagrangian manifolds that support the semiclassical approximations to the elements of the remodeling algebras in Section 4.3. With the remodeling geometry in place, in Section 4.4 we perform the action integral calculations in both models and show that they are related exactly as claimed. Finally, in Section 4.5 we complete the derivation of the asymptotic form of the 6j-symbol by computing the amplitude determinant and Maslov and signature indices in the 4j-model, where they are easiest to analyze.

4.1 Intertwiner States

The states that occur in the various models of the 6j-symbol can all be thought of as direct products of two-, three-, or four-valent intertwiner states. More generally, the states involved in the inner-product models for all $3nj$ -symbols are composed of k -valent intertwiners, where k may vary from 2 to $n + 2$. In this section we treat all k -valent intertwiners as states in

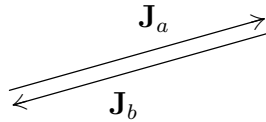


Figure 4.1.1: A point on the diangle manifold \mathcal{L}_K projected onto a pair of vectors in \mathbb{R}^3 of fixed length $|\mathbf{J}_a| = |\mathbf{J}_b| = J$. The two vectors satisfy the condition $\mathbf{J}_a + \mathbf{J}_b = \mathbf{0}$ and can therefore be arranged into a closed chain to form a “diangle”. The two vectors are slightly separated in the drawing so that they do not overlap.

The phase of these $2j$ -intertwiner state is defined such that the components of $|K_{ab}\rangle$ with respect to the standard angular momentum basis vectors are the $2j$ -symbols of Section 3.1.4.

The classical phase space corresponding to \mathcal{H}_{2j} is the $2j$ -phase space $\Phi_{2j} \equiv \Sigma_a \times \Sigma_b$ and the Lagrangian manifold \mathcal{L}_K that supports the semi-classical approximation to the $2j$ -intertwiner state is described as the level set,

$$\mathcal{L}_K = \left(\begin{array}{cc} I_a & \mathbf{J}_{ab} \\ J & \mathbf{0} \end{array} \right) \subset \Phi_{2j} \quad (4.1.3)$$

where the classical function \mathbf{J}_{ab} is the sum $\mathbf{J}_a + \mathbf{J}_b$ and $J = j + 1/2$. We may have also included the level set condition $I_b = J$ in Eq. 4.1.3, however this condition is not independent of the four functions already listed. This manifold is generated by the group $G_K = U(1) \times SU(2)$. The isotropy subgroup is trivial for this manifold so \mathcal{L}_K has the topology and volume

$$\mathcal{L}_K \cong U(1) \times SU(2), \quad V_K = (4\pi)(16\pi^2) = 2^6\pi^3, \quad (4.1.4)$$

where the volume is taken with respect to the Haar measure $d\psi_a \wedge d\alpha \wedge \sin\beta d\beta \wedge d\gamma$.

The projection of \mathcal{L}_K onto the $2j$ -angular momentum space Λ_{2j} consists of the pair of vectors in \mathbb{R}^3 of equal fixed lengths $j + 1/2$ that add to zero. That is, the two vectors \mathbf{J}_a and \mathbf{J}_b are equal and opposite each other. We call the figure formed by placing the two vectors end-to-end in the order $(\mathbf{J}_a, \mathbf{J}_b)$ as in Figure 4.1.1 a “diangle,” in analogy with the triangle formed by the three vectors in the Wigner manifold. We commonly refer to the Lagrangian manifold \mathcal{L}_K as the “diangle manifold” and the state $|K_{ab}\rangle$ as the “diangle state.” The projection of the diangle manifold onto angular momentum space is a manifold generated by the group of rotations $SO(3)$. However, the subgroup of $SO(2)$ rotations about the axis \mathbf{j}_a of \mathbf{J}_a leaves both vectors invariant and thus is an isotropy subgroup. The diangle manifold in Λ_{2j} is thus a two-sphere, parameterized by orientations of \mathbf{j}_a and thus the diangle manifold may be seen as a T^2 bundle over S^2 . The S^1 subset of these fibers generated by the Hamiltonian $\mathbf{j}_a \cdot \mathbf{J}_{ab}$ are Hopf circles over S^2 and thus the manifold may be expressed as $S^1 \times S^3$, as expected for the topology $U(1) \times SU(2)$.

4.1.2 The $3j$ -Intertwiner (“Triangle”) States

Consider the tensor product of three copies of the Schwinger Hilbert space, $\mathcal{H}_{3j} = \mathcal{S}_a \otimes \mathcal{S}_b \otimes \mathcal{S}_c$ where the three Hilbert spaces are labeled by a , b , and c and let \mathcal{C}_{abc} be the $\mathcal{C}_{j_a} \otimes \mathcal{C}_{j_b} \otimes \mathcal{C}_{j_c}$

subspace of \mathcal{H}_{3j} . Let \mathcal{Z}_{abc} be the space of $3j$ -intertwiners $:\mathcal{C}_{abc} \rightarrow \mathbb{C}$. As discussed in Section 3.1.3.3, \mathcal{Z}_{abc} is non-trivial iff the triplet (j_a, j_b, j_c) is triangle-allowed, in which case there is a unique $j = 0$ (one-dimensional) irreducible subspace of \mathcal{C}_{abc} . This subspace is spanned by the Wigner state introduced in Section 3.1.1. As in Section 3.1.2 we will treat the Wigner state as an element of \mathcal{H}_{3j} and label the normalized state in the Dirac notation as $|W_{abc}\rangle$, where the subscripts indicate the three component Schwinger Hilbert spaces in \mathcal{H}_{3j} and it is understood that this state carries the irrep labels j_a, j_b , and j_c . Following Eq. 3.1.9, we define

$$|W_{abc}\rangle = \left| \begin{array}{cccc} \hat{I}_a & \hat{I}_b & \hat{I}_c & \hat{\mathbf{J}}_{abc} \\ j_a & j_b & j_c & \mathbf{0} \end{array} \right\rangle = \begin{array}{c} \uparrow a \\ \bullet \\ \swarrow b \quad \searrow c \end{array} \in \mathcal{S}_a \otimes \mathcal{S}_b \otimes \mathcal{S}_c, \quad (4.1.5)$$

where $\hat{\mathbf{J}}_{abc} = \hat{\mathbf{J}}_a + \hat{\mathbf{J}}_b + \hat{\mathbf{J}}_c$ and the label a, b , and c on the legs of the spin network represent the understood irrep labels j_a, j_b , and j_c . This state is normalized and the phase is defined such that the components of $|W_{abc}\rangle$ with respect to the standard angular momentum basis vectors are the $3j$ -symbols.

The properties of the Lagrangian manifold $\mathcal{L}_W \subset \Phi_{abc} \equiv \Sigma_a \times \Sigma_b \times \Sigma_c$ corresponding to the $3j$ Wigner state were already discussed in detail in Sec. 3.2.2. Specifically, the manifold \mathcal{L}_W was defined as a level set in Eq. 3.2.7 and the topology and volume were given in Eq. 3.2.8. On \mathcal{L}_W the three angular momentum vectors may be configured to form a triangle as in Figure 3.2.3 so \mathcal{L}_W may be called a “triangle manifold” and $|W_{abc}\rangle$ a “triangle state.”

4.1.3 The $4j$ -Intertwiner (“Butterfly”) States

Consider the tensor product of four copies of the Schwinger Hilbert space, $\mathcal{H}_{4j} = \bigotimes \mathcal{S}_r$, with $r = a, b, c, d$ and let \mathcal{C}_{abcd} be the $\mathcal{C}_{j_a} \otimes \mathcal{C}_{j_b} \otimes \mathcal{C}_{j_c} \otimes \mathcal{C}_{j_d}$ subspace of \mathcal{H}_{4j} . Let $\mathcal{Z}_{j_a j_b j_c j_d}$ be the space of $4j$ -intertwiners $:\mathcal{C}_{abcd} \rightarrow \mathbb{C}$. According to the standard rules for addition of angular momenta this space is non-trivial iff the “polygon inequality” $\max\{j_r + 1/2\} \leq \frac{1}{2} \sum (j_r + 1/2)$ is satisfied and $\sum j_r \in \mathbb{Z}$ where the sums are taken over $r = \{a, b, c, d\}$. The polygon inequality is a necessary and sufficient condition for line segments of length $j_r + 1/2$ to be fit together to form a closed polygon in \mathbb{R}^n . The space \mathcal{Z}_{abcd} is spanned by the set of $j = 0$ irreducible subspaces of \mathcal{C}_{abcd} and so may be defined as the simultaneous eigenspace

$$\mathcal{Z}_{abcd} \equiv \left\{ |\psi\rangle \in \mathcal{H}_{4j} \mid \hat{I}_r |\psi\rangle = j_r |\psi\rangle, \hat{\mathbf{J}}_{abcd} |\psi\rangle = \mathbf{0} |\psi\rangle \right\}, \quad (4.1.6)$$

where $r = a, b, c, d$ and $\hat{\mathbf{J}}_{abcd} = \sum_r \hat{\mathbf{J}}_r$. We call elements of \mathcal{Z}_{abcd} “ $4j$ -intertwiner states.” Unlike the space of $2j$ - and $3j$ -intertwiners, the dimension of the space of $4j$ -intertwiners is in general greater than one when the polygon inequality is satisfied. In fact, the $6j$ -symbol may be interpreted in the $4j$ -model as the coefficients for a change-of-basis of \mathcal{Z}_{abcd} . (This is why there is no need to define a rotationally-invariant $3j$ -symbol. The space of intertwiners is one-dimensional so the “change-of-basis” amounts to the normalization condition Eq. 3.1.5.)

Orthonormal basis states in \mathcal{Z}_{abcd} may be constructed by coupling $2j$ and $3j$ Wigner states [28]. Let \mathcal{H}_{6j} be a $6j$ Hilbert space for the six angular momenta a through f . Consider first a coupling scheme that couples angular momenta a and b into the intermediate angular momentum e . Consider the two triangle states $|W_{abe}\rangle \in \mathcal{H}_{abe}$ and $|W_{fcd}\rangle \in \mathcal{H}_{fcd}$ and the dual diangle state $\langle K_{ef}|$. For these states to be non-zero we require $j_e = j_f \equiv j_{ab}$ and (j_a, j_b, j_{ab}) and (j_{ab}, j_c, j_d) to be triangle-allowed triplets. We may treat $\langle K_{ef}|$ as a map $:\mathcal{H}_{6j} \rightarrow \mathcal{H}_{4j}$ which effectively projects a state $|\psi\rangle \in \mathcal{H}_{6j}$ into the simultaneous $(\hat{I}_e, \hat{\mathbf{J}}_{ef})$ -eigenspace of \mathcal{H}_{6j} at eigenvalues $(j_{ab}, \mathbf{0})$ followed by the natural projection of $\mathcal{H}_{abcd} \otimes \mathcal{H}_{ef}$ onto \mathcal{H}_{abcd} . Let $|\psi\rangle$ be the result of $\langle K_{ef}|$ acting on $|W_{abe}W_{fcd}\rangle$. This is an element of \mathcal{Z}_{abcd} since it is an element of the $\hat{\mathbf{J}}_{abc}$, $\hat{\mathbf{J}}_{fcd}$, and $\hat{\mathbf{J}}_{ef}$ null eigenspace and therefore

$$\hat{\mathbf{J}}_{abcd}|\psi\rangle = (\hat{\mathbf{J}}_{abe} + \hat{\mathbf{J}}_{fcd} - \hat{\mathbf{J}}_{ef})|\psi\rangle = 0. \quad (4.1.7)$$

As discussed in Section 3.1.5 the triangle state $|W_{abe}\rangle$ is in the $j_{ab}(j_{ab} + 1)$ -eigenspace of $\hat{\mathbf{J}}_{ab}^2$. Similarly, $|W_{fcd}\rangle$ is in the $j_{ab}(j_{ab} + 1)$ -eigenspace of $\hat{\mathbf{J}}_{cd}^2$. Therefore $|\psi\rangle$ is in the $j_{ab}(j_{ab} + 1)$ -eigenspace of both $\hat{\mathbf{J}}_{ab}^2$ and $\hat{\mathbf{J}}_{cd}^2$. Note that the eigenvalue condition on $\hat{\mathbf{J}}_{ab}^2$ combined with the $SU(2)$ -invariance condition implies the eigenvalue condition on $\hat{\mathbf{J}}_{cd}^2$. We write the normalized state coupled in this way $|B_{a(bc)d}, j_{ab}\rangle$. A different basis arises from acting $\langle K_{ef}|$ on the state $|W_{bce}W_{fad}\rangle$ which couples angular momenta b and c together. The (normalized) states are written in terms of eigenvalues as

$$|B_{(ab)cd}, j_{ab}\rangle = \left| \begin{array}{ccc} \hat{I}_r & \hat{\mathbf{J}}_{ab}^2 & \hat{\mathbf{J}}_{abcd} \\ j_r & j_{ab} & \mathbf{0} \end{array} \right\rangle, \quad |B_{a(bc)d}, j_{bc}\rangle = \left| \begin{array}{ccc} \hat{I}_r & \hat{\mathbf{J}}_{bc}^2 & \hat{\mathbf{J}}_{abcd} \\ j_r & j_{bc} & \mathbf{0} \end{array} \right\rangle, \quad (4.1.8)$$

where the quantum number j_{ab} means that the state is an eigenstate of $\hat{\mathbf{J}}_{ab}^2$ with eigenvalue $j_{ab}(j_{ab} + 1)$. A third basis which couples a and c exists but will not be considered in this work.

In spin network notation we define these $4j$ -intertwiner states to be

$$|B_{(ab)cd}, j_{ab}\rangle = (-1)^{j_a - j_b - j_c + j_d} \sqrt{2j_{ab} + 1} \begin{array}{c} \nearrow a \\ \bullet \\ \searrow b \\ \nearrow d \\ \bullet \\ \searrow c \end{array} \in \mathcal{H}_{abcd}, \quad (4.1.9)$$

$$|B_{a(bc)d}, j_{bc}\rangle = (-1)^{2j_b} \sqrt{2j_{bc} + 1} \begin{array}{c} \nearrow c \\ \bullet \\ \searrow b \\ \nearrow d \\ \bullet \\ \searrow a \end{array} \in \mathcal{H}_{abcd}. \quad (4.1.10)$$

where the phases are chosen to agree with standard recoupling theory results [28]. Following the conventions in Stedman [8] we simplify our spin networks by assuming that all arrows

point away from the $3j$ -nodes and towards the $2j$ -stubs on an internal line with a stub unless explicitly drawn otherwise. Allowing j_{ab} or j_{bc} to run over the full range of triangle-allowed values yields the two bases of \mathcal{Z}_{abcd} that occur in the $6j$ -symbol.

The classical phase space corresponding to \mathcal{H}_{4j} is the $4j$ -phase space $\Phi_{4j} \equiv \Sigma_a \times \Sigma_b \times \Sigma_c \times \Sigma_d$. Following Section 2.4.3, the space of intertwiners \mathcal{Z}_{abcd} corresponds to the co-isotropic manifold

$$L_Z = \begin{pmatrix} I_a & I_b & I_c & I_d & \mathbf{J}_{abcd} \\ J_a & J_b & J_c & J_d & \mathbf{0} \end{pmatrix} \subset \Phi_{4j}. \quad (4.1.11)$$

The Lagrangian manifold $\mathcal{L}_{B,ab}$ and $\mathcal{L}_{B,bc}$ that support the semi-classical approximations to the $4j$ -intertwiner states are Lagrangian manifolds in this co-isotropic submanifold,

$$\mathcal{L}_{B,ab} = \begin{pmatrix} \mathbf{J}_{ab}^2 \\ J_{ab}^2 \end{pmatrix} \subset L_Z \subset \Phi_{4j}, \quad \mathcal{L}_{B,bc} = \begin{pmatrix} \mathbf{J}_{bc}^2 \\ J_{bc}^2 \end{pmatrix} \subset L_Z \subset \Phi_{4j}, \quad (4.1.12)$$

where the contour values are $(j_{ab} + 1/2)^2$ and $(j_{bc} + 1/2)^2$ as shown in Section 3.2.3. It is more convenient to use the Hamiltonians $|\mathbf{J}_{ab}|$ as the Hamiltonian that defines $\mathcal{L}_{B,ab}$ since the angle θ conjugate to $|\mathbf{J}_{ab}|$ is 4π -periodic while period of the angle conjugate to \mathbf{J}_{ab}^2 depends on the contour value J_{ab} . Therefore we choose to use the following equivalent description of $\mathcal{L}_{B,ab}$ and $\mathcal{L}_{B,bc}$,

$$\mathcal{L}_{B,ab} = \begin{pmatrix} |\mathbf{J}_{ab}| \\ J_{ab} \end{pmatrix} \subset L_Z \subset \Phi_{4j}, \quad \mathcal{L}_{B,bc} = \begin{pmatrix} |\mathbf{J}_{bc}| \\ J_{bc} \end{pmatrix} \subset L_Z \subset \Phi_{4j}, \quad (4.1.13)$$

These manifolds are generated by the group $G_B = U(1)^5 \times SU(2)$. Coordinate on G_B are (ψ_r, θ, u) , where ψ_r are the 4π -periodic evolution variables for I_r , θ is the 4π -periodic evolution variable for either $|\mathbf{J}_{ab}|$ or $|\mathbf{J}_{bc}|$, and $u \in SU(2)$. The isotropy subgroup is then generated by two elements, $(2\pi, 2\pi, 2\pi, 2\pi, 0, -1)$ and either $(0, 0, 2\pi, 2\pi, 2\pi, -1)$ or $(2\pi, 0, 0, 2\pi, 2\pi, -1)$ (for the ab - and bc -coupling schemes, respectively). In either case the manifolds have topology and volume

$$\mathcal{L}_B \cong \frac{U(1)^5 \times SU(2)}{(\mathbb{Z}_2)^2}, \quad V_B = \frac{1}{4}(4\pi)^5(16\pi^2) = 2^{12}\pi^7, \quad (4.1.14)$$

where the volume is taken with respect to the Haar measure $(\wedge d\psi_r) \wedge d\theta \wedge d\alpha \wedge \sin\beta d\beta \wedge d\gamma$.

The projection of $\mathcal{L}_{B,ab}$ onto the $4j$ -angular momentum space Λ_{4j} consists of the four vectors in \mathbb{R}^3 with fixed lengths J_r that add to zero and satisfy $|\mathbf{J}_{ab}| = J_{ab}$. We can construct such a figure by placing the four vectors end-to-end in the order $(\mathbf{J}_a, \mathbf{J}_b, \mathbf{J}_c, \mathbf{J}_d)$ adding the fixed-length vector \mathbf{J}_{ab} to the diagram, basing it at the origin, as shown in Figure 4.1.2. The $SU(2)$ group generates $SO(3)$ rotations of the entire figure and the $U(1)$ group generated by $|\mathbf{J}_{ab}| = \mathbf{j}_{ab} \cdot \mathbf{J}_{ab}$ generates $SO(2)$ rotations of vectors \mathbf{J}_a and \mathbf{J}_b about the axis $\mathbf{j}_{ab} \equiv \mathbf{J}_{ab}/|\mathbf{J}_{ab}|$. This leaves the triangle formed by the triplet $(\mathbf{J}_{ab}, \mathbf{J}_c, \mathbf{J}_d)$ invariant. Treating the $(\mathbf{J}_a, \mathbf{J}_b, -\mathbf{J}_{ab})$ and $(\mathbf{J}_{ab}, \mathbf{J}_c, \mathbf{J}_d)$ triangles as “wings” lets this $SO(2)$ rotation be visualized as a “flapping.” Thus the figure is referred to as a “butterfly figure,” with the coupled vector

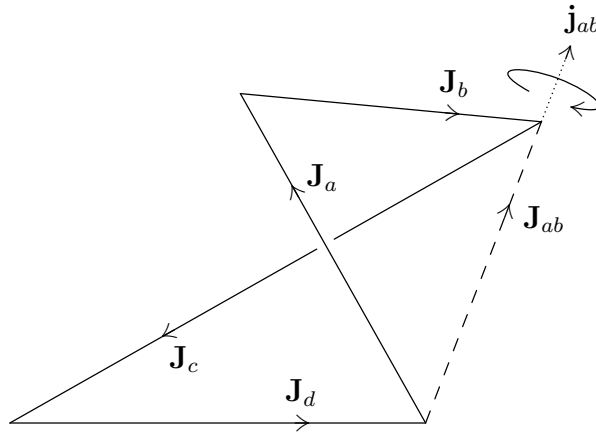


Figure 4.1.2: A point on the butterfly manifold $\mathcal{L}_{B,ab}$ projected onto a set of four vectors in \mathbb{R}^3 of fixed lengths $|\mathbf{J}_r| = J_r$ ($r = a, b, c, d$). The four vectors satisfy the condition $\mathbf{J}_a + \mathbf{J}_b + \mathbf{J}_c + \mathbf{J}_d = \mathbf{0}$ and can therefore be arranged into a closed chain. The length of the vector sum \mathbf{J}_{ab} is constrained to be J_{ab} . The two wings of the “butterfly” are the triangles formed by the triplets $(\mathbf{J}_a, \mathbf{J}_b, -\mathbf{J}_{ab})$ and $(\mathbf{J}_c, \mathbf{J}_d, \mathbf{J}_{ab})$ and the body is the vector \mathbf{J}_{ab} . The “flapping” motion generated by \mathbf{J}_{ab}^2 (or $|\mathbf{J}_{ab}|$) rotates \mathbf{J}_a and \mathbf{J}_b about the axis $\mathbf{j}_{ab} \equiv \mathbf{J}_{ab}/J_{ab}$.

\mathbf{J}_{ab} acting as the body of the butterfly. We call manifolds $\mathcal{L}_{B,ab}$ and $\mathcal{L}_{B,bc}$ the “butterfly manifolds” and the $4j$ -intertwiner states in Eq. 4.1.8 the “butterfly states.”

Finally, consider again the co-isotropic manifold L_Z defined in Eq. 4.1.11. The projection of this manifold onto Λ_{4j} may be interpreted as the set of four vectors \mathbf{J}_a , \mathbf{J}_b , \mathbf{J}_c , and \mathbf{J}_d of fixed lengths arranged end-to-end into a closed chain. By adding vectors \mathbf{J}_{ab} connecting the tail of \mathbf{J}_a to the tip of \mathbf{J}_b and \mathbf{J}_{bc} connecting the tail of \mathbf{J}_b to the tip of \mathbf{J}_c as shown in Figure 4.1.3 we see that each point on L_Z defines a tetrahedron. Thus we may define a volume function on L_Z ,

$$V \equiv \frac{1}{6} \mathbf{J}_a \cdot (\mathbf{J}_b \times \mathbf{J}_c) : L_Z \rightarrow \mathbb{R}. \quad (4.1.15)$$

We may in fact define such a function everywhere on Φ_{4j} , but we may only interpret it as a tetrahedron volume on L_Z .

4.2 Remodeling Algebra of the 6j-Symbol

Connecting the $4j$ - and $12j$ -models of the $6j$ -symbol requires two applications of the remodeling procedure. The first remodel of the $6j$ -symbol, connects the “symmetric” $12j$ -model of Roberts [2] to an “intermediate” $8j$ -model. The product space inner product serves as the $12j$ -model in this case and the target space inner product serves as the $8j$ -model. The two states in the $12j$ -model are a quartet of $3j$ -intertwiners and a sextet of $2j$ -intertwiners while the two states in the $8j$ -model are a quartet of $2j$ -intertwiners and a pair of $4j$ -intertwiners.

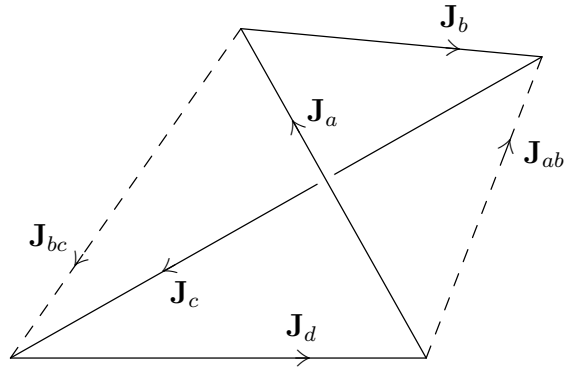


Figure 4.1.3: A point in L_Z projected onto a set of four vectors in \mathbb{R}^3 of fixed lengths $|\mathbf{J}_r| = J_r$ ($r = a, b, c, d$). The four vectors satisfy the condition $\mathbf{J}_a + \mathbf{J}_b + \mathbf{J}_c + \mathbf{J}_d = \mathbf{0}$ and can therefore be arranged into a closed chain. The tetrahedron is formed by including vectors $\mathbf{J}_{ab} \equiv \mathbf{J}_a + \mathbf{J}_b$ and $\mathbf{J}_{bc} \equiv \mathbf{J}_b + \mathbf{J}_c$ in the diagram.

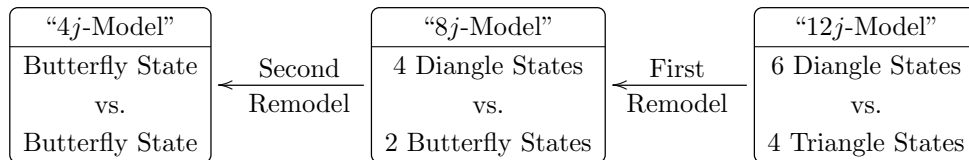


Figure 4.2.1: Schematic of the spaces and states involved in the two remodeling algebras for the 6j-symbol.

The second remodel connects the intermediate 8j-model with the “coupled” or “asymmetric” 4j-model which was explored in Aquilanti *et al* [1]. Here the 8j-model arises from the product space inner product and the target space inner product produces the 4j-model. The two states in the 4j-model are both single copies of a 4j-intertwiner. A schematic of the two remodelings is shown in Figure 4.2.1.

We start in Section 4.2.1 by defining all of the Hilbert spaces that occur in this pair of remodels. In Section 4.2.2 we construct the algebra for the first remodel, connecting the 12j- and 8j-models of the 6j-symbol. Then in Section 4.2.3 we construct the algebra for the second remodel, connecting the 8j- and 4j-models of the 6j-symbol.

4.2.1 Hilbert Spaces for the Remodels of the 6j-Symbol

The symmetric labeling of the 6j-symbol in Eq. 4.0.1 specifies six irrep labels $j_r, r = 1, \dots, 6$. In the symmetric 12j-model of Roberts [2] each of these irreps is assigned to a pair of Schwinger spaces and thus the 12j-model Hilbert space is a space describing twelve angular momenta. We label these pairs of Schwinger spaces \mathcal{S}_r and $\mathcal{S}_{r'}$, where the irrep label j_r picks out the relevant irreducible carrier subspace of *both* \mathcal{S}_r and $\mathcal{S}_{r'}$. The 12j-Hilbert space

is defined as

$$\mathcal{H}_{12j} \equiv \bigotimes_{r=1}^6 \mathcal{S}_r \otimes \mathcal{S}_{r'}. \quad (4.2.1)$$

Spin networks for states in \mathcal{H}_{12j} will therefore contain twelve ket chevrons, labeled by 1 through 6 and 1' through 6', with appropriate irrep labels j_r implied for the legs ending in both the primed and unprimed chevrons.

The 8j-model takes place in a Hilbert space comprised of a subset of eight of the Schwinger spaces comprising \mathcal{H}_{12} . These eight Schwinger spaces may be separated into the four pairs of primed and unprimed spaces for $r = 1, 2, 4, 5$. The 8j-Hilbert space which carries the 8j-model of the 6j-symbol is thus

$$\mathcal{H}_{8j} \equiv \bigotimes_{r \in \{1, 2, 4, 5\}} \mathcal{S}_r \otimes \mathcal{S}_{r'}. \quad (4.2.2)$$

Note that a *different* 8j-model was briefly introduced in Aquilanti *et al* [1], involving the four unprimed spaces for $r = 1, 2, 4, 5$ and the primed and unprimed pairs for $r = 3, 6$. We will not consider this 8j-model in this chapter as it is unrelated to the remodeling algebra that we are setting up here.

The 12j-Hilbert space is the product space of the first remodel and the 8j-Hilbert space is the target space so the dual of the source space must be the 4j-Hilbert space

$$\mathcal{H}_{33'66'} \equiv \mathcal{S}_3 \otimes \mathcal{S}_{3'} \otimes \mathcal{S}_6 \otimes \mathcal{S}_{6'}. \quad (4.2.3)$$

We explicitly label the four angular momenta involved in this 4j-Hilbert space because the pair of remodeling algebras for the 6j-symbol contain a total of three different 4j-Hilbert spaces and their duals, rendering notation “ \mathcal{H}_{4j} ” insufficient. The source space for the first remodel is thus the dual 4j-Hilbert space $\mathcal{H}_{33'66'}^*$. Note that indeed $\mathcal{H}_{8j} \otimes (\mathcal{H}_{33'66'}^*)^* = \mathcal{H}_{12j}$.

In the second remodel the dual of the 8j-Hilbert space \mathcal{H}_{8j}^* serves as the product Hilbert space so the target Hilbert space, which will carry the 4j-model of the 6j-symbol, is a dual 4j-Hilbert space containing a subset of four of the Schwinger spaces comprising \mathcal{H}_{8j}^* . The 4j-model uses irrep labels j_1, j_2, j_4 , and j_5 , with j_3 and j_6 acting as the coupled angular momenta (in the asymmetric labeling of the 6j-symbol, j_3 is replaced by j_{12} , for example). We define the target space as

$$\mathcal{H}_{1245}^* \equiv \mathcal{S}_1^* \otimes \mathcal{S}_2^* \otimes \mathcal{S}_{4'}^* \otimes \mathcal{S}_5^*. \quad (4.2.4)$$

The dual source space is made of the remaining spaces,

$$\mathcal{H}_{1'2'4'5'}^* \equiv \mathcal{S}_{1'}^* \otimes \mathcal{S}_{2'}^* \otimes \mathcal{S}_4^* \otimes \mathcal{S}_{5'}^*, \quad (4.2.5)$$

which means that the source space for the second remodel is $\mathcal{H}_{1'2'4'5'}$.

A summary of the Hilbert spaces introduced in this Section and what roles they take in the remodeling algebras for the 6j-symbol is given in Table 4.1.

remodel. Specifying \mathcal{H}_{12j} as the product Hilbert space means that the network for the M -state must contain one ket chevron for each of the twelve Schwinger spaces (six primed and six unprimed). The spin network for the M -state is therefore the four $3j$ -intertwiners,

$$|M_1\rangle = \begin{array}{cccc} \begin{array}{c} \uparrow 1 \\ \bullet \\ \swarrow 2 \quad \searrow 3 \end{array} & \begin{array}{c} \uparrow 1' \\ \bullet \\ \swarrow 5' \quad \searrow 6 \end{array} & \begin{array}{c} \uparrow 2' \\ \bullet \\ \swarrow 6' \quad \searrow 4 \end{array} & \begin{array}{c} \uparrow 3' \\ \bullet \\ \swarrow 4' \quad \searrow 5 \end{array} \\ \in \mathcal{H}_{12j}, & & & \end{array} \quad (4.2.8)$$

where the ‘1’ subscript in $|M_1\rangle$ is used to highlight that this is the map state of the *first* remodel. In Dirac notation this state is written $|M_1\rangle \equiv |W_{123}\rangle|W_{1'5'6}\rangle|W_{2'6'4}\rangle|W_{3'4'5}\rangle$ which is the simultaneous eigenstate

$$|M_1\rangle = \left| \begin{array}{cccccc} \hat{I}_r & \hat{I}_{r'} & \hat{\mathbf{J}}_{123} & \hat{\mathbf{J}}_{1'5'6} & \hat{\mathbf{J}}_{2'6'4} & \hat{\mathbf{J}}_{3'4'5} \\ j_r & j_r & \mathbf{0} & \mathbf{0} & \mathbf{0} & \mathbf{0} \end{array} \right\rangle \in \mathcal{H}_{12j}, \quad (4.2.9)$$

where $r = 1, \dots, 6$ and $|W_{abc}\rangle$ was defined in Eq. 4.1.5.

The remaining pieces of the spin network form the dual of the product state. Therefore the product state in the first remodel is

$$|ab_1\rangle = \begin{array}{cccccc} \begin{array}{c} \uparrow 1' \\ \downarrow 1 \end{array} & \begin{array}{c} \uparrow 2' \\ \downarrow 2 \end{array} & \begin{array}{c} \uparrow 3' \\ \downarrow 3 \end{array} & \begin{array}{c} \uparrow 4' \\ \downarrow 4 \end{array} & \begin{array}{c} \uparrow 5' \\ \downarrow 5 \end{array} & \begin{array}{c} \uparrow 6' \\ \downarrow 6 \end{array} \\ \in \mathcal{H}_{12j}. & & & & & \end{array} \quad (4.2.10)$$

In terms of the normalized $2j$ -states $|K_{ab}\rangle$ defined in Eq. 4.1.1 this state is the product of $\sqrt{2j_r + 1}|K_{rr'}\rangle$,

$$|ab_1\rangle = \prod_{r=1}^6 \sqrt{2j_r + 1} \left| \begin{array}{cc} \hat{I}_r & \hat{\mathbf{J}}_{rr'} \\ j_r & \mathbf{0} \end{array} \right\rangle \in \mathcal{H}_{12j}, \quad (4.2.11)$$

The $12j$ -model of the $6j$ -symbol is represented by spin network 4.2.7 and is formed from the inner product of the ab -state with the M -state,

$$\text{“12-Model”}: \langle ab_1|M_1\rangle = N_{12} \langle K_{11'} \cdots K_{66'} | W_{123} W_{1'5'6} W_{2'6'4} W_{3'4'5} \rangle, \quad (4.2.12)$$

where N_{12} is the prefactor $\prod_{r=1}^6 \sqrt{2j_r + 1}$.

The a - and b -states are found by splitting the product state spin network into two subnetworks. The a -state is an element of the target space \mathcal{H}_{8j} of the first remodel so its spin network is made of the subnetwork of Eq. 4.2.10 containing ket chevrons for primed and unprimed Schwinger spaces 1, 2, 4, and 5,

$$|a_1\rangle = \begin{array}{cccc} \begin{array}{c} \uparrow 1' \\ \downarrow 1 \end{array} & \begin{array}{c} \uparrow 2' \\ \downarrow 2 \end{array} & \begin{array}{c} \uparrow 4' \\ \downarrow 4 \end{array} & \begin{array}{c} \uparrow 5' \\ \downarrow 5 \end{array} \\ \in \mathcal{H}_{8j}, & & & \end{array} \quad (4.2.13)$$

which in Dirac notation is

$$|a_1\rangle = \prod_{r \in \{1,2,4,5\}} \sqrt{2j_r + 1} \left| \begin{array}{c} \hat{I}_r \quad \hat{\mathbf{J}}_{rr'} \\ j_r \quad \mathbf{0} \end{array} \right\rangle \in \mathcal{H}_{8j}. \quad (4.2.14)$$

The dual of the b -state is then the remaining pieces of the spin network,

$$|b_1\rangle = \begin{array}{c} \uparrow \quad \uparrow \\ 3' \quad 6' \\ | \\ 3 \quad 6 \\ \downarrow \quad \downarrow \end{array} \in \mathcal{H}_{33'66'}. \quad (4.2.15)$$

Thus the b -state is

$$\langle b_1| = \begin{array}{c} \diagup \quad \diagup \\ 3' \quad 6' \\ | \\ 3 \quad 6 \\ \diagdown \quad \diagdown \end{array} = \sqrt{2j_3 + 1} \sqrt{2j_6 + 1} \left\langle \begin{array}{cc|cc} I_3 & I_6 & \mathbf{J}_{33'} & \mathbf{J}_{66'} \\ j_3 & j_6 & \mathbf{0} & \mathbf{0} \end{array} \right| \in \mathcal{H}_{33'66'}^*. \quad (4.2.16)$$

The M -state in the first remodel acts as a map : $\mathcal{H}_{33'66'}^* \rightarrow \mathcal{H}_{8j}$. In particular, each of the four $3j$ -networks in Eq. 4.2.8 acts as a map from a dual Schwinger Hilbert space to a tensor product of two Schwinger Hilbert spaces as in Eq. 3.1.2. Acting this map on the b -state of Eq. 4.2.16 yields the β -state,

$$|\beta_1\rangle = \begin{array}{c} \diagup \quad \diagup \quad \diagup \quad \diagup \\ 1 \quad 5 \\ | \quad | \\ 3 \quad 3 \\ | \quad | \\ 2 \quad 4' \\ \diagdown \quad \diagdown \quad \diagdown \quad \diagdown \end{array} \quad \begin{array}{c} \diagup \quad \diagup \\ 4 \quad 5' \\ | \quad | \\ 6 \quad 6 \\ \diagdown \quad \diagdown \\ 2' \quad 1' \\ \diagdown \quad \diagdown \end{array} \in \mathcal{H}_{8j}, \quad (4.2.17)$$

In terms of the normalized butterfly states defined by Eqs. 4.1.9 and 4.1.10 the β -state is

$$|\beta_1\rangle = \frac{(-1)^{2s+2j_4}}{\sqrt{2j_3 + 1} \sqrt{2j_6 + 1}} |B_{(12)4'5}, j_3\rangle |B_{1'(2'4)5'}, j_6\rangle, \quad (4.2.18)$$

where s is the semi-perimeter,

$$s \equiv \frac{1}{2}(j_1 + j_2 + j_4 + j_5). \quad (4.2.19)$$

By Eqs. 4.1.8 the β -state can therefore be expressed as the simultaneous eigenstate

$$|\beta_1\rangle = \frac{(-1)^{2s+2j_4}}{\sqrt{2j_3 + 1} \sqrt{2j_6 + 1}} \left| \begin{array}{cc|cc|cc} \hat{I}_r & \hat{I}_{r'} & \hat{\mathbf{J}}_{12}^2 & \hat{\mathbf{J}}_{2'4}^2 & \hat{\mathbf{J}}_{124'5} & \hat{\mathbf{J}}_{1'2'45'} \\ j_r & j_{r'} & j_3 & j_6 & \mathbf{0} & \mathbf{0} \end{array} \right\rangle, \quad (4.2.20)$$

where $r = 1, 2, 4, 5$ and the quantum number j for coupled operator $\hat{\mathbf{J}}_{ab}^2$ indicates an eigenvalue $j(j+1)$.

State	Space	Components	Group
$\langle b_1 $	$\mathcal{H}_{33'66'}$	2 Diangle Bras	$(U(1) \times SU(2))^2$
$ ab_1\rangle$	\mathcal{H}_{12j}	6 Diangle Kets	$(U(1) \times SU(2))^6$
$ M_1\rangle$	\mathcal{H}_{12j}	4 Triangle Kets	$(U(1)^3 \times SU(2))^4$
$ a_1\rangle$	\mathcal{H}_{8j}	4 Diangle Kets	$(U(1) \times SU(2))^4$
$ \beta_1\rangle$	\mathcal{H}_{8j}	2 Butterfly Kets	$(U(1)^5 \times SU(2))^2$

Table 4.2: States in the first remodeling algebra for the 6j-symbol.

The 8j-model of the 6j-symbol is represented by spin network 4.2.24 and is formed from the inner product of the a -state with the β -state,

$$\text{“8-Model”}: \langle a_1 | \beta_1 \rangle = N_8 \langle K_{11'} K_{22'} K_{44'} K_{55'} | B_{(12)4'5}, j_3; B_{1'(2'4)5'}, j_6 \rangle, \quad (4.2.21)$$

where N_8 is the prefactor

$$N_8 = (-1)^{2s+2j_4} \frac{\prod_{r=1}^6 \sqrt{2j_r + 1}}{(2j_3 + 1)(2j_6 + 1)}. \quad (4.2.22)$$

The states of the first remodel for the 6j-symbol are summarized in Table 4.2.

Note that the 12j-model allows the 6j-symbol to be expressed as a sum of 3j-symbols. By inserting a resolution of the identity in the standard angular momentum basis between each pair of chevrons in the 12j-model spin network 4.2.7 and using Eqs. 3.0.1 and 3.1.32, the 6j-symbol evaluates to

$$\left\{ \begin{array}{ccc} j_1 & j_2 & j_3 \\ j_4 & j_5 & j_6 \end{array} \right\} = \sum_{m_r} (-1)^{\sum_r j_r - m_r} \begin{pmatrix} j_1 & j_2 & j_3 \\ m_1 & m_2 & m_3 \end{pmatrix} \begin{pmatrix} j_1 & j_5 & j_6 \\ -m_1 & -m_5 & m_6 \end{pmatrix} \\ \begin{pmatrix} j_2 & j_6 & j_4 \\ -m_2 & -m_6 & m_4 \end{pmatrix} \begin{pmatrix} j_3 & j_4 & j_5 \\ -m_3 & -m_4 & m_5 \end{pmatrix}. \quad (4.2.23)$$

Apart from differences in phase conventions which all cancel out in the end, this formula is the same as Eq. (6.2.3) of Edmonds [28].

4.2.3 The Second Remodeling Algebra

Construction of the second remodeling algebra starts with the spin network for the 8j-target space model of the first remodel from Section 4.2.2, which pairs the dual of the a -state with

the β -state of the first remodel,

$$\left\{ \begin{array}{ccc} j_1 & j_2 & j_3 \\ j_4 & j_5 & j_6 \end{array} \right\} = \text{Diagram} \quad (4.2.24)$$

The network can then be separated into two $2j$ -intertwiner networks and four $2j$ -intertwiner networks. These are then separated into three sets which act as the b -, M -, and dual of the a -state for the second remodel. We choose to take the four $2j$ -intertwiners as the map for this remodel,

$$\langle M_2 | = \begin{array}{cccc} \begin{array}{c} \diagup \diagdown \\ | \\ \diagdown \diagup \end{array} & \begin{array}{c} \diagup \diagdown \\ | \\ \diagdown \diagup \end{array} & \begin{array}{c} \diagup \diagdown \\ | \\ \diagdown \diagup \end{array} & \begin{array}{c} \diagup \diagdown \\ | \\ \diagdown \diagup \end{array} \\ 1' & 2' & 4' & 5' \\ | & | & | & | \\ 1 & 2 & 4 & 5 \end{array} \in \mathcal{H}_{8j}^*, \quad (4.2.25)$$

where the ‘2’ subscript in $\langle M_2 |$ is used to highlight that this is the map state of the *second* remodel. The subnetwork containing the $2j$ -intertwiners ends in eight bra chevrons, which is why we need to take the dual of the $8j$ -Hilbert space as the product space in the second remodel. In particular, we treat $\langle M_2 |$ as a map : $\mathcal{H}_{1'2'4'5'} \rightarrow \mathcal{H}_{124'5}^*$. Note that the map state for the second remodel is the dual of the a -state of the first remodel,

$$\langle M_2 | = (|a_1\rangle)^\dagger = \prod_{r \in \{1,2,4,5\}} \sqrt{2j_r + 1} \langle K_{rr'} |. \quad (4.2.26)$$

The remaining pieces of the spin network form the dual of the product state,

$$\langle ab_2 | = \text{Diagram} \in \mathcal{H}_{8j}^*, \quad (4.2.27)$$

This is just the dual of the β -state of the first remodel,

$$\langle ab_2 | = (|\beta_1\rangle)^\dagger = \frac{(-1)^{2s+2j_4}}{\sqrt{2j_3+1}\sqrt{2j_6+1}} \langle B_{(12)4'5}, j_3 | \langle B_{1'(2'4)5'}, j_6 |. \quad (4.2.28)$$

The product space model of the second remodel is the ‘dual model’ of the target space model of the first remodel. We define dual models in the following manner. First consider a general setting, with \mathcal{H} a Hilbert space of kets. The inner product $\langle A|B \rangle$ in this space may be expressed as

$$\langle A|B \rangle = \text{tr}((|A\rangle)^\dagger |B\rangle) = \text{tr}((\langle B|)^\dagger \langle A|). \quad (4.2.29)$$

These forms of the inner product emphasize which Hilbert space the inner product takes place in. The first expression for $\langle A|B\rangle$ shows the inner product in \mathcal{H} of $|A\rangle$ with $|B\rangle$. The second expression shows the “dual model,” which is the inner product of $\langle B|$ with $\langle A|$ in the dual Hilbert space of bras \mathcal{H}^* . It is important to recognize that forming the dual model is *not* the same as forming the Hermitian conjugate of the original model, which would be an inner product $\langle B|A\rangle$.

The product space model in the second remodel is represented by spin network 4.2.24 and is formed from the inner product of the ab -state with the M -state. Since this model takes place in \mathcal{H}_{8j}^* we call it the “dual $8j$ -model” of the $6j$ -symbol,

$$\text{“Dual } 8j\text{-Model”}: \text{tr}(\langle ab_2|)^\dagger \langle M_2|) = \langle M_2|ab_2\rangle = \langle a_1|\beta_1\rangle, \quad (4.2.30)$$

where the first expression is presented in a form that emphasizes that it is an inner product in \mathcal{H}_{8j}^* . The second and third expressions show that the dual $8j$ -model is indeed equal to the dual inner product model of the $8j$ -model of Eq. 4.2.21.

The a -state is an element of the second remodel target space $\mathcal{H}_{124'5}^*$ so its spin network is made of the subnetwork of Eq. 4.2.27 containing bra chevrons for Schwinger spaces 1, 2, 4', and 5,

$$\langle a_2| = \begin{array}{c} \text{---} \\ \diagup \quad \diagdown \\ \bullet \quad \quad \bullet \\ \diagdown \quad \diagup \\ \text{---} \end{array} \begin{array}{c} 1 \quad 5 \\ | \quad | \\ 3 \\ | \\ 4' \end{array} \in \mathcal{H}_{124'5}^*, \quad (4.2.31)$$

while the dual of the b -state is the remaining $4j$ -intertwiner network and thus the b -state is

$$|b_2\rangle = \begin{array}{c} \diagdown \quad \diagup \\ \bullet \quad \quad \bullet \\ \diagup \quad \diagdown \\ \text{---} \end{array} \begin{array}{c} 4 \quad 5' \\ | \quad | \\ 6 \\ | \\ 2' \quad 1' \end{array} \in \mathcal{H}_{1'2'4'5'}. \quad (4.2.32)$$

In terms of the normalized butterfly states defined by Eqs. 4.1.9 and 4.1.10 the a - and b -states are

$$\langle a_2| = \frac{(-1)^{-j_1+j_2+j_4-j_5}}{\sqrt{2j_3+1}} \langle B_{(12)4'5}, j_3|, \quad (4.2.33)$$

$$|b_2\rangle = \frac{(-1)^{2j_2}}{\sqrt{2j_6+1}} |B_{1'(2'4)5'}, j_6\rangle, \quad (4.2.34)$$

The β -state is formed by attaching the four $2j$ -nodes to the b -state of Eq. 4.2.32. Following the rules for converting kets into bras established in Aquilanti *et al* [1], the β state is

$$\langle \beta_2 | = (-1)^{2j_4} \begin{array}{c} \text{---} 4' \text{---} \\ \diagdown \quad \diagup \\ \bullet \quad \bullet \\ \diagup \quad \diagdown \\ \text{---} 2' \text{---} \end{array} \begin{array}{c} \text{---} 5' \text{---} \\ \diagdown \quad \diagup \\ \bullet \quad \bullet \\ \diagup \quad \diagdown \\ \text{---} 1' \text{---} \end{array} \begin{array}{c} \text{---} 6 \text{---} \\ \diagdown \quad \diagup \\ \bullet \quad \bullet \\ \diagup \quad \diagdown \\ \text{---} 1 \text{---} \end{array} = (-1)^{2j_4} \begin{array}{c} \text{---} 4' \text{---} \\ \diagdown \quad \diagup \\ \bullet \quad \bullet \\ \diagup \quad \diagdown \\ \text{---} 2 \text{---} \end{array} \begin{array}{c} \text{---} 5 \text{---} \\ \diagdown \quad \diagup \\ \bullet \quad \bullet \\ \diagup \quad \diagdown \\ \text{---} 1 \text{---} \end{array} \begin{array}{c} \text{---} 6 \text{---} \\ \diagdown \quad \diagup \\ \bullet \quad \bullet \\ \diagup \quad \diagdown \\ \text{---} 1 \text{---} \end{array} \in \mathcal{H}_{1'2'45'}, \quad (4.2.35)$$

where the phase of $(-1)^{2j_4}$ is used to invert the orientation of the stub for the $2j$ -intertwiner $: \mathcal{S}_4 \rightarrow \mathcal{S}_{4'}^*$ in Eq. 4.2.25. Thus the β -state is

$$\langle \beta_2 | = \frac{(-1)^{2j_2+2j_4}}{\sqrt{2j_6+1}} |B_{1(24')5}, j_6\rangle \in \mathcal{H}_{124'5}. \quad (4.2.36)$$

The target space model in the second remodel is formed from the inner product of the a - and β -states,

$$\left\{ \begin{array}{ccc} j_1 & j_2 & j_3 \\ j_4 & j_5 & j_6 \end{array} \right\} = (-1)^{2j_4} \begin{array}{c} \bullet \\ \diagdown \quad \diagup \\ \text{---} 6 \text{---} \\ \diagdown \quad \diagup \\ \bullet \quad \bullet \\ \diagup \quad \diagdown \\ \text{---} 1 \text{---} \\ \diagdown \quad \diagup \\ \bullet \quad \bullet \\ \diagup \quad \diagdown \\ \text{---} 2 \text{---} \\ \diagdown \quad \diagup \\ \bullet \quad \bullet \\ \diagup \quad \diagdown \\ \text{---} 3 \text{---} \\ \diagdown \quad \diagup \\ \bullet \quad \bullet \\ \diagup \quad \diagdown \\ \text{---} 4' \text{---} \\ \diagdown \quad \diagup \\ \bullet \quad \bullet \\ \diagup \quad \diagdown \\ \text{---} 5 \text{---} \\ \diagdown \quad \diagup \\ \bullet \quad \bullet \\ \diagup \quad \diagdown \\ \text{---} \end{array} \cdot \quad (4.2.37)$$

Since this model is interpreted as an inner product between states in the dual space $\mathcal{H}_{124'5}$ we call it the “dual $4j$ -model,”

$$\text{“Dual } 4j\text{-Model”}: \text{tr} ((a_2|)^\dagger \langle \beta_2 |) = N_4 \langle B_{1(24')5}, j_6 | B_{(12)4'5}, j_3 \rangle, \quad (4.2.38)$$

where N_4 is the prefactor

$$N_4 = (-1)^{2s} \frac{1}{\sqrt{2j_3+1} \sqrt{2j_6+1}}. \quad (4.2.39)$$

The dual inner product model of the dual $4j$ -model is the standard $4j$ -model treated, for example, in Aquilanti *et al* [1].

The states of the second remodel of the $6j$ -symbol are summarized in Table 4.3 and the various inner product models of the $6j$ -symbol are presented in Table 4.4.

4.3 Remodeling Geometries of the $6j$ -Symbol

In this section we construct the remodeling geometries for the two inner product remodelings of the $6j$ -symbol. First in Section 4.3.1 we set up the phase spaces and Lagrangian manifolds that occur in the remodeling geometries and then in Section 4.3.2 show how the transport procedure is used to create the butterfly manifolds of the $8j$ - and $4j$ -models. With the remodeling geometries set up, in Section 4.3.3 we describe the stationary phase sets which

State	Space	Components	Group
$ b_2\rangle$	$\mathcal{H}_{1'2'45'}$	1 Butterfly Ket	$U(1)^5 \times SU(2)$
$\langle ab_2 $	\mathcal{H}_{8j}^*	2 Butterfly Bras	$(U(1)^5 \times SU(2))^2$
$\langle M_2 $	\mathcal{H}_{8j}^*	4 Diangle Bras	$(U(1) \times SU(2))^4$
$\langle a_2 $	$\mathcal{H}_{124'5}^*$	1 Butterfly Bra	$U(1)^5 \times SU(2)$
$\langle \beta_2 $	$\mathcal{H}_{124'5}^*$	1 Butterfly Bra	$U(1)^5 \times SU(2)$

Table 4.3: States in the second remodeling algebra for the 6j-symbol.

Name	Space	Remodel	Interpretation	Inner Product
12j-Model	\mathcal{H}_{12j}	First	Product Space Model	$\langle ab_1 M_1\rangle$
8j-Model	\mathcal{H}_{8j}	First	Target Space Model	$\langle a_1 \beta_1\rangle$
Dual 8j-Model	\mathcal{H}_{8j}^*	First	Dual Target Space Model	$\text{tr}((\langle\beta_1)^\dagger\langle a_1)$
		Second	Product Space Model	$\text{tr}((\langle ab_2)^\dagger\langle M_2)$
Dual 4j-Model	$\mathcal{H}_{124'5}^*$	Second	Target Space Model	$\text{tr}((\langle a_2)^\dagger\langle\beta_2)$
4j-Model	$\mathcal{H}_{124'5}$	Second	Dual Target Space Model	$\langle\beta_2 a_2\rangle$

Table 4.4: Summary of the inner product models of the 6j-symbol.

will be needed for the stationary phase approximation of the various inner product models. Finally, in Section 4.3.4 a symplectic reduction is carried out in the 4j-model to create the one-degree-of-freedom phase space on which the amplitude determinant is most easily computed.

4.3.1 Phase Spaces and Lagrangian Manifolds

As in Section 3.2.1, each of the Hilbert spaces \mathcal{S} in the remodeling algebra corresponds semiclassically to a copy of the Schwinger phase space Σ and thus the phase spaces in the remodeling geometries for the 6j-symbol are products of Schwinger phase spaces or their duals. The product, source, and target phase spaces for the first remodel are labeled Φ_{12j} , $\Phi_{33'66'}^*$, and Φ_{8j} , respectively while the product, source, and target phase spaces for the second remodel are labeled Φ_{8j}^* , $\Phi_{1'2'45'}$, and $\Phi_{124'5}^*$. The dual map $G_{8j} : \Phi_{8j} \rightarrow \Phi_{8j}^*$ is used to map the Lagrangian manifolds for the 8j-model of the first remodel to the relevant manifolds of the dual 8j-model of the second remodel. Similarly, we introduce the 4j-phase space $\Phi_{124'5}$ and the dual map $G_{4j}^{-1} : \Phi_{124'5}^* \rightarrow \Phi_{124'5}$ to map the manifolds from the dual 4j-model of the second remodel to the manifolds described in the standard 4j-model of Aquilanti *et al* [1].

Figure 4.3.1 shows the phase spaces in the two remodeling geometries and the relevant maps between these spaces. Subscripts on the two dual maps G^{-1} and G' between the source and dual source phase spaces of the first and second remodels, respectively, have been omitted because they are bulky and we will not be using these maps extensively in the rest of this chapter. Table 4.5 lists the phase spaces, their roles in the remodeling geometries,

$$\begin{array}{ccccccc}
 \Phi_{124'5} & \xleftarrow{G_{4j}^{-1}} & \Phi_{124'5}^* & \xleftarrow{\pi_{4j}} & \Phi_{8j}^* & \xleftarrow{G_{8j}} & \Phi_{8j} & \xleftarrow{\pi_{8j}} & \Phi_{12j} \\
 & & & & \downarrow \pi_{1'2'45'} & & & & \downarrow \pi_{33'66'} \\
 & & & & \Phi_{1'2'45'}^* & \xleftarrow{G'} & \Phi_{1'2'45'} & & \Phi_{33'66'} & \xleftarrow{G^{-1}} & \Phi_{33'66'}^*
 \end{array}$$

Figure 4.3.1: Phase spaces and the maps between them in the remodeling geometries for the $6j$ -symbol.

	First Remodel		Second Remodel	
Name	Phase Space	Dimension	Phase Space	Dimension
Source Space	$\Phi_{33'66'}^*$	16	$\Phi_{1'2'45'}$	16
Dual Source Space	$\Phi_{33'66'}$	16	$\Phi_{1'2'45'}^*$	16
Target Space	Φ_{8j}	32	$\Phi_{124'5}^*$	16
Product Space	Φ_{12j}	48	Φ_{8j}^*	32

Table 4.5: Phase spaces in the remodeling geometries for the $6j$ -symbol.

and their dimensions.

Each of the states in the remodeling algebras for the $6j$ -symbol are tensor products of diangle, triangle, and butterfly states and thus the Lagrangian manifolds that support the semiclassical approximations of these states are simply Cartesian products of the diangle, triangle, and butterfly manifolds described in Section 4.1.

For example, the a -manifold in the first remodel algebra is the product of four diangle manifolds since $|a_1\rangle$ is proportional to the tensor product of four diangle states,

$$\mathcal{L}_{a,1} = \mathcal{L}_{K1} \times \mathcal{L}_{K2} \times \mathcal{L}_{K4} \times \mathcal{L}_{K5}, \quad (4.3.1)$$

where \mathcal{L}_{K_r} is the submanifold of the $2j$ -phase space $\Sigma_r \times \Sigma_{r'}$ defined by the level set conditions in Eq. 4.1.3 and whose topology and volume is given by Eq. 4.1.4. The rest of the states from Sections 4.2.2 and 4.2.3 are translated in a similar manner, with the properties of the triangle manifolds described by Eqs. 3.2.7 and 3.2.8 and the properties of the butterfly manifolds described by Eqs. 4.1.11, 4.1.13, and 4.1.14.

Table 4.6 summarizes the Lagrangian manifolds that occur in the remodeling geometries of the $6j$ -symbol.

4.3.2 Transporting Manifolds

Now we briefly demonstrate how the transport procedure of Section 2.2.2 applies in the two remodel geometries. Rather than use the full machinery of Section 2.4 we will be able to illustrate the transport using an intuitive analysis of the level sets involved.

In the first remodel geometry, the two-diangle manifold $\mathcal{L}_{b,1}$ is transported through the four-triangle manifold $\mathcal{L}_{M,1}$ to become the two-butterfly manifold $\mathcal{L}_{\beta,1}$. The inverse image

Manifold	Phase Space	Momentum Map Components	Topology	Volume
$\mathcal{L}_{b,1}$	$\Phi_{33'66'}^*$	$I_r, \mathbf{J}_{rr'} \ r = 3, 6$	$(\mathcal{L}_K)^2$	$2^{12}\pi^6$
$\mathcal{L}_{M,1}$	Φ_{12j}	$I_1 \cdots I_6$ $I_{1'} \cdots I_{6'}$ $\mathbf{J}_{123}, \mathbf{J}_{1'5'6}, \mathbf{J}_{2'6'4}, \mathbf{J}_{3'4'5}$	$(\mathcal{L}_W)^4$	$2^{36}\pi^{20}$
$\mathcal{L}_{ab,1}$	Φ_{12j}	$I_r, \mathbf{J}_{rr'} \ r = 1 \cdots 6$	$(\mathcal{L}_K)^6$	$2^{36}\pi^{18}$
$\mathcal{L}_{a,1}$	Φ_{8j}	$I_r, \mathbf{J}_{rr'} \ r = 1, 2, 4, 5$	$(\mathcal{L}_K)^4$	$2^{24}\pi^{12}$
$\mathcal{L}_{M,2}$	Φ_{8j}^*			
$\mathcal{L}_{\beta,1}$	Φ_{8j}	I_1, I_2, I_4, I_5 $I_{1'}, I_{2'}, I_{4'}, I_{5'}$ $ \mathbf{J}_{12} , \mathbf{J}_{2'4} , \mathbf{J}_{124'5}, \mathbf{J}_{1'2'45'}$	$(\mathcal{L}_B)^2$	$2^{24}\pi^{14}$
$\mathcal{L}_{ab,2}$	Φ_{8j}^*			
$\mathcal{L}_{b,2}$	$\Phi_{1'2'45'}$	$I_{1'}, I_{2'}, I_4, I_{5'}, \mathbf{J}_{2'4} , \mathbf{J}_{1'2'45'}$	\mathcal{L}_B	$2^{12}\pi^7$
$\mathcal{L}_{a,2}$	$\Phi_{124'5}^*$	$I_1, I_2, I_{4'}, I_5, \mathbf{J}_{12} , \mathbf{J}_{124'5}$	\mathcal{L}_B	$2^{12}\pi^7$
$\mathcal{L}_{\beta,2}$	$\Phi_{124'5}^*$	$I_1, I_2, I_{4'}, I_5, \mathbf{J}_{24'} , \mathbf{J}_{124'5}$	\mathcal{L}_B	$2^{12}\pi^7$

Table 4.6: Topologies and volumes of the Lagrangian manifolds that occur in the remodeling geometries of the 6j-symbol.

$\pi_{33'66'}^{-1}(\mathcal{L}_{\bar{b},1})$ is a co-dimension 8 co-isotropic manifold in the 12j-phase space,

$$\pi_{33'66'}^{-1}(\mathcal{L}_{\bar{b},1}) = \left(\begin{array}{cccc} I_3 & I_6 & \mathbf{J}_{33'} & \mathbf{J}_{66'} \\ J_3 & J_6 & \mathbf{0} & \mathbf{0} \end{array} \right) \subset \Phi_{12j}. \quad (4.3.2)$$

Recall that this pair of diangle conditions also implies the condition $I_{3'} = J_3$ and $I_{6'} = J_6$ on the manifold. The intersection of this inverse image shares a $U(1)^4$ symmetry group with the M -manifold $\mathcal{L}_{M,1}$, generated by momentum map components $I_3, I_{3'}, I_6,$ and $I_{6'}$. Therefore the intersection manifold $\mathcal{I}_1 \equiv \pi_{33'66'}^{-1}(\mathcal{L}_{\bar{b},1}) \cap \mathcal{L}_{M,1}$ has co-dimension $24 + 8 - 4 = 28$ and dimension $48 - 28 = 20$. The group orbits of this symmetry group are purely vertical over Φ_{8j} so the projection onto the target space will be 16-dimensional, as expected. The intersection may be written as the level set

$$\mathcal{I}_1 = \left(\begin{array}{ccccccccc} I_r & I_{r'} & \mathbf{J}_{33'} & \mathbf{J}_{66'} & \mathbf{J}_{123} & \mathbf{J}_{1'5'6} & \mathbf{J}_{2'6'4} & \mathbf{J}_{3'4'5} \\ J_r & J_{r'} & \mathbf{0} & \mathbf{0} & \mathbf{0} & \mathbf{0} & \mathbf{0} & \mathbf{0} \end{array} \right) \subset \Phi_{12j}, \quad (4.3.3)$$

where $r = 1, \dots, 6$. Note that the 30 conditions in Eq. 4.3.3 are not all independent. Since the transported manifold will be 16-dimensional we need to construct sixteen level set conditions in this list that only depend on the target space variables. The eight conditions for I_r and $I_{r'}$ for $r = 1, 2, 4, 5$ make up half of this set. Next consider the combination $\mathbf{J}_{124'5}$. This may be expressed in terms of the functions in Eq. 4.3.3 as $\mathbf{J}_{123} - \mathbf{J}_{33'} + \mathbf{J}_{3'4'5}$ and is thus $\mathbf{0}$ on \mathcal{I}_∞ . Similarly, $\mathbf{J}_{1'2'45'} = \mathbf{J}_{1'5'6} - \mathbf{J}_{66'} + \mathbf{J}_{2'6'4} = \mathbf{0}$. Finally, as in Section 3.2.3, conditions $\mathbf{J}_{123} = \mathbf{0}$ and $I_3 = J_3$ imply the condition $\mathbf{J}_{12}^2 = J_3^2$ and thus $|\mathbf{J}_{12}| = J_3$ and $\mathbf{J}_{2'6'4} = \mathbf{0}$ and $I_6 = J_6$ similarly implies $|\mathbf{J}_{2'4}| = J_6$. Therefore the projection of \mathcal{I}_{12} by π_{8j} is the level set

$$\mathcal{T}_{M,1}(\mathcal{L}_{b,1}) = \left(\begin{array}{cccccc} I_r & I_{r'} & |\mathbf{J}_{12}| & |\mathbf{J}_{2'4}| & \mathbf{J}_{124'5} & \mathbf{J}_{1'2'45'} \\ J_r & J_{r'} & J_3 & J_6 & \mathbf{0} & \mathbf{0} \end{array} \right) \subset \Phi_{8j}. \quad (4.3.4)$$

for $r = 1, 2, 4, 5$. Comparing Eq. 4.3.4 with Eqs. 4.1.11 and 4.1.13 shows

$$\mathcal{T}_{M,1}(\mathcal{L}_{b,1}) \cong \mathcal{L}_{B,12} \times \mathcal{L}_{B,2'4} \cong \mathcal{L}_{\beta,1}, \quad (4.3.5)$$

where $\mathcal{L}_{B,12}$ is the “ab”-coupled butterfly manifold of $\Phi_{124'5}$ and $\mathcal{L}_{B,2'4}$ is the “bc”-coupled butterfly manifold of $\Phi_{1'2'45'}$.

In the second remodel geometry, the butterfly manifold $\mathcal{L}_{b,2}$ is transported through the four-diangle M -manifold to become the butterfly manifold $\mathcal{L}_{\beta,2}$. The inverse image $\pi_{1'2'45'}^{-1}(\mathcal{L}_{\bar{b},2})$ is a co-dimension 8 co-isotropic manifold in the dual $8j$ -phase space,

$$\pi_{1'2'45'}^{-1}(\mathcal{L}_{\bar{b},2}) = \left(\begin{array}{cccc|c|c} I_{1'} & I_{2'} & I_4 & I_{5'} & |\mathbf{J}_{2'4}| & \mathbf{J}_{1'2'45'} \\ J_1 & J_2 & J_4 & J_5 & J_6 & \mathbf{0} \end{array} \right) \subset \Phi_{8j}^*. \quad (4.3.6)$$

This inverse image shares a $U(1)^4$ symmetry group with the M -manifold $\mathcal{L}_{M,2}$, generated by momentum map components $I_{1'}$, $I_{2'}$, I_4 , and $I_{5'}$ and thus the intersection manifold \mathcal{I}_2 between the inverse image and the map manifold has co-dimension $16 + 8 - 4 = 20$ and dimension $32 - 20 = 12$. The group orbits of this symmetry group are purely vertical over $\Phi_{124'5}^*$ so the projection onto the target space will be 8-dimensional, as expected. The intersection may be written as the level set

$$\mathcal{I}_2 = \left(\begin{array}{ccc|c|c} I_r & I_{r'} & |\mathbf{J}_{2'4}| & \mathbf{J}_{rr'} & \mathbf{J}_{1'2'45'} \\ J_r & J_r & J_6 & \mathbf{0} & \mathbf{0} \end{array} \right) \subset \Phi_{8j}^*, \quad (4.3.7)$$

where $r = 1, 2, 4, 5$. The four conditions on I_1 , I_2 , $I_{4'}$, and I_5 only depend on target-space variables and thus apply to the transported manifold. The conditions $\mathbf{J}_{rr'} = \mathbf{0}$ can be used to exchange \mathbf{J}_r with $-\mathbf{J}_{r'}$ in functions $|\mathbf{J}_{2'4}|$ and $\mathbf{J}_{1'2'45'}$ and thus the projection of \mathcal{I}_2 by $\pi_{124'5}$ is the level set

$$\mathcal{T}_{M,2}(\mathcal{L}_{b,2}) = \left(\begin{array}{cccc|c|c} I_1 & I_2 & I_{4'} & I_5 & |\mathbf{J}_{24'}| & \mathbf{J}_{124'5} \\ J_1 & J_2 & J_4 & J_5 & J_6 & \mathbf{0} \end{array} \right) \subset \Phi_{124'5}^*, \quad (4.3.8)$$

which is precisely $\mathcal{L}_{\beta,2}$, the “bc”-coupled butterfly manifold of $\Phi_{124'5}^*$.

4.3.3 Stationary Phase Sets

Now we construct the stationary phase sets for the $12j$ - and $4j$ -models of the $6j$ -symbol. We fix the six values $J_r > 0$ and treat all other variables as continuous. We also assume that the parameters are in the classically allowed region which implies that at least one real intersection point exists and that the polygon inequalities from Section 4.1.3 hold.

The stationary phase set $I^{(12j)}$ for the $12j$ -model is the intersection $\mathcal{L}_{ab,1} \cap \mathcal{L}_{M,1}$ and is comprised of group orbits of the common symmetry group G_{12} shared by the groups that generate $\mathcal{L}_{ab,1}$ and $\mathcal{L}_{M,1}$. As in Table 4.2, the product manifold is generated by the group $(U(1) \times SU(2))^6$ and the map manifold is generated by the group $(U(1)^3 \times SU(2))^4$. The common symmetry group is $U(1)^{12} \times SU(2)$, a 15-dimensional group generated by the

functions I_r , $I_{r'}$, and $\mathbf{J}_{T,12} \equiv \sum_r \mathbf{J}_r + \mathbf{J}_{r'}$, with $r = 1, \dots, 6$. Symplectic reduction by this group yields the 18-dimensional phase space on which Roberts [2] computed a 9×9 -amplitude determinant in his analysis of the $6j$ -symbol. In this work we are only going to use the $12j$ -model to find the action integral piece of the phase and so we are not concerned with this symplectic reduction.

Combining the level set conditions for $\mathcal{L}_{ab,1}$ and $\mathcal{L}_{M,1}$ yields a set of level set conditions for $I^{(12j)}$,

$$I^{(12j)} = \left(\begin{array}{cccccc} I_r & I_{r'} & \mathbf{J}_{rr'} & \mathbf{J}_{123} & \mathbf{J}_{1'5'6} & \mathbf{J}_{2'6'4} & \mathbf{J}_{3'4'5} \\ J_r & J_r & \mathbf{0} & \mathbf{0} & \mathbf{0} & \mathbf{0} & \mathbf{0} \end{array} \right) \subset \Phi_{12j}, \quad (4.3.9)$$

with $r = 1, \dots, 6$. In the $12j$ -angular momentum space Λ_{12j} this is interpreted as the set of twelve angular momentum vectors such that ordered triplets 123, 1'5'6, 2'6'4, and 3'4'5 may be placed end-to-end to form triangles *and* such that each of the six pairs of primed and unprimed vectors are equal and opposite (they form diangles). The diangle conditions may be interpreted as 'gluing' the primed and unprimed edges of two triangles together. Each of the six diangles glues a pair of edges together so that the four triangles and six diangles are the four faces and six edges of a tetrahedron, as shown in Figure 4.3.2. The diangle and triangle conditions are invariant under $O(3)$ transformations. An explicit method for constructing a tetrahedron from six known edge lengths which uses the singular value decomposition of a Gram matrix was given in Appendix A of Littlejohn and Yu [76]. This method shows that any constructible tetrahedron is *unique* (up to $O(3)$ transformations) and therefore we may conclude that $I^{(12j)}$ projected to angular momentum space consists of a single $O(3)$ group orbit. This orbit may be decomposed into two $SO(3)$ group orbits related by time-reversal ($\mathbf{J} \mapsto -\mathbf{J}$). Unless the constructed tetrahedron is flat (in which case the volume of the tetrahedron is zero) these two $SO(3)$ group orbits are disjoint (no proper rotation will map a tetrahedron to its time-reversed image). We label the two disconnected $SO(3)$ group orbits in angular momentum space $\text{Tet}_{12\pm}$, where the sign specifies the sign of the tetrahedron's oriented volume, $V = \frac{1}{6} \mathbf{J}_1 \cdot (\mathbf{J}_2 \times \mathbf{J}_4)$.

The manifolds $I_{\pm}^{(12j)}$ are $U(1)^{12}$ bundles over $\text{Tet}_{12\pm}$ and are $U(1)^{12} \times SU(2)$ group orbits in Φ_{12j} . This group is precisely the common symmetry group G_{12} introduced earlier. The two manifolds $I_+^{(12j)}$ and $I_-^{(12j)}$ are related by time-reversal and their union is the $12j$ -model stationary phase set, $I^{(12j)} = I_+^{(12j)} \cup I_-^{(12j)}$. Let coordinates on G_{12} be $(\psi_r, \psi_{r'}, u)$, where $u \in SU(2)$. In these coordinates the isotropy subgroup on $I^{(12j)}$ consists of only one nontrivial element, $(2\pi, 2\pi, -1)$ and thus each of the two group orbits comprising the intersection manifold have the topology

$$I_{\pm}^{(12j)} \cong \frac{U(1)^{12} \times SU(2)}{\mathbb{Z}_2}. \quad (4.3.10)$$

If the lengths J_r are allowed to take on any value then situations may arise where the only constructible tetrahedra are flat ($V = 0$). In this case the tetrahedron *can* be transformed into the time-reversed tetrahedron by a proper rotation and the two disconnected pieces of $I^{(12j)}$ merge into a single group orbit. However, this never occurs when all six lengths are quantized and constrained so that all four of the triangle manifolds making up $\mathcal{L}_{M,1}$ exist

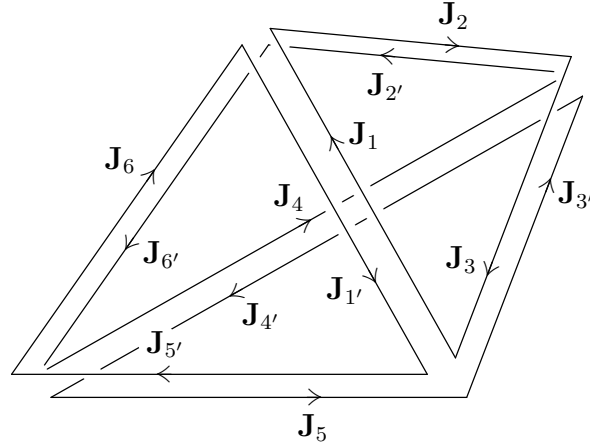


Figure 4.3.2: A point on the stationary phase set $I^{(12j)}$ projected onto a set of twelve vectors in \mathbb{R}^3 of lengths $|\mathbf{J}_r| = |\mathbf{J}_{r'}| = J_r$ ($r = 1, \dots, 6$). The vectors simultaneously obey the six diangle conditions $\mathbf{J}_{rr'} = \mathbf{0}$ and the four triangle conditions $\mathbf{J}_{123} = \mathbf{J}_{1'5'6} = \mathbf{J}_{2'6'4} = \mathbf{J}_{3'4'5} = \mathbf{0}$. Such a point defines a tetrahedron.

(which in part requires the sum of the three quantum numbers j for each triangle to be an integer) [1].

Now we briefly turn to the stationary phase set in the $8j$ -model, which is the intersection between the two manifolds $\mathcal{L}_{a,1}$ and $\mathcal{L}_{\beta,1}$ and, by the results of Section 2.5.1, the projection of $I^{(12j)}$ onto Φ_{8j} . In the $8j$ -angular momentum space Λ_{8j} this involves removing \mathbf{J}_3 , $\mathbf{J}_{3'}$, \mathbf{J}_6 , and $\mathbf{J}_{6'}$ as independent variables and instead expressing them in terms of the other eight angular momenta using the four triangle conditions in Eq. 4.3.9. We may consider the intersection points as places where the four diangles that make up $\mathcal{L}_{a,1}$ are used to glue together the four primed and unprimed pairs of vectors on the border of the two butterfly figures that make up $\mathcal{L}_{\beta,1}$, as shown in Figure 4.3.3.

Next we turn to the stationary phase set $I^{(4j)}$ for the $4j$ -model, which is the intersection $\mathcal{L}_{a,2} \cap \mathcal{L}_{\beta,2}$. This may also be considered the projection of $I^{(8j)}$ in the dual $8j$ -model onto $\Phi_{124'5}$. It is comprised of group orbits of the common symmetry group G_4 shared by the groups that generate $\mathcal{L}_{a,2}$ and $\mathcal{L}_{\beta,2}$. As in Table 4.3, both a - and β -manifolds are generated by the group $U(1)^5 \times SU(2)$. Of the eight independent level set conditions that are needed to specify a Lagrangian manifold in $\Phi_{124'5}$, $\mathcal{L}_{a,2}$ and $\mathcal{L}_{\beta,2}$ share seven, specifying the contour values of I_1 , I_2 , $I_{4'}$, I_5 , and $\mathbf{J}_{124'5}$. These momentum map components generate the common symmetry group $G_4 = U(1)^4 \times SU(2)$. Symplectic reduction by this group yields the 2-dimensional phase space Φ_{4j}^R on which Aquilanti *et al* [1] computed the single Poisson bracket necessary for the amplitude determinant in their analysis of the $6j$ -symbol.

Combining the level set conditions for $\mathcal{L}_{a,2}$ and $\mathcal{L}_{\beta,2}$ yields a set of nine independent level set conditions for $I^{(12j)}$,

$$I^{(4j)} = \left(\begin{array}{cccccc|cc} I_1 & I_2 & I_{4'} & I_5 & \mathbf{J}_{124'5} & |\mathbf{J}_{12}| & |\mathbf{J}_{24'}| \\ J_1 & J_2 & J_4 & J_5 & \mathbf{0} & J_3 & J_6 \end{array} \right) \subset \Phi_{4j}, \quad (4.3.11)$$

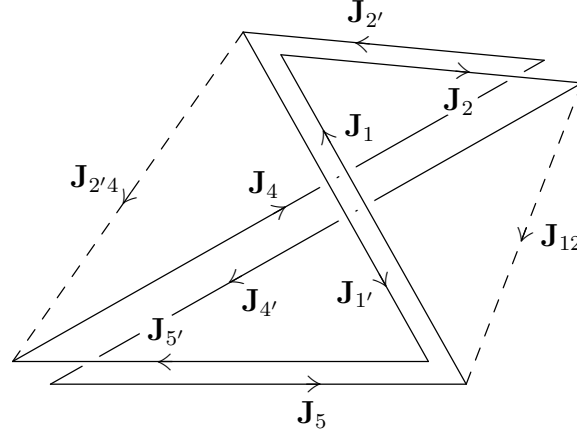


Figure 4.3.3: A point on the stationary phase set $I^{(8j)}$ projected onto a set of eight vectors in \mathbb{R}^3 of lengths $|\mathbf{J}_r| = |\mathbf{J}_{r'}| = J_r$ ($r = 1, 2, 4, 5$). The vectors simultaneously obey the four diangle conditions $\mathbf{J}_{rr'} = \mathbf{0}$ for $r = 1, 2, 4, 5$ and two sets of butterfly conditions, $\mathbf{J}_{124'5} = \mathbf{J}_{1'2'45'} = \mathbf{0}$, $|\mathbf{J}_{12}| = J_3$, $|\mathbf{J}_{2'4}| = J_6$. Such a point defines a tetrahedron.

In the $4j$ -angular momentum space Λ_{4j} this is interpreted as the set of four angular momentum vectors $\mathbf{J}_1, \mathbf{J}_2, \mathbf{J}_{4'}$, and \mathbf{J}_5 of fixed lengths that close when put tip-to-tail and such that in intermediate couplings \mathbf{J}_{12} and $\mathbf{J}_{24'}$ also have fixed lengths. We may again interpret such geometric figures as tetrahedra and, as in the $12j$ -model, the projection of the stationary phase set onto Λ_{4j} yields a pair of $SO(3)$ group orbits $\text{Tet}_{4\pm}$ that are related by time-reversal. The two orbits are labeled by the sign of the oriented volume $V = \frac{1}{6} \mathbf{J}_1 \cdot (\mathbf{J}_2 \times \mathbf{J}_{4'})$.

The manifolds $I_{\pm}^{(4j)}$ are $U(1)^4$ bundles over $\text{Tet}_{4\pm}$ and are $G_4 = U(1)^4 \times SU(2)$ group orbits in Φ_{12j} . The $4j$ -model stationary phase set $I^{(4j)}$ is the union of $I_{+}^{(4j)}$ and its time-reversed image, $I_{-}^{(4j)}$. Let coordinates on G_4 be $(\psi_1, \psi_2, \psi_{4'}, \psi_5, u)$, where $u \in SU(2)$. In these coordinates the isotropy subgroup on $I^{(12j)}$ consists of a single nontrivial element, $(2\pi, 2\pi, 2\pi, 2\pi, -1)$ and thus each of the two connected pieces of the intersection manifold has the topology and volume

$$I_{\pm}^{(4j)} \cong \frac{U(1)^4 \times SU(2)}{\mathbb{Z}_2}, \quad V_{\pm} = \frac{1}{2} (4\pi)^4 (16\pi^2) = 2^{11} \pi^6. \quad (4.3.12)$$

4.3.4 Reduction of the $4j$ -Model

Finally, we consider the symplectic reduction of $\Phi_{12'45}$ by the common symmetry group G_4 to create the reduced $4j$ -phase space Φ_{4j}^R . This phase space is where the amplitude determinant and Maslov index for the $6j$ -symbol will be computed. The reduced space and the features of the reduced $4j$ -model were derived and discussed in Aquilanti *et al* [1].

As usual we perform the symplectic reduction in stages. First we reduce by the $U(1)^4$ subgroup generated by $I_1, I_2, I_{4'}$, and I_5 to get the manifold $(S^2)^4$, the symplectic leaf in the $4j$ -angular momentum space Λ_{4j} obtained by fixing the lengths of all four angular momentum

vectors. The remaining $SU(2)$ symmetry projects to an $SO(3)$ symmetry on this reduced space and so next we reduce by the $SO(3)$ symmetry generated by $\mathbf{J}_{124'5}$ at the fixed point value $\mathbf{0}$.

The first stage in this reduction is to form the level set of the momentum map in $(S^2)^4$,

$$L_Z^R \equiv \left(\begin{array}{c} \mathbf{J}_{124'5} \\ \mathbf{0} \end{array} \right) \subset (S^2)^4 \subset \Lambda_{4j}. \quad (4.3.13)$$

The “Z” subscript is a mnemonic for “zero” and the inverse image of this level set under the projection map of the first symplectic reduction is precisely the level set $L_Z \subset \Phi_{124'5}$ from Eq. 4.1.11. In this level set the four angular momentum vectors \mathbf{J}_1 , \mathbf{J}_2 , $\mathbf{J}_{4'}$, and \mathbf{J}_5 can be formed into a closed, four-sided, generically non-planar polygon. By adding in intermediate angular momenta \mathbf{J}_{12} and $\mathbf{J}_{24'}$ we see points on L_Z^R may all be represented as tetrahedra. Since this level set is at a fixed point under the $SO(3)$ action the group orbits generated by $\mathbf{J}_{124'5}$ are entirely contained within L_Z^R and the reduced space is the “shape space” of tetrahedra with four fixed edge lengths modulo $SO(3)$ rotations. Such phase spaces seem to have first appeared in the work of Kapovich and Millson [77, 78]. Any rotational invariant associated with a tetrahedron, such as the Hamiltonians $|\mathbf{J}_{12}|$ and $|\mathbf{J}_{24'}|$ which define the reduced α - and β -manifolds, the dihedral angle between two faces, and the volume, is a well-defined function on Φ_{4j}^R .

The Hamiltonian $|\mathbf{J}_{12}|$ generates the “flapping” motion about the \mathbf{j}_{12} -axis as described in Section 4.1.3. The conjugate angle to J_{12} on angular momentum space is the 2π -periodic angle ϕ_{12} . This angle is related to the interior dihedral angle α_{12} about the edge \mathbf{J}_{12} of the tetrahedron. In this work we consider all interior dihedral angles α to lie in the range $0 \leq \alpha \leq \pi$. Thus if V is the oriented tetrahedral volume, $\phi_{12} = \pm\alpha_{12}$ when $\text{sgn } V = \pm 1$. Note that the interior dihedral angles are all rotational invariants and thus well-defined functions on the reduced space. Similar statements hold for the Hamiltonian $|\mathbf{J}_{24'}|$, with $\phi_{24'} = \mp\alpha_{24'}$ for $\text{sgn } V = \pm 1$. By construction the α - and β -manifolds project onto (one-dimensional) Lagrangian manifolds on the reduced space and are defined by

$$\mathcal{L}_{\alpha,2}^R = \left(\begin{array}{c} |\mathbf{J}_{12}| \\ J_3 \end{array} \right) \subset \Phi_{4j}^R, \quad \mathcal{L}_{\beta,2}^R = \left(\begin{array}{c} |\mathbf{J}_{24'}| \\ J_6 \end{array} \right) \subset \Phi_{4j}^R. \quad (4.3.14)$$

The projection of the $4j$ -model stationary phase set $I^{(4j)}$ becomes a pair of points in Φ_{4j}^R which are related by time-reversal.

By allowing J_3 or J_6 to take on a continuum of values we may create a Lagrangian foliation of Φ_{4j}^R and thus when computing the Maslov index we may use a “ $|\mathbf{J}_{24'}|$ ”-representation on this reduced phase space. This foliation also allows the topology of the reduced space to be determined. For a real tetrahedron to be constructible J_3 must lie in the triangle-allowed range $|J_1 - J_2| \leq J_3 \leq J_1 + J_2$. On the interior of this range, varying ϕ_{12} creates different tetrahedra and thus the group orbit generated by $|\mathbf{J}_{12}|$ is a circle. However when J_3 saturates one of the inequalities then only a single tetrahedron (modulo proper rotations)

is constructible and thus the group orbit generated by $|\mathbf{J}_{12}|$ degenerates to a point. See, for example, Figure 49 of Aquilanti *et al* [1]. Thus Φ_{4j}^R must have the topology of a sphere,

$$\Phi_{4j}^R = (S^2, d|\mathbf{J}_{12}| \wedge \phi_{12}). \quad (4.3.15)$$

Note that $(|\mathbf{J}_{12}|, \phi_{12})$ are precisely the action-angle variables discovered by Kapovich and Millson [77, 78]. A similar analysis holds for the Hamiltonian $|\mathbf{J}_{24'}|$ and the conjugate angle $\phi_{24'}$. It was noted in Aquilanti *et al* [1] that, given quantized values for all six lengths J_r , the symplectic volume of Φ_{4j}^R is $2\pi \dim \mathcal{Z}_{124'5}$. That is, the reduced manifold contains one Planck cell of area 2π for each state in the space of $4j$ -intertwiners, as expected.

Another interesting function on Φ_{4j}^R is the volume V . As in Eq. 4.1.15, we define the volume on the level set $L_Z^R \subset \Lambda_{4j}$ as

$$V = \frac{1}{6} \mathbf{J}_1 \cdot (\mathbf{J}_2 \times \mathbf{J}_{4'}). \quad (4.3.16)$$

Since this expression is rotationally invariant V may be projected to a function on Φ_{4j}^R . In this chapter we are only concerned with this function insofar as it appears as part of a Poisson bracket in the amplitude determinant. However, the volume itself may be considered a Hamiltonian and the semiclassical version of a volume operator \hat{V} on the Hilbert space of $4j$ -intertwiners. Some works about this operator include Chakrabarti [79], Lèvi-Leblond and Lèvi-Nahas [80], Ashtekar and Lewandowski [20], Major and Seifert [81], Carbone *et al* [82], Neville [83], Brunneman and Thiemann [84], Brunneman and Rideout [85, 86], Ding and Rovelli [87], and Bianchi and Haggard [88, 89], among others. The volume operator plays an important role in loop quantum gravity, where the volume of a spatial region is determined by spin network nodes with valence of four or higher, as described in Rovelli and Smolin [19] and Thiemann [90]. These nodes may themselves be recoupled into the $4j$ -intertwiners introduced earlier. Bianchi and Haggard [88] applied Bohr-Sommerfeld quantization to V on a space similar to Φ_{4j}^R and derived the semiclassical spectrum of the volume operator in terms of complete elliptic integrals of the third kind and found the spectra to be remarkably in agreement with the spectrum computed in loop quantum gravity.

4.4 Action Integrals in the $6j$ -Remodeling Geometry

Now we turn to the relative phase between the two disconnected group orbits that make up the stationary phase set. As usual the relative phase consists of an action integral and a correction due to the Maslov and signature indices. As shown in Section 2.5 the action integrals are the same in models connected by a remodeling geometry, as are the combined Maslov and signature indices. In Section 4.4.1 we construct a closed path between the two pieces $I_+^{(12j)}$ and $I_-^{(12j)}$ of the stationary phase set of the $12j$ -model and compute the action integral. This is the calculation performed by Roberts [2]. The symmetry of the $12j$ -model allows for a very simple construction of the path in terms of Hamiltonian flows

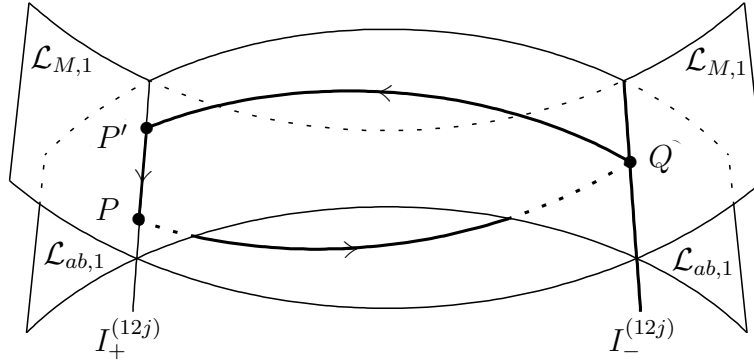


Figure 4.4.1: The closed path for computing the action integral in the $12j$ model. The path starts at P on the intersection manifold $I_+^{(12j)}$, traverses $\mathcal{L}_{M,1}$ to a point Q on $I_-^{(12j)}$, traverses $\mathcal{L}_{ab,1}$ to a point P' on $I_+^{(12j)}$ on the same Hopt fiber over $12j$ -angular momentum space as P , and then finally closes the path by traversing the Hopf fiber in $I_+^{(12j)}$ back to P .

and the Ponzano-Regge phase [27], minus the Maslov correction, emerges naturally. Then in Section 4.4.2 we review a similar calculation for the $4j$ -model which was performed in Aquilanti *et al* [1]. We will see how the asymmetric treatment of the angular momenta results in a more complicated path and thus highlight the advantages of working in a higher-dimensional model when analyzing action integrals.

4.4.1 The Action Integral in the $12j$ -Model

The goal of this section is to compute the action integral part of the relative phase between the two connected pieces $I_+^{(12j)}$ and $I_-^{(12j)}$ of the stationary phase set in the $12j$ -model. We start by constructing an appropriate closed path that starts on $I_+^{(12j)}$, traverses $\mathcal{L}_{M,1}$ to $I_-^{(12j)}$, and then returns to the starting point along $\mathcal{L}_{ab,1}$. This path is sketched in Figure 4.4.1.

Let P be an arbitrary starting point on $I_+^{(12j)}$. The twelve vectors $\mathbf{J}_r, \mathbf{J}_{r'}$ fit together into a tetrahedron Tet_+ of positive volume at point P , as in Figure 4.3.2. Let \mathbf{n}_{123} be the normal vector to the triangle formed by the ordered triplet of vectors $(\mathbf{J}_1, \mathbf{J}_2, \mathbf{J}_3)$, with similar definitions for $\mathbf{n}_{1'5'6}$, $\mathbf{n}_{2'6'4}$, and $\mathbf{n}_{3'4'5}$. It is convenient to define a map $\Delta : \{r, r'\} \rightarrow \{123, 1'5'6, 2'6'4, 3'4'5\}$ from the twelve angular momentum indices to the four ordered triplets that define the four triangles of $\mathcal{L}_{M,1}$ that picks out which of the four triplets the index belongs to (so, for example, $\Delta(1) = 123$ and $\Delta(1') = 1'5'6$).

The Hamiltonian vector fields associated with $\mathbf{J}_{\Delta(r)}$ are tangent to $\mathcal{L}_{M,1}$ for all r, r' so we may generate the path from $I_+^{(12j)}$ to $I_-^{(12j)}$ by flows under these Hamiltonians. In particular, we take the path $\Gamma_{M,1}$ to be the flow of the following Hamiltonian function

$$H_{M,1} \equiv \sum \mathbf{n}_{\Delta(r)}(P) \cdot \mathbf{J}_r, \quad (4.4.1)$$

where the sum is over both primed and unprimed r . Written explicitly in terms of the momentum map components of $\mathcal{L}_{M,1}$, this Hamiltonian is

$$\mathbf{n}_{123}(P) \cdot \mathbf{J}_{123} + \mathbf{n}_{1'5'6}(P) \cdot \mathbf{J}_{1'5'6} + \mathbf{n}_{2'6'4}(P) \cdot \mathbf{J}_{2'6'4} + \mathbf{n}_{3'4'5}(P) \cdot \mathbf{J}_{3'4'5}. \quad (4.4.2)$$

We define the start of the path to be $\Gamma_{M,1}(0) = P$. Since $\mathbf{n}_{\Delta(r)}$ is by definition perpendicular to \mathbf{J}_r a flow by π generates a time-reversal on all twelve angular momentum vectors and thus we take the endpoint of the path to be $Q \equiv \Gamma_{M,1}(\pi) \in I_-^{(12j)}$. Explicitly, the spinors and angular momentum vectors at Q are

$$z_r(Q) = e^{-i\pi \mathbf{n}_{\Delta(r)} \cdot \boldsymbol{\sigma}/2} z_r(P), \quad (4.4.3)$$

$$\mathbf{J}_r(Q) = R(\mathbf{n}_{\Delta(r)}, \pi) \mathbf{J}_r(P) = -\mathbf{J}_r(P), \quad (4.4.4)$$

where r runs over both primed and unprimed values. By Equation A.4.7 the action accumulated along this path is

$$\int_{\Gamma_{M,1}} \theta_{12} = \sum_r (\mathbf{n}_{\Delta(r)} \cdot \mathbf{J}_r)|_P \pi = 0, \quad (4.4.5)$$

where the sum evaluates to zero since $\mathbf{J}_{123} = \mathbf{J}_{1'5'6} = \mathbf{J}_{2'6'4} = \mathbf{J}_{3'4'5} = \mathbf{0}$ on $\mathcal{L}_{M,1}$.

Next, since the Hamiltonian vector fields associated with $\mathbf{J}_{rr'}$ for $r = 1, \dots, 6$ are all tangent to $\mathcal{L}_{ab,1}$ we may generate the path from $Q \in I_-^{(12j)}$ back to $I_+^{(12j)}$ by flows under these Hamiltonians. In particular, we take the path $\Gamma_{ab,1}$ to be the flow of the following Hamiltonian function

$$H_{ab,1} \equiv \sum_r \mathbf{n}_{\Delta(r')}(P) \cdot \mathbf{J}_{rr'}. \quad (4.4.6)$$

We define the start of the path to be $\Gamma_{ab,1}(0) = Q$. Since $\mathbf{n}_{\Delta(r')}(P)$ is perpendicular to $\mathbf{J}_{r'}(P)$ and the angular momenta at Q are related to the angular momenta at P by time-reversal $\mathbf{n}_{\Delta(r')}(P)$ is perpendicular to $\mathbf{J}_{r'}(Q)$. Moreover, on $\mathcal{L}_{ab,1}$ the six diangle conditions hold so $\mathbf{J}_r = -\mathbf{J}_{r'}$ and thus $\mathbf{n}_{\Delta(r')}$ is also perpendicular to $\mathbf{J}_r(Q)$. Therefore the flow of $H_{ab,1}$ by $-\pi$ generates a time-reversal on all twelve angular momentum vectors and thus we take the endpoint of the path to be $P' \equiv \Gamma_{ab,1}(-\pi) \in I_+^{(12j)}$. Explicitly, the spinors and angular momentum vectors at P' are

$$\begin{pmatrix} z_r \\ z_{r'} \end{pmatrix}_{P'} = e^{+i\pi \mathbf{n}_{\Delta(r')}(P) \cdot \boldsymbol{\sigma}/2} \begin{pmatrix} z_r \\ z_{r'} \end{pmatrix}_Q, \quad (4.4.7)$$

$$\begin{pmatrix} \mathbf{J}_r \\ \mathbf{J}_{r'} \end{pmatrix}_{P'} = R(\mathbf{n}_{\Delta(r')}(P), -\pi) \begin{pmatrix} \mathbf{J}_r \\ \mathbf{J}_{r'} \end{pmatrix}_P = - \begin{pmatrix} \mathbf{J}_r \\ \mathbf{J}_{r'} \end{pmatrix}_Q. \quad (4.4.8)$$

By Equation A.4.7 the action accumulated along this path is

$$\int_{\Gamma_{ab,1}} \theta_{12} = \sum_r (\mathbf{n}_{\Delta(r')}(P) \cdot \mathbf{J}_{rr'}(Q)) \pi = 0, \quad (4.4.9)$$

Finally we close the loop by creating a path $\Gamma_{I,1} \in I_+^{(12j)}$ from P' to P . The net result of following $\Gamma_{M,1}$ followed by $\Gamma_{ab,1}$ leaves the primed spinors unaltered,

$$z_{r'}(P') = e^{+i\pi\mathbf{n}_{\Delta(r')}\cdot\boldsymbol{\sigma}/2} e^{-i\pi\mathbf{n}_{\Delta(r')}\cdot\boldsymbol{\sigma}/2} z_{r'}(P) = z_{r'}(P). \quad (4.4.10)$$

The unprimed spinors at P' are

$$z_r(P') = e^{+i\pi\mathbf{n}_{\Delta(r')}\cdot\boldsymbol{\sigma}/2} e^{-i\pi\mathbf{n}_{\Delta(r')}\cdot\boldsymbol{\sigma}/2} z_r(P). \quad (4.4.11)$$

The rotation matrices by π can be simplified by noting that, given a unit vector \mathbf{a} ,

$$e^{\pm i\pi\mathbf{a}\cdot\boldsymbol{\sigma}/2} = \cos(\pi/2) \pm i \sin(\pi/2)\mathbf{a} \cdot \boldsymbol{\sigma} = \pm i\mathbf{a} \cdot \boldsymbol{\sigma}. \quad (4.4.12)$$

Thus,

$$e^{+i\pi\mathbf{a}\cdot\boldsymbol{\sigma}/2} e^{-i\pi\mathbf{b}\cdot\boldsymbol{\sigma}/2} = (\mathbf{a} \cdot \boldsymbol{\sigma})(\mathbf{b} \cdot \boldsymbol{\sigma}) = \mathbf{a} \cdot \mathbf{b} + i(\mathbf{a} \times \mathbf{b}) \cdot \boldsymbol{\sigma}. \quad (4.4.13)$$

For spinor z_r , the unit vectors \mathbf{a} and \mathbf{b} are the normal vectors $\mathbf{n}_{\Delta(r)}$ and $\mathbf{n}_{\Delta(r')}$, respectively. Let ψ_r be the exterior dihedral angle of the two faces of the tetrahedron sharing edge \mathbf{J}_r . Then Eq. 4.4.11 reduces to

$$z_r(P') = \cos(\psi_r) + i \sin(\psi_r)\mathbf{j}_r \cdot \boldsymbol{\sigma} z_r = e^{+i\psi_r\mathbf{j}_r\cdot\boldsymbol{\sigma}} z_r(P) = e^{+i\psi_r} z_r(P), \quad (4.4.14)$$

where \mathbf{j}_r is the unit vector for the unprimed angular momentum \mathbf{J}_r at P . Thus we form $\Gamma_{I,1}$ by following the flows of each of the six Hamiltonians I_r by angle $2\psi_r$. Note that these Hamiltonians are components of the momentum map for the common symmetry group G_{12} and the Hamiltonian flow vectors are all tangent to $I_+^{(12j)}$. Under these flows the primed spinors are unaffected and the unprimed spinors transform as

$$z_r(P') \mapsto e^{-i(2\psi_r)/2} z_r(P') = e^{-i\psi_r} e^{+i\psi_r} z_r(P) = z_r(P). \quad (4.4.15)$$

By Equation A.4.4 the action accumulated along this path is

$$\int_{\Gamma_{I,1}} \theta = \sum_r I_r(P)(2\psi_r) = 2 \sum_r (j_r + 1/2)\psi_r. \quad (4.4.16)$$

The total action integral in the 12j-model of the 6j-symbol is thus

$$S_{12} \equiv \int_{\Gamma_{M,1} + \Gamma_{ab,1} + \Gamma_{I,1}} \theta = 2 \sum_r (j_r + 1/2)\psi_r = 2\Psi_{\text{pr}}, \quad (4.4.17)$$

where Ψ_{pr} is the Ponzano-Regge phase [27], defined as

$$\Psi_{\text{pr}} \equiv \sum_r (j_r + 1/2)\psi_r. \quad (4.4.18)$$

Note that the entirety of this phase came from the path that closes the loop. This fact was exploited in Hedeman *et al* [51] to create a purely symplectic proof of the Schläfli identity [91].

4.4.2 The Action Integral in the 4j-Model

Now we construct the same phase in the 4j-model of the 6j-symbol to highlight the advantages of using the more symmetric 12j-model to find the action integral. We choose to work in the standard 4j-model (an inner product in $\mathcal{H}_{124'5}$), rather than the dual 4j-model (an inner product in $\mathcal{H}_{124'5}^*$) that is the target space model of the second remodel because this is the model considered by Aquilanti *et al* [1]. This will not affect our conclusions since the path used to compute the phase in a given model is just the inverse of the path used in the dual model.

The main difficulty in the 4j-model is in constructing an appropriate closed path that starts on $I_+^{(4j)}$, traverses $\mathcal{L}_{a,2}$ to $I_-^{(4j)}$, and then returns to the starting point along $\mathcal{L}_{\beta,2}$. Recall that $\mathcal{L}_{a,2}$ is the butterfly manifold in $L_Z \subset \Phi_{124'5}$ satisfying $|\mathbf{J}_{12}| = J_3$ and $\mathcal{L}_{\beta,2}$ is the manifold satisfying $|\mathbf{J}_{24'}| = J_6$. We construct a path similar to the path used in Aquilanti *et al* [1] except we choose to start on the piece of the stationary phase set where the oriented tetrahedral volume is positive and we continue using the “symmetric” labeling of the angular momenta.

Let P be an arbitrary starting point on $I_+^{(4j)}$. The four vectors \mathbf{J}_1 , \mathbf{J}_2 , $\mathbf{J}_{4'}$, and \mathbf{J}_5 and the two “coupled” vectors \mathbf{J}_{12} and $\mathbf{J}_{24'}$ form the six edges of a tetrahedron Tet_+ of positive volume at point P . Let α_r be the interior dihedral angle between the two faces sharing edge \mathbf{J}_r for the tetrahedron Tet_+ and let \mathbf{j}_r be the unit vectors for angular momenta \mathbf{J}_r , with $r = 1, 2, 12, 4', 5, 24'$.

We may generate the path $\Gamma_{a,2}$ from $I_+^{(4j)}$ to $I_-^{(4j)}$ along $\mathcal{L}_{a,2}$ by following the flow of $|\mathbf{J}_{12}| = \mathbf{j}_{12} \cdot \mathbf{J}_{12}$ to a point $Q \in I_-^{(4j)}$. We define the start of the path to be $\Gamma_{a,2}(0) = P$. The time-reversed tetrahedron is characterized by the same dihedral angles as Tet_+ so the appropriate angle of evolution for this flow is, $-2\alpha_{12}$, which takes the conjugate angle ϕ_{12} from $+\alpha_{12}$ (since $V > 0$ at P) to $-\alpha_{12}$ (since $V < 0$ at Q). Explicitly, the spinors and angular momentum vectors at Q are

$$z_r(Q) = \begin{cases} e^{+i\alpha_{12}\mathbf{j}_{12}\cdot\boldsymbol{\sigma}} z_r(P), & r = 1, 2, \\ z_r(P), & r = 4', 5, \end{cases} \quad (4.4.19)$$

$$\mathbf{J}_r(Q) = \begin{cases} R(\mathbf{j}_{12}, -2\alpha_{12})\mathbf{J}_r(P), & r = 1, 2, \\ \mathbf{J}_r(P), & r = 4', 5. \end{cases} \quad (4.4.20)$$

Already we see that we are generating a more complicated path since this flow does not bring us cleanly to the time-reversed image of Tet_+ but rather a tetrahedron related to Tet_+ by both time-reversal and an overall $SO(3)$ rotation. By Equation A.4.7 the action accumulated along this path is

$$\int_{\Gamma_{a,2}} \theta_4 = \sum_{r=1,2} (\mathbf{j}_{12} \cdot \mathbf{J}_r)|_P (-\alpha_{12}) = -(\mathbf{j}_{12} \cdot \mathbf{J}_{12})|_P \alpha_{12} = -J_3 \alpha_{12}. \quad (4.4.21)$$

Since the tetrahedron at Q is related to the tetrahedron at P by a time-reversal (up to an overall $SO(3)$ rotation) and the Hamiltonian flow of $|\mathbf{J}_{12}|$ leaves $\mathbf{J}_{4'}$ and \mathbf{J}_5 invariant, we

may consider the net result of this rotation to be a reflection of all four angular momentum vectors through the plane defined by $\mathbf{J}_{4'}(P)$ and $\mathbf{J}_5(P)$. This characterization of the rotation will be needed to determine the proper angles needed to close the path later.

Next we generate the path $\Gamma_{\beta,2}$ from Q back to $I_+^{(4j)}$ along $\mathcal{L}_{\beta,2}$ by following the flow of $|\mathbf{J}_{24'}| = \mathbf{j}_{24'} \cdot \mathbf{J}_{24'}$. This flow rotates the “2 – 4' – 24' wing” about the $\mathbf{J}_{24'}(Q)$ axis. Let $\alpha_{24'}$ be the interior dihedral angle for edge $\mathbf{J}_{24'}$ and define P' to be the endpoint of this flow. As with the \mathbf{J}_{12}^2 flow along $\mathcal{L}_{a,2}$, the appropriate angle of evolution is $-2\alpha_{24'}$, which takes the conjugate angle $\phi_{24'}$ from $+\alpha_{24'}$ (since $V < 0$ at Q) to $-\alpha_{24'}$ (since $V > 0$ at P'). Explicitly, the spinors and angular momentum vectors at P' are

$$z_r(P') = \begin{cases} e^{+i\alpha_{24'}\tilde{\mathbf{j}}_{24'}\cdot\boldsymbol{\sigma}} z_r(Q), & r = 2, 4', \\ z_r(Q), & r = 1, 5, \end{cases} \quad (4.4.22)$$

$$\mathbf{J}_r(P') = \begin{cases} R(\tilde{\mathbf{j}}_{24'}, -2\alpha_{24'})\mathbf{J}_r(Q), & r = 2, 4', \\ \mathbf{J}_r(Q), & r = 1, 5, \end{cases} \quad (4.4.23)$$

where $\tilde{\mathbf{j}}_{24'}$ is the unit vector for $\mathbf{J}_{24'}(Q)$. The action accumulated along this path is

$$\int_{\Gamma_{\beta,2}} \theta_4 = (\tilde{\mathbf{j}}_{24'} \cdot \mathbf{J}_{24'})|_Q (-\alpha_{24'}) = -J_6\alpha_{24'}. \quad (4.4.24)$$

We may again consider the net result of this rotation to be a reflection of all four angular momenta, this time through the plane defined by $\mathbf{J}_1(Q)$ and $\mathbf{J}_5(Q)$.

Now we need to close the path by following flows along $I_+^{(4j)}$. First we close the path in the 4j-angular momentum space Λ_{4j} along a path $\Gamma_{I,2}$ which follows a global $SO(3)$ flow (generated by the $SU(2)$ subgroup of the common symmetry group G_4). To find the appropriate axis and angle of rotation for the $SU(2)$ path we treat the two rotations generated by $|\mathbf{J}_{12}|(P)$ and $|\mathbf{J}_{24'}|(Q)$ as reflections and use the fact that the product of two reflections is itself a rotation, following Aquilanti *et al* [1]. Let $A(\mathbf{n})$ be a reflection through the plane normal to \mathbf{n} . Given planes with outward-pointing normals \mathbf{n} and \mathbf{n}' and interior dihedral angle α ,

$$A(\mathbf{n})A(\mathbf{n}') = R\left(\frac{\mathbf{n} \times \mathbf{n}'}{\sin \alpha}, 2\alpha\right). \quad (4.4.25)$$

The path from P to P' amounts to the product of reflections $A(\mathbf{n}_{15}(Q))$ and $A(\mathbf{n}_{4'5}(P))$ acting on all four angular momentum vectors. The axis of rotation in Eq. 4.4.25 is thus

$$(\mathbf{J}_1(Q) \times \mathbf{J}_5(Q)) \times (\mathbf{J}_{4'}(P) \times \mathbf{J}_5(P)) \propto -\mathbf{j}_5, \quad (4.4.26)$$

where $\mathbf{J}_5(Q) = \mathbf{J}_5(P)$ and the negative sign is due to the negative volume of the tetrahedron at Q . Since the two reflection planes contain the tetrahedron faces that share edge \mathbf{j}_5 the appropriate interior dihedral angle to be used in Eq. 4.4.25 is α_5 . The tetrahedron at P' is thus the tetrahedron at P rotated about the \mathbf{j}_5 axis by angle $-2\alpha_5$. Thus the path $\Gamma_{I,2}$ follows the flow of the Hamiltonian $\mathbf{j}_5 \cdot \mathbf{J}_{124'5}$ by angle $2\alpha_5$. Let P'' be the endpoint of this

flow. By construction P and P'' lie on the same T^4 fiber over angular momentum space. Explicitly, the spinors at P' are

$$z_r(P'') = e^{-i\alpha_5 \mathbf{j}_5 \cdot \boldsymbol{\sigma}} z_r(P'), \quad (4.4.27)$$

The action accumulated along this path is

$$\int_{\Gamma_{I,2}} \theta_4 = (\mathbf{j}_5 \cdot \mathbf{J}_{124'5})|_{P'} (-\alpha_5) = 0, \quad (4.4.28)$$

since $\mathbf{J}_{124'5} = \mathbf{0}$ on $I_+^{(4j)}$.

Finally we close the path in $\Phi_{124'5}$ along a path $\Gamma_{I',2}$ which follows the flows generated by I_r . To properly close the loops each of the products of $SU(2)$ transformation matrices in Eqs. 4.4.19, 4.4.22, and 4.4.27 must be combined and written as $z_r(P'') = e^{i\theta_r \mathbf{j}_r \cdot \boldsymbol{\sigma}/2} z_r(P)$ for some angles θ_r , in which case θ_r becomes the appropriate angle of evolution for the flow of I_r . In Aquilanti *et al* [1] these angles were found using the Rodrigues-Hamilton formula [92] and considering the paths traced out by individual angular momenta as the edges of a spherical triangle to make the product of $SO(3)$ rotations the identity and then determining the \mathbb{Z}_2 homotopy class of the path in $SU(2)$. After much work the appropriate evolution angles θ_1 , θ_2 , $\theta_{4'}$, and θ_5 were determined to be $-2\alpha_1 + 2\pi$, $-2\alpha_2$, $-2\alpha_{4'} + 2\pi$, and $-2\alpha_5$, respectively. By Equation A.4.4 the action accumulated along this last bit of path is

$$\int_{\Gamma_{I',2}} \theta = \sum_r I_r(P'')(\theta_r) = -2(J_1\alpha_1 + J_2\alpha_2 + J_4\alpha_{4'} + J_5\alpha_5) + 2\pi(J_1 + J_4). \quad (4.4.29)$$

The exterior dihedral angles ψ_r are given by $\pi - \alpha_r$. Treating α_{12} and $\alpha_{24'}$ as α_3 and α_6 , respectively, the total action integral around the path $\Gamma_2 = \Gamma_{a,2} + \Gamma_{\beta,2} + \Gamma_{I,2} + \Gamma_{I',2}$ for the $4j$ -model is therefore

$$S_4 \equiv \oint_{\Gamma_2} \theta = 2 \sum_r J_r \psi_r + 2\pi(J_1 + J_4) = 2\Psi_{\text{pr}} + 2\pi(J_1 + J_4). \quad (4.4.30)$$

The final term must be an integer multiple of 2π for triangle-allowed values of the quantum numbers j_r and thus

$$S_4 = S_{12} \bmod 2\pi. \quad (4.4.31)$$

The reason the action integrals are only equal modulo 2π is because lifting the path Γ_2 into the $12j$ -phase space using the methods of Section 2.5.2 yields a different path than the one described in Section 4.4.1. However, as discussed in Section 2.5.6 this difference in paths at most contributes a difference of integer multiples of 2π , as demonstrated in Eq. 4.4.31.

Comparing the calculations for the action integral in the $12j$ -model and the $4j$ -model it is clear that the symmetric treatment of the angular momenta in the $12j$ -model offers many advantages over the asymmetric treatment of the $4j$ -model. For one, the entirety of the action integral in the $12j$ -model is accumulated by flows along the common symmetry

group orbits whereas the path in the $4j$ -model asymmetrically splits up the contributions to the phase over all legs of the path. The asymmetric treatment makes a condensed analysis inherently harder as well. In general the symmetric treatment of the larger models offers the cleanest construction of the paths because the manifolds in these models will simply be the products of triangle and diangle manifolds, as will be discussed in Section 5.1. In particular, constructing a path to find the relative phase between two stationary phase points related by time-reversal is very easy to implement on the manifolds of such a symmetric model. Implementing time-reversal on smaller phase spaces where the Lagrangian manifolds are more complicated is more involved. In this treatment, we did not even bother to connect two time-reversed tetrahedra with our paths, only concerning ourselves with mapping to a tetrahedron with the opposite signed volume.

4.5 Asymptotics of the $6j$ -Symbol

Now we are ready to compute the remaining pieces of the stationary phase approximation for the $6j$ -symbol. We saw in Section 3.3.2 that the smaller dimensionality of the $2j$ -target space models made the amplitude determinant easier to compute than in the $3j$ -product space model of the $3j$ -symbol. This is even more apparent in the remodeling geometries of the $6j$ -symbol, where the 9×9 amplitude determinant computed by Roberts [2] in the $12j$ -model simplifies to a single Poisson bracket in the $4j$ -model. Since we find the amplitude in the $4j$ -model the appropriate semiclassical expression for the inner product $\langle B_{1(24')5} | B_{(12)4'5} \rangle$ is, up to an overall phase,

$$\langle B_{1(24')5}, j_6 | B_{(12)4'5}, j_3 \rangle \approx \frac{(2\pi)^{(n_4-s_4)/2}}{\sqrt{V_{a,2}V_{\beta,2}}} \sum_{\pm} V_{\pm} \left| \tilde{\Omega}_{\pm}^{4j} \right|^{1/2} e^{i\varphi_{\pm}}, \quad (4.5.1)$$

where V_{\pm} was defined in Eq. 4.3.12, $n_4 = 8$ is the number of degrees of freedom in Φ_{4j} , and $s_4 = 7$ is the dimension of the common symmetry group G_4 . By Eq. 4.2.38 the $6j$ -symbol is thus approximated in the $4j$ -model as

$$\left\{ \begin{array}{ccc} j_1 & j_2 & j_3 \\ j_4 & j_5 & j_6 \end{array} \right\} \approx \frac{1}{\sqrt{2j_3+1}\sqrt{2j_6+1}} \frac{\sqrt{2\pi}}{\sqrt{V_{a,2}V_{\beta,2}}} \sum_{\pm} V_{\pm} \left| \tilde{\Omega}_{\pm}^{4j} \right|^{1/2} e^{i\varphi_{\pm}}. \quad (4.5.2)$$

Plugging in the volumes from Table 4.6 and Eq. 4.3.12 and using $2j_r + 1 = 2J_r$ yields

$$\left\{ \begin{array}{ccc} j_1 & j_2 & j_3 \\ j_4 & j_5 & j_6 \end{array} \right\} \approx \frac{1}{2\sqrt{J_3J_6}\sqrt{2\pi}} \sum_{\pm} \left| \tilde{\Omega}_{\pm}^{4j} \right|^{1/2} e^{i\varphi_{\pm}}. \quad (4.5.3)$$

In Section 4.5.1 we find the amplitude in the $4j$ -model. We already found the action integral piece of the relative phase between $I_+^{(4j)}$ and $I_-^{(4j)}$ for the $4j$ -model in Section 4.4.2, though as we saw we could have confined that calculation to the $12j$ -model. In Section 4.5.2 we continue the calculation of the relative phase by computing the Maslov index using the

method developed in Esterlis *et al* [55]. Finally, in Section 4.5.3 we compute the signature index and put everything together to find the Ponzano-Regge formula for the asymptotics of the 6j-symbol.

4.5.1 Computing the Amplitude in the 4j-Model

Consider the calculation of the amplitude determinant in the 12j-model. Initially, the amplitude determinant is a 24×24 -singular matrix of Poisson brackets on Φ_{12j} . Upon symplectic reduction by the 15-dimensional common symmetry group G_{12} this becomes a non-singular 9×9 matrix of Poisson brackets on the 18-dimensional reduced phase space of the 12j-model. Even though many entries of this matrix are zero, the computation, carried out by Roberts [2], is computationally intense when compared to the calculation in the 4j-model. As seen in Section 3.3.2 we get the same amplitude determinant (up to a factor that will be compensated for by the volume factors in Eq. 4.5.1) in both models. Therefore, we just consider the amplitude determinant in the 4j-model.

The amplitude of the 6j-symbol in the 4j-model is found by taking the determinant of the appropriate matrix of Poisson brackets. As in Section 3.3.2 we need only consider the projection of the manifolds $\mathcal{L}_{a,2}$ and $\mathcal{L}_{\beta,2}$ of the 4j-model onto the reduced space Φ_{4j}^R introduced in Section 4.3.4. The reduced manifolds in Φ_{4j}^R are the level sets of Hamiltonians $|\mathbf{J}_{12}|$ and $|\mathbf{J}_{24'}|$, as in Eq. 4.3.14. Since the reduced 4j-model is two-dimensional, the amplitude determinant is given by a single Poisson bracket,

$$\tilde{\Omega}_{\pm}^{4j} = \{|\mathbf{J}_{24'}|, |\mathbf{J}_{12}|\}_{\pm}^{-1}, \quad (4.5.4)$$

where the subscript indicates on which of the two stationary phase points in the reduced phase space the expression is to be evaluated. To compute this Poisson bracket we lift the bracket into angular momentum space Λ_{4j} , which is a Poisson manifold whose Poisson bracket is given by

$$\{f, g\} = \sum_r \mathbf{J}_r \cdot \left(\frac{\partial f}{\partial \mathbf{J}_r} \times \frac{\partial g}{\partial \mathbf{J}_r} \right), \quad (4.5.5)$$

where $r = 1, 2, 4', 5$ and f and g are any functions on Λ_{4j} . Therefore

$$\{|\mathbf{J}_{24'}|, |\mathbf{J}_{12}|\} = \mathbf{J}_2 \cdot \left(\frac{\partial |\mathbf{J}_2 + \mathbf{J}_{4'}|}{\partial \mathbf{J}_2} \times \frac{\partial |\mathbf{J}_1 + \mathbf{J}_2|}{\partial \mathbf{J}_2} \right). \quad (4.5.6)$$

This evaluates to

$$\{|\mathbf{J}_{24'}|, |\mathbf{J}_{12}|\} = \frac{\mathbf{J}_2 \cdot (\mathbf{J}_{24'} \times \mathbf{J}_{12})}{|\mathbf{J}_{24'}| |\mathbf{J}_{12}|} = \frac{\mathbf{J}_2 \cdot (\mathbf{J}_{4'} \times \mathbf{J}_1)}{|\mathbf{J}_{12}| |\mathbf{J}_{24'}|} = \frac{6V}{|\mathbf{J}_{12}| |\mathbf{J}_{24'}|}, \quad (4.5.7)$$

where the numerator is $6V$ due to cyclic property of the scalar triple product. Note that this volume function is a rotational invariant and thus projects to Φ_{4j}^R . On the stationary phase points $J_{12} = J_3$ and $J_{24} = J_6$ so

$$\tilde{\Omega}_{\pm}^{4j} = \pm \frac{J_3 J_6}{6 |V|}, \quad (4.5.8)$$

where $V = \pm |V|$ on the projection of $I_{\pm}^{(4j)}$ to Φ_{4j}^R .

Plugging these results into Eq. 4.5.3 and pulling out an overall phase yields

$$\left\{ \begin{array}{ccc} j_1 & j_2 & j_3 \\ j_4 & j_5 & j_6 \end{array} \right\} \approx \frac{1}{2} \frac{1}{\sqrt{J_3 J_6} \sqrt{2\pi}} \sqrt{\frac{J_3 J_6}{6 |V|}} \sum_{\pm} e^{i\varphi_{\pm}} = \frac{\cos(\Delta\varphi/2)}{\sqrt{12\pi |V|}}, \quad (4.5.9)$$

where $\Delta\varphi$ is the sum of the action integral around the closed path in the 4j-model, Eq. 4.4.30, and the Maslov and signature index corrections.

$$\Delta\varphi \equiv 2\Psi_{\text{pr}} - \mu(\Gamma) \frac{\pi}{2} + \Delta\sigma \frac{\pi}{4} \pmod{2\pi}. \quad (4.5.10)$$

4.5.2 Computing the Maslov Index in the 4j-Model

We review here the method developed in Esterlis *et al* [55] for the computation of the Maslov index applied to a one degree-of-freedom phase space. Let H be a Hamiltonian and let \mathcal{L} be a level set of this Hamiltonian and let x define the representation. The caustics occur at points on \mathcal{L} where the function $e \equiv \{x, H\}$ is zero. At a caustic we define functions u and v (up to a scale factor) such that $udx = -vdH$. The Maslov index along a path on \mathcal{L} that follows the flow of H is given by

$$\mu = \sum_i \text{sgn} [u \{e, H\} v]_i, \quad (4.5.11)$$

where i indexes the caustic points encountered along the path.

Now we apply this method to the calculation of the Maslov index in the 4j-model of the 6j-symbol. We choose to work in the reduced 4j-phase space Φ_{4j}^R and work in the $|\mathbf{J}_{24'}|$ -representation. Let Γ_2^R be the projection of the path $\Gamma_2 \subset \Phi_{4j}$ from the 4j-model onto the reduced phase space. The reduced space path is much simpler to construct than the full path Γ_2 since we do not need to concern ourselves with overall rotations or phases. The path starts at the projection of $I_+^{(4j)}$, follows the flow of $|\mathbf{J}_{12}|$ along the reduced a -manifold to the projection of $I_-^{(4j)}$, and then follows the flow of $|\mathbf{J}_{24'}|$ along the reduced β -manifold. We denote the two legs of this path $\Gamma_{a,2}^R$ and $\Gamma_{\beta,2}^R$. The reduced a - and β -manifolds were defined in Eq. 4.3.14 by the level set conditions $|\mathbf{J}_{12}| = J_3$ and $|\mathbf{J}_{24'}| = J_6$, respectively.

Since $\mathcal{L}_{\beta,2}^R$ is one of the manifolds that defines the $|\mathbf{J}_{24'}|$ -representation there is no Maslov contribution from $\Gamma_{\beta,2}^R$. In particular, $x = H = |\mathbf{J}_{24'}|$ so $e = 0$ (every point on $\Gamma_{\beta,2}^R$ is a caustic) and $\{e, H\} = 0$, so the argument of the sign function in Eq. 4.5.11 is uniformly zero and thus $\mu = 0$. For $\Gamma_{a,2}^R$ we still have $x = |\mathbf{J}_{24'}|$ but now $H = |\mathbf{J}_{12}|$. On the reduced a -manifold $e = \{|\mathbf{J}_{24'}|, |\mathbf{J}_{12}|\}$, which we determined in Eq. 4.5.7 to be $6V/|\mathbf{J}_{12}||\mathbf{J}_{24'}|$. The caustics on $\mathcal{L}_{a,2}^R$ are therefore points where $V = 0$, which corresponds to flat configurations of the tetrahedron. Since the start and end points of $\Gamma_{a,2}^R$ are related by time-reversal and the flat tetrahedra are related to their time-reversed image by a proper rotation $\Gamma_{a,2}^R$ crosses a caustic exactly once. The entirety of the Maslov index for the 4j-model in the $|\mathbf{J}_{24'}|$ -representation, then, occurs at the single point where the path crosses a caustic on the reduced a -manifold.

To find u and v we need to satisfy $ud|\mathbf{J}_{24'}| = -vd|\mathbf{J}_{12}|$ at the caustic. We find u and v by first finding a general differential relation between V , $|\mathbf{J}_{12}|$, and $|\mathbf{J}_{24'}|$ and then setting $V = 0$ at the caustic. First note that on Φ_{4j}^R we have canonically conjugate pairs $(|\mathbf{J}_{24'}|, -\phi_{24'})$ and $(|\mathbf{J}_{12}|, -\phi_{12})$ and therefore, by Eq. 4.5.7 and definition of the Poisson bracket,

$$\{|\mathbf{J}_{24'}|, |\mathbf{J}_{12}|\} = -\frac{d|\mathbf{J}_{12}|}{d\phi_{24'}} = +\frac{d|\mathbf{J}_{24'}|}{d\phi_{12}} = \frac{6V}{|\mathbf{J}_{12}||\mathbf{J}_{24'}|}. \quad (4.5.12)$$

Next we find the Poisson brackets $\{V, |\mathbf{J}_{12}|\}$ and $\{V, |\mathbf{J}_{24'}|\}$. To do this we define the vectors $\mathbf{A}_{rs} \equiv \mathbf{J}_r \times \mathbf{J}_s$ and let $A_{rs} \equiv |\mathbf{A}_{rs}|$, which is twice the area of the face spanned by \mathbf{J}_r and \mathbf{J}_s . By Eq. 4.5.5,

$$\{V, |\mathbf{J}_{12}|\} = \sum_{r=1}^2 \mathbf{J}_r \cdot \left(\frac{\partial V}{\partial \mathbf{J}_r} \times \frac{\partial |\mathbf{J}_{12}|}{\partial \mathbf{J}_r} \right) = -\frac{\mathbf{A}_{4'5} \cdot \mathbf{A}_{12}}{6|\mathbf{J}_{12}|}, \quad (4.5.13)$$

where the second equality follows from $\mathbf{J}_1 = -\mathbf{J}_2 - \mathbf{J}_{4'} - \mathbf{J}_5$ (valid on the level set L_Z on which the Poisson bracket is being evaluated), the properties of the scalar triple product, and the definition of \mathbf{A}_{rs} . Since the planes defined by \mathbf{A}_{12} and $\mathbf{A}_{4'5}$ intersect along \mathbf{J}_{12} , $\mathbf{A}_{4'5} \cdot \mathbf{A}_{12} = A_{12}A_{4'5} \cos \psi_{12}$, where $\psi_{12} = \pi - \phi_{12}$ is the exterior dihedral angle about edge \mathbf{J}_{12} . Therefore,

$$\{V, |\mathbf{J}_{12}|\} = \frac{dV}{d\phi_{12}} = \frac{A_{12}A_{4'5} \cos \phi_{12}}{6|\mathbf{J}_{12}|} = \{|\mathbf{J}_{24'}|, |\mathbf{J}_{12}|\} \frac{\partial V}{\partial |\mathbf{J}_{24'}|}, \quad (4.5.14)$$

where the last expression is a different way of expanding out the Poisson bracket. Combining Eqs. 4.5.12 and 4.5.14, and performing a similar analysis on the bracket $\{V, |\mathbf{J}_{24'}|\}$ yields

$$\frac{\partial V}{\partial |\mathbf{J}_{24'}|} = \frac{A_{12}A_{4'5} |\mathbf{J}_{24'}| \cos \phi_{12}}{36V}, \quad \frac{\partial V}{\partial |\mathbf{J}_{12}|} = \frac{A_{24'}A_{15} |\mathbf{J}_{12}| \cos \phi_{24'}}{36V}. \quad (4.5.15)$$

Thus the sought-for differential relation between V , $|\mathbf{J}_{12}|$, and $|\mathbf{J}_{24'}|$ is

$$36VdV = A_{12}A_{4'5} |\mathbf{J}_{24'}| \cos \phi_{12} d|\mathbf{J}_{24'}| + A_{24'}A_{15} |\mathbf{J}_{12}| \cos \phi_{24'} d|\mathbf{J}_{12}|. \quad (4.5.16)$$

At the caustic $V = 0$ and $ud|\mathbf{J}_{24'}| + vd|\mathbf{J}_{12}| = 0$ so Eq. 4.5.16 implies

$$u = A_{12}A_{4'5} |\mathbf{J}_{24'}| \cos \phi_{12}, \quad v = A_{24'}A_{15} |\mathbf{J}_{12}| \cos \phi_{24'}. \quad (4.5.17)$$

We may also use the above results to find

$$\{e, |\mathbf{J}_{12}|\}_{V=0} = \{ \{ |\mathbf{J}_{24'}|, |\mathbf{J}_{12}|\}, |\mathbf{J}_{12}|\}_{V=0} = \frac{A_{24'}A_{15} \cos \phi_{24'}}{|\mathbf{J}_{12}|\mathbf{J}_{24'}^2}. \quad (4.5.18)$$

Using Eqs. 4.5.17 and 4.5.18 in Eq. 4.5.11, then, gives the Maslov index for a path on $\mathcal{L}_{a,2}^R$ following the Hamiltonian flow of $|\mathbf{J}_{12}|$ through a caustic

$$\mu = \operatorname{sgn} \left. \frac{A_{12}A_{4'5}A_{24'}^2A_{15}^2 \cos^2 \phi_{24'} \cos \phi_{12}}{|\mathbf{J}_{24'}|} \right|_{V=0} = \operatorname{sgn}(\cos \phi_{12})|_{V=0}. \quad (4.5.19)$$

The caustic condition $V = 0$ implies the tetrahedron is flat at the caustic points and thus all dihedral angles are either 0 or π . Thus $\mu = +1$ when $\phi_{12} = 0$ and $\mu = -1$ when $\phi_{12} = \pi$.

As described in Section 4.4.2, the path $\Gamma_{a,2}^R$ follows the flow of $|\mathbf{J}_{12}|$ through a *negative* angle $-2\alpha_{12}$, which takes the angle ϕ_{12} through 0 from $+\alpha_{12}$ to $-\alpha_{12}$. Thus the path $\Gamma_{a,2}^R$ is more accurately described as following the Hamiltonian flow of $-|\mathbf{J}_{12}|$. By Eq. 4.5.19 the Maslov index for the flow by $|\mathbf{J}_{12}|$ as it passes through $\phi_{12} = 0$ is $+1$ and thus the Maslov index for the flow by $-|\mathbf{J}_{12}|$ which defines $\Gamma_{a,2}^R$ is -1 . We may conclude then that the total Maslov index for the path Γ_2^R is $\mu = -1$.

4.5.3 The Asymptotic Expression for the 6j-Symbol

Finally, we turn our attention to the signature index. We wish to compute the signature index σ at the two intersection points in Φ_{4j}^R in the $|\mathbf{J}_{24'}|$ -representation. As in Cappell, Lee, and Miller [59] and Section C.5, we may express this signature index in terms of the Lagrangian signature,

$$\sigma = \sigma(\Lambda_x, \Lambda_a, \Lambda_\beta), \quad (4.5.20)$$

where Λ_a and Λ_β are the tangent planes to $\mathcal{L}_{a,2}^R$ and $\mathcal{L}_{\beta,2}^R$ at the stationary phase points and Λ_x is the plane tangent to the Lagrangian manifold in the Lagrangian foliation that defines the representation. Since $\mathcal{L}_{\beta,2}^R$ is itself part of the representation-defining foliation Λ_x and Λ_β are equal and, due to the antisymmetry of the Lagrangian signature, Eq. 4.5.20 evaluates to zero at both stationary phase points.

Plugging in the Maslov and signature indices into Eq. 4.5.10 yields a relative phase $\Delta\varphi = 2\Psi_{\text{pr}} + \pi/2$. Thus the asymptotic expression for the 6j-symbol is, up to an overall phase,

$$\left\{ \begin{array}{ccc} j_1 & j_2 & j_3 \\ j_4 & j_5 & j_6 \end{array} \right\} \approx \frac{\cos(\Psi_{\text{pr}} + \pi/4)}{\sqrt{12\pi|V|}}, \quad (4.5.21)$$

where Ψ_{pr} is the Ponzano-Regge phase given in Eq. 4.4.18. This is indeed the well-established asymptotic formula for the 6j-symbol [27, 38, 42, 2, 1]. Note that we have routinely ignored the contributions of overall phases in our calculations of the 6j-symbol. Since the 6j-symbol is real the overall phase correction for Eq. 4.5.21 amounts to a sign ± 1 .

4.6 Summary

The remodeling of the 6j-symbol demonstrates many of the advantages of working with different models. The pair of remodels that were used in the remodeling algebra generalizes to the 3nj-symbols, with a maximally symmetric 6nj-model connected via two remodels to a minimally-sized $(n+2)j$ -model.

The manifolds in the symmetric model will all be products of diangle and triangle manifolds and this simple geometry allows for the construction of particularly simple paths between the stationary phase points. The action integrals are thus easy to compute in these

models. In particular the only contribution to the action integrals will come from flows generated by the $6nj$ I maps on the phase space, and thus all action integrals take on the form of an obvious generalization of the Ponzano-Regge phase. We saw that a similar action integral for the $6j$ -symbol in the $4j$ -model was much messier to calculate since the flapping motion of the butterfly manifolds also generates non-zero action integrals and thus the Ponzano-Regge phase is asymmetrically split and is generated by a combination of I and $|\mathbf{J}|$ flows.

The semiclassical approximation in the $(n+2)j$ -model has the advantage of taking place in a phase space containing significantly fewer degrees of freedom than the symmetric model. Moreover symplectic reduction of the model yields a reduced phase space with merely $n-1$ degrees of freedom. This is the phase space model with the fewest dimensions and is thus ideal for computing any quantity that involves a determinant, such as the amplitude or Maslov phase. In the case of the $6j$ -symbol we are able to express the amplitude as a single Poisson bracket and we were able to compute the Maslov index in a one degree-of-freedom context. This has significant advantages over similar calculations in the larger symmetric model which involve 9×9 determinants. These advantages are only increased in the other $3nj$ -symbols with the reduced symmetric model involving $6n-3$ degrees of freedom in contrast with the $n-1$ degrees of freedom in the reduced $(n+2)j$ -model.

Chapter 5

Other Applications

Now that we have seen in detail how the various aspects of the remodeling of an inner product apply to the $3j$ - and $6j$ -symbols we turn to other applications. First in Section 5.1 we consider the $3nj$ -symbols, which may be interpreted as recoupling coefficients for $n + 1$ angular momenta. As with the $6j$ -symbol we form three models, an $(n + 2)j$ -, a $2(n + 2)j$ -, and a $6nj$ -model, and connect them with two applications of an inner product remodeling. In Section 5.2 we introduce $SU(2)$ rotation operators into our spin networks. We call such operators “ g -insertions” since they involve adding a line carrying a group element g to our spin networks. The g -inserted spin networks ultimately may be interpreted as the amplitudes of loop quantum gravity. That is, we may treat spin network states in loop quantum gravity as wavefunctionals on the space of connections. The action of a spin network state on a connection will be equivalent to performing a g -insertion on all legs of the spin network. Once the loop quantum gravity amplitudes are expressed in terms of spin networks they may be subjected to remodeling, producing models in Schwinger Hilbert spaces as well as models in the space of wavefunctions on the group manifold $SU(2)$. Finally, in Section 5.3 we analyze how the remodeling geometry may be used to associate a Lagrangian manifold in a certain product phase space to a co-isotropic manifold. This relationship enables us to consider the quantization of co-isotropic manifolds.

5.1 $3nj$ -Symbols ($n \geq 2$)

We define $k \equiv n + 2$ for the rest of this section. Let \mathcal{Z}_k be the space of kj -intertwiners. When $n = 1$ ($k = 3$) this space is non-trivial iff the three irreps involved form a triangle-allowed triplet, in which case the space \mathcal{Z}_3 of $3j$ -intertwiners is one-dimensional. When $n = 2$ and the four irreps satisfy the polygon inequalities the space \mathcal{Z}_4 of $4j$ -intertwiners is non-trivial and, in general, has a dimension greater than one. As we saw in Section 4, we may put different bases on \mathcal{Z}_4 , corresponding to different ways of coupling the four angular momenta into an $SU(2)$ -invariant. The $6j$ -symbol is then interpreted as the components for a unitary change-of-basis in \mathcal{Z}_4 . In general, we define the $3nj$ -symbols for $n \geq 2$ which are interpreted

as the components for a unitary change-of-basis for the space of $(n + 2)j$ -intertwiners \mathcal{Z}_{n+2} .

The $3nj$ -symbols have applications in molecular, atomic, and nuclear physics but our primary interest in them comes from their applications to quantum gravity. Just as the $6j$ -symbol is the basic building block of the Ponzano-Regge model [27] for the state sum in $3d$ -Euclidean quantum gravity, the $15j$ -symbol is the basic building block of models for $4d$ -Lorentzian gravity. The $15j$ -symbol appears, for example, in analogues of the Ponzano-Regge and Turaev-Viro [29] models in $4d$ such as the Ooguri model [30] and the Archer [31, 32], Crane-Yetter [33], and Roberts [34] models which involve the q -deformed $15j$ -symbol. Of particular note is the Barrett-Crane model [35] which generalizes these models to a Lorentzian setting. The $15j$ -symbol enters because the amplitude is fundamentally a state sum over four-simplices. The fifteen irrep labels represent the areas of the ten triangular faces of the four-simplex as well as five recoupling irreps. The $15j$ -symbol has also recently been used in loop quantum gravity and spin-foam models by Engle *et al* [36], Livine and Speziale [93], and Freidel and Krasnow [37].

We start in Section 5.1.1 by introducing “ k -valent nodes” into the spin network notation. These nodes allow us to discuss general kj -intertwiners. With this notation we then proceed to construct the myriad inner product models of the $3nj$ -symbols, paying special attention to the $9j$ -symbol and the $15j$ -symbol. Then in Section 5.1.2 we construct the remodeling algebras that link these inner product models together. Finally in Section 5.1.3 we construct the remodeling geometries corresponding the the remodeling algebras and describe how the Kapovich-Millson shape space [77, 78] emerges as a symplectic reduction of the “ kj -model” of the $3nj$ -symbol.

5.1.1 Inner Product Models of the $3nj$ -Symbol

Define $k \equiv n + 2$ for this section. Given k -irrep labels j_1, \dots, j_k , we may schematically write a general state in \mathcal{Z}_k as

$$\begin{array}{c}
 \nearrow 1 \\
 \vdots \\
 \circ k \\
 \vdots \\
 \searrow k
 \end{array} \in \mathcal{Z}_k. \tag{5.1.1}$$

We call such a spin network a “ k -valent node.” Since the space of intertwiners \mathcal{Z}_k greater than one-dimensional for $k \geq 4$ ($n \geq 2$) we need to label or “color” such nodes when they occur to indicate which element of \mathcal{Z}_k the network represents. The coloring of the k -valent node in spin network 5.1.1 is indicated by the label “ v ” to the left of the node.

One way of representing such a node is to expand it in a basis of recoupled angular momenta, as we did with the “butterfly states” in \mathcal{Z}_4 in Section 4.1.3. In particular, consider a trivalent spin network containing n trivalent nodes connected by $n - 1$ internal lines (each carrying an irrep label) and $n + 2 = k$ external lines (each carrying an irrep label) ending in ket chevrons. The internal lines represent a definite coupling scheme in this network.

Following terminology from Feynman diagrams we call such networks “tree-level networks” since there are no internal “loops” or “bubbles.” A basis of \mathcal{Z}_k may be formed from any tree-level network, with the individual basis states differing only by the irrep labels on the $n - 1$ internal lines. For example, a general four-valent node may be written,

$$\begin{array}{c} \nearrow a \\ \circlearrowleft 4 \\ \searrow b \end{array} \begin{array}{c} \nearrow d \\ \circlearrowright v \\ \searrow c \end{array} = \sum_{ab} c_{ab} \begin{array}{c} \nearrow a \\ \bullet \\ \searrow b \end{array} \begin{array}{c} \text{---} ab \text{---} \\ | \\ \bullet \end{array} \begin{array}{c} \nearrow d \\ \bullet \\ \searrow c \end{array}, \tag{5.1.2}$$

where v is a coloring of the four-valent intertwiner and we have expanded \mathcal{Z}_4 in the (ab) -coupled basis of Eq. 4.1.9 and c_{ab} are the expansion coefficients.

The $3nj$ -symbol is fundamentally a matrix element of a transformation from one basis in the space \mathcal{Z}_k of kj -intertwiners to another. The bases in question represent the different recoupling schemes for the k angular momenta. We express any $3nj$ -symbol spin network as

$$\text{“}3nj\text{-symbol”} = \begin{array}{c} 1 \\ \curvearrowright \\ \circlearrowleft k \\ v_1 \end{array} \begin{array}{c} \curvearrowleft \\ \vdots \\ \curvearrowright \\ k \end{array} \begin{array}{c} \circlearrowright k \\ v_2 \end{array}, \tag{5.1.3}$$

where each of the two k -valent nodes stands for a specific tree-level network in \mathcal{Z}_k representing a particular recoupling scheme. The colorings v_1 and v_2 label the recoupling schemes and the irrep labels on the internal lines. The “ $3n$ ” j labels of the $3nj$ -symbol are the $n + 2$ irreps $1, \dots, k$ explicitly shown in Eq. 5.1.3 and the two sets of $n - 1$ irrep labels on the internal lines of the expansion of the k -valent nodes into tree-level networks. For example, $n = 2$ gives the $6j$ -symbol. In the “coupled” labeling, we may express Eq. 4.0.1 as the four-valent spin network

$$\left\{ \begin{array}{ccc} j_1 & j_2 & j_{12} \\ j_3 & j_4 & j_{23} \end{array} \right\} = \begin{array}{c} 1 \\ \curvearrowright \\ \circlearrowleft 4 \\ 12 \end{array} \begin{array}{c} \curvearrowleft \\ 2 \\ \curvearrowright \\ 3 \end{array} \begin{array}{c} \circlearrowright 4 \\ 23 \end{array}, \tag{5.1.4}$$

where the four-valent nodes on the left and right represent the dual of the spin network in Eq. 4.2.31 and the spin network in Eq. 4.2.35, respectively. The colorings “12” and “23” on the nodes indicate the intermediate (hidden) couplings in the four-valent intertwiners.

By cutting the spin network in Eq. 5.1.3 down the middle we form an inner product in

momenta on an equal footing and is thus the most symmetric model. In the case of $n = 2$, this is the $12j$ -model of the $6j$ -symbol as defined in Eqs. 4.2.12 and 4.2.7.

The kj -, $2kj$ -, and $6nj$ -models are not the only models that may be formed. Let $m \neq 2n$ be a factor of $2n$. Then we may form a $\frac{2n(m+2)}{m}j$ -model of the $3nj$ symbol by splitting the spin network into a set of $\frac{2n}{m}(m+2)j$ -intertwiner states and $\frac{n(m+2)}{m}2j$ -intertwiner states. Note that $m = n$ reproduces the $2kj$ -model of Eq. 5.1.6 and $m = 1$ reproduces the $6nj$ -model of Eq. 5.1.7. Another interesting distinct case for $n > 2$ is $m = 2$, which is a $4nj$ -model containing n $4j$ -intertwiner states and $2n$ $2j$ -intertwiner states. Thus we may always form a “ $4j$ -vs.- $2j$ ” model of the $3nj$ -symbol,

$$\text{“}4nj\text{-Model”}: \quad n \times \begin{array}{c} \swarrow \quad \searrow \\ \textcircled{4} \\ \nwarrow \quad \nearrow \end{array}, \quad 2n \times \begin{array}{c} \swarrow \quad \searrow \\ | \\ \nwarrow \quad \nearrow \end{array}. \quad (5.1.8)$$

One consequence of this construction is that we may insert resolutions of the identity in different bases in \mathcal{Z}_4 to each of the $4j$ -intertwiner states in the $4nj$ -model and thus express the $3nj$ -symbols as sums of products of n $6j$ -symbols [7, 8].

Consider for example the $9j$ -symbol ($n = 3, k = 5$),

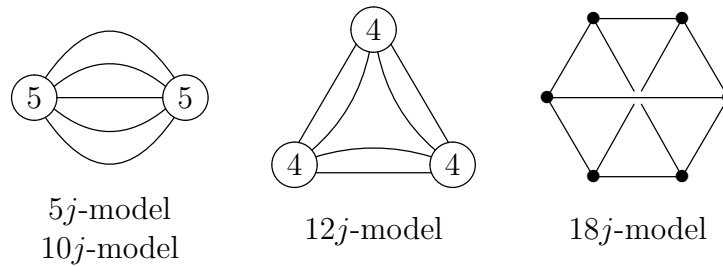
$$\left\{ \begin{array}{ccc} j_1 & j_2 & j_{12} \\ j_3 & j_4 & j_{34} \\ j_{13} & j_{24} & j_5 \end{array} \right\} = \begin{array}{c} \begin{array}{c} \bullet \\ | \\ \begin{array}{c} \swarrow \quad \searrow \\ \text{---} \\ \nwarrow \quad \nearrow \end{array} \\ | \\ \bullet \end{array} \\ \begin{array}{c} \swarrow \quad \searrow \\ \text{---} \\ \nwarrow \quad \nearrow \end{array} \\ \begin{array}{c} \bullet \\ | \\ \begin{array}{c} \swarrow \quad \searrow \\ \text{---} \\ \nwarrow \quad \nearrow \end{array} \\ | \\ \bullet \end{array} \\ \begin{array}{c} \swarrow \quad \searrow \\ \text{---} \\ \nwarrow \quad \nearrow \end{array} \\ \bullet \end{array}, \quad (5.1.9)$$

where we use a coupled, rather than symmetric, labeling and the convention that all lines have arrows pointing away from the trivalent nodes and towards the stubs. In addition to the $5j$ -model there are three relevant models of the $9j$ -symbol: $m = 3$ gives a $10j$ -model (a $5j$ -vs.- $2j$ model), $m = 2$ gives a $12j$ -model (a $4j$ -vs.- $2j$ model), and $m = 1$ gives the symmetric $18j$ -model (a $3j$ -vs.- $2j$ -model). The spin networks for these models are sketched schematically (without decorations such as irrep labels, stubs, arrows, or chevrons) in Figure 5.1.1.

As stated earlier, the four-valent spin network for $9j$ -symbol may be used to express the $9j$ -symbol as a sum over a triple product of $6j$ -symbols [66],

$$\left\{ \begin{array}{ccc} j_1 & j_2 & j_{12} \\ j_3 & j_4 & j_{34} \\ j_{13} & j_{24} & j_5 \end{array} \right\} = \sum_J (-1)^{2J} \sqrt{2J+1} \left\{ \begin{array}{ccc} j_1 & j_2 & j_{12} \\ j_{34} & j_5 & J \end{array} \right\} \left\{ \begin{array}{ccc} j_3 & j_4 & j_{34} \\ j_2 & J & j_{24} \end{array} \right\} \left\{ \begin{array}{ccc} j_{13} & j_{24} & j_5 \\ J & j_1 & j_3 \end{array} \right\}. \quad (5.1.10)$$

Because of its central importance to $4d$ -Lorentzian gravity spin-foam models we also mention here the various models of the $15j$ -symbol ($n = 5$). There are in fact five physically

Figure 5.1.1: Spin network schematics for models of the $9j$ -symbol.

distinct types of $15j$ -symbol, which in Yutsis [7] are called the $15j$ -symbols of the first through fifth kind. We also refer to these in this section as Type I through Type V. The trivalent spin networks are sketched schematically (without decorations such as irrep labels, stubs, arrows, or chevrons) in Figure 5.1.2(a) through (e). These may be cut as described above to produce a $30j$ -model ($m = 1$ or $3j$ -vs- $2j$ model). For each of the five types of $15j$ -symbol there is a single $30j$ -model. We may also recouple these networks into a spin network containing a pair of seven-valent nodes. This spin network may be cut as described above to produce the $7j$ - and $14j$ -models of the $15j$ -symbols. Note that there are may be different $7j$ - and $14j$ -models for a given type of $15j$ -symbol depending on how the angular momenta have been recoupled. All $7j$ - and $14j$ -models may be schematically represented by the seven-valent spin network shown in Figure 5.1.2(j). Finally, we may couple pairs of trivalent nodes together in the trivalent spin networks to produce four-valent spin networks. There are four distinct types of four-valent spin networks that occur when the five types of trivalent spin networks are coupled in this fashion. We label these in this section as Types A through D. The four-valent spin networks that represent the various types of $15j$ -symbol are shown in Figure 5.1.2(f) through (i). Cutting the four-valent spin networks as described above yields various $20j$ -models. The $15j$ -symbol of the first kind (Type I) may be recoupled to give all four types of four-valent spin networks and thus admits four distinct $20j$ -models. The $15j$ -symbol of the second kind (Type II) on the other hand can not be recoupled to give the four-valent spin network of Type D thus admits only three distinct $20j$ -models (corresponding to the four-valent spin networks of Type A, B, and C). Similarly the $15j$ -symbol of the fourth kind (Type IV) admits three $20j$ -models, corresponding to the four-valent spin networks of Type B, C, and D. The $15j$ -symbol of the third kind (Type III) only admits two distinct $20j$ -models, corresponding to the four-valent spin networks of Type C and D. Finally, the $15j$ -symbol of the fifth kind (Type V) only admits a single $20j$ -model, corresponding to the four-valent spin network of Type D.

Of particular importance to the Barrett-Crane model is the four-valent spin network of Type D, as shown in Figure 5.1.2(i). We call this spin network the “four-simplex spin network” since it is comprised of five four-valent nodes with each node connected to every other node by an edge, just as the spin network for the $6j$ -symbol may be considered a “three-simplex” or “tetrahedron spin network” since it is comprised of four three-valent nodes with each node connected to every other node by an edge. The four-simplex spin network

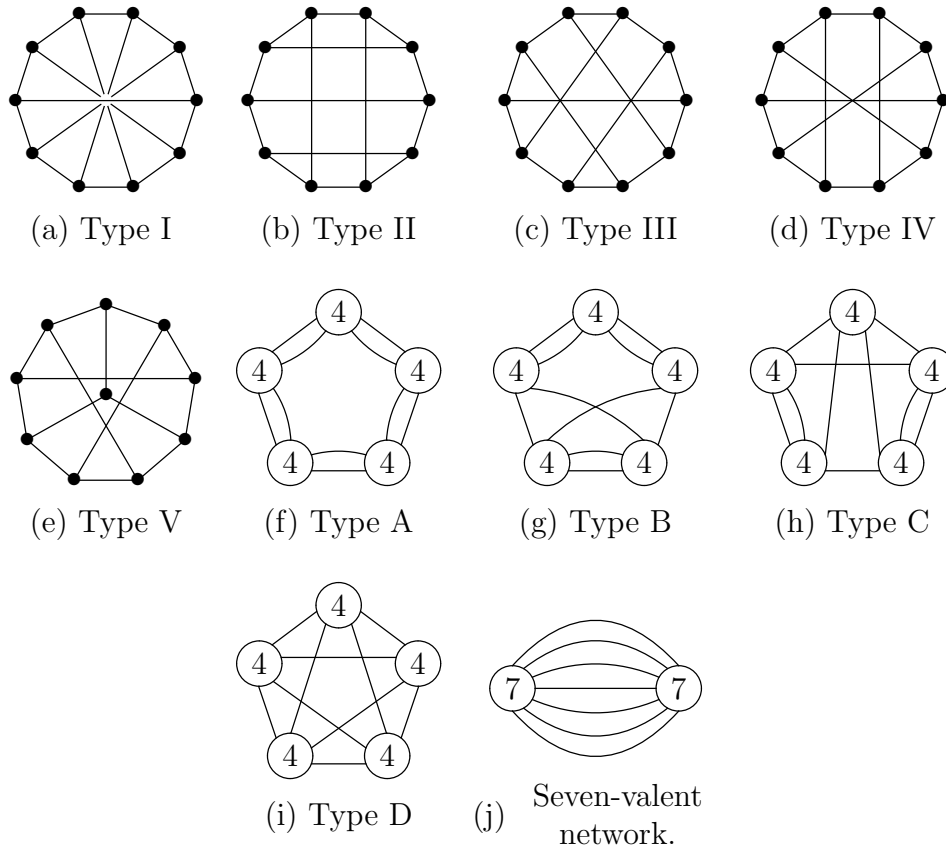


Figure 5.1.2: Spin network schematics for the various types of $15j$ -symbol.

represents the “Riemannian $10j$ -symbol” (Barrett and Crane [35], Barrett [94], Barrett and Williams [95], Baez and Christensen [96], Christensen and Egan [97], Baez *et al* [49], Freidel and Louapre [50], Barrett and Steele [98]). The ten irrep values (one for each of the ten lines connecting two four-valent nodes) physically represent the areas of the ten triangular faces in the four-simplex. Note that five additional colorings are needed for each of the five four-valent nodes in the $10j$ -spin network. If the four-valent nodes are allowed to represent arbitrary elements of the space of $4j$ -intertwiners then this network may be expanded into a basis of $15j$ -symbols of the first, third, fourth, or fifth kind (but not the second kind). For example, Baez and Christensen [96] use an expansion of the four-simplex spin network into $15j$ -symbols of the first kind in order to prove the positivity of the $10j$ -symbol.

5.1.2 Remodeling Algebras for the $3nj$ -Symbols

Just as we connected the symmetric $12j$ -model of the $6j$ -symbol with the small $4j$ -model of the $6j$ -symbol in Section 4.2 we may connect the symmetric $6nj$ -model to the small kj -model of the $3nj$ symbol via two applications of the remodeling of an inner product. The

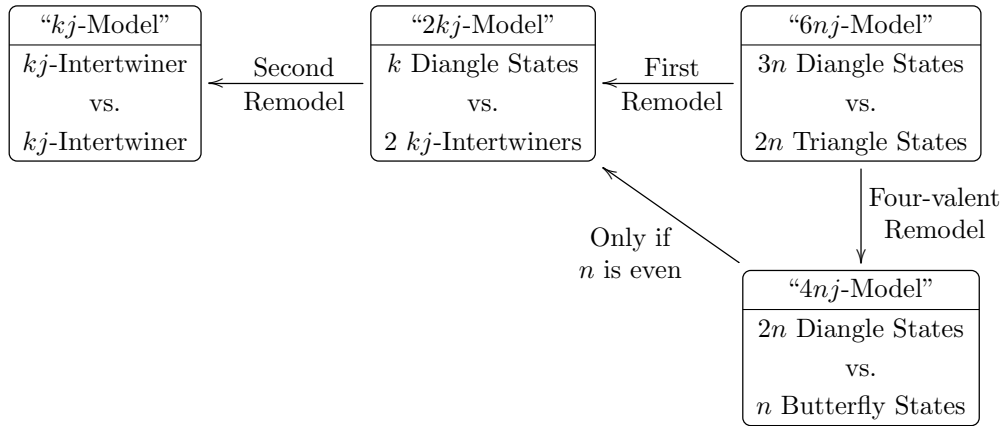


Figure 5.1.3: Schematic of the spaces and states in the remodeling algebras for the $3nj$ -symbols.

first remodel connects the symmetric $6nj$ -model (represented schematically by a trivalent spin network) to an intermediate $2kj$ -model (represented schematically by a k -valent spin network). The product space inner product serves as the $6nj$ -model in this case and the target space inner product serves as the $2kj$ -model. Note that to set up such a remodeling algebra we need to commit to a particular coupling scheme for the two kj -intertwiner states that appear in the $2kj$ -model.

The second remodel connects the “dual $2kj$ -model” with the “dual kj -model” (also represented schematically by a trivalent spin network). The dual inner product models are used here for the same reason they were used in the $6j$ -symbol, as will be discussed below. The dual $2kj$ -model is the product space inner product and the target space inner product produces the dual kj -model. We may also perform a separate remodel to connect the $6nj$ -model to the $4nj$ -model (represented schematically by a four-valent spin network). The $6nj$ -model again serves as the product space model but the target-space model is now the $4nj$ -model inner product. If n is even then the $4nj$ -model may itself serve as a product space model for a remodel connecting it to the $2kj$ -model. However if n is odd no such direct remodel exists. A schematic of the remodelings for the $3nj$ -symbol is shown in Figure 5.1.3. These remodels are by no means an exhaustive list (in particular we may also connect the $6nj$ -model to any of the $\frac{2n(m+2)}{m}j$ -models and other remodels may exist between these models) but rather a highlighting of the remodels that connect the models of most physical interest and calculational use.

To construct the remodeling algebra for the first remodel we first begin with the standard trivalent spin network with stubs inserted on each line and arrows pointing away from all trivalent nodes and towards all stubs. The remodel is then constructed by severing all $6nj$ legs of the trivalent spin network. This network can then be separated into a set of $2n$ $3j$ -intertwiners and $3n$ $2j$ -intertwiners. We separate these into three sets which act as the b -, M -, and dual of the a -state for the first remodel. In particular the $2n$ $3j$ -intertwiners is

a ket in the $6nj$ -Hilbert space \mathcal{H}_{6nj} and acts as the M -state $|M_1\rangle$ for the first remodel,

$$|M_1\rangle = \bigotimes_{\Delta=1}^{2n} \begin{array}{c} \uparrow \\ \Delta_1 \\ \bullet \\ \swarrow \Delta_2 \quad \searrow \Delta_3 \end{array} \in \mathcal{H}_{6nj}. \quad (5.1.11)$$

In Eq. 5.1.11 Δ indexes the $2n$ trivalent nodes and Δ_1 , Δ_2 , and Δ_3 are the three Hilbert space labels for the three angular momenta coupled together at a given trivalent node. The remaining $3n$ $2j$ -intertwiner states form the dual of the product state. Therefore the product state in the first remodel is

$$|ab_1\rangle = \begin{array}{c} \uparrow \\ 1' \\ | \\ 1 \\ \downarrow \end{array} \cdots \begin{array}{c} \uparrow \\ 3n' \\ | \\ 3n \\ \downarrow \end{array} \in \mathcal{H}_{6nj}. \quad (5.1.12)$$

The $6nj$ -model of the $3nj$ -symbol is then the inner product of the ab -state with the M -state,

$$\text{“}6nj\text{-Model”}: \langle ab_1 | M_1 \rangle. \quad (5.1.13)$$

Note that this model is the product space model for both the first remodel and the “four-valent remodel” referred to in Figure 5.1.3.

The a - and b -states for the first remodel are found by splitting the product state spin network into two subnetworks. The a -state is an element of the target space \mathcal{H}_{2kj} of the first remodel so its spin network is made of the subnetwork of Eq. 5.1.12 containing ket chevrons for the set of primed and unprimed Schwinger spaces for the k irrep labels that appear in the $2kj$ -model under consideration.

$$|a_1\rangle = \begin{array}{c} \uparrow \\ r'_1 \\ | \\ r \\ \downarrow \end{array} \cdots \begin{array}{c} \uparrow \\ r'_k \\ | \\ r_k \\ \downarrow \end{array} \in \mathcal{H}_{2kj}. \quad (5.1.14)$$

The dual of the b -state is then the remaining pieces of the spin network,

$$|b_1\rangle = \bigotimes_{r \neq r_1, \dots, r_k} \begin{array}{c} \uparrow \\ r' \\ | \\ r \\ \downarrow \end{array} \in \mathcal{H}_{4(n-1)j}. \quad (5.1.15)$$

Note that since $k \equiv n + 2$, the source space in the first remodel contains $6n - 2k = 4(n - 1)$ copies of the dual Schwinger Hilbert space.

The M -state in the first remodel acts as a map: $\mathcal{H}_{4(n-1)j}^* \rightarrow \mathcal{H}_{6nj}$. In particular, the $2n$ $3j$ -networks in Eq. 5.1.11 can be broken up into two set of n $3j$ -networks and each of these

sets acts as a map from a $2(n-1)j$ -dual Schwinger Hilbert space to a kj -Hilbert space. The b -state itself contains two pairs of $(n-1)2j$ -intertwiners which are used to couple the two sets of n trivalent nodes into a pair of kj -intertwiners and the $2j$ -intertwiners in the b -state become the internal lines of these intertwiners. Thus the β -state of the first remodel is

$$|\beta_1\rangle = \begin{array}{c} \begin{array}{c} \nearrow 1 \\ \circlearrowleft k \\ \searrow k \end{array} \\ v_1 \end{array} \quad \begin{array}{c} \begin{array}{c} \nearrow 1' \\ \circlearrowleft k \\ \searrow k' \end{array} \\ v_2 \end{array} \in \mathcal{H}_{2kj}, \quad (5.1.16)$$

where v_1 and v_2 represent the coloring of the kj -nodes. The target space model is thus the $2kj$ -model of the $3nj$ -symbol,

$$\text{“}2kj\text{-Model”}: \langle a_1 | \beta_1 \rangle. \quad (5.1.17)$$

Construction of the second remodeling algebra takes the dual of the $2kj$ -target space model of the first remodel as the product space and thus is an inner product in the dual space \mathcal{H}_{2kj}^* with $|\beta_1\rangle$ now acting as the dual of the product state $\langle ab_2 |$ of the second remodel and $\langle a_1 |$ acting as the M -state $\langle M_2 |$ of the second remodel,

$$\text{“Dual } 2kj\text{-Model”}: \langle M_2 | ab_{12} \rangle = \langle a_1 | \beta_1 \rangle. \quad (5.1.18)$$

The map state in the second remodel is thus the set of k $2j$ -intertwiner bras,

$$\langle M_2 | = \begin{array}{c} \begin{array}{c} \diagup \\ r'_1 \\ \diagdown \end{array} \\ \vdots \\ \begin{array}{c} \diagdown \\ r_1 \\ \diagup \end{array} \end{array} \cdots \begin{array}{c} \begin{array}{c} \diagup \\ r'_k \\ \diagdown \end{array} \\ \vdots \\ \begin{array}{c} \diagdown \\ r_k \\ \diagup \end{array} \end{array} \in \mathcal{H}_{2kj}^*, \quad (5.1.19)$$

where the ‘2’ subscript in $\langle M_2 |$ is used to highlight that this is the map state of the *second* remodel. In particular, we treat $\langle M_2 |$ as a map $:\mathcal{H}_{kj'} \rightarrow \mathcal{H}_{kj}^*$, where \mathcal{H}_{kj} and $\mathcal{H}_{kj'}$ are kj -Hilbert spaces for two different sets of k angular momenta. The product state is just the dual of the β -state of the first remodel,

$$\langle ab_2 | = \begin{array}{c} \begin{array}{c} \diagdown \\ \vdots \\ \diagup 1 \end{array} \\ \vdots \\ \begin{array}{c} \diagdown \\ \vdots \\ \diagup k \end{array} \end{array} \begin{array}{c} \begin{array}{c} \diagdown \\ \vdots \\ \diagup 1' \end{array} \\ \vdots \\ \begin{array}{c} \diagdown \\ \vdots \\ \diagup k' \end{array} \end{array} \in \mathcal{H}_{2kj}^*, \quad (5.1.20)$$

bras rather than $2(n-1)$ as in the first remodel. The map M acts as n versions of a map $:\mathcal{H}_{2j}^* \rightarrow \mathcal{H}_{4j}$ and the action is to map a $2j$ -intertwiner bra into a $4j$ -intertwiner ket as described in Section 4.2.2.

5.1.3 Remodeling Geometries for the $3nj$ -Symbols

As in Sections 3.2.1 and 4.3.1, each of the Hilbert spaces \mathcal{S} in the remodeling algebra corresponds semiclassically to a copy of the Schwinger phase space Σ and thus the phase spaces in the remodeling geometries for the $3nj$ -symbol are products of Schwinger phase spaces or their duals. The product, source, and target phase spaces for the first remodel are labeled Φ_{6nj} , $\Phi_{2(n-1)j}^*$, and Φ_{2kj} , respectively while the product, source, and target phase spaces for the second remodel are labeled Φ_{2kj}^* , $\Phi_{kj'}$, and Φ_{kj}^* . The dual map $G_{kj} : \Phi_{kj} \rightarrow \Phi_{kj}^*$ is used to map the Lagrangian manifolds for the kj -model of the first remodel to the relevant manifolds of the dual kj -model of the second remodel. Similarly, we introduce the kj -phase space Φ_{kj} and the dual map $G_{kj}^{-1} : \Phi_{kj}^* \rightarrow \Phi_{kj}$ to map the manifolds from the dual kj -model of the second remodel to the manifolds of the regular kj -model.

Each of the states in the remodeling algebras are tensor products of intertwiner states and thus the Lagrangian manifolds that support the semiclassical approximations of these states are simply Cartesian products of the diangle, triangle, and butterfly manifolds described in Section 4.1 as well as k -edged polygon manifolds that support the semiclassical approximations of the kj -intertwiner states. In general these manifolds are the level sets of the k conditions on the k outer edge lengths of the polygon ($I_r = j_r + 1/2$ for $r = 1, \dots, k$), the closure condition $\mathbf{J}_T \equiv \sum_1^k \mathbf{J}_r = \mathbf{0}$, as well as $n-1$ other conditions specified by the coloring of the intertwiner state, such as the edge length $|\mathbf{J}_{12}|$ for the $k=4$ (butterfly) manifolds,

$$\mathcal{L}_{kj} \subset \left(\begin{array}{ccc} I_1 & \cdots & I_k \\ J_1 & & J_k \end{array} \begin{array}{c} \mathbf{J}_T \\ \mathbf{0} \end{array} \right) \subset \Phi_{kj}. \quad (5.1.24)$$

Let $\mathcal{L}_{kj,1}$ and $\mathcal{L}_{kj,2}$ be the two Lagrangian manifolds supporting the semiclassical approximations of the two kj -intertwiner states in the kj -model. The stationary phase set in this case is the intersection $\mathcal{L}_{kj,1} \cap \mathcal{L}_{kj,2}$. By Eq. 5.1.24 this intersection is the union of group orbits for the group $G = U(1)^k \times SU(3)$ generated by I_r , $r = 1, \dots, k$ and \mathbf{J}_T . This is a $(k+3)$ -dimensional group. Symplectic reduction by this group yields a reduced kj -phase space Φ_{kj}^R . This phase space is where the amplitude determinant and Maslov index for the kj -symbol are easiest to compute. This reduction yields the Kapovich-Millson shape space [77, 78] for a k -sided non-planar polygon. This symplectic reduction eliminates a total of $(k+3)$ degrees of freedom from the $2k$ -degree of freedom phase space Φ_{kj} . The reduced phase space therefore contains $k-3$ or $n-1$ degrees of freedom and $\dim \Phi_{kj}^R = 2(n-1)$. As a result, the amplitude for the $3nj$ -symbol may be written in terms of the determinant of an $(n-1) \times (n-1)$ matrix of Poisson brackets. For example, in Section 4.5.1 the amplitude determinant of the $6j$ -symbol ($n=2$) was a single Poisson bracket. Similarly, in Haggard and Littlejohn [45] the amplitude of the $9j$ -symbol ($n=3$) was expressed in terms of a 2×2 matrix of Poisson brackets.

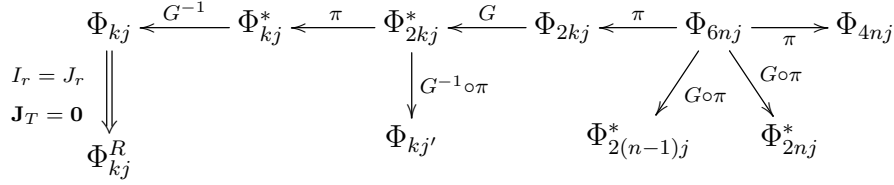


Figure 5.1.4: Phase spaces and the maps between them in the remodeling geometries for the $3nj$ -symbol.

Model	Phase Space	Dimension
$6nj$ -model	Φ_{6nj}	$24n$
$4nj$ -model	Φ_{4nj}	$16n$
$2kj$ -model	Φ_{2kj}	$8k$
Dual $2kj$ -model	Φ_{2kj}^*	$8k$
Dual kj -model	Φ_{kj}^*	$4k$
kj -model	Φ_{kj}	$4k$
Reduced kj -model	Φ_{kj}^R	$2(n-1)$

Table 5.2: Phase spaces for models in the remodeling geometries of the $3nj$ -symbols.

The phase space for the $6nj$ -model has the largest dimensionality ($24n$) but treats all $6n$ angular momenta on an equal footing. Therefore this is the most symmetric model and construction of the path and evaluation of the action integral should be easiest in this space.

Figure 5.1.4 shows the phase spaces in the two remodeling geometries and the relevant maps between these spaces. Subscripts on the dual maps and projection maps have been omitted. Table 5.2 lists the phase spaces, their roles in the remodeling geometries, and their dimensions.

As we demonstrated in Chapter 4, the amplitude and Maslov contributions to the semiclassical analysis of the $3nj$ -symbol are easiest to compute in the reduced kj -phase space and the action integral is easiest to compute in the symmetric $6nj$ -phase space. For example, Haggard and Littlejohn [45] used a symplectic reduction of the $5j$ -model to derive the amplitude of the $9j$ -symbol and reported a Ponzano-Regge-like term for the action integral that resulted from an analysis of the $18j$ -model. The derivation of this action integral follows very closely the derivation from Section 4.4.1 and the analyses of Roberts [2] and Hedeman *et al* [51] for the Ponzano-Regge phase in the $6j$ -symbol.

5.2 g -Insertions

As stated in Chapter 1, a spin network basis state of loop quantum gravity consists of a decorated spin networks along with a specification of the knot class of the embedding of the network into a three-dimensional spacelike slice of spacetime [17, 5]. The basis states can be identified with “wavefunctionals” of the connection, maps from the space of connections

to \mathbb{C} [18]. Acting a basis state on the connection amounts to inserting an $SU(2)$ rotation operator on each edge of the spin network to represent the holonomy along the embedding of that edge. We call the addition of these $SU(2)$ rotation operators to a spin network edge a “ g -insertion”.

The $SU(2)$ group action $\hat{U}(g) : \mathcal{S} \rightarrow \mathcal{S}$ is a linear map on the Schwinger Hilbert space that subjects the states in \mathcal{S} to a rotation. Following Stedman [8], we express the spin network for $\hat{U}(g)$ as

$$\hat{U}(g) = \left\langle \begin{array}{c} | \\ g \\ \hline \leftarrow \quad \rightarrow \end{array} \right\rangle. \quad (5.2.1)$$

The dashed line represents the g -insertion and is oriented so that it is counterclockwise of the bra chevron and clockwise of the ket chevron. Note that inserting the identity element $e \in SU(2)$ yields the identity map. Generalizing the rules for Hermitian conjugation established in Aquilanti *et al* [1], the spin network for $\hat{U}^\dagger(g)$ and thus, by unitarity, $\hat{U}(g^{-1})$, may be expressed as,

$$\hat{U}^\dagger(g) = \left\langle \begin{array}{c} \hline \leftarrow \quad \rightarrow \\ | \\ g \end{array} \right\rangle = \left\langle \begin{array}{c} | \\ g^{-1} \\ \hline \leftarrow \quad \rightarrow \end{array} \right\rangle = \hat{U}(g^{-1}). \quad (5.2.2)$$

Note that the spin networks in Eqs. 5.2.1 and 5.2.2 may also represent maps $\mathcal{S}^* \rightarrow \mathcal{S}^*$ in which case the group action on \mathcal{S}^* is represented by $\hat{U}^\dagger(g)$ rather than $\hat{U}(g)$. By the group representation property $\hat{U}(g)\hat{U}(h) = \hat{U}(gh)$, two consecutive g -insertions can be combined to a single g -insertion,

$$\left\langle \begin{array}{c} | \\ g \\ \hline \leftarrow \leftarrow \rightarrow \end{array} \right\rangle = \left\langle \begin{array}{c} | \\ gh \\ \hline \leftarrow \quad \rightarrow \end{array} \right\rangle, \quad \left\langle \begin{array}{c} \hline \leftarrow \leftarrow \rightarrow \\ | \\ g \end{array} \right\rangle = \left\langle \begin{array}{c} \hline \leftarrow \quad \rightarrow \\ | \\ hg \end{array} \right\rangle. \quad (5.2.3)$$

The components of the $SU(2)$ rotation matrices in the standard angular momentum basis form the D -matrices (also called the Wigner rotation matrices). In Section 5.2.1 we construct a remodeling algebra which connects two models of the D -matrix, one which takes place in a $2j$ -Schwinger Hilbert space and one which takes place in a $1j$ -Schwinger Hilbert space. Then in Section 5.2.2 we introduce a third model, which treats the D -matrix as a wavefunction on the group manifold $SU(2)$. Thus the third model takes place in the Hilbert space $L^2SU(2)$. We construct a remodeling algebra connecting this third model with the $2j$ -model of the D -matrix and identify an isomorphism between $L^2SU(2)$ and a subspace of $\mathcal{S} \otimes \mathcal{S}^*$. We also explore the phase space $T^*SU(2)$ which contains the Lagrangian manifolds that support the semiclassical approximation of states in $L^2SU(2)$. In Section 5.2.3 we discuss intertwiners in the context of g -insertions. Finally, in Section 5.2.4 we discuss how the remodeling algebras for the $3nj$ -symbols are modified to accommodate general g -inserted spin networks. We conclude that section by discussing how the amplitudes in loop quantum gravity may be interpreted as g -inserted spin networks.

5.2.1 Models of the D -Matrix

The D -matrices (or the Wigner rotation matrices) are the components of $\hat{U}(g)$ with respect to the standard angular momentum basis of \mathcal{S} ,

$$D_{mm'}^j(g) = \langle jm | \hat{U}(g) | jm' \rangle = *m \leftarrow \begin{array}{c} | g \\ \vdots \\ j \end{array} \leftarrow m'. \quad (5.2.4)$$

We may consider the D -matrix as a g -inserted version of the inner product $\langle jm | jm' \rangle$. The asymptotic formula for the D -matrices has been known for a long time (Brussard and Tolhoek [99], Ponzano and Regge [27], Braun *et al* [100], Sokolovski and Connor [101], Littlejohn and Yu [76]) but it is useful to see how the remodeling algebra applies to this matrix element to elucidate of the geometrical issues that arise in its asymptotics.

We set up the remodeling algebra for the D -matrix by considering the matrix element in Eq. 5.2.4. The remodeling algebra is formed by first cutting the spin network in Eq. 5.2.4 on both of the legs,

$$*m \text{---} \begin{array}{c} \llcorner \\ j \end{array} \llcorner \begin{array}{c} | g \\ \vdots \\ j \end{array} \llcorner \begin{array}{c} \llcorner \\ j \end{array} \text{---} m'. \quad (5.2.5)$$

We make the choice in this spin network to place an irrep label on all three segments. The operator in the middle segment is thus the projection of the rotation operator $\hat{U}(g)$ onto the carrier space \mathcal{C}_j . We write this restriction $\hat{U}_j(g)$ to distinguish it from the rotation operator acting on the full Schwinger Hilbert space. This map serves as the M -state of the remodeling algebra,

$$\hat{M} = \hat{U}_j(g) = \left\langle \begin{array}{c} | g \\ \vdots \\ j \end{array} \right\rangle \in \mathcal{S} \otimes \mathcal{S}'^* \quad (5.2.6)$$

We can just as well set up the remodeling algebra with the full rotation operator $\hat{U}(g)$ acting as the M -state. However, the choice of $\hat{U}_j(g)$ has the advantage that the states in the remodeling algebra and the Lagrangian manifolds in the remodeling geometry now share a larger common symmetry group. We take the source Hilbert space to be \mathcal{S}' and the target Hilbert space to be \mathcal{S} , where the prime is used to distinguish between the two copies of the Schwinger Hilbert space. The map $\hat{U}_j(g)$ is an element of the product Hilbert space $\mathcal{S} \otimes \mathcal{S}'^*$. Note that the image of $\hat{U}_j(g)$ is the carrier subspace $\mathcal{C}_j \subset \mathcal{S}$ and the orthogonal compliment of the kernel of $\hat{U}_j(g)$ is the carrier subspace $\mathcal{C}_j \subset \mathcal{S}'$.

The a - and b -states of this remodeling algebra are the standard basis kets $|jm\rangle \in \mathcal{S}$ and $|jm'\rangle \in \mathcal{S}'$, respectively, and the product state is $|jm\rangle\langle jm'| \in \mathcal{S} \otimes \mathcal{S}'^*$,

$$|a\rangle = m \xrightarrow{j} \in \mathcal{S}; \quad |b\rangle = m' \xrightarrow{j} \in \mathcal{S}'. \quad (5.2.7)$$

$$|a\rangle\langle b| = \left\langle \begin{array}{c} j \\ \text{---} m \end{array} \right\rangle *m' \xrightarrow{j} \in \mathcal{S} \otimes \mathcal{S}'^*. \quad (5.2.8)$$

Note that $|b\rangle \in (\ker \hat{U}_j(g))_\perp$.

Finally, the β -state is the map $\hat{U}_j(g)$ acting on the b -state,

$$|\beta\rangle = \hat{U}_j(g)|jm'\rangle = \left\langle \begin{array}{c} | \\ \vdots \\ g \\ | \\ j \end{array} \leftarrow m' \in \mathcal{S} \right. \quad (5.2.9)$$

The β -state is a simultaneous eigenstate of \hat{I} and a component of $\hat{\mathbf{J}}$. We demonstrate thus using the adjoint formula, which relates the action of the $SU(2)$ rotation operators with the adjoint representation generators $\hat{\mathbf{J}}$,

$$\hat{U}(g)\hat{\mathbf{J}}\hat{U}^\dagger(g) = \mathbf{R}^{-1}(g)\hat{\mathbf{J}} : \mathcal{S} \rightarrow \mathcal{S}, \quad (5.2.10)$$

where $\mathbf{R}(g)$ is the 3×3 representation matrix of the group element g in the adjoint representation on \mathbb{R}^3 and $\mathbf{R}(g)\hat{\mathbf{J}} = R_{ij}(g)\hat{J}_j$. Since $\hat{U}(g) : \mathcal{S}' \rightarrow \mathcal{S}$ the conjugation of the source space angular momentum operator is a rotated target space angular momentum operator. Thus, by the invariance of the inner product under rotation and unitarity of the rotation operators,

$$\hat{U}(g)(\mathbf{z} \cdot \hat{\mathbf{J}}') = (\mathbf{R}(g)\mathbf{z}) \cdot \hat{\mathbf{J}}\hat{U}(g). \quad (5.2.11)$$

Note that the operator $\hat{U}(g)$ may be replaced by the restricted operator $\hat{U}_j(g)$ in both Eqs. 5.2.10 and 5.2.11 since the operator that defines the representation is a Casimir and commutes with the rotation operators. Acting $\hat{U}_j(g)$ on the eigenvalue equation $\mathbf{z} \cdot \hat{\mathbf{J}}'|jm'\rangle = m'|jm'\rangle$ for the b -state gives

$$(\mathbf{R}(g)\mathbf{z}) \cdot \hat{\mathbf{J}}\hat{U}_j(g)|jm'\rangle = m'\hat{U}_j(g)|jm'\rangle. \quad (5.2.12)$$

Define $\mathbf{n} \equiv \mathbf{R}(g)\mathbf{z}$ and let $\hat{J}_n \equiv \mathbf{n} \cdot \hat{\mathbf{J}}$. Then we may write the β -state as the simultaneous eigenstate

$$|\beta\rangle = \hat{U}_j(g)|jm'\rangle = \left| \begin{array}{cc} \hat{I} & \hat{J}_n \\ j & m' \end{array} \right\rangle \in \mathcal{S}. \quad (5.2.13)$$

This state $\hat{U}_j(g) \in \mathcal{S} \otimes \mathcal{S}'$ is the simultaneous eigenstate of operators \hat{I} and $\hat{\mathbf{J}} - \mathbf{R}(g)\hat{\mathbf{J}}'^\top$ as we now show. First,

$$\hat{I}\hat{U}_j(g) = j\hat{U}_j(g), \quad (5.2.14)$$

as can be seen by acting both sides of the equation on an arbitrary bra from the right. Next, recall that the operator $\hat{\mathbf{J}}'^\top$ is the action of $\hat{\mathbf{J}}'$ on \mathcal{S}^* from the right. Consider $\hat{\mathbf{J}} - \mathbf{R}(g)\hat{\mathbf{J}}'^\top$ acting on $\hat{U}_j(g)$,

$$(\hat{\mathbf{J}} - \mathbf{R}(g)\hat{\mathbf{J}}'^\top)(\hat{U}_j(g)) = \hat{\mathbf{J}}\hat{U}_j(g) - \mathbf{R}(g)\hat{U}_j(g)\hat{\mathbf{J}}'. \quad (5.2.15)$$

By Eq. 5.2.10 $\hat{U}_j(g)\hat{\mathbf{J}}' = \mathbf{R}(g^{-1})\hat{\mathbf{J}}\hat{U}_j(g)$. Therefore

$$(\hat{\mathbf{J}} - \mathbf{R}(g)\hat{\mathbf{J}}'^\top)(\hat{U}_j(g)) = \mathbf{0}. \quad (5.2.16)$$

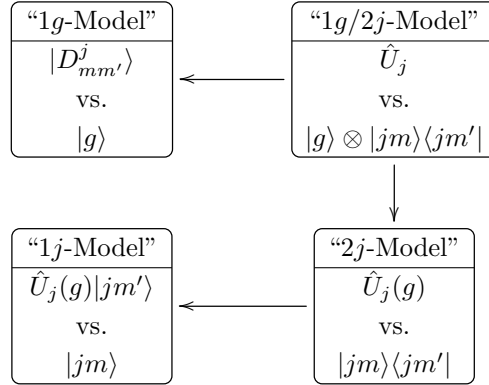


Figure 5.2.1: Schematic of the spaces and states in the remodeling algebras for the D -matrix.

and the M -state is the map $\hat{U}_j : \mathcal{S}^* \otimes \mathcal{S}' \rightarrow \mathcal{H}_{SU(2)} : |jm'\rangle\langle jm| \mapsto |D_{mm'}^j\rangle$. Note that by definition $\langle g|\hat{U}_j = \hat{U}_j(g)$.

A schematic of the remodelings for the D -matrix is shown in Figure 5.2.1.

A similar remodeling algebra can be set up for the map $\hat{U}^\dagger : \mathcal{H}_{SU(2)} \rightarrow \mathcal{S} \otimes \mathcal{S}'^* : |g\rangle \mapsto \hat{U}(g)$. Note that we are no longer restricting to a given irrep label. The kernel of this map is zero and thus orthogonal complement of the kernel of this map is the full space $\mathcal{H}_{SU(2)}$. The image of this map is the zero eigenspace of $\hat{I} - \hat{I}'^\top$. Thus the core isomorphism identifies $L^2SU(2)$ with the zero eigenspace of $\hat{I} - \hat{I}'^\top$ in $\mathcal{S} \otimes \mathcal{S}'^*$.

The classical phase space associated with $\mathcal{H}_{SU(2)}$ is the cotangent bundle $T^*SU(2)$. As discussed in Hedeman *et al* [51], points on $T^*SU(2)$ may be written as pairs (\mathbf{J}, g) or (g, \mathbf{J}') , where \mathbf{J} and \mathbf{J}' are the momentum maps for the right- and left-translation actions of $SU(2)$ on itself, respectively (these are similar to the space and body coordinates of a rigid body). The two choices of angular momenta \mathbf{J} and \mathbf{J}' in the fiber over g are related by $\mathbf{J} = \mathbf{R}(g)\mathbf{J}'$.

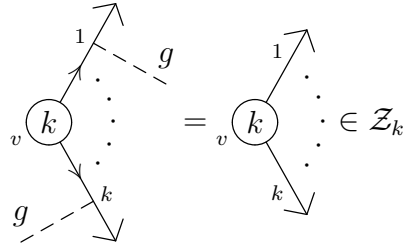
In Hedeman *et al* [51] we found that symplectic reduction of the $2j$ -phase space $\Sigma \times \Sigma'^*$ by the $U(1)$ group generated by $I - I'$ yields a phase space that is isomorphic to the cotangent bundle $T^2SU(2)$ with the exception of the zero section, which is identified with a single point. This same phase space arises in the theory of “symplectic implosion” [102]. A similar reduction is performed in the analysis of “twisted geometries” by Freidel and Speziale [103] in connection with the classical phase spaces associated with spin networks in loop quantum gravity. As in Hedeman *et al* [51] we write this phase space minus the zero point as \dot{Q} . We may specify coordinates on \dot{Q} by the pair (\mathbf{J}, g) , which is the projection of the $I - I'$ group orbit in $\Sigma \times \Sigma'$ such that the projection of z onto angular momentum space is \mathbf{J} and $z' = g^{-1}z$. We may also use coordinates (g, \mathbf{J}') , where the projection of z' onto angular momentum space is \mathbf{J}' and $z = gz'$. The core geometry associated with the map \hat{U}^\dagger thus contains $T^*SU(2)$ as the source space and $\Sigma \times \Sigma'^*/(I - I' = 0)$ as the reduced target space. A point (\mathbf{J}, g) in the source space is mapped by the core symplectomorphism to the point (\mathbf{J}, g) in \dot{Q} . The symplectic structure of these spaces may be given by the symplectic

potential, which we expressed in Hedeman *et al* [51] as

$$\theta = i\mathbf{J} \cdot \text{tr}(g^\dagger \boldsymbol{\sigma} dg) = -i\mathbf{J}' \cdot \text{tr}(g \boldsymbol{\sigma} dg^\dagger). \quad (5.2.20)$$

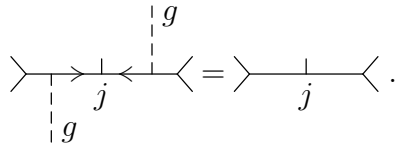
5.2.3 g -Inserted Intertwiners

Recall that an intertwiner is a linear map between vector spaces that commutes with the actions of $SU(2)$ on the two spaces. Let $\mathcal{H}_{kj} = \bigotimes \mathcal{S}_r$, $r = 1, \dots, k$ and let $\mathcal{Z}_{kj} \subset \mathcal{H}_{kj}$ be the space of intertwiners $:\mathcal{H}_{kj}^* \rightarrow \mathbb{C}$. Since \mathbb{C} is a carrier space for the $j = 0$ irrep of $SU(2)$ the intertwiner property implies that all elements of \mathcal{Z}_{kj} are $SU(2)$ invariants. A rotation by group element $g \in SU(2)$ on \mathcal{H}_{kj} is tensor product $\hat{U}_1(g) \otimes \dots \otimes \hat{U}_k(g)$, where $\hat{U}_r(g)$ is the $SU(2)$ rotation operator acting only on \mathcal{S}_r . We may therefore represent the intertwiner property in spin network language by



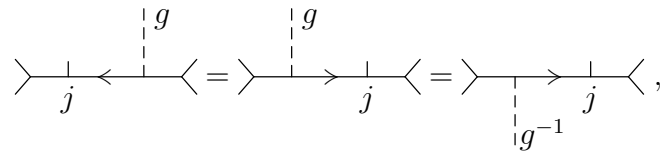
$$\text{Spin network with node } k \text{ and legs } 1, k \text{ with } g \text{ insertions} = \text{Spin network with node } k \text{ and legs } 1, k \in \mathcal{Z}_k. \quad (5.2.21)$$

Applying this to the $2j$ -intertwiner yields



$$\text{Stub with legs } j \text{ and } g \text{ insertion} = \text{Stub with legs } j. \quad (5.2.22)$$

Note that the orientations for both g -insertions are such that the dashed lines represent the operator $\hat{U}(g)$. Eq. 5.2.22 implies that we can “push” a g -insertion through a stub,



$$\text{Stub with legs } j \text{ and } g \text{ insertion} = \text{Stub with legs } j \text{ and } g \text{ insertion} = \text{Stub with legs } j \text{ and } g^{-1} \text{ insertion}, \quad (5.2.23)$$

which can be seen by replacing the stub in Eq. 5.2.23 with the g -inserted stub network in Eq. 5.2.22 (with group element g^{-1}) and then using Eq. 5.2.2 and Eq. 5.2.3 to replace the two g -insertions to the right of the stub with the identity. Note that in the first equality of Eq. 5.2.23 pushing the g -insertion through the stub inverts the orientation of the dashed line with respect to the external chevrons or internal arrows. Note that the g -insertions in the first two spin networks of Eq. 5.2.23 are the representation matrices on \mathcal{S} and \mathcal{S}^* , respectively. In fact, we may consider Eq. 5.2.23 to be the intertwiner property applied to

the map $\hat{K}_j : \mathcal{C}_j \rightarrow \mathcal{C}_j^*$ introduced in Section 3.1.4, $\hat{K}_j \circ \hat{U}(g) = \hat{U}^\dagger(g) \circ \hat{K}_j$, where $\hat{U}(g)$ and $\hat{U}^\dagger(g)$ are the unitary representation operators for \mathcal{S} and \mathcal{S}^* , respectively. Eqs. 5.2.22 and 5.2.23 hold for the full intertwiner $\hat{K} : \mathcal{S} \rightarrow \mathcal{S}^*$ as well as the intertwiner restricted to the irrep carrier spaces.

Performing a g -insertion on a diangle state $|K_{ab}\rangle \in \mathcal{S}_a \otimes \mathcal{S}_b$ (as defined in Section 4.1.1) yields a ‘‘bent diangle’’ state,

$$\hat{U}_a(g)|K_{ab}\rangle = \left| \begin{array}{c} \hat{I}_a \\ j \end{array} \begin{array}{c} \hat{\mathbf{J}}_a + \mathbf{R}(g)\hat{\mathbf{J}}_b \\ \mathbf{0} \end{array} \right\rangle = \frac{1}{\sqrt{2j+1}} g \begin{array}{c} \uparrow b \\ \text{---} \\ \downarrow a \end{array} \in \mathcal{S}_a \otimes \mathcal{S}_b, \quad (5.2.24)$$

where the a subscript on the rotation operator indicates that it is only acting on the \mathcal{S}_a piece of $\mathcal{S}_a \otimes \mathcal{S}_b$. Note that if we pushed the dashed line of the g -insertion to the other side of the stub it would represent the conjugated operator $\hat{U}^\dagger(g)$ rather than $\hat{U}(g)$. Unless otherwise noted all g -insertions in the remainder of this work will be oriented as in Eq. 5.2.1. We have suppressed a downward-pointing arrow on the internal line between the stub and the g -insertion since the orientation is clear from context. We will continue to suppress arrows on internal lines when the orientation is clear by context. This state is a $\mathbf{0}$ -eigenstate of the operator $\hat{\mathbf{J}}_a + \mathbf{R}(g)\hat{\mathbf{J}}_b$ as can be seen from the considering $|K_{ab}\rangle$ as a map : $\mathcal{S}_b^* \rightarrow \mathcal{S}'_a$ and $\hat{U}(g)$ as a map : $\mathcal{S}'_a \rightarrow \mathcal{S}_a$ (so that $\hat{U}(g) \in \mathcal{S}_a \otimes \mathcal{S}'_a^*$ as before). Consider the map $(\hat{\mathbf{J}}_a + \mathbf{R}(g)\hat{\mathbf{J}}_b)(\hat{U}_a(g)|K_{ab}\rangle)$ acting on some arbitrary $\psi_b \in \mathcal{S}_b$,

$$\left[(\hat{\mathbf{J}}_a + \mathbf{R}(g)\hat{\mathbf{J}}_b)(\hat{U}_a(g)|K_{ab}\rangle) \right] (\langle \psi_b |) = \langle \psi_b | \mathbf{R}(g)(\hat{\mathbf{J}}'_a + \hat{\mathbf{J}}_b) | K_{ab} \rangle, \quad (5.2.25)$$

where we have used $\hat{\mathbf{J}}_a(\hat{U}(g)) = \mathbf{R}(g)\hat{\mathbf{J}}_a^\top(\hat{U}(g))$. Since $|K_{ab}\rangle$ is a $\mathbf{0}$ -eigenstate of $\hat{\mathbf{J}}'_a + \hat{\mathbf{J}}_b$ this expression is zero for all $\langle \psi_b |$ and thus $(\hat{\mathbf{J}}_a + \mathbf{R}(g)\hat{\mathbf{J}}_b)(\hat{U}_a(g)|K_{ab}\rangle) = \mathbf{0}$. We write the Hermitian conjugate of the bent diangle state as

$$\left(\begin{array}{c} \uparrow b \\ \text{---} \\ \downarrow a \end{array} \right)^\dagger = \begin{array}{c} \text{---} \\ \uparrow b \\ \downarrow a \end{array} \in \mathcal{S}_a^* \otimes \mathcal{S}_b^*, \quad (5.2.26)$$

where we have pushed the g -insertion through the stub so that the dashed line again has the correct orientation to stand for the group action by g on \mathcal{S} rather than \mathcal{S}^* .

Applying Eq. 5.2.21 to the $3j$ -intertwiner yields

$$\begin{array}{c} \uparrow \\ \text{---} \\ \downarrow \\ \text{---} \\ \downarrow \end{array} \begin{array}{c} j_1 \\ \text{---} \\ j_2 \\ \text{---} \\ j_3 \end{array} \begin{array}{c} \uparrow \\ \text{---} \\ \downarrow \\ \text{---} \\ \downarrow \end{array} \begin{array}{c} g \\ \text{---} \\ g \end{array} = \begin{array}{c} \uparrow \\ \downarrow \\ \downarrow \end{array} \begin{array}{c} j_1 \\ \downarrow \\ j_3 \end{array}, \quad (5.2.27)$$

where there is an implied arrow pointing away from the node on all three lines coming out of the node. Eq. 5.2.27 implies that we can always “push” a g -insertion on one line connected to a trivalent node onto the other two lines. In particular,

$$\begin{array}{c} \uparrow \\ | \\ j_1 \text{ --- } g_1 \\ | \\ \bullet \\ / \quad \backslash \\ j_2 \quad j_3 \end{array} = \begin{array}{c} \uparrow \\ | \\ j_1 \\ | \\ \bullet \\ / \quad \backslash \\ j_2 \quad j_3 \\ \quad \quad \backslash \\ \quad \quad \quad g^{-1} \end{array} . \tag{5.2.28}$$

If there is a g -insertion on all three legs of a $3j$ -intertwiner we may use Eq. 5.2.28 to eliminate one of the group elements,

$$\begin{array}{c} \uparrow \\ | \\ j_1 \text{ --- } g_1 \\ | \\ \bullet \\ / \quad \backslash \\ j_2 \quad j_3 \\ \quad \quad \backslash \\ \quad \quad \quad g_3 \end{array} \quad g_2 \text{ --- } \quad = \quad \begin{array}{c} \uparrow \\ | \\ j_1 \\ | \\ \bullet \\ / \quad \backslash \\ j_2 \quad j_3 \\ \quad \quad \backslash \\ \quad \quad \quad g_3 g_1^{-1} \end{array} \quad g_2 g_1^{-1} \text{ --- } . \tag{5.2.29}$$

Given a tree-level kj -intertwiner ket we may perform a g -insertion on each of the $n - 1$ internal lines. By Eq. 5.2.29 and the tree-structure of the spin network we may always move the g -insertions on an internal line to the external lines. For example, consider the $4j$ -intertwiner butterfly state in the ab -coupling scheme of Eq. 4.1.9 with a g -insertion performed on the internal line,

$$\begin{array}{c} \uparrow \quad \quad \uparrow \\ | \quad \quad | \\ a \quad \quad d \\ | \quad \quad | \\ \bullet \quad \quad \bullet \\ | \quad \quad | \\ b \quad \quad c \\ | \quad \quad | \\ ab \quad \quad g \end{array} . \tag{5.2.30}$$

We are again using the convention that all internal arrows are pointing away from trivalent nodes and towards stubs and the placement and orientation of the g -insertion is chosen so the g -insertion stands for the group action by g on \mathcal{S} rather than \mathcal{S}^* . The g -insertion may be pushed through the trivalent node on the right which yields a g -insertion by g^{-1} on the two external lines on the right. We may also push the g -insertion first through the stub by using the second equality of Eq. 5.2.23 and then through the trivalent node on the left which

yields a g -insertion by g on the two external lines on the left,

$$(5.2.31)$$

A general g -inserted tree-level $4j$ -intertwiner may thus be written

$$(5.2.32)$$

where the level set conditions defining the Lagrangian manifold in the $4j$ phase space Φ_{4j} that supports the semiclassical approximation of the g -inserted $4j$ -intertwiner is given in the expression on the right and $r = a, b, c, d$.

5.2.4 g -Inserted Spin Networks

We define a “ g -inserted spin network” to be a closed spin network (of arbitrary valence) where all stubs have been replaced by combinations of stubs and g -insertions. This is akin to replacing all diangle states with “bent diangle” states. For example, consider the g -inserted $6j$ -symbol,

$$(5.2.33)$$

This is a symmetric formulation since all six diangle bras are treated on an equal footing. However we may also assign the g -insertions asymmetrically by pushing the g -insertion on diangles ‘3’ and ‘6’ through the trivalent nodes. We make the replacements

$$g_1 \mapsto g_1; \quad g_2 \mapsto g_2 g_6^{-1}; \quad g_4 \mapsto g_6 g_4 g_3^{-1}; \quad g_5 \mapsto g_3 g_5, \quad (5.2.34)$$

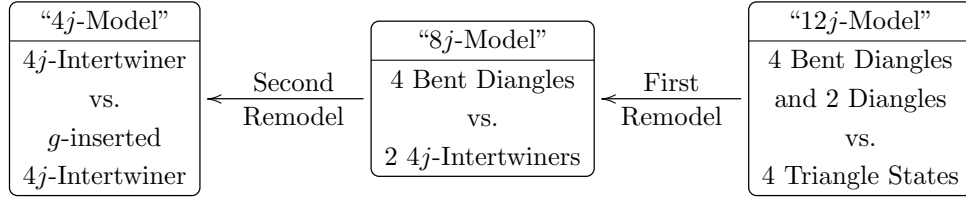
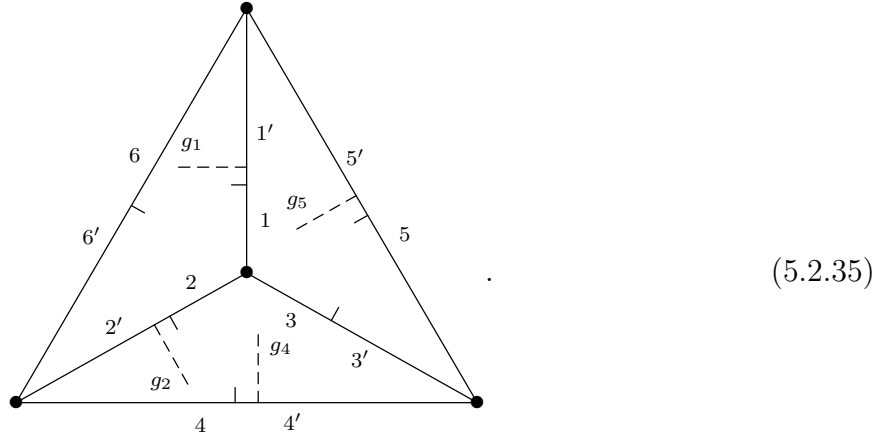


Figure 5.2.2: Schematic of the spaces and states in the remodeling algebras for the g -inserted $6j$ -symbol.

in which case the spin network in Eq. 5.2.33 becomes



This is the most convenient form for construction of the remodeling algebras of the g -inserted $6j$ -symbol.

This spin network may be cut as in Eq. 4.2.7 to create a remodel of the $6j$ -symbol in which case the M -state, b -state, and β -states are identical to the states Eqs. 4.2.8, 4.2.16, and 4.2.17 in the first remodel of the $6j$ -symbol as discussed in Section 4.2.2. The difference is that the a -state is now g -inserted version of the a -state Eq. 4.2.13 of the first remodel of the $6j$ -symbol,

$$|a_1\rangle = \begin{array}{c} \begin{array}{c} \uparrow \\ | \\ \downarrow \end{array} \\ \begin{array}{c} \uparrow \\ | \\ \downarrow \end{array} \\ \begin{array}{c} \uparrow \\ | \\ \downarrow \end{array} \\ \begin{array}{c} \uparrow \\ | \\ \downarrow \end{array} \end{array} \in \mathcal{H}_{8j}, \quad (5.2.36)$$

The first remodel now connects a g -inserted $12j$ -model with a g -inserted $8j$ -model. A second remodel connects the $8j$ -model with a $4j$ -model. The a - and b -states of the second remodel are identical to the states Eqs. 4.2.31 and 4.2.32 in the second remodel of the $6j$ -symbol as discussed in Section 4.2.3. The M -state is now four bent diangle bras and the β -state is proportional to a g -inserted $4j$ -intertwiner ket, with all g -insertions on the external legs as in Eq. 5.2.32. A schematic of the two remodelings of the g -inserted $6j$ -symbol are given in Figure 5.2.2.

Now we can see how g -inserted spin networks represent the amplitudes in loop quantum gravity. References for the geometry explored here include Baez and Muniain [104] and Gambini and Pullin [22] and standard references and review articles for loop quantum gravity include Rovelli [5], Ashtekar and Lewandowski [12], and Thiemann [13].

Let Σ be a spacelike hypersurface and $\Gamma \in \Sigma$ a path. An $SU(2)$ connection \mathbf{A} on Σ is a $\mathfrak{su}(2)$ -valued one-form on Σ . The (open-path) holonomy H_A is then a map from the space of paths in Σ to the group $SU(2)$ given by the path-ordered exponential,

$$H_A(\Gamma) = P \exp \left(i \int_{\Gamma} \mathbf{A} \right). \quad (5.2.37)$$

Given two paths Γ_1 and Γ_2 such that the final point $\Gamma_1(1)$ of the first path is the initial point $\Gamma_2(0)$ of the second path, the holonomy over the concatenated path $\Gamma_1 \circ \Gamma_2$ is the group product of the holonomies,

$$H_A(\Gamma_1 \circ \Gamma_2) = H_A(\Gamma_1)H_A(\Gamma_2). \quad (5.2.38)$$

A gauge transformation by gauge function $g : \Sigma \rightarrow SU(2)$ changes the connection via $\mathbf{A}(x) \mapsto g(x)\mathbf{A}g^{-1}(x) + g(x)dg^{-1}(x)$. Under a gauge transformation the open-path holonomy transforms as

$$H_A(\Gamma) \mapsto g(\Gamma(0)) H_A(\Gamma) g^{-1}(\Gamma(1)), \quad (5.2.39)$$

where $\Gamma(0)$ and $\Gamma(1)$ are the initial and final points of the path Γ . Given a closed path Γ in Σ , the Wilson loop is the trace in $SU(2)$ of the closed-path holonomy,

$$W_A(\Gamma) = \text{tr } H_A(\Gamma). \quad (5.2.40)$$

The Wilson loops are all invariant under gauge transformations.

As stated in Chapter 1 a spin network basis state $|S, k\rangle$ is specified by a decorated spin network S and a discrete label k that gives the knot class of the embedding of S into Σ . This state may be considered a wavefunctional $\Psi_{S,k}[\mathbf{A}]$ on the space of connections, with the $\Psi_{S,k}[\mathbf{A}]$ being the holonomy with respect to connection \mathbf{A} around the loop defined by the embedding of the spin network S into Σ [17, 5]. These wavefunctionals represent the amplitudes of loop quantum gravity. The diffeomorphism invariance of the spin network states is manifested in the freedom (up to a specification of the knot class) in choosing the embedding of the spin network in Σ . Each edge of the spin network maps to an open oriented path $\Gamma \subset \Sigma$ under the embedding. In this work we choose to place stubs on all internal lines so that all arrows on internal lines point away from nodes of valence three or higher and point towards stubs. The orientation of the stub then determines the orientation of the path in the embedding; the node counterclockwise of the stub is the initial point of the path and the node clockwise of the stub is the final point, as shown in Figure 5.2.3. Thus a holonomy may be assigned to each edge of the spin network. We may interpret these holonomies as maps from the tangent space at the embedding of the initial node to the tangent space at the embedding of the final node. The interpretation of the holonomy as a g -insertion is most

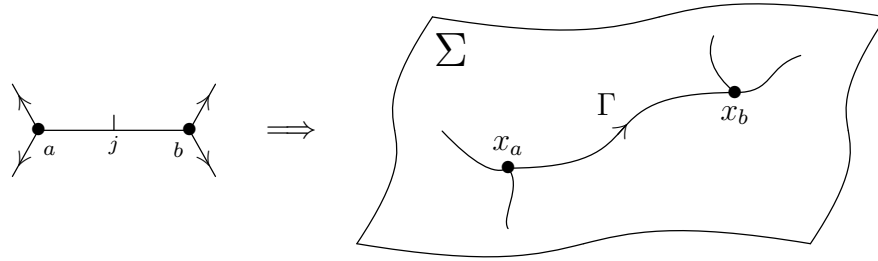


Figure 5.2.3: The embedding of a spin network edge into a path Γ in Σ .

easily seen by considering a closed-path holonomy which is a map from the tangent space at the embedding of a node to itself. The action of the holonomy group element acting on the tangent vector \mathbf{J}_i to Γ at the start of the path gives the vector \mathbf{J}_f tangent to Γ at the end of the path,

$$\mathbf{R}(H_A^{-1}(\Gamma))\mathbf{J}_i = \mathbf{J}_f. \quad (5.2.41)$$

Note that the holonomy must be inverted in order to satisfy the homomorphism property Eq. 5.2.38. Let $\mathbf{J}_a = \mathbf{J}_i$ and $\mathbf{J}_b = -\mathbf{J}_f$ so that \mathbf{J}_a and \mathbf{J}_b both point along the path Γ . Then the holonomy implies

$$\mathbf{J}_a + \mathbf{R}(H_A(\Gamma))\mathbf{J}_b = \mathbf{0}. \quad (5.2.42)$$

This is precisely the classical version of the statement that the bent diangle bra of Eq. 5.2.26 is a $\mathbf{0}$ -eigenvalue of the operator $\hat{\mathbf{J}}_a + \mathbf{R}(g)\hat{\mathbf{J}}_b$. Thus we may represent the action of a spin network edge on a connection with a g -insertion,

$$\left(\begin{array}{c} \nearrow \\ \bullet \\ \searrow \end{array} \right)_a \text{---} \overset{j}{\text{---}} \text{---} \left(\begin{array}{c} \nearrow \\ \bullet \\ \searrow \end{array} \right)_b \Big|_k [\mathbf{A}] = \begin{array}{c} \overset{H_A(\Gamma)}{\text{---}} \\ \nearrow \\ \bullet \\ \searrow \end{array} \text{---} \overset{j}{\text{---}} \text{---} \begin{array}{c} \nearrow \\ \bullet \\ \searrow \end{array}. \quad (5.2.43)$$

The spin network in the expression on the left in Eq. 5.2.43 represents a segment of a spin network in a spin network basis state and the subscript k indicates the knot class of the embedding (both the spin network and the knot class labels are required to specify a spin network basis state). The left-hand side of Eq. 5.2.43 thus is a spin network basis state treated as a wavefunctional and acting on a connection \mathbf{A} . The expression on the right is a g -inserted spin network with $H_A(\Gamma)$ the holonomy along Γ , the embedding of the internal edge into Σ .

The gauge invariance of the spin network states is manifested in the intertwiner property of the nodes. For example, consider the following segment of a spin network state,

$$\begin{array}{c} b \\ \bullet \\ | \\ \bullet \\ \swarrow \quad \searrow \\ c \quad \quad d \\ a \end{array}. \quad (5.2.44)$$

Let this spin network be embedded in Σ such that node r is at point $x_r \in \Sigma$ with $r = a, b, c, d$ and the edge going from node r to node s follows the path $\Gamma_{rs} \subset \Sigma$. The three edges of this spin network give three oriented paths Γ_{ba} , Γ_{ca} , and Γ_{ad} , where the orientation of the stub determines which node marks the beginning of the path and which node marks the end. Let the space Σ carry the connection \mathbf{A} and define $h_{rs} \equiv H_A(\Gamma_{rs})$ to be the holonomy along the oriented edge connecting node r to node s . Following Eq. 5.2.43 the evaluation of this spin network segment on the connection \mathbf{A} is the g -inserted spin network,

$$\left(\left(\begin{array}{c} b \\ | \\ a \\ / \quad \backslash \\ c \quad d \end{array} \right) \right)_k [\mathbf{A}] = \begin{array}{c} b \\ | \\ \text{---} h_{ba} \text{---} \\ | \\ a \\ / \quad \backslash \\ \text{---} h_{ca} \text{---} \quad \text{---} h_{ad} \text{---} \\ c \quad d \end{array} \quad (5.2.45)$$

Now suppose \mathbf{A} is subjected to a gauge transformation $\mathbf{A} \mapsto \mathbf{A}'$. By Eq. 5.2.39 the holonomies transform as $h_{rs} \mapsto g_r h_{rs} g_s^{-1}$, where g_r is the gauge function evaluated at x_r . The spin network state acting on the connection after the gauge transformation is thus

$$\left(\left(\begin{array}{c} b \\ | \\ a \\ / \quad \backslash \\ c \quad d \end{array} \right) \right)_k [\mathbf{A}'] = \begin{array}{c} b \\ | \\ \text{---} g_b h_{ba} g_a^{-1} \text{---} \\ | \\ a \\ / \quad \backslash \\ \text{---} g_c h_{ca} g_a^{-1} \text{---} \quad \text{---} g_a h_{ad} g_d^{-1} \text{---} \\ c \quad d \end{array} \quad (5.2.46)$$

By Eqs. 5.2.3 and 5.2.23 these g -insertions may be broken up,

$$\left(\left(\begin{array}{c} b \\ | \\ a \\ / \quad \backslash \\ c \quad d \end{array} \right) \right)_k [\mathbf{A}'] = \begin{array}{c} b \\ | \\ \text{---} g_b^{-1} \text{---} \quad \text{---} h_{ba} \text{---} \\ | \\ \text{---} g_a^{-1} \text{---} \\ | \\ a \\ / \quad \backslash \\ \text{---} h_{ca} \text{---} \quad \text{---} h_{ad} \text{---} \\ \text{---} g_c^{-1} \text{---} \quad \text{---} g_d^{-1} \text{---} \\ c \quad d \end{array} \quad (5.2.47)$$

Note that there is a g -insertion by the same group element (g_a^{-1}) abutting node a on each of the three edges that meet at node a . By the intertwiner property Eq. 5.2.27 we may make the replacement

$$\begin{array}{c} \text{---} g_a^{-1} \text{---} \\ | \\ \text{---} g_a^{-1} \text{---} \\ | \\ \text{---} g_a^{-1} \text{---} \\ / \quad \backslash \\ \text{---} \quad \text{---} \\ c \quad d \end{array} = \begin{array}{c} \text{---} \\ | \\ \text{---} \\ / \quad \backslash \\ \text{---} \quad \text{---} \\ c \quad d \end{array}, \quad (5.2.48)$$

A similar manipulation happens at each node of the spin network if the spin network has no external edges. Therefore the g -inserted spin network in Eq. 5.2.47 simplifies to the g -inserted spin network in Eq. 5.2.45 and we conclude that the spin network amplitude is invariant under gauge transformations, as expected.

Thus the fundamental amplitudes of loop quantum gravity can be expressed in terms of g -inserted spin networks. Performing a semiclassical approximation therefore amounts to semiclassically evaluating these g -inserted spin networks. We may construct the same remodeling algebras as in Section 5.1 to form different inner product models or we may perform a remodel as in Section 5.2.2 to interpret these states in some power of $L^2SU(2)$ as is done in the twisted geometries approach [103].

5.3 Co-Isotropic Manifolds

The semiclassical interpretation of a linear map $\hat{M} : \mathcal{H}_2 \rightarrow \mathcal{H}_1$ as a Lagrangian manifold \mathcal{L}_M in the product phase space $\Phi_1 \times \Phi_2^*$ is one example of Weinstein's symplectic creed [105], "everything is a Lagrangian manifold!" In this section we use the remodeling algebra and geometry to explore another example, wherein we may relate certain classes of co-isotropic manifolds to Lagrangian manifolds of a larger space. In particular, we may use the remodeling geometry to associate a canonical Lagrangian manifold in a product phase space with a co-isotropic manifold in a target phase space.

Consider a Hilbert space \mathcal{H} and a symmetry group G on \mathcal{H} generated by the dual Lie algebra-valued operator $\hat{\mathbf{A}} : \mathcal{H} \rightarrow \mathfrak{g}^* \times \mathcal{H}$. Let $\mu \in \mathfrak{g}^*$ be a fixed point under the Ad^* -action of G on \mathfrak{g}^* and define \mathcal{H}_μ as the simultaneous μ -eigenspace of the operator $\hat{\mathbf{A}}$,

$$\mathcal{H}_\mu \equiv \left\{ |\psi\rangle \in \mathcal{H} \mid \hat{\mathbf{A}}|\psi\rangle = \mu|\psi\rangle \right\}. \quad (5.3.1)$$

Let Φ be the classical phase space corresponding to \mathcal{H} and let \mathbf{A} be the Ad^* -equivariant momentum map for the symplectic action of G on Φ . As in Section 2.4.3 the eigenspace \mathcal{H}_μ may be represented semiclassically by two different manifolds. If \mathcal{H}_μ is interpreted as a subspace of \mathcal{H} then the associated semiclassical object is the co-isotropic level set $\mathbf{A}^{-1}(\mu) \subset \Phi$. If \mathcal{H}_μ is interpreted as a Hilbert space then the associated semiclassical object is the phase space Φ_μ obtained by the symplectic reduction $\Phi//(\mathbf{A} = \mu)$. Note that by definition of the symplectic reduction there is an inclusion map $\iota_\mu : \mathbf{A}^{-1}(\mu) \rightarrow \Phi$ and projection map $\pi_\mu : \mathbf{A}^{-1}(\mu) \rightarrow \Phi_\mu$ such that $\iota_\mu^* \omega = \pi_\mu^* \omega_\mu$, where ω and ω_μ are the symplectic forms on Φ and Φ_μ , respectively.

Consider \mathcal{H}_μ as a Hilbert space in its own right and let $\hat{\mathcal{I}} : \mathcal{H}_\mu \rightarrow \mathcal{H}$ be the inclusion map. That is, $\hat{\mathcal{I}}$ maps the Hilbert space \mathcal{H}_μ to the subspace $\mathcal{H}_\mu \subset \mathcal{H}$. We may set up a remodeling algebra and geometry for such a map, with the Hilbert space \mathcal{H}_μ and the reduced phase space Φ_μ acting as the source spaces and the original Hilbert space \mathcal{H} and phase space Φ acting as the target spaces. Then $\hat{\mathcal{I}}$ is identified as a vector in the product Hilbert space $\mathcal{H} \otimes \mathcal{H}_\mu$ and the semiclassical approximation to $\hat{\mathcal{I}}$ is supported by a Lagrangian manifold $\mathcal{L}_{\mathcal{I}}$

$$\begin{array}{ccc}
 \Phi & \xleftarrow{\pi_1} & \Phi \times \Phi_\mu^* \\
 \uparrow \iota_\mu & & \downarrow G_2^{-1} \circ \pi_2 \\
 \mathbf{A}^{-1}(\mu) & \xrightarrow{\pi_\mu} & \Phi_\mu
 \end{array}$$

Figure 5.3.1: Phase spaces and the maps between them for the symplectic reduction and remodeling geometry associated with the inclusion map $\hat{\mathcal{I}}$.

in the product phase space $\Phi \times \Phi_\mu^*$. The phase spaces of the remodeling geometry and the spaces involved in the symplectic reduction are shown in Figure 5.3.1.

We may determine the structure of $\mathcal{L}_{\mathcal{I}}$ by using the transport procedure of Section 2.2.2. Let $|\psi\rangle \in \mathcal{H}_\mu$ be a vector of the subspace \mathcal{H}_μ and thus an element of both Hilbert spaces \mathcal{H}_μ and \mathcal{H} . Let \mathcal{L} be the Lagrangian manifold in Φ corresponding to $|\psi\rangle \in \mathcal{H}$ and let $\mathcal{L}^R \subset \Phi_\mu$ be the Lagrangian manifold in Φ_μ corresponding to $|\psi\rangle \in \mathcal{H}_\mu$. By definition of \mathcal{H}_μ , $\hat{\mathbf{A}}|\psi\rangle = \mu|\psi\rangle$ and thus $\mathcal{L} \subset \mathbf{A}^{-1}(\mu)$. This manifold projects onto the Lagrangian manifold \mathcal{L}^R in the reduced space, Alternatively we could have started with the manifold $\mathcal{L}^R \subset \Phi_\mu$ and formed by the manifold \mathcal{L} by pulling back by forming the inverse image of \mathcal{L}^R under the projection of the symplectic reduction and then pushing forward by the inclusion map,

$$\mathcal{L}^R = \pi_\mu(\mathcal{L}), \quad \mathcal{L} = \iota_\mu(\pi_\mu^{-1}(\mathcal{L}^R)). \quad (5.3.2)$$

Since $\hat{\mathcal{I}}_\mu$ maps $|\psi\rangle \in \mathcal{H}_\mu$ to the same vector in \mathcal{H} we expect the transport of \mathcal{L}^R through \mathcal{L}_μ to give \mathcal{L} ,

$$\mathcal{L} = \mathcal{T}(\mathcal{L}^R) = \pi_1(\mathcal{L}_{\mathcal{I}} \cap \pi_2^{-1}(G_2\mathcal{L}^R)). \quad (5.3.3)$$

Let points on Φ and Φ_μ be written z_1 and z_2 so point on the product space are (z_1, z_2) . Eqs. 5.3.2 and 5.3.3 hold for any Lagrangian manifold $\mathcal{L}^R \subset \Phi_\mu$ so we may assume that

$$\iota_\mu(\pi_\mu^{-1}(z_2)) \cong \pi_1(\mathcal{L}_{\mathcal{I}} \cap \pi_2^{-1}(G_2(z_2))), \quad \forall z_2 \in \Phi_\mu. \quad (5.3.4)$$

The left-hand side of Eq. 5.3.4 is the set

$$\iota_\mu(\pi_\mu^{-1}(z_2)) = \{z_1 \in \mathbf{A}^{-1}(\mu) \mid \pi_\mu(z_1) = z_2\} \subset \Phi, \quad (5.3.5)$$

while the right-hand side of Eq. 5.3.4 is the set

$$\pi_1(\mathcal{L}_{\mathcal{I}} \cap \pi_2^{-1}(G_2(z_2))) = \{z_1 \in \Phi \mid (z_1, z_2) \in \mathcal{L}_{\mathcal{I}}\}, \quad (5.3.6)$$

where we have used $\pi_2^{-1}(G_2(z_2)) = \Phi \times \{z_2\}$. Comparing Eqs. 5.3.5 and 5.3.6 yields

$$\mathcal{L}_{\mathcal{I}} = \{(z_1, z_2) \in \Phi \times \Phi_\mu^* \mid \mathbf{A}(z_1) = \mu, \pi_\mu(z_1) = z_2\}. \quad (5.3.7)$$

In terms of level sets Eq. 5.3.7 implies

$$\mathcal{L}_{\mathcal{I}} = \left(\begin{array}{c} \mathbf{A} \\ \mu \end{array} \quad z_2 - \pi_\mu(z_1) \right) \in \Phi \times \Phi_\mu^*, \quad (5.3.8)$$

where \mathbf{A} has been pulled back by π_1 to a function on the product space and π_μ is the projection map of the symplectic reduction. This is the expected answer since the core geometry of this setup has Φ_μ as both reduced target and source spaces and the reduced manifold $\mathcal{L}_{\mathcal{I}}^R$ is simply the graph of the identity map. We may construct a map $\mathbf{A}^{-1}(\mu) \rightarrow \mathcal{L}_{\mathcal{I}} : z_1 \mapsto (z_1, \pi_\mu(z_1))$. This map by construction is one-to-one and by Eq. 5.3.7 is onto. Therefore,

$$\mathbf{A}^{-1}(\mu) \cong \mathcal{L}_{\mathcal{I}}, \quad (5.3.9)$$

where $\mathbf{A}^{-1}(\mu)$ is a co-isotropic manifold in Φ and $\mathcal{L}_{\mathcal{I}}$ is a Lagrangian manifold in $\Phi \times \Phi^*$. We have thus successfully reinterpreted a co-isotropic level set in one space as a Lagrangian manifold in another space.

5.3.1 Quantization of I

For a Lagrangian manifold to properly support the semiclassical approximation to a quantum state, the Lagrangian manifold must be “quantized” in the sense of Bohr-Sommerfeld quantization [106, 58]. That is, the action integral with Maslov correction around any closed path on the Lagrangian manifold must be an integer multiple of 2π . This requirement is essentially a consistency requirement for the WKB wavefunction. If a Lagrangian manifold is specified as the level set of a momentum map then the Bohr-Sommerfeld quantization conditions lead to the discrete spectrum of classical contour values that the momentum map components can take. For example, applying Bohr-Sommerfeld quantization to the $1jm$ -torus of Eq. 3.2.1 constrains I to be a half-integer and $I + J_z$ to be an integer, replicating the usual conditions for quantum numbers j and m [44]. The restriction of possible contour values J of I to half-integers does not just hold for the jm -tori, however. In general we find that, given a Lagrangian manifold in an nj -classical phase space, partially specified by the level set condition $I_r = J_r$, Bohr-Sommerfeld quantization implies that J_r must be a half-integer. In this section we apply the Bohr-Sommerfeld quantization to a Lagrangian manifold associated with the coisotropic manifold $I^{-1}(J)$ in the Schwinger Hilbert space to reproduce the quantized contour values of I .

It will be more convenient in this section to set up the remodeling geometry for the projection operator $\hat{\Pi}_j : \mathcal{S} \rightarrow \mathcal{C}_j$, where \mathcal{S} is a Schwinger Hilbert space and \mathcal{C}_j is the j -eigenspace of the operator \hat{I} on \mathcal{S} . Considering \mathcal{C}_j as a Hilbert space in its own right yields a remodeling geometry similar to Figure 5.3.1, with the roles of the source and target space reversed, as shown in Figure 5.3.2. As in Appendix A, Σ is the Schwinger phase space $(\mathbb{C}^2, idz^\dagger \wedge dz)$. As usual let $J = j + 1/2$. The level set $I^{-1}(J)$ has the topology of a 3-sphere of radius J and the projection onto the reduced phase space \mathcal{C}_J is a 2-sphere of radius J , with the projection of the symplectic reduction being the Hopf map $: S^3 \rightarrow S^2$.

The Lagrangian manifold in $\Sigma_J \times \Sigma^*$ that supports the semiclassical approximation to $\hat{\Pi}_j$ is the manifold

$$\mathcal{L}_{\mathcal{I}} = \{(\mathbf{J}, z) \in \Sigma_J \times \Sigma^* \mid I(z) = J, \mathbf{J} = \pi(z)\} \cong S^3. \quad (5.3.10)$$

$$\begin{array}{ccc}
 \Sigma_J & \xleftarrow{\pi_1} & \Sigma_J \times \Sigma^* \\
 \uparrow \pi & & \downarrow G_2^{-1} \circ \pi_2 \\
 \mathbf{I}^{-1}(J) \subset & \longrightarrow & \Sigma
 \end{array}$$

Figure 5.3.2: Phase spaces and the maps between them for the symplectic reduction and remodeling geometry associated with the projection map $\hat{\Pi}$.

We may find the quantized contour values of I in many ways. The first, as mentioned earlier, is to apply Bohr-Sommerfeld quantization directly to Lagrangian manifolds whose description contains the level set condition $I = J$, such as the jm -tori. Another method is inspired by geometric quantization [69, 70, 71], in which we require a compact phase space to contain an integer number of Planck cells equal to the dimension of the Hilbert space. The reduced space Σ_J carries the symplectic form $Jd\Omega$ and thus has volume $4\pi J$. Requiring $4\pi J = 2\pi n$ for some integer n (the number of Planck cells) yields the quantized contour values $J = n/2$. This phase space corresponds to the carrier space \mathcal{C}_j of dimension $n = 2j + 1$ which fixes $J = j + 1/2$.

In light of the connection between co-isotropic manifolds and Lagrangian manifolds, however, we have a third method of finding the quantized contour values of I . In particular, we require that the Lagrangian manifold $\mathcal{L}_{\mathcal{I}}$ be quantized in the sense of Bohr-Sommerfeld. We will not directly apply Bohr-Sommerfeld quantization to the manifold S^3 in $\Sigma_J \times \Sigma^*$ since the product phase space is topologically non-trivial and we can not define a global symplectic potential θ on it and thus we would need to modify the definition of the action integral and Maslov index. Instead we use the fact that Σ_J is a symplectic reduction and lift the product space into $\Sigma \times \Sigma^*$, which is flat and has a globally well-defined symplectic potential. We say that $\mathcal{L}_{\mathcal{I}}$ is quantized if the lifted version of the Lagrangian manifold is quantized on $\Sigma \times \Sigma^*$. This is how, for example, the Lagrangian manifolds on Σ_J corresponding to the states $|jm\rangle \in \mathcal{C}_j$ are quantized [44]. The lift of $\mathcal{L}_{\mathcal{I}}$ into $\Sigma \times \Sigma^*$ is the manifold that supports the semiclassical approximation to $\hat{\Pi}_j : \mathcal{S} \rightarrow \mathcal{C}_j$ with \mathcal{C}_j now interpreted as a subspace of \mathcal{S} rather than an independent Hilbert space. In particular, both target and source phase spaces are copies of the Schwinger phase space.

Let I be the momentum map on Σ and let I' be the momentum map on Σ^* , in which case $\Sigma_J \times \Sigma^*$ is a symplectic reduction by I at contour value J . The group orbits of I are circles and thus the lift of $\mathcal{L}_{\mathcal{I}}$ is an S^1 bundle over S^3 . We quantize this manifold by considering contours that follow the Hamiltonian flow of I . The Hamiltonian I is conjugate to the 4π -periodic angle ψ so by Eq. A.4.4 of Appendix A the action integral around such a contour is $4\pi J$. As shown in Aquilanti *et al* [44] the Maslov index for this contour is $\mu = 4$ and thus the Bohr-Sommerfeld quantization condition is

$$4\pi J - 2\pi = 2\pi n, \quad \implies \quad J = \frac{n + 1}{2}, \quad (5.3.11)$$

which is the familiar restriction on the values of J .

5.4 Conclusions

During the writing of this dissertation we have begun to turn our attention to q -deformed spin networks. The methods of semiclassical analysis used extensively in this work are not immediately applicable to such systems since the Lagrangian manifolds that support the semiclassical approximations of states involved can not be interpreted as level sets of momentum maps of some groups or as group orbits. This is because there is no Lie group underlying the q -deformed spin networks. Rather, these networks are built upon the Hopf algebras $SL_q(2)$. The group theory used to construct the invariant densities on the Lagrangian manifolds is no longer applicable, for instance. In order to tackle such networks we first need to modify the semiclassical methods used and then analyze how the modifications affect the various aspects of the remodeling procedure.

The work presented in this dissertation is meant to provide a framework for simplifying semiclassical calculations of the objects that occur in Loop Quantum Gravity and in spin-foam models. Sections 5.1 and 5.2 outlined exactly how the inner product remodeling applies to the $3nj$ -symbols and the g -inserted spin networks. The next natural step would be to carry out the semiclassical approximations of physically relevant objects such as the $15j$ -symbol using the structures set up in this chapter to simplify the calculations. It is the hope of the author that the remodeling procedure will be a valuable tool in determining the semiclassical and asymptotic behavior of spin network based approaches to quantum gravity.

Bibliography

- [1] V. Aquilanti et al. “Semiclassical mechanics of the Wigner $6j$ -symbol”. In: *Journal of Physics A: Mathematical and Theoretical* 45.6 (2012), p. 065209.
- [2] J. Roberts. “Classical $6j$ -symbols and the tetrahedron”. In: *Geometry and Topology* 3 (1999), pp. 21–66.
- [3] R. Penrose. “Angular momentum: an approach to combinatorial space-time”. In: *Quantum Theory and Beyond* (1971), pp. 151–180.
- [4] S. A. Major. “A spin network primer”. In: *American Journal of Physics* 67.11 (1999), pp. 972–980.
- [5] C. Rovelli. *Quantum gravity*. Cambridge University Press, 2004.
- [6] I. B. Levinson. “Sums of Wigner coefficients and their graphical representation”. In: *Proceed. Physical-Technical Inst. Acad. Sci. Lithuanian SSR* 2.17 (1956), p. 4.9.
- [7] A. P. Yutsis, V. Vanagas, and I. B. Levinson. *Mathematical apparatus of the theory of angular momentum*. Israel program for scientific translations, 1962.
- [8] G. Stedman. *Diagram Techniques in Group Theory*. Cambridge University Press, 1990. ISBN: 0521327873.
- [9] L. Kauffman and S. Lins. *Temperley-Lieb recoupling theory and invariants of 3-manifolds*. 134. Princeton University Press, 1994.
- [10] V. Aquilanti et al. “Quantum and semiclassical spin networks: from atomic and molecular physics to quantum computing and gravity”. In: *Physica Scripta* 78.5 (2008), p. 058103.
- [11] B. Hasslacher and M. J. Perry. “Spin networks are simplicial quantum gravity”. In: *Physics Letters B* 103.1 (1981), pp. 21–24.
- [12] A. Ashtekar and J. Lewandowski. “Background independent quantum gravity: a status report”. In: *Classical and Quantum Gravity* 21.15 (2004), R53.
- [13] T. Thiemann. *Modern canonical quantum general relativity*. Vol. 26. Cambridge University Press Cambridge, 2007.
- [14] R. Arnowitt, S. Deser, and C. W. Misner. “The dynamics of general relativity”. In: *Gravitation: An Introduction to Current Research*. Ed. by L. Witten. New York; London: Wiley, 1962, pp. 227–265.

- [15] J. Schwinger. “Quantized gravitational field”. In: *Physical Review* 130.3 (1963), p. 1253.
- [16] A. Ashtekar. “New variables for classical and quantum gravity”. In: *Physical Review Letters* 57.18 (1986), pp. 2244–2247.
- [17] C. Rovelli and L. Smolin. “Spin networks and quantum gravity”. In: *Physical Review D* 52.10 (1995), pp. 5743–5759.
- [18] R. W. Jackiw. “Schrödinger picture for boson and fermion quantum field theories”. In: *Mathematical Quantum Field Theory and Related Topics: Proceedings of the 1987 Montréal Conference Held September 1-5, 1987*. Ed. by J. Feldman et al. Vol. 9. American Mathematical Society, 1988, p. 107.
- [19] C. Rovelli and L. Smolin. “Discreteness of area and volume in quantum gravity”. In: *Nuclear Physics B* 442.3 (1995), pp. 593–619.
- [20] A. Ashtekar and J. Lewandowski. “Quantum theory of geometry. 2. Volume operators”. In: *Advances in Theoretical and Mathematical Physics* 1 (1998), pp. 388–429.
- [21] A. Ashtekar and C. Rovelli. “A loop representation for the quantum Maxwell field”. In: *Classical and Quantum Gravity* 9.5 (1992), p. 1121.
- [22] R. Gambini and J. Pullin. *Loops, knots, gauge theories and quantum gravity*. Cambridge University Press, 2000.
- [23] J. C. Baez. “An introduction to spin foam models of BF theory and quantum gravity”. In: *Geometry and quantum physics*. Springer, 2000, pp. 25–93.
- [24] D. Oriti. “Spacetime geometry from algebra: spin foam models for non-perturbative quantum gravity”. In: *Reports on Progress in Physics* 64.12 (2001), p. 1703.
- [25] A. Perez. “Spin foam models for quantum gravity”. In: *Classical and Quantum Gravity* 20.6 (2003), R43.
- [26] A. Perez. “The spin-foam approach to quantum gravity”. In: *Living Rev. Relativity* 16.3 (2013), p. 1205.2019.
- [27] G. Ponzano and T. Regge. “Semiclassical limit of Racah coefficients”. In: *Spectroscopic and group theoretical methods in physics*. Ed. by F Bloch et al. Amsterdam: North-Holland, 1968, pp. 1–98.
- [28] A. R. Edmonds. *Angular momentum in quantum mechanics*. Princeton University Press, 1996.
- [29] V. G. Turaev and O. Y. Viro. “State sum invariants of 3-manifolds and quantum $6j$ -symbols”. In: *Topology* 31.4 (1992), pp. 865–902.
- [30] H. Ooguri. “Topological lattice models in four dimensions”. In: *Modern Physics Letters A* 7.30 (1992), pp. 2799–2810.
- [31] F. J. Archer. *A simplicial approach to topological quantum field theory*. University of Cambridge, 1993.

- [32] F. J. Archer. “A topological quantum field theory construction on piecewise linear manifolds”. In: *Journal of Geometry and Physics* 16.1 (1995), pp. 39–70.
- [33] L. Crane and D. Yetter. “Categorical Construction of 4D Topological Quantum Field Theories”. In: *Quantum Topology*. Ed. by L. Kauffman and R. Baadhio. World Scientific, 1993.
- [34] J. Roberts. “Skein theory and Turaev-Viro invariants”. In: *Topology* 34.4 (1995), pp. 771–787.
- [35] J. W. Barrett and L. Crane. “Relativistic spin networks and quantum gravity”. In: *Journal of Mathematical Physics* 39.6 (1998), pp. 3296–3302.
- [36] J. Engle, R. Pereira, and C. Rovelli. “Loop-quantum-gravity vertex amplitude”. In: *Physical Review Letters* 99.16 (2007), p. 161301.
- [37] L. Freidel and K. Krasnov. “A new spin foam model for 4D gravity”. In: *Classical and Quantum Gravity* 25.12 (2008), p. 125018.
- [38] D. Neville. “A technique for solving recurrence relations approximately and its application to the $3\text{-}J$ and $6\text{-}J$ symbols”. In: *Journal of Mathematical Physics* 12.12 (1971), pp. 2438–2453.
- [39] W. H. Miller. “Classical-limit quantum mechanics and the theory of molecular collisions”. In: *Advances in Chemical Physics* 25.1 (1974), pp. 69–177.
- [40] K. Schulten and R. G. Gordon. “Exact recursive evaluation of $3j$ and $6j$ coefficients for quantummechanical coupling of angular momenta”. In: *Journal of Mathematical Physics* 16.10 (1975), pp. 1961–1970.
- [41] K. Schulten and R. G. Gordon. “Semiclassical approximations to $3j$ and $6j$ coefficients for quantummechanical coupling of angular momenta”. In: *Journal of Mathematical Physics* 16.10 (1975), pp. 1971–1988.
- [42] L. C. Biedenharn and J. D. Louck. *The Racah-Wigner algebra in quantum theory*. Addison-Wesley, 1981.
- [43] L. Charles. “On the quantization of polygon spaces”. In: *Asian Journal of Mathematics* 14.1 (2010), pp. 109–152.
- [44] V. Aquilanti et al. “Semiclassical analysis of Wigner $3j$ -symbol”. In: *Journal of Physics A: Mathematical and Theoretical* 40.21 (2007), p. 5637.
- [45] H. M. Haggard and R. G. Littlejohn. “Asymptotics of the Wigner $9j$ -symbol”. In: *Classical and Quantum Gravity* 27.13 (2010), p. 135010.
- [46] H. M. Haggard. “Asymptotic analysis of spin networks with applications to quantum gravity”. PhD thesis. University of California - Berkeley.
- [47] L. Yu. “Semiclassical analysis of $SU(2)$ spin networks”. PhD thesis. University of California - Berkeley, 2010.

- [48] V. Bonzom and P. Fleury. “Asymptotics of Wigner $3nj$ -symbols with small and large angular momenta: an elementary method”. In: *Journal of Physics A: Mathematical and Theoretical* 45.7 (2012), p. 075202.
- [49] J. C. Baez, J. D. Christensen, and G. Egan. “Asymptotics of $10j$ symbols”. In: *Classical and Quantum Gravity* 19.24 (2002), p. 6489.
- [50] L. Freidel and D. Louapre. “Asymptotics of $6j$ and $10j$ symbols”. In: *Classical and Quantum Gravity* 20.7 (2003), p. 1267.
- [51] A. Hedeman et al. *Symplectic and semiclassical aspects of the Schläfli identity*. 2014. arXiv:1409.7117 [math-ph].
- [52] A. Martinez. *An introduction to semiclassical and microlocal analysis*. Springer, 2002.
- [53] A. S. Mishchenko, B. Y. Sternin, and V. E. Shatalov. *Lagrangian manifolds and the Maslov operator*. Springer, 1990.
- [54] R. G. Littlejohn. “Semiclassical structure of trace formulas”. In: *Journal of Mathematical Physics* 31.12 (1990), pp. 2952–2977.
- [55] I. Esterlis et al. “Maslov indices, Poisson brackets, and singular differential forms”. In: *Europhysics Letters* 106.5 (2014), p. 50002.
- [56] R. Abraham and J. E. Marsden. *Foundations of mechanics*. Assistance by Raiu, Tudor S and Cushman, Richard. Benjamin/Cummings Publishing Company Reading, Massachusetts, 1978.
- [57] S. Roman. *Advanced linear algebra*. Vol. 135. Springer, 2007.
- [58] S. Bates and A. Weinstein. *Lectures on the Geometry of Quantization*. American Mathematical Soc., 1997.
- [59] S. E. Cappell, R. Lee, and E. Y. Miller. “On the Maslov index”. In: *Communications on Pure and Applied Mathematics* 47.2 (1994), pp. 121–186.
- [60] G. Lion and M. Vergne. *The Weil representation, Maslov index and Theta series*. Springer, 1980.
- [61] M. de Gosson. *Maslov classes, metaplectic representation and lagrangian quantization*. Akademie Verlag, 1997.
- [62] J. Schwinger. “On angular momentum, USAEC Report NYO-3071 (unpublished)”. In: *Quantum theory of angular momentum*. Ed. by L. Biedenharn and H. van Dam. Academic Press, New York, 1952, pp. 229–279.
- [63] V. Bargmann. “On the representations of the rotation group”. In: *Reviews of Modern Physics* 34.4 (1962), p. 829.
- [64] D. A. Varshalovich, A. N. Moskalev, and V. K. Khersonskii. *Quantum theory of angular momentum*. World Scientific, 1988.
- [65] S. Sternberg. *Group theory and physics*. Cambridge University Press, 1995.

- [66] A. Messiah. *Quantum mechanics, volume II*. North Holland Publ. Co., Amsterdam, 1962.
- [67] V. I. Arnol'd. *Mathematical methods of classical mechanics*. Vol. 60. Springer, 1989.
- [68] R. H. Cushman and L. M. Bates. *Global aspects of classical integrable systems*. Vol. 94. Springer, 1997.
- [69] A. A. Kirillov and E. Hewitt. *Elements of the Theory of Representations*. Springer, 1976.
- [70] N. M. J. Woodhouse. *Geometric quantization*. Clarendon Press, 1980.
- [71] V. Guillemin and S. Sternberg. *Geometric asymptotics*. 14. American Mathematical Soc., 1990.
- [72] M. Dupuis and E. R. Livine. “Pushing the asymptotics of the $6j$ -symbol further”. In: *Physical Review D* 80.2 (2009), p. 024035.
- [73] M. Dupuis and E. R. Livine. “The $6j$ -symbol: recursion, correlations and asymptotics”. In: *Classical and Quantum Gravity* 27.13 (2010), p. 135003.
- [74] T. Regge. “General relativity without coordinates”. In: *Il Nuovo Cimento* 19.3 (1961), pp. 558–571.
- [75] V. G. Turaev. “Quantum invariants of 3-manifold and a glimpse of shadow topology”. In: *Quantum groups*. Springer, 1992, pp. 363–366.
- [76] R. G. Littlejohn and L. Yu. “Uniform semiclassical approximation for the Wigner $6j$ -symbol in terms of rotation matrices”. In: *The Journal of Physical Chemistry A* 113.52 (2009), pp. 14904–14922.
- [77] M. Kapovich and J. Millson. “On the moduli space of polygons in the Euclidean plane”. In: *Journal of Differential Geometry* 42.1 (1995), pp. 133–164.
- [78] M. Kapovich and J. Millson. “The symplectic geometry of polygons in Euclidean space”. In: *Journal of Differential Geometry* 44.3 (1996), pp. 479–513.
- [79] A. Chakrabarti. “On the coupling of 3 angular momenta”. In: *Annales de l'institut Henri Poincaré (A) Physique théorique*. Vol. 1. 3. Gauthier-villars, 1964, pp. 301–327.
- [80] J. LévyLeblond and M. LévyNahas. “Symmetrical coupling of three angular momenta”. In: *Journal of Mathematical Physics* 6.9 (1965), pp. 1372–1380.
- [81] S. A. Major and M. D. Seifert. “Modelling space with an atom of quantum geometry”. In: *Classical and Quantum Gravity* 19.8 (2002), p. 2211.
- [82] G. Carbone, M. Carfora, and A. Marzuoli. “Quantum states of elementary three-geometry”. In: *Classical and Quantum Gravity* 19.14 (2002), p. 3761.
- [83] D. Neville. “Volume operator for spin networks with planar or cylindrical symmetry”. In: *Physical Review D* 73.12 (2006), p. 124004.

- [84] J. Brunnemann and T. Thiemann. “Simplification of the spectral analysis of the volume operator in loop quantum gravity”. In: *Classical and Quantum Gravity* 23.4 (2006), p. 1289.
- [85] J. Brunnemann and D. Rideout. “Properties of the volume operator in loop quantum gravity: I. Results”. In: *Classical and Quantum Gravity* 25.6 (2008), p. 065001.
- [86] J. Brunnemann and D. Rideout. “Oriented matroids - combinatorial structures underlying loop quantum gravity”. In: *Classical and Quantum Gravity* 27.20 (2010), p. 205008.
- [87] Y. Ding and C. Rovelli. “The volume operator in covariant quantum gravity”. In: *Classical and Quantum Gravity* 27.16 (2010), p. 165003.
- [88] E. Bianchi and H. M. Haggard. “Discreteness of the volume of space from Bohr-Sommerfeld quantization”. In: *Physical Review Letters* 107.1 (2011), p. 011301.
- [89] E. Bianchi and H. M. Haggard. “Bohr-Sommerfeld quantization of space”. In: *Physical Review D* 86.12 (2012), p. 124010.
- [90] T. Thiemann. “Closed formula for the matrix elements of the volume operator in canonical quantum gravity”. In: *Journal of Mathematical Physics* 39.6 (1998), pp. 3347–3371.
- [91] L. Schläfli. “On the multiple integral...” In: *Quarterly Journal of Mathematics* 2 (1858), pp. 269–300.
- [92] E. T. Whittaker. *A treatise on the analytical dynamics of particles and rigid bodies: with an introduction to the problem of three bodies*. CUP Archive, 1970.
- [93] E. R. Livine and S. Speziale. “Solving the simplicity constraints for spinfoam quantum gravity”. In: *Europhysics Letters* 81.5 (2008), p. 50004.
- [94] J. W. Barrett. “The classical evaluation of relativistic spin networks”. In: *Advances in Theoretical and Mathematical Physics* 2 (1998), pp. 593–600.
- [95] J. W. Barrett and R. M. Williams. “The asymptotics of an amplitude for the four simplex”. In: *Advances in Theoretical and Mathematical Physics* 3 (1999), pp. 209–215.
- [96] J. C. Baez and J. D. Christensen. “Positivity of spin foam amplitudes”. In: *Classical and Quantum Gravity* 19.8 (2002), p. 2291.
- [97] J. D. Christensen and G. Egan. “An efficient algorithm for the Riemannian $10j$ symbols”. In: *Classical and Quantum Gravity* 19.6 (2002), p. 1185.
- [98] J. W. Barrett and C. M. Steele. “Asymptotics of relativistic spin networks”. In: *Classical and Quantum Gravity* 20.7 (2003), p. 1341.
- [99] P. J. Brussaard and H. A. Tolhoek. “Classical limits of clebsch-gordan coefficients, racah coefficients and $D_{mn}^l(\varphi, \theta, \psi)$ -functions”. In: *Physica* 23.6 (1957), pp. 955–971.

- [100] P. A. Braun et al. “Semiclassics of rotation and torsion”. In: *Zeitschrift für Physik B Condensed Matter* 100.1 (1996), pp. 115–127.
- [101] D. Sokolovski and J. N. L. Connor. “Semiclassical nearside-farside theory for inelastic and reactive atom-diatom collisions”. In: *Chemical Physics Letters* 305.3 (1999), pp. 238–246.
- [102] V. Guillemin, L. J. Jeffrey, and R. S. Sjamaar. “Symplectic implosion”. In: *Transformation Groups* 7.2 (2002), pp. 155–185.
- [103] L. Freidel and S. Speziale. “Twisted geometries: a geometric parametrization of $SU(2)$ phase space”. In: *Physical Review D* 82.8 (2010), p. 084040.
- [104] J. C. Baez and J. P. Muniain. *Gauge fields, knots and gravity*. Vol. 6. World Scientific Singapore, 1994.
- [105] A. Weinstein. “Symplectic geometry”. In: *Bulletin of the American Mathematical Society* 5.1 (1981), pp. 1–13.
- [106] M. V. Berry and K. E. Mount. “Semiclassical approximations in wave mechanics”. In: *Reports on Progress in Physics* 35.1 (1972), p. 315.
- [107] E. U. Condon and G. H. Shortley. *The theory of atomic spectra*. Cambridge University Press, 1935.
- [108] Y. Weissman. “Semiclassical approximation in the coherent states representation”. In: *The Journal of Chemical Physics* 76.8 (1982), pp. 4067–4079.
- [109] A. Voros. “Wentzel-Kramers-Brillouin method in the Bargmann representation”. In: *Physical Review A* 40.12 (1989), p. 6814.
- [110] M. Stone, K.-S. Park, and A. Garg. “The semiclassical propagator for spin coherent states”. In: *Journal of Mathematical Physics* 41.12 (2000), pp. 8025–8049.
- [111] M. Baranger et al. “Semiclassical approximations in phase space with coherent states”. In: *Journal of Physics A: Mathematical and General* 34.36 (2001), p. 7227.
- [112] R. G. Littlejohn. “The semiclassical evolution of wave packets”. In: *Physics Reports* 138.4 (1986), pp. 193–291.
- [113] J. E. Marsden and T. S. Ratiu. *Introduction to mechanics and symmetry: a basic exposition of classical mechanical systems*. Vol. 17. Springer, 1999.
- [114] J.-P. Ortega and T. S. Ratiu. *Momentum maps and Hamiltonian reduction*. Vol. 222. Springer, 2004.
- [115] J. Butterfield. “On symplectic reduction in classical mechanics”. In: *Philosophy of Physics* 2 (2006), p. 1.
- [116] D. D. Holm et al. *Geometric mechanics and symmetry: from finite to infinite dimensions*. 12. Oxford University Press London, 2009.
- [117] C. T. C. Wall. “Non-additivity of the signature”. In: *Inventiones Mathematicae* 7.3 (1969), pp. 269–274.

- [118] L. Hörmander. “Fourier integral operators. I”. In: *Acta Mathematica* 127.1 (1971), pp. 79–183.
- [119] A. Einstein. “Zum quantensatz von Sommerfeld und Epstein”. In: *Verhandl. Dtsch. Phys. Ges.* 19 (1917), pp. 82–92.
- [120] L. Brillouin. “Remarques sur la mécanique ondulatoire”. In: *Journal de Physique et Le Radium* 7.12 (1926), pp. 353–368.
- [121] J. B. Keller. “Corrected Bohr-Sommerfeld quantum conditions for nonseparable systems”. In: *Annals of Physics* 4.2 (1958), pp. 180–188.
- [122] I. C. Percival. “Regular and irregular spectra”. In: *Journal of Physics B: Atomic and Molecular Physics* 6.9 (1973), p. L229.
- [123] M. V. Berry and M. Tabor. “Closed orbits and the regular bound spectrum”. In: *Proceedings of the Royal Society of London. A. Mathematical and Physical Sciences* 349.1656 (1976), pp. 101–123.
- [124] M. C. Gutzwiller. *Chaos in classical and quantum mechanics*. Vol. 1. Springer, 1990.
- [125] M. Brack and R. K. Bhaduri. *Semiclassical physics*. Vol. 14. Addison-Wesley Reading, 1997.
- [126] M. Cargo et al. “Quantum normal forms, Moyal star product and Bohr–Sommerfeld approximation”. In: *Journal of Physics A: Mathematical and General* 38.9 (2005), p. 1977.
- [127] V. P. Maslov and M. V. Fedoriuk. *Semi-classical approximation in quantum mechanics*. Vol. 7. Springer, 2001.
- [128] R. G. Littlejohn and J. M. Robbins. “A new way to compute Maslov indices”. In: *Physical Review A* 36.6 (1987), p. 2953.
- [129] C. Emmrich and A. Weinstein. “Geometry of the transport equation in multicomponent WKB approximations”. In: *Communications in Mathematical Physics* 176.3 (1996), pp. 701–711.
- [130] H. Weyl. *The theory of groups and quantum mechanics*. Courier Dover Publications, 1950.
- [131] E. Wigner. “On the quantum correction for thermodynamic equilibrium”. In: *Physical Review* 40.5 (1932), p. 749.
- [132] M. V. Berry. “Semi-classical mechanics in phase space: a study of Wigner’s function”. In: *Philosophical Transactions of the Royal Society of London. Series A, Mathematical and Physical Sciences* 287.1343 (1977), pp. 237–271.
- [133] N. L. Balazs and B. K. Jennings. “Wigner’s function and other distribution functions in mock phase spaces”. In: *Physics Reports* 104.6 (1984), pp. 347–391.
- [134] A. M. O. De Almeida. “The Weyl representation in classical and quantum mechanics”. In: *Physics Reports* 295.6 (1998), pp. 265–342.

- [135] H. J. Groenewold. *On the principles of elementary quantum mechanics*. Springer, 1946.
- [136] J. E. Moyal. “Quantum mechanics as a statistical theory”. In: *Mathematical Proceedings of the Cambridge Philosophical Society*. Vol. 45. 01. Cambridge Univ Press, 1949, pp. 99–124.

Appendix A

Representations of Angular Momenta

A.1 The Schwinger Hilbert Space

We begin by outlining our notation for the Schwinger formalism for representing angular momentum operators in terms of harmonic oscillators [62, 63]. The method begins with a pair of harmonic oscillators $\hat{H}_\mu = (1/2)(\hat{x}_\mu^2 + \hat{p}_\mu^2)$, $\mu = 1, 2$, which act on the (Schwinger) Hilbert space $\mathcal{S} = L^2(\mathbb{R}^2)$ containing wavefunctions $\psi(x)$, $x = (x_1, x_2) \in \mathbb{R}^2$ (or ket vectors). We denote the dual space by \mathcal{S}^* which we also think of as a space of wavefunctions (or bra vectors). To distinguish quantum mechanical operators from their classical counterparts, we put hats on operators. Let $\hat{a}_\mu = (\hat{x}_\mu + i\hat{p}_\mu)/\sqrt{2}$ and $\hat{a}_\mu^\dagger = (\hat{x}_\mu - i\hat{p}_\mu)/\sqrt{2}$ ($\mu = 1, 2$) be the usual creation and annihilation operators and define

$$\hat{I} = \frac{1}{2}\hat{a}^\dagger\hat{a}, \quad \hat{\mathbf{J}} = \frac{1}{2}\hat{a}^\dagger\boldsymbol{\sigma}\hat{a}, \quad (\text{A.1.1})$$

where $\boldsymbol{\sigma}$ is the vector of Pauli matrices and contractions are implied among the two components of \hat{a} , \hat{a}^\dagger and the components of the Pauli matrices. The operator \hat{I} is half the sum of the two harmonic oscillator Hamiltonians, with the zero point energy subtracted off, $\hat{I} = (1/2)(\hat{H}_1 + \hat{H}_2 - 1)$. These operators satisfy the commutation relations

$$[\hat{I}, \hat{J}_a] = 0; \quad [\hat{J}_a, \hat{J}_b] = i\epsilon_{abc}\hat{J}_c, \quad (\text{A.1.2})$$

as well as the operator identity

$$\hat{\mathbf{J}}^2 = \hat{I}(\hat{I} + 1) \quad (\text{A.1.3})$$

The operator $\hat{\mathbf{J}}$ thus forms an $SU(2)$ algebra on \mathcal{S} , with \hat{I} a Casimir operator. The spectrum of \hat{I} is the set of all non-negative half-integers, $j = 0, 1/2, 1, \dots$ and the eigenspaces of \hat{I} are in a one-to-one correspondence with the carrier spaces of the $SU(2)$ irreps. These carrier spaces will be written as \mathcal{C}_j wherever they arise. Since each irrep occurs precisely once, $\mathcal{S} = \bigoplus_j \mathcal{C}_j$. Since $\hat{\mathbf{J}}$ commutes with \hat{I} we may interpret the operator $\hat{\mathbf{J}}$ as either an operator on the full Schwinger Hilbert space \mathcal{S} or on the irreducible subspaces \mathcal{C}_j . We use the standard physics phase conventions for the harmonic oscillator states and the Condon

and Shortley [107] phase conventions for the standard angular momentum basis vectors $|jm\rangle$. With these phase conventions the basis vectors $|jm\rangle$ in \mathcal{C}_j are identical to harmonic oscillator eigenvectors $|n_1 n_2\rangle$, with $n_1 = j + m$ and $n_2 = j - m$.

The dual Schwinger Hilbert space \mathcal{S}^* is the space of bra vectors, or equivalently the space of linear maps $\mathcal{S} \rightarrow \mathbb{C}$. For each operator on the Schwinger Hilbert space, there is an associated operator on the dual space. Let $\hat{A} : \mathcal{H} \rightarrow \mathcal{H}$ be a linear operator and define the transpose $\hat{A}^\top : \mathcal{H}^* \rightarrow \mathcal{H}^*$ as the operator \hat{A} acting on bras from the right,

$$\hat{A}^\top(\langle\phi|) = \langle\phi|\hat{A}. \quad (\text{A.1.4})$$

The map from operators to their dual is an anti-homomorphism with respect to the commutation algebra. That is, if $[\hat{A}, \hat{B}] = \hat{C}$, then $[\hat{A}^\top, \hat{B}^\top] = -\hat{C}^\top$. Note that $[-\hat{\mathbf{J}}_a^\top, -\hat{\mathbf{J}}_b^\top] = i\epsilon_{abc}(-\hat{\mathbf{J}}_c^\top)$ so the components of the operator $-\hat{\mathbf{J}}^\top$ form an $SU(2)$ algebra on \mathcal{S}^* , with \hat{I}^\top a Casimir operator.

The nj -Hilbert space for a collection of n angular momenta is the tensor product of n copies of the Schwinger Hilbert spaces \mathcal{S}_i , $\mathcal{H}_{nj} = \mathcal{S}_1 \otimes \cdots \otimes \mathcal{S}_n$, where the index is used to distinguish copies of the Schwinger Hilbert space. Operators on the component spaces can be lifted into operators on the full nj -Hilbert space. For example, an operator \hat{A} on \mathcal{S}_2 becomes an operator on the $2j$ -Hilbert space $\mathcal{H}_{2j} = \mathcal{S}_1 \otimes \mathcal{S}_2$ defined by $\hat{I}d_1 \otimes \hat{\mathbf{J}}_2$, where $\hat{I}d_1$ is the identity on \mathcal{H}_1 and $\hat{\mathbf{J}}_2$ is the angular momentum operator defined on \mathcal{H}_2 . In a slight abuse of notation, we will let $\hat{\mathbf{J}}_2$ stand for both the map $\mathcal{S}_2 \rightarrow \mathcal{S}_2$ and the map $\mathcal{H}_{2j} \rightarrow \mathcal{H}_{2j}$.

A.2 The Schwinger Phase Space

The Schwinger phase space Σ is defined as the classical phase space for two harmonic oscillators, $\Sigma = (\mathbb{R}^4, \sum_\mu dp_\mu \wedge dx_\mu)$, where $\mu = 1, 2$ labels the oscillator. Complex coordinates (z_μ, \bar{z}_μ) on Σ are defined by

$$z_\mu = \frac{1}{\sqrt{2}}(x_\mu + ip_\mu), \quad \bar{z}_\mu = \frac{1}{\sqrt{2}}(x_\mu - ip_\mu). \quad (\text{A.2.1})$$

The coordinates z_1 and z_2 can be combined in a column vector to form a two-component spinor z . In these coordinates, the Schwinger phase space is $(\mathbb{C}^2, idz^\dagger \wedge dz)$, where $dz^\dagger \wedge dz = \sum_\mu d\bar{z}_\mu \wedge dz_\mu$. The connection between \mathcal{S} and Σ is established in part by the Weyl correspondence which maps operators that act on \mathcal{S} into functions (or ‘‘symbols’’) on Σ , as discussed in more detail in Section C.3. In addition, the phase of a WKB wavefunction $\psi(x)$ in \mathcal{S} is given in part by the integral of the symplectic potential $\theta = p dx$ along the Lagrangian manifold in Σ that supports the semiclassical approximation, as discussed in Section C.1. The WKB phase of coherent state wavefunctions is given by the integral of the symplectic potential $\theta = \Im(dz^\dagger z)$ along complexified versions of these Lagrangian manifolds [108, 109, 110, 111]. The coherent states themselves live on \mathbb{C}^2 and provide another link between the classical and quantum descriptions of the Schwinger oscillators [63].

Interesting functions on Σ are

$$I = \frac{1}{2}z^\dagger z = \frac{1}{4}(x_1^2 + p_1^2 + x_2^2 + p_2^2); \quad \mathbf{J} = \frac{1}{2}z^\dagger \boldsymbol{\sigma} z, \quad (\text{A.2.2})$$

where we perform contractions as in Eq. A.1.1. The function I is the Weyl symbol of $\hat{I} + 1/2$ (it is one half of the sum of the classical harmonic oscillator Hamiltonians), and \mathbf{J} is the Weyl symbol of $\hat{\mathbf{J}}$. These functions satisfy the identities

$$\mathbf{J}^2 = I^2; \quad z z^\dagger = I \mathbf{1} + \mathbf{J} \cdot \boldsymbol{\sigma}. \quad (\text{A.2.3})$$

The definition of \mathbf{J} defines a map $\pi : \mathbb{C}^2 \rightarrow \mathbb{R}^3$ (where $\mathbb{R}^3 \cong \mathfrak{su}(2)^*$ is “angular momentum space”) which is the projection of the Hopf fibration, in which the Hamiltonian flow generated by I defines the fibers (the Hopf circles) of the fibration. Thus, π is the projection map of Poisson reduction under the $U(1)$ symmetry generated by I . If π_j is the projection map whose domain is restricted to the level set $I = j + 1/2$ (a 3-sphere in \mathbb{C}^2), then it is the projection map of symplectic reduction, and the reduced symplectic manifold (the symplectic leaf in \mathbb{R}^3) is a 2-sphere with radius $|\mathbf{J}| = j + 1/2$.

Consider a vector $\mathbf{J} \in \mathbb{R}^3$ of length I . The inverse image of \mathbf{J} under π is a Hopf circle of spinors $z \in \mathbb{C}^2$ parametrized by $0 \leq \psi < 4\pi$. Let θ and ϕ be the polar and azimuthal angles of \mathbf{J} with respect to the z -axis. Then the vector $\mathbf{J} \in \mathbb{R}^3$ and the spinor $z \in \mathbb{C}^2$ are

$$\mathbf{J} = I \begin{pmatrix} \sin \theta \cos \phi \\ \sin \theta \sin \phi \\ \cos \theta \end{pmatrix}, \quad z = \sqrt{2I} e^{-i\psi/2} \begin{pmatrix} \cos(\theta/2) e^{-i\phi/2} \\ \sin(\theta/2) e^{+i\phi/2} \end{pmatrix}. \quad (\text{A.2.4})$$

Plugging this spinor into the symplectic form $dz^\dagger \wedge dz$ on Σ yields

$$\omega = dI \wedge d\psi + dJ_z \wedge d\phi. \quad (\text{A.2.5})$$

We associate the dual Schwinger Hilbert space \mathcal{S}^* with the dual Schwinger phase space $\Sigma^* = (\mathbb{R}^4, -dp \wedge dx)$, which differs from Σ in having the opposite symplectic form. Let \hat{G} be the metric on the Schwinger Hilbert space, an antiunitary map

$$\hat{G} : \mathcal{S} \rightarrow \mathcal{S}^* : |\psi\rangle \mapsto \langle \psi| : \psi(x) \mapsto \psi(x)^*. \quad (\text{A.2.6})$$

It corresponds to the classical antisymplectic “dual” map

$$G : \Sigma \rightarrow \Sigma^* : (x, p) \mapsto (x, p) : (z, \bar{z}) \mapsto (z, \bar{z}), \quad (\text{A.2.7})$$

which is not the identity map because the two copies of (x, p) belong to different spaces. The map G is antisymplectic because the pullback of the symplectic form $-dp \wedge dx$ on Σ^* is minus the symplectic form $dp \wedge dx$ on Σ .

Operators that act on \mathcal{S}^* are mapped into functions on Σ^* by a “dual Weyl correspondence,” which may be defined as follows. Let $\hat{A} : \mathcal{H} \rightarrow \mathcal{H}$ be a linear operator with

corresponding Weyl symbol $A(x, p) : \Phi \rightarrow \mathbb{C}$. Let $\hat{A}^\top : \mathcal{H}^* \rightarrow \mathcal{H}^*$ be the map defined in Eq. A.1.4. The “dual Weyl symbol” $A^\top(x, p) : \Phi^* \rightarrow \mathbb{C}$ is defined to be the composition $A^\top(x, p) \equiv A \circ G^{-1}(x, p)$. That is, the functional forms of $A^\top(x, p)$ and $A(x, p)$ are the same. Note that with this definition the Weyl symbol of the non-Hermitian operator \hat{a} on \mathcal{S} is the z -coordinate of Σ , while the dual Weyl symbol of \hat{a}^\top on \mathcal{S}^* is the z -coordinate of Σ^* . The symplectic form on Σ^* in these complex coordinates is $-idz^\dagger \wedge dz$. The Weyl symbols of operators \hat{I}^\top and $\hat{\mathbf{J}}^\top$ on \mathcal{S}^* under the dual Weyl correspondence are given by Eq. A.2.2 (they are the same functions in terms of the (x, p) or (z, \bar{z}) coordinates, but defined on a different space). The semiclassical approximations to WKB wavefunctions in \mathcal{S}^* are supported by Lagrangian manifolds in Σ^* , in which the phase is computed in part as the integral of the symplectic potential $-\int p dx$ along the Lagrangian manifold.

The classical nj -phase space for a collection of n angular momenta is the direct product of the Schwinger phase spaces Σ_r , with $r = 1, \dots, n$, labeling the angular momenta,

$$\Phi_{nj} = \Sigma_1 \times \dots \times \Sigma_n. \quad (\text{A.2.8})$$

This phase space can alternatively be written $(\mathbb{R}^{4n}, \omega_{nj})$, where the symplectic form is the sum of the symplectic forms on the component phase spaces,

$$\omega_{nj} = \sum_{r=1}^n \sum_{\mu=1}^2 dp_{\mu r} \wedge dx_{\mu r} = \sum_{r=1}^n idz_r^\dagger \wedge dz_r. \quad (\text{A.2.9})$$

Functions on the component spaces can be lifted into operators on the full Nj -phase space. For example, the operator for the 2nd angular momentum on $\Phi_{2j} = \Sigma_1 \times \Sigma_2$ maps $(z_1, z_2) \mapsto \mathbf{J}_2(z_2)$. In a slight abuse of notation, we will let \mathbf{J}_2 stand for both the function $:\Sigma_2 \rightarrow \mathbb{R}^3$ and the map $:\Phi_{2j} \rightarrow \mathbb{R}^3$.

A.3 Group Actions

Each Schwinger Hilbert space \mathcal{S} carries a unitary representation $\hat{U}(g) : \mathcal{S} \rightarrow \mathcal{S}$ of $SU(2)$ generated by the operators $\hat{\mathbf{J}}$, defined in Eq. A.1.1. The matrix elements of $\hat{U}(g)$ in the jm -basis form the Wigner D -matrix,

$$D_{mm'}^j(g) = \langle jm | \hat{U}(g) | jm' \rangle. \quad (\text{A.3.1})$$

The dual Hilbert space \mathcal{S}^* also carries a unitary representation $\hat{U}^{\dagger\top}(g) : \mathcal{S}^* \rightarrow \mathcal{S}^* : \langle \psi | \mapsto \langle \psi | \hat{U}^{\dagger\top}(g)$ of $SU(2)$ generated by the operators $-\hat{\mathbf{J}}^\top$. This is a left action.

Just as the operators $\hat{\mathbf{J}}$ generate a unitary $SU(2)$ action on \mathcal{S} , so also do the classical functions \mathbf{J} defined in Eq. A.2.2 generate a symplectic $SU(2)$ action on Σ under their Hamiltonian flows. These flows are linear symplectic maps of Σ onto itself, providing a real representation of $SU(2)$ as a subgroup of $Sp(4)$. See Appendix A of Littlejohn [112] for more information about the relation between the quantum and classical action of $SU(2)$. Let

$z \in \mathbb{C}^2$ be the coordinates of a point in Σ . For an element $g \in SU(2)$, the $SU(2)$ action is given by $z \mapsto gz$. The classical angular momentum functions \mathbf{J} transform as a vector under the $SU(2)$ action, $\mathbf{J}(g^{-1}z) = \mathbf{R}(g)\mathbf{J}(z)$, where $\mathbf{R}(g) \in SO(3)$ is the representation matrix on \mathbb{R}^3 .

As a specific example, consider an $SO(3)$ rotation about an axis \mathbf{n} by angle ϕ , $\mathbf{R}(\mathbf{n}, \phi)$. In $SO(3)$, ϕ ranges from 0 to 2π . An arbitrary $SU(2)$ rotation can also be expressed in axis-angle form if we allow ϕ to range from 0 to 4π to compensate for the fact that $SU(2)$ is a double-cover of $SO(3)$. This rotation is represented on \mathcal{S} by the operator $\hat{U}(\mathbf{n}, \phi) = \exp(-i\phi\mathbf{n} \cdot \hat{\mathbf{J}})$. Classically, the rotation corresponds to a Hamiltonian flow by angle ϕ under the $U(1)$ subgroup of $SU(2)$ generated by $\mathbf{n} \cdot \mathbf{J}$ which is the spinor transformation,

$$z \mapsto e^{-i\phi\mathbf{n} \cdot \sigma/2} z. \quad (\text{A.3.2})$$

The map $\mathbf{J} : \Sigma \rightarrow \mathbb{R}^3$ is a Poisson map [113], giving \mathbb{R}^3 the Poisson structure $\{J_a, J_b\} = \epsilon_{abc} J_c$. We denote \mathbb{R}^3 with this Poisson structure by Λ . The map \mathbf{J} can also be interpreted as the momentum map [56] of the $SU(2)$ action on Σ , so that Λ or angular momentum space is identified with $\mathfrak{su}(2)^*$.

Similarly, there is an $SU(2)$ action on Σ^* . It is generated by the Hamiltonian flows of $-\mathbf{J} : \Sigma^* \rightarrow \mathbb{R}^3$, which are the Weyl symbols of $-\hat{\mathbf{J}}^\top$. The action generated by \mathbf{J} on coordinates $(x, p) \in \Sigma$ is the same as the action generated by $-\mathbf{J}$ on coordinates $(x, p) \in \Sigma^*$. This is because the negative sign in the generators cancels the negative sign on the symplectic form on Σ^* .

The operator \hat{I} acting on \mathcal{S} (defined in Equation A.1.1) serves as the generator for the group $U(1)$ and carries the representation $\hat{U} = \exp(-i\psi\hat{I})$. The Hamiltonian flow of I is a symplectic $U(1)$ action on Σ ,

$$z \mapsto e^{-i\psi/2} z, \quad (\text{A.3.3})$$

where ψ is the variable conjugate to I . The orbit of the $U(1)$ action generated by I passing through any point $z \neq 0$ on Σ is a Hopf circle on which ψ is a coordinate, covered once when $0 \leq \psi < 4\pi$. The level set $I^{-1}(j + 1/2)$ is a 3-sphere of radius $j + 1/2$.

A.4 Representations in the Schwinger Phase Space

In the x -representation of the Schwinger phase space, the two harmonic oscillator coordinates x_μ are taken to be the configuration variables and the coordinates p_μ are the conjugate momenta. The states $|x_1 x_2\rangle \in \mathcal{S}$ correspond to Lagrangian planes in Σ defined by the vanishing of the one-forms dx_μ , $\mu = 1, 2$. The planes are integral surfaces of the tangent vectors $X_{x_\mu} = \partial/\partial p_\mu$. Configuration space is the plane \mathbb{R}^2 . In this representation the symplectic potential is $\theta = \sum_\mu p_\mu dx_\mu$.

Transforming this to complex coordinates yields

$$\theta = \sum_\mu p_\mu dx_\mu = \frac{i}{2} \sum_\mu (\bar{z}_\mu dz_\mu - z_\mu d\bar{z}_\mu) + dF, \quad (\text{A.4.1})$$

where $F = -i \sum_{\mu} (z_{\mu}^2 - \bar{z}_{\mu}^2)/4 = \sum_{\mu} x_{\mu} p_{\mu}/2$.

Consider the x -representation action integral $S_{\Gamma} = \int_{\Gamma} \theta$ over some path $\Gamma \subset \Sigma$. The exact one-form dF will only contribute a boundary term to the action integral and will be dropped for now. Ultimately we are only concerned with action integrals around closed loops in which case these boundary terms cancel out. This is expected because the precise form of the symplectic potential depends on the representation and the action integral around a closed loop is a representation-independent quantity. First let Γ be a path starting at z_0 and generated by the Hamiltonian flow of I . Parametrize the flow by s so that $z(s) = e^{-is/2} z_0$ and let s range from 0 to ψ . The one-form dz restricted to this path is

$$dz|_{\Gamma} = \frac{dz(s)}{ds} ds = \frac{-i}{2} z(s) ds, \quad (\text{A.4.2})$$

and thus the symplectic potential from Eq. A.4.1 restricted to Γ is

$$\theta|_{\Gamma} = \frac{1}{2} \bar{z}(s) z(s) ds = I(s) ds, \quad (\text{A.4.3})$$

where $z \in \mathcal{S}$ is a two-component complex spinor, $I(s)$ is the function I defined in Eq. A.2.2 evaluated at $z(s)$, and the contribution from the exact one-form dF has been dropped. Under the $U(1)$ phase rotation the value of I remains constant and thus $I(s) = I_0$, the value of I at the starting point of the path. The action integral therefore evaluates to

$$S_{\Gamma} = \int_0^{\psi} I(s) ds = I_0 \psi, \quad (\text{A.4.4})$$

up to a correction from the boundary term.

Next let Γ be the path based at z_0 and formed by the Hamiltonian flow of $\mathbf{n} \cdot \mathbf{J}$ for some fixed axis \mathbf{n} . Parametrize the flow by s so that $z(s) = U(\mathbf{n}, s) z_0$ and let s range from 0 to ϕ . The one-form dz restricted to this path is

$$dz|_{\Gamma} = \frac{dz(s)}{ds} ds = \frac{-i}{2} \mathbf{n} \cdot \boldsymbol{\sigma} z(s) ds, \quad (\text{A.4.5})$$

and the canonical one-form restricted to Γ is

$$\theta|_{\Gamma} = \frac{1}{2} \bar{z}(s) (\mathbf{n} \cdot \boldsymbol{\sigma}) z(s) ds = \mathbf{n} \cdot \mathbf{J}(s) ds, \quad (\text{A.4.6})$$

where $\mathbf{J}(s)$ is the function \mathbf{J} defined in Eq. A.2.2 evaluated at $z(s)$ and the contribution from the exact one-form dF has been dropped. Under a rotation about \mathbf{n} the component $\mathbf{n} \cdot \mathbf{J}$ remains constant and thus $\mathbf{n} \cdot \mathbf{J}(s) = \mathbf{n} \cdot \mathbf{J}_0$, the \mathbf{n} -component of \mathbf{J} at the starting point of the path. The action integral therefore evaluates to

$$S_{\Gamma} = \int_0^{\phi} \mathbf{n} \cdot \mathbf{J}(s) ds = (\mathbf{n} \cdot \mathbf{J}_0) \phi, \quad (\text{A.4.7})$$

up to a correction from the boundary term.

The results in Eq. A.4.4 and Eq. A.4.7 are useful in computing action integrals for $SU(2)$ spin networks.

Appendix B

Symplectic Geometry

B.1 Symplectic Manifolds

A symplectic vector space is a pair (V, ω) where V is a vector space and $\omega \in \Omega^2(V)$ is a closed, non-degenerate two-form. The non-degeneracy condition implies that the dimension of V is even, so we set $\dim V = 2n$. Consider a subspace $W \subset V$. The symplectic complement $W^\omega \subset V$ is the set of all vectors $v \in V$ such that the one-form $\iota_v \omega$ annihilates W . That is,

$$W^\omega = \{v \in V \mid \omega(v, w) = 0, \forall w \in W\}. \quad (\text{B.1.1})$$

Let $\omega|_W$ be the symplectic form restricted to W . One interpretation of $\omega|_W$ is as a map $: W \rightarrow W^*$, where W^* is the set of linear maps $: W \rightarrow \mathbb{C}$, which allows definition of the kernel $\ker \omega|_W \subset W$. The maximal dimension of $\ker \omega|_W$ is n , half the dimension of V . Physically relevant subspaces of V typically fall into one of the following categories based on the relationship between the subspace and its symplectic complement. A subspace W is symplectic when $W^\omega \cap W = 0$. That is, the symplectic form restricted to W is non-degenerate. The pair $(W, \omega|_W)$ is thus a symplectic vector space and necessarily has an even dimension, $\dim W = 2m$, with $m \leq n$. A subspace is co-isotropic when $W^\omega \subset W$. The smallest dimension a co-isotropic subspace can have is half the dimension of V , so $n \leq \dim W \leq 2n$. A subspace is isotropic when $W^\omega \supset W$. Therefore the symplectic form restricted to W vanishes on an isotropic subspace, $\omega|_W = 0$. The largest dimension an isotropic subspace can have is half the dimension of V , so $0 \leq \dim W \leq n$. Finally, a subspace is Lagrangian when $W^\omega = W$. Lagrangian subspaces are both isotropic and co-isotropic and therefore a Lagrangian subspace must have exactly half the dimension of V , $\dim W = n$. A maximally isotropic subspace (an isotropic subspace with dimension n) or a minimally co-isotropic subspace (a co-isotropic subspace with dimension n) is necessarily Lagrangian if V is finite-dimensional.

Consider a co-isotropic subspace $W \subset V$ and let $\omega|_W$ be the symplectic form restricted to W . The kernel of $\omega|_W$ is an isotropic submanifold of V . Let W_R be the quotient vector space $W/\ker \omega|_W$ and let $\pi_R : W \rightarrow W_R$. Then by construction there exists a non-degenerate

closed form $\omega_R \in \Omega^2(W_R)$ such that $\pi_R^*\omega_R = \omega|_W$. The pair (W_R, ω_R) defines a symplectic vector space called a “reduced” vector space of W .

A phase space or symplectic manifold is a pair (M, ω) where M is a manifold of dimension $\dim M = 2n$ and $\omega \in \Omega^2(M)$ is a closed, non-degenerate two-form on M . The tangent space to any point on M is a symplectic vector space. Submanifolds of a symplectic manifold fall into the same categories as subspaces of a symplectic vector space based on the categorization of their tangent spaces. A typical example of a phase space is the co-tangent bundle T^*Q of some configuration space Q , although not all symplectic manifolds can be interpreted as co-tangent bundles (the two-sphere, for example). Darboux’s theorem (Darboux 1882) says that there always exists a set of local coordinates (q_i, p_i) around a point $P \in M$ ($i = 1, \dots, n$) such that the symplectic form evaluated at P can be expressed in the form

$$\omega = \sum_{i=1}^n dp_i \wedge dq_i. \quad (\text{B.1.2})$$

We usually write this symplectic form as simply $dp \wedge dq$ with a sum over index i implied. Since ω is closed it is locally exact. The symplectic potential θ (also called the symplectic, tautological, Liouville, Poincaré, or canonical one-form) is locally defined such that $\omega = d\theta$. In Darboux coordinates, $\theta = p dq$, where a sum over i is implied. The symplectic potential is not unique since we may add any closed one-form to it without affecting the symplectic form.

A map $F : M_1 \rightarrow M_2$ between two symplectic manifolds (M_1, ω_1) and (M_2, ω_2) is called “symplectic” if it preserves the symplectic form, $F^*\omega_2 = \omega_1$. A symplectomorphism is a symplectic map that is also a diffeomorphism. What is traditionally called a canonical transformation is a coordinate representation of a symplectomorphism. Under symplectomorphisms the canonical one-form may be shifted by a closed one-form but the symplectic form remains invariant.

An important result that inspired the development of the remodeling geometry is that the “graph” of a canonical transformation is a Lagrangian manifold [56, 39]. In particular let $\Phi_1 = (\Phi, \omega)$ be a phase space, and let Φ_2^* be the dual phase space $(\Phi, -\omega)$. Define the product phase space Φ_{12} as the manifold $\Phi \times \Phi$ with symplectic form $\pi_1^*\omega - \pi_2^*\omega$, where π_1 and π_2 are the projections from $\Phi \times \Phi$ to the first and second copies of Φ , respectively. Let $F : \Phi \rightarrow \Phi$ be a canonical transformation and define the graph of F to be the set of points $(z, z') \in \Phi \times \Phi^*$ satisfying $z = F(z')$. A vector $X \in T_{(F(z'), z')} \Phi_{12}$ tangent to the graph satisfies $\pi_{1*}X = F_* \circ \pi_{2*}X$. The product space symplectic form acting on any two tangent vectors to the graph at a point $(F(z'), z')$ is thus

$$\begin{aligned} (\pi_1^*\omega - \pi_2^*\omega')(X, Y) &= \omega(\pi_{1*}X, \pi_{1*}Y) - \omega(\pi_{2*}X, \pi_{2*}Y) \\ &= F^*\omega(\pi_{2*}X, \pi_{2*}Y) - \omega(\pi_{2*}X, \pi_{2*}Y) = 0, \end{aligned} \quad (\text{B.1.3})$$

where the last equality is due to the fact that F is a canonical transformation and thus $F^*\omega = \omega$. Therefore the graph of a canonical transformation is isotropic in the product phase

space. Since this transformation is an isomorphism the graph itself has the same dimension as Φ and thus half the dimension of the product phase space and we may conclude that the graph is a Lagrangian manifold.

A smooth function $H : M \rightarrow \mathbb{R}$ on a phase space is called a Hamiltonian. Given an Hamiltonian H we may define a Hamiltonian vector field $X_H \in \mathfrak{X}(M)$, defined such that

$$X_H \equiv \omega^{-1}(dH), \quad \iota_{X_H} \omega = dH, \quad (\text{B.1.4})$$

where ω^{-1} in the first expression is interpreted as a map from one-forms to vector fields on Φ . The Poisson bracket of two Hamiltonians A, B is defined by

$$\{A, B\} = -\omega(X_A, X_B) = \sum_{i=1}^n \frac{\partial A}{\partial q_i} \frac{\partial B}{\partial p_i} - \frac{\partial A}{\partial p_i} \frac{\partial B}{\partial q_i}, \quad (\text{B.1.5})$$

where the last expression is the Poisson bracket expressed in terms of local Darboux coordinates.

A phase space representation is a foliation of a phase space Φ into a family of Lagrangian manifolds. ‘‘Representation space’’ \mathcal{Q} is the space formed under a quotient operation where two points in Φ are considered equivalent if they lie on the same Lagrangian leaf. This is the semiclassical setting for discussing representations in quantum mechanics. Let q_i be local coordinates on \mathcal{Q} so that a particular Lagrangian leaf is uniquely specified by the set of q_i . The forms dq_i all vanish when restricted to a particular Lagrangian leaf and the leaves are the integral surfaces of the Hamiltonian vector fields X_{q_i} . Consider a point z in phase space and let p_i be a locally-defined set of conjugate momenta to the q_i so that the set (q_i, p_i) form local Darboux coordinates (this involves an arbitrary choice of local Lagrangian section in the leaf bundle over \mathcal{Q}). In this case we may form a local symplectic potential $\theta = p dx$. Given one representation we may change to another representation via a canonical transformation. This generically will cause the local symplectic potential to change by a closed one-form. The action integrals and Maslov indices along an open path are both representation-dependent quantities. However, physical quantities such as the semiclassical approximations to inner products will ultimately wind up being independent of representation.

B.2 Momentum Maps

A symmetry on a Hamiltonian system (a phase space with a Hamiltonian) allows for many useful structures to be added to the phase space, such as group actions and momentum maps [56, 114]. The group actions represent the application of the symmetry to the phase space and the momentum maps act as the ‘‘conserved quantities’’ associated with the symmetry under Noether’s theorem.

Let Φ be a symplectic manifold and G a connected Lie group with a symplectic action $\varphi_g : \Phi \rightarrow \Phi$, Lie algebra \mathfrak{g} , and dual algebra \mathfrak{g}^* . Let $\{\xi_i\}$ be a basis of \mathfrak{g} and let c_{ij}^k be the

structure constants of the algebra in this basis, so $[\xi_i, \xi_j] = c_{ij}^k \xi_k$. Let $X_i \in \mathfrak{X}(\Phi)$ be the infinitesimal generators of the action φ corresponding to the basis vectors ξ_i ,

$$X_i \equiv \left. \frac{d}{dt} \right|_{t=0} \varphi_{\exp t\xi_i}. \quad (\text{B.2.1})$$

Consider a map $\mathbf{P} : \Phi \rightarrow \mathfrak{g}^*$. Let $P_i \equiv \langle \mathbf{P}, \xi_i \rangle : \Phi \rightarrow \mathbb{R}$ be the components of \mathbf{P} with respect to this basis and let $X_{P_i} = \omega^{-1}(dP_i)$ be the associated Hamiltonian vector fields. The map \mathbf{P} is called a ‘‘momentum map’’ if the flow vectors X_i are the same as the Hamiltonian vector fields X_{P_i} for all i . The map $\mathfrak{g} \rightarrow \mathfrak{X}(\Phi)$ that takes a vector ξ to the infinitesimal generator X_ξ is a Lie Algebra antihomomorphism,

$$[X_{\xi_1}, X_{\xi_2}] = -X_{[\xi_1, \xi_2]}. \quad (\text{B.2.2})$$

The group G has a coadjoint action on the dual Lie algebra, $\text{Ad}_g^* : \mathfrak{g}^* \rightarrow \mathfrak{g}^*$. A momentum map is called Ad^* -equivariant if $\mathbf{P} \circ \varphi_g = \text{Ad}_{g^{-1}}^* \circ \mathbf{P}$ for all $g \in G$. If \mathbf{P} is an Ad^* -equivariant momentum map then the component functions P_i close under the Poisson bracket. In particular,

$$\{P_i, P_j\} = \langle \mathbf{P}, [\xi_i, \xi_j] \rangle = c_{ij}^k P_k. \quad (\text{B.2.3})$$

Given a semisimple group G the existence of a corresponding Ad^* -equivariant momentum map is guaranteed [56].

On the Schwinger phase space the maps $I : \Sigma \rightarrow \mathbb{R}$ and $\mathbf{J} : \Sigma \rightarrow \mathbb{R}^3$ defined in Section A.2 are the momentum maps for the $U(1)$ and $SU(2)$ actions on Σ . Note that $\mathfrak{u}(1)^*$ is identified with \mathbb{R} and $\mathfrak{su}(2)^*$ is identified with \mathbb{R}^3 .

B.3 Level Sets, Orbits, and Lagrangian Manifolds

Let Φ be a phase space and G be a connected, semisimple Lie group with a symplectic group action φ on Φ and an Ad^* -equivariant momentum map $\mathbf{P} : \Phi \rightarrow \mathfrak{g}^*$. The group orbit $B \subset \Phi$ passing through z is the set $\{\varphi_g(z)\}$ for all $g \in G$. The tangent space $T_z B$ to the group orbit at z is spanned by the vectors X_i defined in Eq. B.2.1 evaluated at z . The rank of the vectors is $\dim B \equiv m \leq \dim G$. We call the dual Lie algebra element $\mu \equiv \mathbf{P}(z) \in \mathfrak{g}^*$ the ‘‘generalized momentum’’ at z . The level sets of the momentum map are the sets of all phase space points with the same generalized momentum. Let $L \equiv \mathbf{P}^{-1}(\mu)$ be the level set passing through z . The forms dP_i all annihilate the tangent space $T_z L$. Since ω by definition is nonsingular, the rank of the dP_i is identical to the rank of the X_i and thus L has co-dimension m .

The isotropy subgroup $H_\mu \subset G$ is the group that leaves μ invariant under the coadjoint action, $H_\mu \equiv \{h \in G \mid \text{Ad}_h^* \mu = \mu\}$. Let $\mathcal{I} \subset B$ be the orbit of the isotropy subgroup at z . By Ad^* -equivariance, $\mathbf{P}(\varphi_h(z)) = \mathbf{P}(z)$ and we can conclude that $\mathcal{I} \subset L$. Therefore, $\mathcal{I} \subset L \cap B$. Let $z' \in L \cap B$. Since $z' \in B$, there exists a $g \in G$ such that $z' = \varphi_g z$. By Ad^* -equivariance, $\mathbf{P}(z') = \text{Ad}_g^* \mathbf{P}(z)$. Since $z' \in L$, $\mathbf{P}(z') = \mu = \mathbf{P}(z)$ and $\text{Ad}_g^* \mu = \mu$. Therefore $g \in H$ and z'

is an element the isotropy subgroup orbit. Since z' is an arbitrary element of $L \cap B$ we may conclude that $L \cap B \subset \mathcal{I}$. Therefore the intersection of the level set and the group orbit is the isotropy subgroup orbit, $\mathcal{I} = L \cap B$.

An arbitrary vector $Y \in T_z B$ can be expressed as linear combinations of the flow vectors, $Y = \sum a_i X_i$. An arbitrary vector $Z \in T_z L$ is annihilated by the forms dP_i for all i . From these properties it follows that $\omega(Y, Z) = 0$, so $T_z B$ and $T_z L$ are symplectic complements of one another. It also follows that the symplectic form acting on any two vectors in $T_z \mathcal{I}$ vanishes, so \mathcal{I} is an isotropic manifold.

Now let $\mu \in \mathfrak{g}^*$ be a fixed point of the coadjoint action, $\text{Ad}_g^* \mu = \mu$ for all $g \in G$. By differentiation and contraction with an arbitrary element of \mathfrak{g} this implies $\langle \mu, [\xi_i, \xi_j] \rangle = 0$ for all i, j . Therefore, $c_{ij}^k \mu_k = 0$ and $\{P_i, P_j\} = c_{ij}^k P_k = 0$ for all points $z \in \mathbf{P}^{-1}(\mu)$. In other words, the momentum map components P_i , which in general form a nontrivial Lie algebra on Φ , have vanishing Poisson brackets among themselves on L . This in turn implies that the P_i 's are constant along each other's flows on B , that is, $X_i(P_j) = -\{P_j, A_i\} = 0$, so $B \subset L$. Alternatively, the isotropy subgroup for a fixed point is the full group G so $\mathcal{I} = B$ and $B \subset L$. It follows that B is an isotropic submanifold of Φ and L is a coisotropic submanifold of Φ whenever μ is a fixed point. In terms of dimensions, this implies that $\dim B = n \leq N$ and $\dim L = 2N - n \geq N$. In the case that L is compact and these inequalities are saturated the group orbit and the level set coincide. In such a case $L = B$ is a Lagrangian submanifold of Φ .

In spin networks, we will be primarily dealing with groups that are direct products of $U(1)$ and $SU(2)$ groups. Since $U(1)$ is an abelian group, every element of $\mathfrak{u}(1)^* = \mathbb{R}$ is a fixed point. The coadjoint action of $SU(2)$ on $\mathfrak{su}(2)^* = \mathbb{R}^3$ takes the form of a rotation on angular momentum space \mathbb{R}^3 . The only fixed point of such an action is the zero vector $\mathbf{0}$.

B.4 Symplectic Reduction

Symplectic reduction [56, 115, 116] is a way of eliminating the symmetries of a Hamiltonian system. Let Φ be a phase space and let G be a Lie group with a symplectic group action on Φ and an Ad^* -equivariant momentum map \mathbf{P} . We may define symplectic reduction for any generalized momenta $\mu \in \mathfrak{g}^*$ but we are only concerned in this work with the case where μ is a fixed point of the coadjoint action and so we restrict our attention to such a case. Let $L = \mathbf{P}^{-1}(\mu)$ be the level set of the momentum map at a fixed point. As discussed in Section B.3 since μ is a fixed point the group orbit passing through any point $z \in L$ is completely contained within L . Define an equivalence relation such that two points on L are equivalent if they lie on the same group orbit and let Φ_μ be the space of equivalence classes L/G . Define the map $\pi : L \rightarrow \Phi_\mu$ as the projection map under this quotient operation. The conditions listed above ensure that Φ_μ is itself a manifold and ensures the existence of a symplectic form ω_μ on Φ_μ which satisfies $\pi^* \omega_\mu = \iota^* \omega$. Thus the manifold Φ_μ with symplectic form ω_μ has the structure of a phase space. We call Φ_μ with this form the ‘‘symplectic reduction of Φ by G ’’. This reduced space is sometimes written as $\Phi // G$ or $\Phi // (\mathbf{P} = \mu)$. Let

$\dim \Phi = 2n$ and let L have co-dimension m (note that m is not necessarily the dimension of the group G). Then, as discussed in Section B.3, the group orbits are m -dimensional and thus the reduced phase space has dimension $\dim \Phi_\mu = 2(n - m)$.

A Hamiltonian A on Φ may be projected down to a reduced Hamiltonian H^R on Φ_μ only if it is constant on the group orbits of G in L . Conversely, we may lift a Hamiltonian H^R from the reduced space into the level set L by demanding that the lifted function be G -invariant (and thus constant along the G -group orbits). In terms of Poisson brackets this means that $\{H, \mathbf{P}\} = 0$ on L . Given two functions G -invariant Hamiltonian A and B on L the Hamiltonian $C = \{A, B\}$ is then also a G -invariant function as a result of the Jacobi identity. These Hamiltonians may all be projected down to the reduced space Hamiltonians A^R, B^R , and C^R . As discussed in Abraham and Marsden [56], the projection of the Poisson bracket is then the Poisson bracket of the projection, $C^R = \{A^R, B^R\}$. Alternatively, the Poisson bracket on Φ_μ of two Hamiltonians on the reduced space is the Poisson bracket on Φ of the lifted Hamiltonians.

Let $X, Y \in T_z L$ be tangent vectors in the level set at some point $z \in L$. Pushing forward by ι allows these vectors to be interpreted as vectors in $T_z \Phi$ (this is equivalent to considering $T_z L$ a vector subspace of $T_z \Phi$). We may also push these vectors forward by π to get the reduced vectors $X^R = \pi_* X, Y^R = \pi_* Y$. By the definition of the reduced symplectic form,

$$\omega_\mu(X^R, Y^R) = \pi^* \omega_\mu(X, Y) = \omega(X, Y). \quad (\text{B.4.1})$$

If X and Y are tangent to a manifold $M \subset L$ then X^R and Y^R are tangent to the reduced manifold formed by the push-forward of the manifold under the projection, $M^R = \pi(M)$. If M^R is isotropic then by definition $\omega(X, Y) = 0$ and thus $\omega_\mu(X^R, Y^R) = 0$. Therefore the projection of an isotropic manifold in L under symplectic reduction is itself an isotropic manifold of the reduced space. Now consider a Lagrangian manifold $\mathcal{L} \subset L \subset \Phi$ which necessarily has dimension n since $\dim \Phi = 2n$. Since \mathcal{L} is isotropic the reduced manifold $\mathcal{L}^R = \pi(\mathcal{L})$ is also isotropic and thus $\dim \mathcal{L}^R \leq n - m$ since $\dim \Phi_\mu = 2(n - m)$. However, the group orbits in L are m -dimensional and $\dim \pi(\mathcal{L}) \geq n - m$. We conclude that the reduced manifold must have dimension $n - m$ and is thus an isotropic manifold of maximum dimensionality. Therefore a Lagrangian manifold completely in the level set of a symplectic reduction projects onto a Lagrangian manifold in the reduced space.

As an explicit example of symplectic reduction, consider the Schwinger phase space Σ with the $U(1)$ group action given in A.3.3. The momentum map for this action is the function I , defined in Eq. A.2.2. Given a value $J \neq 0$, the level set $I^{-1}(J)$ is a three-sphere $S^3 \in \mathbb{C}^2$ of radius J . The symplectic form in Eq. A.2.5 restricted to S^3 is $\iota^* \omega = dJ_z \wedge d\phi$ since $dI = 0$ on this level set. The $U(1)$ group orbits are all circles which are the Hopf circles of the Hopf fibration. The projection map of symplectic reduction is the Hopf map $\pi : S^3 \rightarrow S^2$ and the reduced symplectic manifold is a 2-sphere of radius J . Moreover the function \mathbf{J} is invariant under this group action and so is a good function on the reduced space. By choosing $\omega_\mu = dJ_z \wedge d\phi$ we satisfy $\pi^* \omega_\mu = \iota^* \omega$ and thus the symplectic reduction

of the Schwinger phase space by the momentum map I is

$$\Sigma // (I=J) = (S^2, dJ_z \wedge d\phi). \quad (\text{B.4.2})$$

B.5 The Lagrangian Signature

Consider the $2n$ -dimensional symplectic vector space (V, ω) . The Lagrangian Grassmannian $\text{Lag}(V)$ is defined as the space of all Lagrangian vector subspaces of V . Elements $\Lambda \in \text{Lag}(V)$ are isomorphic to \mathbb{R}^n and are called Lagrangian planes. The Maslov indices that appear in WKB theory can be interpreted as different manifestations of a signature defined on a triplet of Lagrangian planes, $\sigma : \text{Lag}(V)^3 \rightarrow \mathbb{Z}$ [61]. We refer to this map as the Lagrangian signature, though it is also known as the Wall-Kashiwara signature and the Maslov triple index. It is closely related to the triple index defined by Kashiwara as described in Lions and Vergne [60], the triple index defined by Wall [117], and the higher-index structures defined by Hörmander [118]. The Lagrangian signature is completely antisymmetric in its three arguments and invariant under symplectic transformations,

$$\sigma(\Lambda_1, \Lambda_2, \Lambda_3) = \sigma(s\Lambda_1, s\Lambda_2, s\Lambda_3) \quad \forall s \in Sp(2n). \quad (\text{B.5.1})$$

Furthermore, we require the property of symplectic additivity so that

$$\sigma_{V \times W}(\Lambda_1 \oplus \Lambda'_1, \Lambda_2 \oplus \Lambda'_2, \Lambda_3 \oplus \Lambda'_3) = \sigma_V(\Lambda_1, \Lambda_2, \Lambda_3) + \sigma_W(\Lambda'_1, \Lambda'_2, \Lambda'_3), \quad (\text{B.5.2})$$

where $\Lambda_i \in \text{Lag}(V)$, $\Lambda'_i \in \text{Lag}(W)$ and the subscripts on σ indicate the symplectic vector space on which the signature is defined. Up to a normalization these properties uniquely define the Lagrangian signature [59]. The Lagrangian signature can be explicitly defined as follows. Consider a triplet of Lagrangian planes $\Lambda_1, \Lambda_2, \Lambda_3 \in \text{Lag}(V)$ and construct the quadratic form

$$\begin{aligned} Q_{123} : \Lambda_1 \times \Lambda_2 \times \Lambda_3 &\rightarrow \mathbb{R} \\ (\vec{z}_1, \vec{z}_2, \vec{z}_3) &\mapsto \omega(\vec{z}_1, \vec{z}_2) + \omega(\vec{z}_2, \vec{z}_3) + \omega(\vec{z}_3, \vec{z}_1). \end{aligned} \quad (\text{B.5.3})$$

Let $\{e_{r,i}\}$, $i = 1, \dots, n$ be a basis of Λ_r for $r = 1, 2, 3$ so that $z_r \in \Lambda_r = \sum_i z_r^i e_{r,i}$. Let \hat{Q}_{123} be the symmetric $3n \times 3n$ -matrix representation of Q_{123} with respect to this basis,

$$\hat{Q}_{123} = \left[\begin{array}{c|c|c} 0 & \omega(e_{1,i}, e_{2,j}) & -\omega(e_{1,i}, e_{3,j}) \\ \hline -\omega(e_{2,i}, e_{1,j}) & 0 & \omega(e_{2,i}, e_{3,j}) \\ \hline \omega(e_{3,i}, e_{1,j}) & -\omega(e_{3,i}, e_{2,j}) & 0 \end{array} \right]. \quad (\text{B.5.4})$$

Since \hat{Q}_{123} is a real, symmetric matrix we may define the matrix signature $\text{sgn } \hat{Q}_{123}$, which is the number of positive eigenvalues minus the number of negative eigenvalues that occur in the spectrum of \hat{Q}_{123} .

We define the Lagrangian signature as the matrix signature of the matrix \hat{Q}_{123} associated with Q_{123} ,

$$\sigma : \text{Lag}(V)^3 \rightarrow \mathbb{Z} : (\Lambda_1 \times \Lambda_2 \times \Lambda_3) \mapsto \text{sgn } \hat{Q}_{123}. \quad (\text{B.5.5})$$

This map by construction satisfies the requirements detailed earlier as well as a cocycle condition [60, 61]. Given a set of four Lagrangian planes in $\text{Lag}(V)$,

$$\sigma(\Lambda_1, \Lambda_2, \Lambda_3) - \sigma(\Lambda_2, \Lambda_3, \Lambda_4) + \sigma(\Lambda_3, \Lambda_4, \Lambda_1) - \sigma(\Lambda_4, \Lambda_1, \Lambda_2) = 0. \quad (\text{B.5.6})$$

The Lagrangian signature may also be associated with the matrix signature of a pair of real, symmetric $n \times n$ -matrices. Let $\Lambda_x \in \text{Lag}(V)$ be a fixed reference Lagrangian plane and let $\Lambda_p \in \text{Lag}(V)$ be a choice of transverse plane to Λ_x so that $\Lambda_x \cap \Lambda_p = 0$. The vector space V can then be expressed as the direct sum $V = \Lambda_x \oplus \Lambda_p$ and any vector $\vec{z} \in V$ projects uniquely into a pair of n -component vectors $\vec{x} \in \Lambda_x$ and $\vec{p} \in \Lambda_p$. Each real, symmetric matrix \hat{A} generates a Lagrangian plane $\Lambda_A \in \text{Lag}(V)$ such that, for all $\vec{z} \in \Lambda_A$, $\vec{x} = \hat{A}\vec{p}$. The zero-matrix in this scheme generates Λ_p itself. Note that only the set of planes transverse to Λ_x can be generated this way. Let $\Lambda_A, \Lambda_B \in \text{Lag}(V)$ be a pair of Lagrangian planes generated by a pair of real, symmetric matrices \hat{A}, \hat{B} . The Lagrangian signature of the triplet of planes Λ_x, Λ_A , and Λ_B is then

$$\sigma(\Lambda_x, \Lambda_A, \Lambda_B) = \text{sgn}(\hat{A} - \hat{B}). \quad (\text{B.5.7})$$

Note that while the transverse plane Λ_p is needed to generate the planes, the resulting signature is invariant under the particular choice of plane. A special case of Eq. B.5.7 is when $\Lambda_B = \Lambda_p$ so \hat{B} is zero,

$$\sigma(\Lambda_x, \Lambda_A, \Lambda_p) = \text{sgn } \hat{A}. \quad (\text{B.5.8})$$

Another special case that is essential to the proof in Section 2.5.5 is the case where the three Lagrangian planes satisfy $\Lambda_1 \subset (\Lambda_1 \cap \Lambda_2) \oplus (\Lambda_1 \cap \Lambda_3)$. Note that if $\Lambda_2 \cap \Lambda_3 = 0$ then this subset relation is saturated. Then the characteristic polynomial for finding the eigenvalues of \hat{Q}_{123} is

$$\det(\hat{Q}_{123} - \lambda \mathbf{1}_{3n}) = \lambda^m f(\lambda^2) = 0, \quad (\text{B.5.9})$$

where $\mathbf{1}_{3n}$ is the $3n \times 3n$ identity matrix, $m \geq n$ is the rank of the kernel of \hat{Q}_{123} and f is a polynomial. Eigenvalues of \hat{Q}_{123} are therefore either 0 or solutions of $f(\lambda^2) = 0$. Thus the non-zero eigenvalues must come in pairs $\pm\lambda$ and the number of positive eigenvalues n_+ is equal to the number of negative eigenvalues n_- yielding

$$\sigma(\Lambda_1, \Lambda_2, \Lambda_3) = \text{sgn } \hat{Q}_{123} = n_+ - n_- = 0. \quad (\text{B.5.10})$$

Appendix C

The Semiclassical Approximation

In this section we review the various aspects of the semiclassical approximation of an inner product. We are primarily interested in integrable systems, the semiclassics of which have been studied for a long time (Einstein [119], Brillouin [120], Keller [121], Percival [122], Berry and Tabor [123], Gutzwiller [124], Brack and Bhaduri [125], Cargo *et al* [126], and Aquilanti *et al* [44], among others). The link between the classical objects in phase space and the quantum objects in a Hilbert space is provided by WKB theory. For modern treatments of WKB theory, see Martinez [52] or Mishchenko *et al* [53].

For simplicity in this section we work in a flat phase space $\Phi \equiv \mathbb{R}^{2n}$ which is considered the co-tangent bundle over a Euclidean configuration space $\mathcal{Q} \equiv \mathbb{R}^n$. Coordinates on \mathbb{R}^{2n} are (x, p) with $x \in \mathcal{Q}$ the configuration variables.

C.1 The WKB Wavefunction

The semiclassical approximation to the x -space wavefunction $\langle x|\psi\rangle$ is given in the allowed region by the WKB wavefunction

$$\psi(x) = N \sum_{\text{branches } k} |\Omega_k(x)|^{1/2} e^{i(S_k(x) - \mu_k \pi/2)}, \quad (\text{C.1.1})$$

where N is a normalization, k is a branch index, $\Omega_k(x)$ is an amplitude, $S_k(x)$ is an “action integral” and μ_k is a Maslov index. We have set $\hbar = 1$ as usual but it is worth noting that when restored the action integral is $S_k(x)/\hbar$ and thus in the limit of small \hbar (or, more physically, in the limit of large quantum numbers), the phase is rapidly oscillating. For the WKB approximation to be valid we require that the amplitude be “slowly varying.” That is, the amplitude does not change appreciably over the wavelength.

The action integral is a generating function for the momentum, $p_k \equiv \partial S_k(x)/\partial x$. The pair (x, p_k) then describes points in phase space belonging to a Lagrangian submanifold \mathcal{L} . The branches k of the WKB wavefunction are the same as the branches of the projection $\pi : \mathcal{L} \rightarrow \mathcal{Q}$ from the Lagrangian manifold to configuration space, assumed to be locally invertible.

Consider a reference point $z_0 \in \mathcal{L}$ and a point z on the k -th branch of \mathcal{L} over $x \in \mathcal{Q}$, so $\pi(z) = x$. Let Γ be a path on \mathcal{L} starting at z_0 and ending at z . The action integral $S_k(x)$ in the WKB wavefunction Eq. C.1.1 may then be expressed as

$$S_k(x) \equiv \int_{\Gamma} \theta, \quad (\text{C.1.2})$$

where $\theta = p dx$ is the symplectic potential in the x -representation.

Caustic points on \mathcal{L} are points where the Lagrangian manifold is “vertical” over configuration space. That is, the caustic points are points where the projection map $\pi : \mathcal{L} \rightarrow \mathcal{Q}$ is less than full rank. The x -representation foliates phase space into Lagrangian leaves \mathcal{L}_x . Caustic points may also be considered points where the tangent space to \mathcal{L} and the tangent space to the Lagrangian leaf \mathcal{L}_x have a non-trivial intersection (the intersection represents the directions in which \mathcal{L} is vertical over \mathcal{Q}).

The idea underlying the Maslov method in WKB theory is that caustic points may be avoided in stationary phase integrals by transforming from one representation to another [127]. In particular, to get from a stationary phase point one branch of \mathcal{L} to another requires passing through a caustic point. The stationary phase integral suffers a singularity at this point. To properly perform the integral a Fourier transform is used to change from the x -representation to the p -representation in a neighborhood of the caustic. Then we transform back to the x -representation after the caustic has been cleared. The cost of this procedure is an additional phase of $e^{-i\mu\pi/2}$, where μ is the Maslov index, an integer. The Maslov index is only accumulated at the caustic points. If $T(p)$ is the momentum-representation generating function for \mathcal{L} at the caustic point then the Maslov index accumulated along a path that passes through a caustic is the change in the matrix signature of the Hessian matrix,

$$\mu = \Delta \text{sgn} \frac{\partial^2 T(p)}{\partial p_i \partial p_j}. \quad (\text{C.1.3})$$

The Maslov index may also be expressed in terms of the Lagrangian signature defined in Section B.5. Since we are assuming a Euclidean phase space \mathbb{R}^{2n} the tangent spaces $T_z \Phi$ can all be trivially and uniquely identified which means that a single global Lagrangian Grassmannian $\text{Lag}(V)$ can be used for the phase space. Consider a point z near a caustic in \mathcal{L} . The manifold is locally described by $x_i(p) = -\partial T / \partial p_i$. The tangent plane at z to \mathcal{L} is a Lagrangian plane $T_z \mathcal{L} \in \text{Lag}(V)$ and is spanned by the vectors $\frac{\partial}{\partial p_i} + \frac{\partial x_j}{\partial p_i} \frac{\partial}{\partial x_j}$. The projections onto the representation planes are then related by $\vec{x} = \hat{A} \vec{p}$, where

$$\hat{A}_{ij} \equiv \frac{\partial x_j}{\partial p_i} = -\frac{\partial^2 T(p)}{\partial p_i \partial p_j}. \quad (\text{C.1.4})$$

Thus $\mu = -\Delta \text{sgn} A_{ij}$. Thus by Eq. B.5.8 the Maslov index along a path passing through a caustic may be expressed as the change in a Lagrangian signature,

$$\mu = \Delta \sigma(\Lambda_x, \Lambda_A, \Lambda_p), \quad (\text{C.1.5})$$

where Λ_x and Λ_p are Lagrangian planes defining the x - and p -representations and Λ_A is the tangent plane to the manifold \mathcal{L} .

In Esterlis *et al* [55] we developed a method for computing the Maslov index that relies only on Poisson brackets and simple linear algebra. We also developed a singular differential form whose integral along a curve results in the Maslov index for the curve.

A Lagrangian manifold \mathcal{L} is said to be quantized if, for all *closed* paths Γ on \mathcal{L} , the action integral (including Maslov correction) around the path is an integer multiple of 2π ,

$$\oint_{\Gamma} \theta - \mu(\Gamma) \frac{\pi}{2} = 0 \pmod{2\pi}, \quad \forall \Gamma \subset \mathcal{L}. \quad (\text{C.1.6})$$

This amounts to a consistency condition on the WKB wavefunction Eq. C.1.1. Littlejohn and Robbins [128] showed that the closed-path Maslov indices of the type that occur here may alternatively be expressed as winding numbers in the complex plane.

C.2 Densities

The function $\Omega_k(x)$ in Eq. C.1.1 on a given branch of the WKB wavefunction satisfies a set of n amplitude-transport equations on \mathcal{Q} [129, 44]. Given a point $z \in \mathcal{L}$ on branch k over representation-point x (with coordinates x_1, \dots, x_n), a volume form $\sigma \in \Omega^n(\mathcal{L})$ can be constructed on the Lagrangian manifold,

$$\sigma|_z = \Omega_k(x) dx_1 \wedge \dots \wedge dx_n. \quad (\text{C.2.1})$$

Let \mathcal{L} be the a group orbit for some group G with a symplectic action on phase space and let \mathbf{P} be the momentum map for this group action. The amplitude-transport equations for $\Omega(x)$ imply that the density σ is invariant under the (left) action of the group.

If $\dim G = \dim \mathcal{L}$ then the left- and right-invariant forms and vector fields on the group manifold G can be locally pushed-forward into vector fields and forms on \mathcal{L} . In particular the Hamiltonian vector field generated by a component of \mathbf{P} is the push-forward of a right-invariant vector field on G . Let \mathcal{L} be described as the level set of a momentum map \mathbf{P} for an n -dimensional group G , $\mathcal{L} = \mathbf{P}^{-1}(\mu)$, where μ is a fixed point of \mathfrak{g}^* . The set of Hamiltonian vector fields $\{X_i\}$ at any point $z \in \mathcal{L}$ span the tangent space $T_z \mathcal{L}_\mu$. Let $\{\lambda_i\}$ be a set of n 1-forms on \mathcal{L} dual to the vectors X_i , that is, $\lambda_i(X_j) = \delta_{ij}$. These are locally the push-forwards of right-invariant forms on G . The density σ may then be expressed in terms of the right-invariant one-forms,

$$\sigma_{\mathcal{L}} \equiv \lambda_1 \wedge \dots \wedge \lambda_n \in \Omega^n(\mathcal{L}). \quad (\text{C.2.2})$$

This volume form is uniquely determined once an ordered choice of basis vectors $\{\xi_i\}$ is made. The density defined this way is locally the pullback of the right-invariant Haar measure on G . We will only be concerned with compact groups G in this work in which case the left- and

right-invariant Haar measures on G are the identical. Note that σ is the unique left-invariant volume form on \mathcal{L} up to an overall normalization factor.

The amplitudes $\Omega_k(x)$ may be determined by acting both volume forms on the n Hamiltonian flow vectors X_i . The σ acting on the flow vectors is

$$\sigma(X_1, \dots, X_n) = \det [\lambda_i(X_j)] = \det [\delta_{ij}] = 1. \quad (\text{C.2.3})$$

Eq. C.2.1 acting on the vectors gives

$$\Omega_k(x)(dx_1 \wedge \dots \wedge dx_n)(X_1, \dots, X_n) = \Omega_k(x) \det [dx_i(X_j)]. \quad (\text{C.2.4})$$

Each of the entries of the $n \times n$ matrix in the determinant is a Poisson bracket,

$$dx_i(X_j) = \omega^{-1}(dx_i, dP_j) = \{x_i, P_j\}. \quad (\text{C.2.5})$$

Therefore the amplitude $\Omega_k(x)$ is expressed as the inverse of an $n \times n$ matrix of Poisson brackets,

$$\Omega_k(x) = \frac{1}{\det [\{x_i, P_j\}]}, \quad (\text{C.2.6})$$

where the brackets are evaluated at the point $z \in \mathcal{L}$ on branch k over configuration point x .

Let $V_{\mathcal{L}} = \int_{\mathcal{L}} \sigma$ be the volume of the Lagrangian manifold with respect to the left-invariant density. When \mathcal{L} is a single connected group orbit, as we assume in all applications, $V_{\mathcal{L}}$ is related to the volume V_G of the group G with respect to the Haar measure μ_G . Let $H \subset G$ be the isotropy subgroup of G with respect to the group action on \mathcal{L} . That is, H is the set of elements $h \in G$ such that $\varphi_h z = z$ for all $z \in \mathcal{L}$. If H only contains discrete elements then the group orbit covers \mathcal{L} exactly $|H|$ times, where $|H|$ is the cardinality of the isotropy subgroup. Consider the map $\phi : G \rightarrow \mathcal{L} : g \mapsto \varphi_g z_0$, where z_0 is some arbitrary reference point on \mathcal{L} . Then the Haar measure is the pull-back of the density, $\mu_G = \phi^* \sigma$. Carrying out the volume integral yields

$$V_G = \int_G \mu_G = \int_G \phi^* \sigma = \int_{\phi(G)} \sigma = |H| \int_{\mathcal{L}} \sigma = |H| V_{\mathcal{L}}. \quad (\text{C.2.7})$$

Therefore the volume of a Lagrangian manifold is given by

$$V_{\mathcal{L}} = \frac{V_G}{|H|}. \quad (\text{C.2.8})$$

As shown in Aquilanti *et al* [44] the overall normalization of the WKB wavefunction in Eq. C.1.1 is

$$N = \frac{1}{\sqrt{V_{\mathcal{L}}}}. \quad (\text{C.2.9})$$

Changing the basis of \mathfrak{g}^* or changing the momentum map description of \mathcal{L} changes the density form σ by a scale factor. This in turn causes the amplitude $\Omega_k(x)$ and the volume $V_{\mathcal{L}}$ to change by the same scale factor. However, only the combination $\sqrt{\Omega_k(x)/V_{\mathcal{L}}}$ appears in the WKB wavefunction so this dependence on the choice of basis of \mathfrak{g}^* cancels out.

C.3 The Wigner-Weyl Transform

In this work we typically describe a quantum state as a non-degenerate eigenvector $|A\rangle$ in a Hilbert space \mathcal{H} of a set of observables \hat{A}_i on \mathcal{H} . Note that these observables do not necessarily commute on the entire space \mathcal{H} . The classical analog to $|A\rangle$ will be a Lagrangian manifold \mathcal{L}_a in the phase space Φ that corresponds to \mathcal{H} as seen in the “semi-classical dictionary” presented in Chapter 2 of Bates and Weinstein [58]. As discussed in Littlejohn [54] and Aquilanti *et al* [44], this Lagrangian manifold will be the level set of the classical observables A_i (without the hats) for appropriate contour values.

Classical observables on Φ are formed by taking the Wigner-Weyl transform of operators on \mathcal{H} (Weyl [130], Wigner [131], Berry [132], Balazs and Jennings [133], Littlejohn [112], de Almeida [134]). The function $A : \Phi \rightarrow \mathbb{C}$ corresponding to the operator $\hat{A} : \mathcal{H} \rightarrow \mathcal{H}$ is called the “Weyl symbol” of the operator. For example, the complex coordinates (z_μ, \bar{z}_μ) on Σ are the Weyl symbols of the annihilation and creation operators $(\hat{a}_\mu, \hat{a}_\mu^\dagger)$ on \mathcal{S} . Let operator \hat{A} be expressed in terms of the canonically conjugate configuration and momentum operators \hat{q}, \hat{p} on \mathcal{H} , $\hat{A}(\hat{q}, \hat{p})$ (an ordering convention is needed to make this notation meaningful). The principal symbol of \hat{A} , $A_{pr}(q, p)$ is formed by replacing operators \hat{q}, \hat{p} with classical coordinates q, p . The principal symbol is the lowest-order contribution to the Weyl symbol. For operators that are linear or quadratic in \hat{q} and \hat{p} the principal symbol and Weyl symbol agree.

Let \hat{A} and \hat{B} be operators on some Hilbert space \mathcal{H} and with Weyl symbols A and B , respectively, on the corresponding phase space Φ . The Moyal star product [135, 136] is defined so that $A \star B$ is the Weyl symbol of the operator $\hat{A}\hat{B}$. Let the coordinates on Φ be z_μ with $\mu = 1, \dots, 2n$ (these are real coordinates on an arbitrary phase space, not to be confused with the complex coordinates on the Schwinger phase space) and let the Poisson tensor in these coordinates be $J^{\mu\nu}$. The star product can then be expressed in terms of the “Janus operator” $\overleftrightarrow{\mathcal{L}} \equiv \overleftarrow{\partial}_\mu J^{\mu\nu} \overrightarrow{\partial}_\nu$ where the arrows on the derivatives indicate whether the derivative acts to the left or to the right. In this notation $A \overleftrightarrow{\mathcal{L}} B = A_{,\mu} J^{\mu\nu} B_{,\nu} = \{A, B\}$. The Moyal star product then is

$$A \star B = A e^{\frac{i\hbar}{2} \overleftrightarrow{\mathcal{L}}} B, \quad (\text{C.3.1})$$

where \hbar has been temporarily restored as an expansion parameter [135]. To second order in \hbar ,

$$A \star B = AB + \frac{i\hbar}{2} \{A, B\} - \frac{\hbar^2}{8} A_{,\mu\nu} J^{\mu\rho} J^{\nu\sigma} B_{,\rho\sigma} + \mathcal{O}(\hbar^3). \quad (\text{C.3.2})$$

If operator \hat{A}_i has the Weyl symbol A_i then the eigenvalue condition $\hat{A}_i|A\rangle = a_i|A\rangle$ translates into the level set condition $A_i = a_i$ to lowest order in \hbar . Note that we do *not* adopt the convention that removing the hat gives the Weyl symbol in the case of the operator \hat{I} defined in Eq. A.1.1. Instead, the Weyl symbol of \hat{I} is the function $I - 1/2$, where I is defined as in Eq. A.2.2. Therefore the Lagrangian manifold corresponding to a state in the j -eigenspace of \mathcal{S} will lie in the $I = j + 1/2$ level set of Σ . For example, the Lagrangian

manifold corresponding to the standard basis vector $|jm\rangle \in \mathcal{S}$ is the simultaneous level set of $I = j + 1/2$ and $J_z = m$ in Σ .

The Weyl symbol for operators that are quartic in \hat{z} differ from their principal symbols by a term of order \hbar^2 (all higher-order terms will vanish however). The operator $\hat{\mathbf{J}}^2$ for a single angular momentum has the Weyl symbol $\mathbf{J}^2 - 3\hbar^2/8$, which is consistent with the operator relation $\hat{\mathbf{J}}^2 = \hat{I}(\hat{I} + 1)$. The error term is of relative order \hbar^2 which is the error expected in lowest-order semiclassical approximations. However, the operator identity allows the quartic-operator eigenvalue condition on $\hat{\mathbf{J}}^2$ to be replaced by a quadratic-operator eigenvalue condition on \hat{I} . The Weyl symbol of the coupled-angular momentum operator $\hat{\mathbf{J}}_{12}^2$ is $\mathbf{J}_{12}^2 - 3\hbar^2/4$. There is no quadratic operator \hat{I}_{12} which could be used to replace the quartic operator to obtain exact eigenvalues in this case.

C.4 WKB Approximation of Inner Products

Let \mathcal{H} be a Hilbert space describing n classical degrees of freedom and let Φ be the associated $2n$ -dimensional phase space. Consider two vectors $|a\rangle, |b\rangle \in \mathcal{H}$ with x -representation WKB wavefunctions $\psi_a(x), \psi_b(x)$ and let $\mathcal{L}_a, \mathcal{L}_b \subset \Phi$ be the two Lagrangian manifolds that support the semiclassical approximations. The inner product $\langle a|b\rangle$ is approximated by

$$\langle a|b\rangle = \int dx \sum_{k,k'} |\Omega_{a,k}(x)\Omega_{b,k'}(x)|^{1/2} e^{i(S_{b,k'}(x) - S_{a,k}(x) - (\mu_{b,k'} - \mu_{a,k})\pi/2)}, \quad (\text{C.4.1})$$

where k and k' index the x -representation branches of \mathcal{L}_a and \mathcal{L}_b . The stationary phase points occur when $\partial S_{b,k'}/\partial x - \partial S_{a,k}/\partial x = 0$ which is equivalent to $p_{b,k'}(x) = p_{a,k}(x)$. Thus the stationary phase set is geometrically interpreted in phase space as the intersection points of \mathcal{L}_a and \mathcal{L}_b .

Let the states $|a\rangle$ and $|b\rangle$ be simultaneous non-degenerate eigenstates of sets of observables \hat{A}_i and \hat{B}_i ($i = 1, \dots, n$) and let \hat{A}_i and \hat{B}_i form Lie algebras for the groups G_A and G_B under the commutator. The Lagrangian manifolds \mathcal{L}_a and \mathcal{L}_b that support the semiclassical approximations to $|a\rangle$ and $|b\rangle$ may then be described as the simultaneous level sets of momentum map components A_i and B_i , respectively. These are both n -dimensional manifolds in a $2n$ -dimensional phase space. As in Section C.2 the amplitude $\Omega_{a,k}(x)$ is related to the determinant of a matrix of Poisson brackets, as is $\Omega_{b,k'}(x)$.

Let \mathcal{I} be the intersection $\mathcal{L}_a \cap \mathcal{L}_b$. When this intersection is a discrete set of points the stationary phase approximation of Eq. C.4.1 evaluates to

$$\langle a|b\rangle \approx \frac{(2\pi i)^{n/2}}{\sqrt{V_A V_B}} \sum_{z \in \mathcal{I}} |\Omega_z|^{1/2} e^{i\varphi_z}, \quad (\text{C.4.2})$$

where V_A and V_B are the volumes of \mathcal{L}_a and \mathcal{L}_b with respect to the densities defined in Section C.2. The phase φ_z is

$$\varphi_z = S_{b,k'_z}(\pi(z)) - S_{a,k_z}(\pi(z)) - (\mu_{b,k'_z} - \mu_{a,k_z})\frac{\pi}{2} + \sigma_z(b, a)\frac{\pi}{4}, \quad (\text{C.4.3})$$

where $\pi(z)$ is the projection of the intersection points onto \mathcal{Q} and k_z, k'_z are the branches of \mathcal{L}_a and \mathcal{L}_b that contain z , V_A and V_B and σ_z is the “signature index,” which will be discussed in Section C.5. As shown by Littlejohn [54], the amplitudes in this expression may be expressed as the inverse of an $n \times n$ matrix of Poisson brackets,

$$\Omega_z = (\det \{A_i, B_j\}_z)^{-1}, \quad (\text{C.4.4})$$

where the Poisson brackets are to be evaluated at the intersection point z in phase space. In this context Ω_z is called the “amplitude determinant.”

The states in the inner product may feature a “common symmetry group” which manifests itself as higher-dimensional intersections of the two Lagrangian manifolds that support the WKB wavefunctions of the states. The intersection of \mathcal{L}_a and \mathcal{L}_b is then a set of disconnected group orbits of this common symmetry group. Let H be the common symmetry group which generates flows along the connected pieces of the intersection manifold $\mathcal{I} = \mathcal{L}_a \cap \mathcal{L}_b$ and let both H and the group orbits have dimension s . As shown in Aquilanti *et al* [1] the common symmetry group may be made explicit by choosing a basis of the Lie algebras for G_A and G_B such that the first s components of the momentum maps \mathbf{A} and \mathbf{B} are identical. Let \mathcal{I} in this case be divided up into a discrete set of H -group orbits indexed by κ . The stationary phase approximation of Eq. C.4.1 in the presence of a common symmetry group evaluates to

$$\langle a|b \rangle \approx \frac{(2\pi i)^{(n-s)/2}}{\sqrt{V_A V_B}} \sum_{\kappa \in \mathcal{I}} V_{H,\kappa} \left| \tilde{\Omega}_\kappa \right|^{1/2} e^{i\varphi_z}, \quad (\text{C.4.5})$$

where $V_{H,\kappa}$ is the volume of the group orbit with respect to the Haar measure on H . The phase is the same as in Eq. C.4.3, with z an arbitrary point on the group orbit, but $\tilde{\Omega}_\kappa$ is a “reduced” amplitude determinant involving an $(n-s) \times (n-s)$ -matrix of Poisson brackets of the last $(n-s)$ components of \mathbf{A} and \mathbf{B} (the components that are not common to both momentum maps). This is interpreted as the amplitude determinant in the symplectic reduction of the phase space by the common symmetry group. The choice of point z on the common symmetry group orbit is irrelevant because the path connecting one point on the group orbit to another is completely contained within both \mathcal{L}_a and \mathcal{L}_b by definition of the common symmetry group as the generator of the intersection. Therefore the action integrals and Maslov indices on both the a - and b -manifolds change by equal amounts and the total relative phase in Eq. C.4.5 is unaffected.

Note that in some cases the intersection manifold may be generated by a group which is *not* a subgroup of G_A or G_B . In this case the bases of the Lie algebras in which the first s momentum map components are identical are not fixed and in fact depend on the location in phase space. This is an area of ongoing research and has applications to the $2j$ -symbol and its q -deformed version.

C.5 Phases in the WKB Inner Product Approximation

Suppose there is a unique intersection point $z_0 \in \Phi$ and consider the phase φ defined in Eq. C.4.3 at this intersection point. The expression $\sigma_{z_0}(b, a)$ is called the “signature index” and is a way of rewriting the imaginary units that result from the stationary phase determinant. Let $H_{b,a}(z_0)$ be the Hessian matrix defined as

$$[H_{b,a}(z_0)]_{ij} \equiv \left. \frac{\partial^2(S_{bk'_0} - S_{ak_0})}{\partial x_i \partial x_j} \right|_{\pi(z_0)}, \quad (\text{C.5.1})$$

where k_0 and k'_0 are the branches of \mathcal{L}_a and \mathcal{L}_b where the intersection occurs. Then,

$$\sigma_{z_0}(b, a) \equiv \text{sgn } H_{b,a}(z_0), \quad (\text{C.5.2})$$

where the matrix signature $\text{sgn } A$ of a real, symmetric matrix A is the number of positive eigenvalues minus the number of negative eigenvalues that occur in the spectrum of A .

The signature index in Eq. C.5.2 may be expressed in terms of the Lagrangian signature defined in Section B.5. Let Φ be a Euclidean phase space isomorphic to \mathbb{R}^{2n} . The tangent spaces $T_z\Phi$ can all be trivially and uniquely identified which means that a single global Lagrangian Grassmannian $\text{Lag}(V)$ can be used for the phase space. Let \mathcal{L} be a Lagrangian submanifold of Φ and consider a point $z \in \mathcal{L}$. In the x -representation, z is on some branch of \mathcal{L} which carries the action function $S_k(x)$. Locally, the manifold is described by $p_i(x) = \partial S_k / \partial x_i$. The tangent plane at z to \mathcal{L} is a Lagrangian plane $T_z\mathcal{L} \in \text{Lag}(V)$ and is spanned by the vectors $\frac{\partial}{\partial x_i} + \frac{\partial p_j}{\partial x_i} \frac{\partial}{\partial p_j}$. The projections onto the representation planes are then related by $\vec{p} = \hat{A}\vec{x}$, where

$$\hat{A}_{ij} \equiv \frac{\partial p_j}{\partial x_i} = \frac{\partial^2 S_k}{\partial x_i \partial x_j}. \quad (\text{C.5.3})$$

Given an x -representation, the tangent plane to a point z on a Lagrangian manifold is the plane generated by the Hessian of the local action in that representation. Now consider two Lagrangian manifolds, \mathcal{L}_a and \mathcal{L}_b with intersection point z on branches k, k' , respectively. Let $(\hat{A})_{ij} \equiv \partial^2 S_{ak} / \partial x_i \partial x_j$ and $(\hat{B})_{ij} \equiv \partial^2 S_{bk'} / \partial x_i \partial x_j$. From equation C.5.2, the signature index $\sigma(b, a)$ is the matrix signature $\text{sgn}(\hat{B} - \hat{A})$. Thus by Eq. B.5.7 the signature index can be expressed as the Lagrangian signature of the triplet of Lagrangian planes

$$\sigma(b, a) = \sigma(\Lambda_x, \Lambda_B, \Lambda_A), \quad (\text{C.5.4})$$

where Λ_x is the representation plane and Λ_A, Λ_B are the tangent planes to the manifolds $\mathcal{L}_a, \mathcal{L}_b$ at the intersection point.

In general, there will be more than one intersection point. Label the intersection points with the index i and define paths $\Gamma_{0i}^{(a)} \subset \mathcal{L}_a$ and $\Gamma_{0i}^{(b)} \subset \mathcal{L}_b$ be paths from the reference points

$z_{a0} \in \mathcal{L}_a$ and $z_{b0} \in \mathcal{L}_b$ to the i -th intersection point $z_i \in \mathcal{L}_a \cap \mathcal{L}_b$. The approximation of $\langle a|b \rangle$ will then be a sum of terms $A_i e^{i\varphi_i}$. The phases can be written

$$\varphi_i = \int_{\Gamma_{0i}^{(b)}} \theta - \int_{\Gamma_{0i}^{(a)}} \theta - \left(\mu(\Gamma_{0i}^{(b)}) - \mu(\Gamma_{0i}^{(a)}) \right) \frac{\pi}{2} + \sigma_i(a, b) \frac{\pi}{4}. \quad (\text{C.5.5})$$

Typically, we will only be concerned with the *relative* phase between terms in the semiclassical approximation, since the overall phase depends on the phase conventions of the individual states and is not physically relevant. Let $\Delta\varphi_{ij} \equiv \varphi_j - \varphi_i$ be the relative phase of the term due to intersection point z_j with respect to the term due to intersection point z_i . Define paths $\Gamma_{ij}^{(a)} \equiv -\Gamma_{0i}^{(a)} + \Gamma_{0j}^{(a)}$, $\Gamma_{ij}^{(b)} \equiv -\Gamma_{0i}^{(b)} + \Gamma_{0j}^{(b)}$, and $\Gamma_{ij} \equiv \Gamma_{ij}^{(b)} - \Gamma_{ij}^{(a)}$. Note that path Γ_{ij} is a *closed* path that starts at point z_i , goes to point z_j along \mathcal{L}_b , and comes back to z_i along \mathcal{L}_a . Given an algebraic function \mathcal{F} on paths,

$$\begin{aligned} \mathcal{F}(\Gamma_{0j}^{(b)}) - \mathcal{F}(\Gamma_{0j}^{(a)}) &= \mathcal{F}(\Gamma_{0i}^{(b)} + \Gamma_{ij}^{(b)}) - \mathcal{F}(\Gamma_{0i}^{(a)} + \Gamma_{ij}^{(a)}) \\ &= \mathcal{F}(\Gamma_{0i}^{(b)}) - \mathcal{F}(\Gamma_{0i}^{(a)}) + \mathcal{F}(\Gamma_{ij}). \end{aligned} \quad (\text{C.5.6})$$

Since the integral $\int_{\Gamma} \theta$ and the Maslov index $\mu(\Gamma)$ are algebraic functions of paths, the above result allows the phase difference $\Delta\varphi_{ij}$ to be written in terms of the closed path Γ_{ij} :

$$\Delta\varphi_{ij} = \oint_{\Gamma_{ij}} \theta - \mu(\Gamma_{ij}) \frac{\pi}{2} + \Delta\sigma_{ij}(b, a) \frac{\pi}{4}. \quad (\text{C.5.7})$$

Note that the change in the signature index will generically be a multiple of 2 and so the signature index is sometimes treated as another type of Maslov index. Also note that the Bohr-Sommerfeld quantization condition on Lagrangian manifolds \mathcal{L}_a and \mathcal{L}_b imply that choosing different paths will only change the relative phase by integer multiples of 2π .

The action integral part of the phase difference is independent of both reference point and representation. Let the path Γ_{ij} be the boundary of some surface S . Then,

$$\oint_{\Gamma_{ij}} \theta = \int_S d\theta = \int_S \omega. \quad (\text{C.5.8})$$

The symplectic form ω is representation-independent. Changing the reference point on one of the Lagrangian manifolds amounts to adding an additional piece of surface δS that lies entirely in that Lagrangian manifold, which adds zero symplectic area.